CHARACTERISATION OF CARBOHYDRATE CONFORMATIONS BY CHIROPTICAL METHODS

David Thom

A thesis presented for the Degree of

Doctor of Philosophy

University of Edinburgh

1973

GEN EX B/3L UNIVERSITY OF EDINB
CHEMISTRY LIBRARY

TO HAZEL AND EWAN

ACKNOWLEDGEMENTS

I should like to express my most sincere thanks to Professor D.A. Rees for his expert guidance and constant enthusiasm during the course of this study. I should also like to thank my internal supervisor, Dr. J.C.P. Schwarz, and all of my colleagues and in particular Dr. E.R. Morris for the many helpful discussions throughout the course of this work.

My thanks are also due to Professor Cadogan for the provision of laboratory facilities at the University of Edinburgh and to Unilever Ltd. for the provision of laboratory facilities at Colworth House, Sharnbrook during the latter part of this study.

Finally, I should like to thank the Science Research Council for the provision of a maintenance grant.

ABSTRACT

An introduction to the use of the empirical methods for the prediction of the molecular rotation $[M]$ and linkage rotation $[\Lambda]$ of carbohydrates is given. From knowledge of conformations the major factors determining the sign of the optical rotatory dispersion (o.r.d.) curves and the first circular dichroism (c.d.) band of unsubstituted sugars are considered. The o.r.d. and c.d. of polysaccharides and polysaccharide derivatives containing accessible chromophores are discussed.

In Section A of this Thesis the variation with temperature of the compensated molecular rotation (c.m.r.) of a series of monosaccharide methyl glycosides has been measured in water, dimethyl sulphoxide and dioxan and compared with Reeves' earlier measurements in N NaOH. The change in the c.m.r. values with temperature and solvent cannot be rationalised solely by changes in the conformational equilibria around the C(5) - C(6) and C(1) —— OCH_3 bonds. An explanation is given in terms of changes in the empirical parameters used to estimate monosaccharide molecular rotations. The change in the c.m.r. values on replacing water by any other simple solvent are greater than those observed on interchanging other simple solvents. A possible explanation for this is given in terms of the theoretical description of dilute aqueous solutions of simple carbohydrates.

The variation of $[\Lambda]_D$ with temperature has been measured for several disaccharides in the solvents mentioned. For α-linked disaccharides in water it is suggested that the molecules spend considerable time in "folded" conformations where the hydrophobic glucose surfaces are screened from solvent. This is not possible for β-linked disaccharides. The anomalous $[\Lambda_{obs}]_D$ for cyclohexaamylose

is explained by an "intramolecular inclusion complex" in which one linkage approaches a folded conformation. The consequences of these suggestions on the conformations of α-1,4-linked oligosaccharides and amylose are also discussed.

In Section B of this Thesis it is shown that c.d. has great scope for alginate characterisation. A rapid, sensitive, non-destructive method for the estimation of alginate composition is given. Moreover both guluronate and mannuronate residues can occur in the chains between two like or two unlike residues and this has predictable second order influences on the spectra. By mixing the "canonical spectra" of the three types of block found in alginates, using a computer, alginate spectra can be accurately reproduced giving a direct index of block structure.

Using calcium alginate as a model the use of c.d. to characterise the specific interactions between polysaccharide polyelectrolytes and inorganic cations has been explored. Alginate gelation has been studied by diffusing divalent metal ions directly into a c.d. cell filled with alginate solution. The striking spectral changes which occur elucidate the cooperative mechanism for the formation of the gel network by association of like regions of the chains into ordered bundles. An explicit chemical structure is also proposed for these "microcyrstallite" regions which is in very good agreement with other experimental evidence.

CONTENTS

GENERAL INTRODUCTION

GENERAL INTRODUCTION

The extraordinary sensitivity of the closely related chiroptical techniques of optical rotatory dispersion (o.r.d.) and circular dichroism (c.d.) to the 3-dimensional geometry of the molecules under observation makes them extremely valuable tools for gaining information about molecular structure and conformation. Unfortunately, although the theory is quite well understood in general terms, we do not yet have a detailed enough understanding to predict spectra from shape accurately, except in a few extremely limited cases, and must, therefore, rely on more empirical approaches. Such methods have been most widely used in chemistry of natural products, but although carbohydrates were to the fore in demonstrating their usefulness (Hudson 1909[1], Harris, Hirst and Wood 1934[2]) they have contributed little to the fundamental theory compared with recent developments in the steroid field. The main reasons for this are a scarcity of suitable chromophores in unsubstituted carbohydrates and the complexity of the stereochemical problem, due to possible interconversion between the less rigidly-defined carbohydrate conformations.

Both techniques give essentially the same information and examine the differences in the interaction of left and right circularly polarised light with the electrons of dissymmetric molecules[3,4]; optical rotation is a measure of different rates of propagation, while c.d. arises from differential absorption.

Optical Rotation at a Single Wavelength

The electric vector of plane-polarised light is composed of two electric vectors of equal amplitude (E_R and E_L), for right and left circularly polarised light, which make equal angles with the

axis of propagation (x). On passing through an optically active medium, light of one helical sense, E_L say, is slowed down relative to the other and on emerging the vectors no longer make the same angle with the x axis. This leads to rotation of the plane of the polarised light, as shown in fig. 1.

Optical rotations are generally measured in solution and the "specific rotation $[\alpha]$" of a compound is defined as

$$[\alpha]^{\text{Temp. of measurement}}_{\lambda,\ \text{wavelength of measurement}} = \frac{\alpha \times 100}{l \times c}$$

where α is the observed rotation, l is the length of the sample tube in decimetres and c is the concentration of the solution in g/100 ml. In quantitative comparisons of different compounds it is more convenient to use the "molecular rotation [M]";

$$\text{Molecular rotation } [M] = \frac{[\alpha] \times \text{mol. weight}}{100}$$

In some publications, however, particularly in carbohydrate chemistry, the product is not divided by 100.

Monosaccharides

The earliest and best known of the rules correlating optical rotation with carbohydrate configuration are Hudson's "rules of isorotation"[1]. They apply to derivatives of pyranose sugars and assume that the rotation of each anomeric form of corresponding derivatives is the sum of two independent contributions. Anomerisation causes the contribution which is characteristic of C(1) to be reversed in sign but does not change the contribution dependent on the configuration from C(2) onward. Quantitative values show that the rules hold for many aldohexose derivatives but for

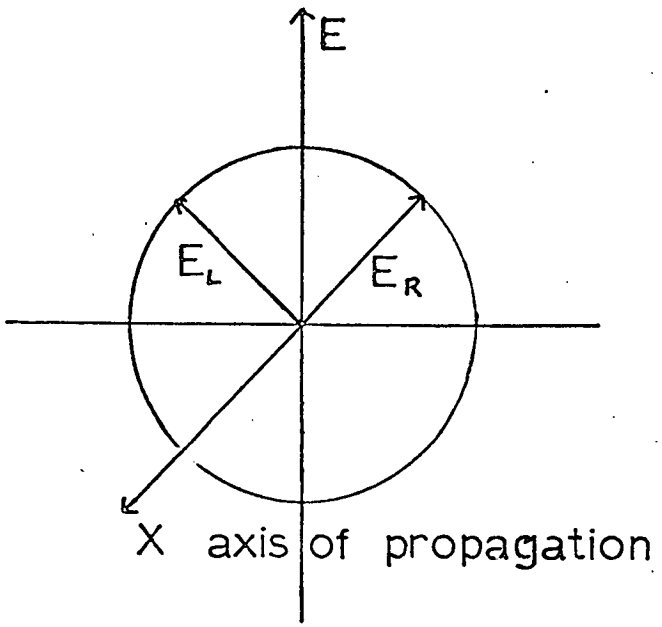

Fig. 1(a) Superposition of the electric vectors for left and right circularly polarised light before entering an optically active sample.

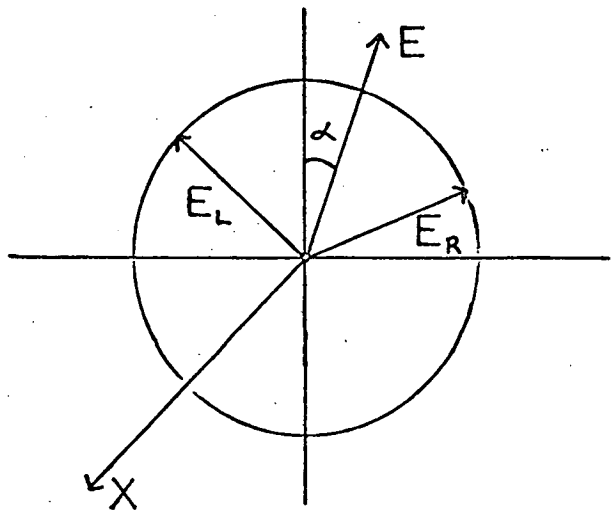

Fig. 1(b) Superposition on leaving the optically active sample; this shows the rotation of plane polarised light by delay of one circularly polarised component relative to the other.

sugars with an axial group at C(2) the values are constant but very different from those expected. This discrepancy has provoked much speculation but can be readily explained by later theories[5].

Kauzmann[6] recognised the fundamental unsoundness of the Van't Hoff superposition principle, and Hudson's rules which were derived from it, and pointed out that the quantum theories suggest that optical rotation is a result of the modification of electron motions by interactions between groups. The terms to be considered, in summing the interaction effects between groups, are of the type AB ("pairwise interactions"), ABC ("three-way interactions"), ABCD ("four-way interactions") and so on.

An important empirical development, which only considered one type of interaction, was made by Whiffen[7], who proposed that the observed rotation of a carbohydrate molecule could be regarded as the algebraic sum of partial rotatory contributions due to various conformational elements of assymmetry arising from chains of four atoms such as UC-CX (fig. 2). The value of these contributions would depend

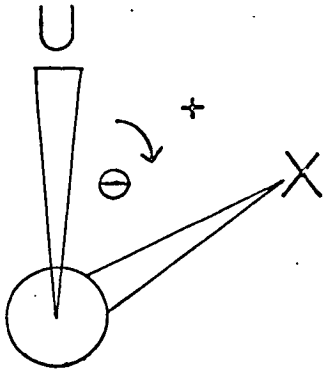

Fig. 2 Looking along the connecting carbon - carbon bond

on the size of the angle θ and was given by an expression of the type $\sum_{n=0}^{\infty} a_n \sin(\theta_n)$; but by the conformational assumptions made θ was restricted to $\pm \pi/3$ or π. Empirical values were assigned to combinations of these contributions which allowed a fairly accurate estimation of the net rotation of various cyclic sugars and cyclitols. The main features of this approach are given in more detail in Appendix I along with an example of its use in the calculation of monosaccharide molecular rotations.

This empirical approach was extended by Brewster[8] to apply to a wide range of cyclic and acyclic compounds. His hypothesis was that " a centre of optical activity can be described as an assymmetric screw pattern of polarisability" and it distinguished three different ways in which this could arise.

(a) "Atomic assymmetry" where if the sole source of assymmetry was the atom X in a compound X ABCD (fig. 3) the net rotation of a randomly oriented assembly of molecules would be dextro for the

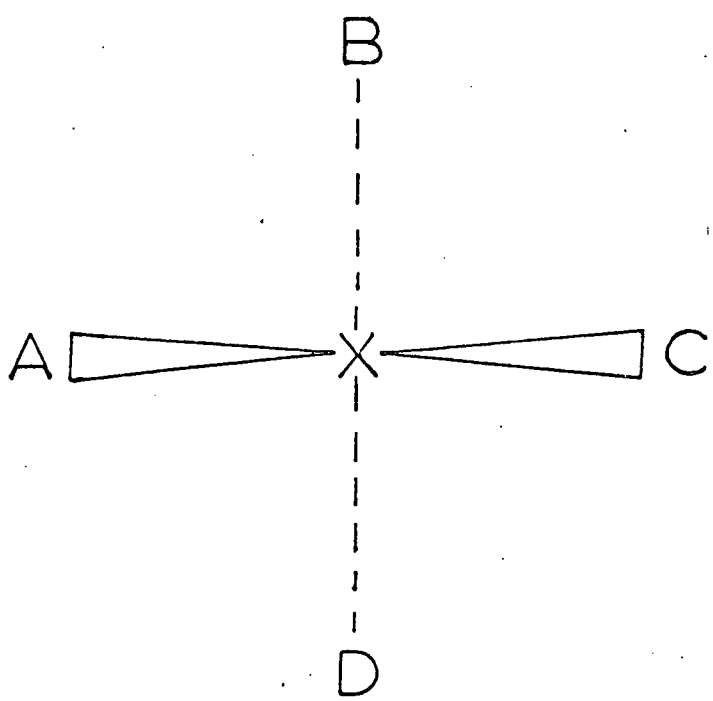

Fig. 3

configuration where the polarisability decreased in the order A > B > C > D. The earlier empirical rules of Marker[9] were equivalent to this assumption but such contributions were small and were more likely to apply under conditions where types (b) and (c) did not arise. For the determination of cyclic carbohydrate rotations Brewster neglected these contributions.

(b) "Conformational assymmetry" whose contributions to the optical rotation of a molecule were dealt with in a manner very similar to that of Whiffen except that more explicit rules were given for computing the magnitudes of the contributions by given pairs of groups.

(c) "Permolecular assymmetry" due to the inherent axis of polarisability, in a carbohydrate ring, which passes through the oxygen atom and C(3). The presence of dissimilar axial groups at C(1) and C(5) or at C(2) and C(4) would introduce a further axis of polarisability difference in each case which would form a screw pattern of polarisability with the axis of the ring.

In hexopyranose rings the rotational assymmetry of the hydroxymethyl group at C(5) necessitated a further empirical correction and also the large correction of 105° in molecular rotation was found for the rotational assymmetry of the glycosidic methyl group at C(1) (dextro for an α-D-form; levo for a β-D-form).

Brewster compared his own and Whiffen's calculated values, for carbohydrates and their derivatives, with the observed rotations and concluded that a wide range of constants could be employed when this series was considered alone. Although Whiffen's constants gave slightly more accurate results Brewster's values allowed the series to become part of a wide range of compounds where the application of these empirical methods can be usefully employed. Also in considering

permolecular effects Brewster's theory was more consistent with the observed origins of the contributions. Brewster's assumptions and values for his rotational constants are given in Appendix I and an example of the calculation of the molecular rotation of methyl-α-D-galactopyranoside is also given.

A more detailed evaluation of the possible application of pairwise interactions to the determinations of optical rotation and conformational analysis was carried out by Kauzmann and co-workers[10]. Also, good agreement was found, using the above methods, between calculated and experimental rotations for the conformationally unambiguous 1,6 anhydro-β-D-hexopyranosides and their derivatives[11]. Lemieux and Martin[12] simplified and reduced the number of empirical parameters required by Whiffen's theory to calculate optical rotations (Appendix I) and in addition combined n.m.r. spectral and optical rotatory data to study the effect of solvent environment on conformational equilibria[13,14]. This follows from the fact that if a molecule can exist in a number of different conformations each will make a discrete contribution to the overall spectrum. Changes in the populations of different conformational states with temperature or with change of solvent will be reflected by changes in chiroptical measurements. However, changes in the temperature and solvent also change the contribution to the optical rotation from direct spectroscopic perturbations, from solvent interactions and intramolecular hydrogen bonding. Although these are not large enough to obscure large conformational changes comparable with a change in conformation of the sugar ring, their magnitude, as shown in Section A of this thesis, can be comparable to that arising from changes in

the conformation of the C(1)-O-methyl or C(5) hydroxymethyl groups under the same conditions.

Di, Oligo and Polysaccharides

In more recent applications[15,16], Kauzmann's additivity principles for optical rotation coupled with Brewster's empirical treatment in terms of screw patterns of polarisation have been used to empirically relate the single-wavelength optical rotations, of di, oligo and polysaccharides, to their solution conformations at the glycosidic linkage in terms of the dihedral angles ϕ and ψ (fig. 4). The expressions are applicable to those di, oligo and polymers in which the sugar residues have the D configuration and can be fairly reliably predicted to be in the Reeves C(1) conformation.

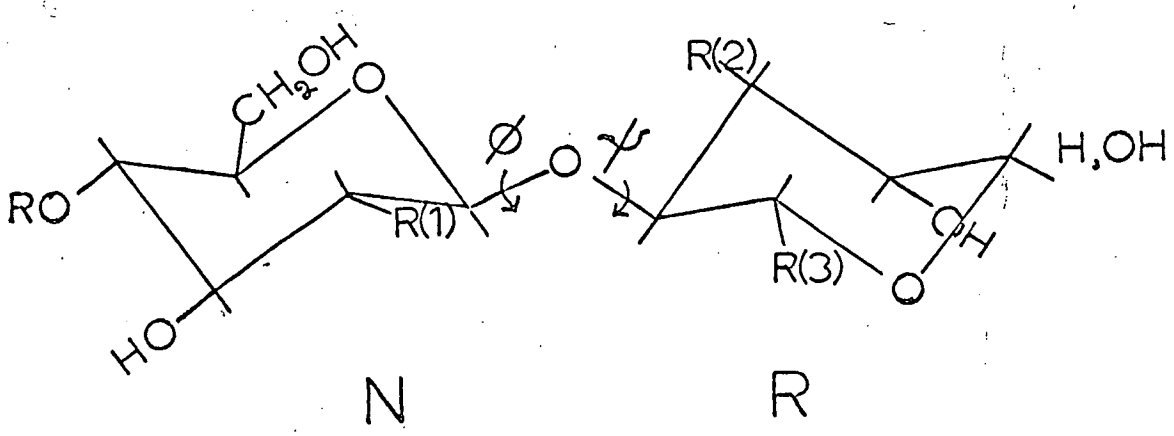

Fig. 4 The dihedral angles θ and ψ.

The linkage rotation $[\Lambda]$ for a given wavelength can be defined as;

$$[\Lambda] = [M_{NR}] - ([M_N] + [M_R]) \quad \text{-------(1)}$$

where $[M_{NR}]$ is the molecular rotation for a disaccharide containing a non-reducing (N) and a reducing (R) residue, $[M_N]$ the molecular rotation of the methyl glycoside of N and $[M_R]$ the molecular rotation of the reducing sugar R. For trial purposes the corresponding equations for the disaccharide glycosides can be used to avoid any error due to differences in the mutarotation equilibria of R and NR. The linkage rotation represents the optical rotation arising from interactions across the glycoside linkage minus any contributions to $[M_{ME-N}]$ and $[M_R]$ by interaction of the glycosidic methyl and the hydrogen atom lost from N and R, respectively, in the formation of the disaccharide NR.

The empirical treatment now makes the assumption that only interactions between bonded atoms will contribute to $[\Lambda]$ since spectroscopic perturbation of one residue by the other will tend to be quenched in polar, strongly hydrogen bonding solvents, such as water or dimethyl sulphoxide. Using Brewster's conformational asymmetry terms, the partial rotatory contributions from chains of bonded atoms, taken four at a time, will depend on the dihedral angle and will make positive contributions when the angle is as shown in fig. 2. For a 1,4 linkage for example the interaction C(2) - C(1) - O - C(4') makes the contribution

$$[\Phi_1]_D = \text{const} \times \sin\theta \qquad \text{- - - - - - - - - - (2)}$$

where the constant can be calculated from Brewster's conformation XLV[8] (fig. 5) as $105 \times 2/\sqrt{3} = 120^\circ$ for the sodium D line. Summing this plus the contributions from O(5) - C(1) - O - C(4'), C(1) - O - C(4') - C(5') and C(1) - O - C(4') - C(3') remembering to subtract the C_{methyl} - O - C(1) - O(5) and C_{methyl} - O - C(1) - C(2) gives an equation for $[\Lambda]$ of the form:

$$[\Lambda_{calc}]_D = A \pm 120 (\sin \Delta\phi + \sin \Delta\psi) \quad (3)$$

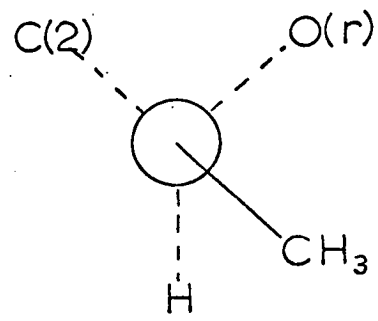

Fig. 5 Brewsters conformation XLV[8] which was assigned the empirical value of 105°.

The constant A has the value A = -105 for an α linkage and A = +105 for a β linkage since it is deduced from the C-methyl interactions. The dihedral angles, denoted $\Delta\phi$ and $\Delta\psi$ to avoid confusion with earlier computing conventions, are zero when the relevant C-H and C-O bonds are eclipsed.

The empirical relationship suggests that the observed linkage rotations will always be within the ranges quoted in table 1, but rarely approach the extremes because of the resulting steric compression. This reasoning is in excellent agreement with the observed values (table 1).

Table 1

$[\Lambda]_D$	β-linkages		α-linkages	
Calculated	-135	+345	-245	+135
Observed	- 41	+106	- 61	+ 83
	(42 observations)		(19 observations)	

Since the conformation is deduced in terms of two variables, and experimental measurement gives only one value, unambiguous interpretation is impossible. Calculation can show, however, that oligosaccharide crystal conformations, as might be reasonably expected, do not necessarily dominate in solution. The solution conformations suggested by n.m.r. and conformational analysis in terms of energy calculations can also be tested in this way. An example of these calculations is given in Appendix I and a more detailed discussion of the information which can be obtained using this approach is given in Chapter 2 of this thesis.

This study[16] also spectacularly demonstrates that internally consistent, rough predictions can be made about the average linkage conformations in solution by hard sphere map computer calculations. An increase in the number of accessible conformations results from the presence of smaller substituents next to the glycosidic oxygen. Also, for di-equatorial glycosidic linkages the numerically averaged values of $\Delta\phi$ and $\Delta\psi$ are almost independent; $\Delta\phi$ being determined by the nature of R_1, while R_2 and R_3 control $\Delta\psi$ (fig. 4). Therefore, on the basis of their conformational maps, glucosyl oligomers can be assigned the cellobiose $\Delta\phi$ value and that of lactose is applicable to the galactosyl homologues. When a large number of compounds are analysed in this way and their $\Delta\psi$ values calculated from equation 3 the results consistently demonstrate that:

(1) each group of compounds having similar substitution around the glycosidic oxygen shows only very small variations in this angle and that

(2) replacement of a substituent with a less bulky one causes this narrow range to shift in the direction expected from steric considerations.

The factors affecting $\Delta\phi$ and $\Delta\psi$ for α-linkages are less easy to separate but the same general picture is observed if it is assumed that, as in the β-series, $\Delta\phi$ is the same for related compounds. This assumption requires that for α-linkages, even in water, the exo-anomeric effect[13,17] overrides the steric clashes suggested by computer calculations and dominates the conformation around C(1).

In the case of 1,6 linkages there is a third angle of rotation ($\Delta\omega$) about C(5) - C(6). It is expected that $\Delta\phi$ and $\Delta\omega$ will have similar values to those in the isolated monomers and the remaining variable angle can be estimated directly from the relationship:

$$[\Lambda_{calc}]_D = 120 \sin \Delta\psi$$

Finally, perhaps the most dramatic illustration, in carbohydrate chemistry, of the usefulness of optical rotation measurements at a single wavelength is the demonstration[18,19] of the cooperative formation of double helices in solutions and gels of iota and kappa carrageenan. That this tertiary structure formation can cause multiple cross-linking and hence tangled networks has been demonstrated by controlled degradation and chemical modification[20] to give a sample which showed a clean coil to helix transition with a corresponding doubling of molecular weight[21]. A further confirmation of these results has been obtained by a simple extension[22] of the above methods. The linkage terms for the double helix are calculated from X-ray diffraction studies[23] for the solid state by substituting the values $\Delta\phi^{AB}$, $\Delta\psi^{AB}$, $\Delta\phi^{BA}$ and $\Delta\psi^{BA}$ for the alternating carrageenan structure (fig. 6) into equation 3. For the random coil the conformational terms are assumed to be the same as in the corresponding

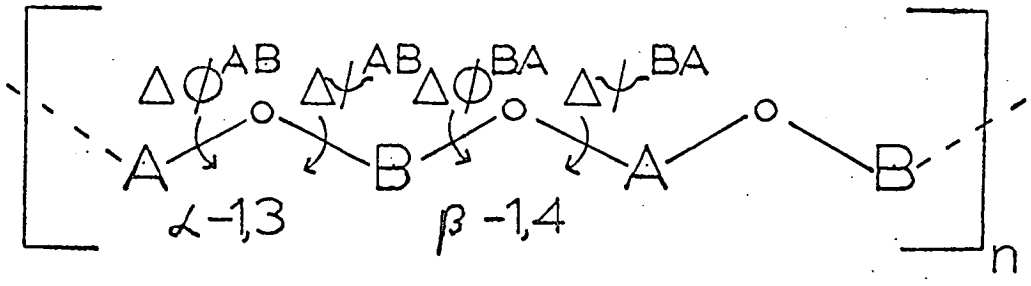

Fig. 6 Schematic representation of the alternating structure for carrageenan

disaccharides. When these calculated values are compared with measured values for the solution in which the transition occurs excellent agreement is obtained.

More recent work[19,24] using these optical rotation methods has shown the first example of polysaccharide quaternary structure. This is the cooperative association of unlike polysaccharide chains in the binding of polysaccharide helices to galactomannans. Moreover this binding of galactomannan stabilises the helix under conditions where it is not stable alone and thus represents a ligand induced change of polysaccharide conformation.

All the above empirical treatments are only applicable for compounds which do not have chromophores which absorb in the near u.v., so that direct spectroscopic perturbations, from solvent interactions or intra-molecular hydrogen bonding, do not have large enough contributions to affect those from which the relationships are derived. Where such chromophores are present,

however, secondary influences on them may swamp the far u.v. conformational contributions and the relationships should only be applied along with studies of the Cotton effects due to these chromophores.

O.R.D. and C.D.

If the specific rotation (or [M]) is measured as a function of wavelength, then greater absolute values are generally obtained at shorter wavelengths. This is a result of the usual form of the "plain curve" and we can use this, in spectral regions remote from an absorption band to estimate the position of its maximum absorption by making use of the Drude[25] equation.

In the region of an absorption band, left and right handed circularly polarised light are not only propagated with different velocities, in chiral molecules, but are also absorbed to different extents. Thus the lengths of the two vectors E_R and E_L are now different, after passing through the optically active medium, and the emergent wave is no longer truly plane polarised; in fact the point of the resultant electric vector describes an ellipse as shown in Fig. 7. The plane of polarisation is now defined by the major axis of this ellipse and the minor axis provides a measure of the c.d. The angle θ is known as the "ellipticity" but for meaningful comparisons of the c.d. of various samples the "molecular ellipticity" $[\theta]$ may be employed where;

$$[\theta] = \frac{\theta \times \text{mol. weight (g)}}{l \times c} \quad \text{degree cm}^2/\text{decimole}$$

and l is the pathlength (mm) of the sample cell; c is the concentration of the solution (g/cm^3).

Due to this differential absorption an s-shaped component is superimposed on the plain o.r.d. curve. A curve of this type is

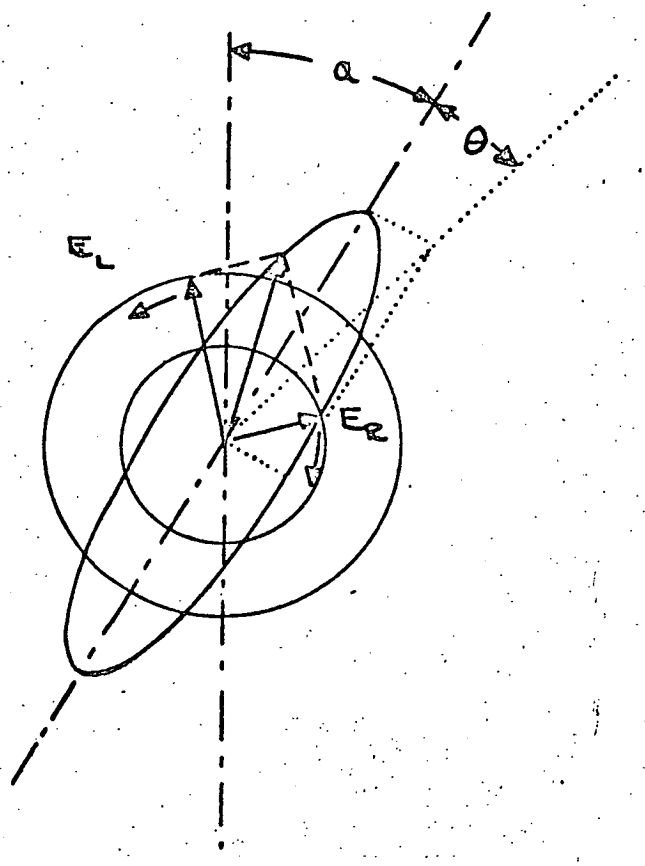

Fig. 7 Effect of an optically active absorbing sample on plane polarised light.

Optical rotation - α

Circular dichroism - θ

described as "anomalous o.r.d." and both effects, c.d. and anomalous o.r.d., are known as the "Cotton effect". Because of the common physical origin of the chiroptical methods, if either of the two curves is known over the entire spectral range, the other can be calculated using the Kronig-Kramer's transform equations[4]. For an isolated chromophore the c.d. and o.r.d. bands have the form shown in fig. 8. Since c.d. is an absorption phenomenon, the band is bell shaped, as in u.v., but may be either positive or negative depending on whether the dissymmetric system absorbs left or right circularly polarised light more strongly. While c.d. drops off rapidly, and only has non negligible values at wavelengths restricted to the immediate region about λ_{max}, the optical rotation remains significant even at wavelengths remote from the absorption band. This has the advantage of allowing o.r.d. to be used even when there is no absorption in the accessible region because of the still appreciable contribution from groups which absorb in the far u.v. Indeed the previously discussed empirical theories based on rotations at a single wavelength essentially make greatly simplifying assumptions concerning what will give rise to relevant absorption bands since, formally, the optical rotation at any wavelength can be regarded as the algebraic sum of the contributions due to the various optically active bands. However, the disadvantage is always present in o.r.d. that resolution of the spectra from different chromophores is much more difficult than for c.d. because of these appreciable "background" rotations, along with the inherently more complex shape of the o.r.d. band.

Early c.d. measurements were usually obtained by the modification of spectropolarimeters and, consequently, looked at the ellipticity

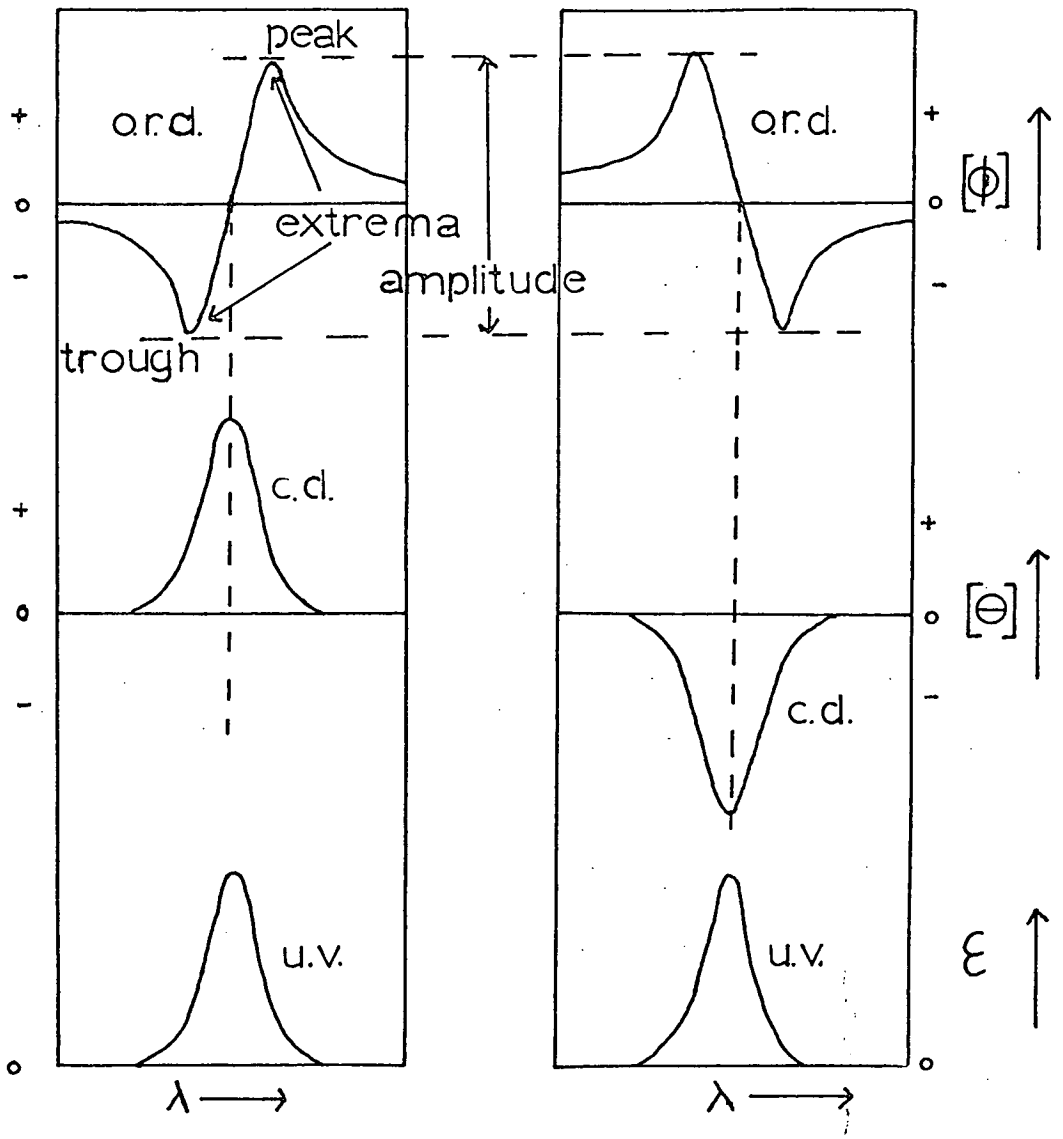

Fig. 8 Idealised u.v., c.d. and o.r.d. spectra for an isolated chromophore.

Left: dextrorotatory molecule: positive Cotton effect.

Right: laevorotatory molecule: negative Cotton effect.

of the emergent light. This is extremely susceptible to cell strain and light scattering artefacts, causing c.d. to be overshadowed by o.r.d. until the development[3], in the early 1960's, of new commercial instruments. These measure directly the difference in absorption of right and left circularly polarised light and have led to the rapid development of this potentially superior technique.

Plain Curves

When an electron moves from its initial energy state to a state of higher energy by absorbing light, the wavelength required for most electrons in an organic molecule is shorter than the minimum obtainable with present instruments (around 185 nm). In particular this is true of the electrons of the saturated bonds of the ring forms of carbohydrates and the absence of any discernible Cotton effect in the region of carbonyl absorption ($\sim$ 290 nm) confirms that only tiny amounts of open chain forms are present under equilibrium conditions. In unsubstituted carbohydrates, of the chromophores responsible for optical rotation, the ring oxygen and methoxyl absorb below 180 nm while the hydroxyl group absorption occurs near 150 nm. In the accessible region below 200 nm, unsubstituted monosaccharides show the onset of a dichroism band[26] attributable to light absorption by the ring oxygen; the sign and magnitude of this band are determined by the stereochemical arrangement of groups around the ring oxygen. It has been demonstrated[27,27a] that, although the sign of the o.r.d. curve is significantly influenced by the configuration at the anomeric carbon atom, the major effect in determining the sign of the first c.d. band is the introduction of a new axis of polarisability difference in the molecule due to the replacement of the equatorial hydroxyl at C(2) or C(4) with an axial one (c.f. Brewster's permolecular

effect). Another important factor is perhaps the influence of the C(4) configuration on the conformation of the freely rotating hydroxy methyl group at C(5).

Similarly in the plain o.r.d. curves[27], although the data express the contributions of all asymmetric centres, as the far u.v. transitions of the ring oxygen are approached, their contributions reach a maximum and become dominant in relation to the contributions from other optically active bands. Table 2 summarises the direction of rotatory contributions of individual asymmetric configurations, in the D-pyranose series, in the accessible region below 210 nm and in the visible region.

Table 2

Configuration about	C1 Conformation		1C Conformation	
Carbon No.	600–250nm	Below 210nm	600–250nm	Below 210nm
1(a) a in C1 conformation	+	+	−	−
1(e) a in 1C conformation	−	−	+	+
2(a)	−	+	+	−
2(e)	+	−	−	+
3(a)	−	−	+	+
4(a)	+	−	−	+
5(e) with 4(e)	+	+	−	−
5(e) with 4(a) and 1(a)	+	−	−	+
5(e) with 4(a) and 1(e)	−	−	+	+

(a) and (e) denote axial and equatorial substituents respectively.

The magnitude of the C(3) configurational contribution is smaller than the rest, as expected since it lies on the existing axis of polarisability of the ring. The results also indicate that interactions between a bulky substituent and a neighbouring group

may affect the optical rotation, a possibility that is not always considered in the single wavelength calculations.

Cotton Effect Curves

Although most unsubstituted carbohydrates show only plain curves and the onset of dichroic bands, electronic systems which have a smaller difference in energy between their initial and excited states will absorb light of longer wavelengths. The transition most studied by the chiroptical techniques is the ketone $n \longrightarrow \pi^*$ transition in which a non bonding electron on the oxygen atom is promoted to a higher energy anti-bonding orbital of the carbonyl group[25,28,29].

For a number of chromophores, the effect of the spatial distribution of other atoms or groups on optical activity has been systematised into rules. The best known of these are the carbonyl octant rule[25], which has greatly simplified the use of chiroptical methods in the determination of steroid ketone stereochemistry, and the peptide quadrant rule[29], which has helped the development of the techniques to the point where spectra from the helix, pleated sheet and random coil conformations of polypeptides can be interpreted qualitatively. In favourable cases protein spectra can also be matched quantitatively by mixtures of these three extremes[30].

Unfortunately in carbohydrate chemistry these better understood chromophores are seldom encountered, although similar transitions are exhibited by the carboxyl, amide and acetyl groups present in some naturally occurring plant and animal polysaccharides. If an accessible derivative is not present in the carbohydrates, suitable derivatives may, of course, be prepared by substitution of the hydroxyl groups on the sugar residues, but this could

substantially alter the preferred conformation. A recent review of polysaccharide c.d. has been made by Morris and Sanderson[31].

Polysaccharides Containing Accessible Chromophores

Polysaccharides in this category are most responsive to the chiroptical methods because they contain sugar residues which possess an accessible optically active chromophore. The individual monomeric residues of the polymers have been extensively studied to gain an insight into the spectral behaviour of the natural material.

(a) Acidic Sugars: Chiroptical studies of the uronic acids[32,33] show a main Cotton effect around 210 nm typical of the carboxyl $n \rightarrow \pi^*$ transition. An interesting small negative band, which has been attributed to an identical transition for a particular conformation or solvation state, also appears at higher wavelength for uronosides possessing an equatorial hydroxyl group at C(4). This is not observed for the corresponding methyl glycosides which have an axial hydroxyl at C(4). It has been suggested[33] that a hydrogen bonded, stabilised conformation of the carboxyl group is possible, for equatorial C(4) hydroxyl groups, in which the chromophore and the ring oxygen lie in the same plane and allow the stabilisation of the excited state by conjugation with the non-bonding electrons of the ring oxygen. This would reduce the energy required for the transition and account for the observed, small longer wavelength band. The corresponding stabilised conformation of this type is impossible for an axial hydroxyl group at C(4) since it does not have the chromophore aligned in this way. This agrees with the absence of the lower energy transition when the C(4) hydroxyl is axial. Support for this interpretation[32] comes from the relative increases in the size of the longer wavelength band in non polar solvents where there

will be increased intramolecular hydrogen bonding.

The recent study[33] also demonstrates that methyl-β-D-mannuronoside and methyl-α-L-guluronoside give spectra which are completely different. This suggests that the structure of the commercially important, seaweed polysaccharide alginic acid may be determined by an application of the chiroptical methods and the successful investigation of this direct, rapid index of composition is described in Chapter 3 of this thesis. In Chapter 4 is described the application of c.d. to the study of alginate gelation, by diffusing calcium ions directly into a cell filled with sodium alginate solution. The striking spectral changes which occur have led to the elucidation of the cooperative mechanism[34] for the formation of the gel network by association of like regions of the molecular chains into ordered bundles. An explicit chemical structure is also proposed for these "microcrystallite" regions which is in very good agreement with other experimental evidence.

These chiroptical studies may also be applied to pectin, a 1,4 linked poly-α-D-galactopyranosyl uronic acid similar to alginate but complicated by the presence of high (70%) or low (30%) degrees of methyl esterification along with neutral sugars, which occur either as side chains[34] or as "kinks"[35] in the main chain. Esterification appreciably affects the position of the c.d. peak[36] and the calcium gelation of low methoxy pectin can also be monitored as for alginates and a similar mechanism postulated. The gelation of high methoxy pectin requires the pH to be low and sucrose or sorbitol must be added to depress the activity of the water. The gels are formed by cooling heated pectin solutions, which satisfy the above conditions, in a c.d. cell and this results in a large increase in the spectrum

intensity, without altering its shape or position[36]. Although a very small increase is observed on cooling such solutions under non-gelling conditions, the c.d. indicates, as expected, a different gelation mechanism from that of the low-methoxy calcium gels. This is believed to take place by the association of regions of uronic ester, with the possible incorporation of occasional acidic residues since these occupy no more space than the ester and are also electrostatically neutral[34].

(b) 2-Deoxy-2-Acetamido Sugars: Replacement of the C(2) hydroxyl group of a sugar residue by an acetamido group occurs in many biologically important macromolecules and monomeric studies have shown[37] that substitution of an equatorial acetamido group leads to a negative c.d. band centred around 210 nm. The corresponding axial chromophore gives a smaller positive band at the same wavelength. The spectrum of N-acetyl-D-glucosamine together with that of muramic acid have been combined to show that the separation and freedom of

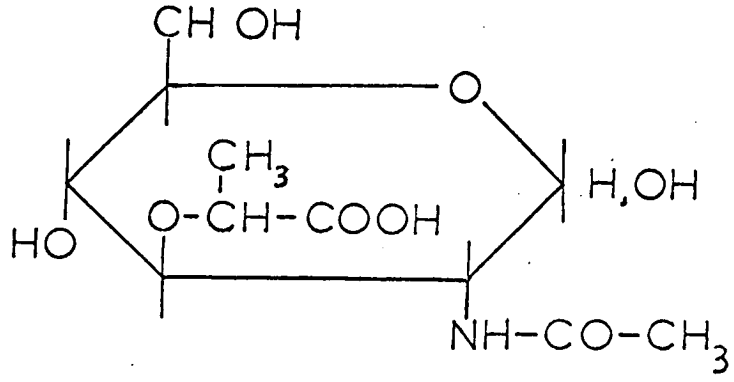

Fig. 9 N-acetyl-muramic acid

rotation of these chromophores in N-acetyl-muramic acid (fig. 9)[38] leads to very little interaction between them and each essentially

experiences the same electrostatic environment as in their monosubstituted sugars. From this has been deduced the N-acetyl muramic acid conformation which will be an important factor in the determination of the precise shape and function of bacterial cell wall, peptidoglycan networks, since it is a major component of the peptidoglycan.

Probably the most important group of polysaccharides containing acetamido chromophores are the mucopolysaccharides which, after extensive structural studies[39], have been shown to have the characteristic disaccharide repeats shown in table 3. Stone[40] has extensively examined the chiroptical effects, in these polysaccharides, arising from the electronic transitions of the acetamido and carboxyl groups in the sugar residues and these are shown in fig. 10. The magnitude of the 208 nm negative band, present in all the spectra, varies in magnitude and all also show other distinctive features. Dermatan sulphate (D S) shows an additional c.d. minimum around 190 nm and hyaluronic acid (HA) and the chondroitin 4 (CH-4-S) and 6 (CH-6-S) sulphates show the beginning of this negative band. In contrast heparin (H), heparitin sulphate (HS) and keratan sulphate (KS) show an additional positive band centred near 190 nm in addition to the 208 band. Thus the c.d. spectra define two broad groups correlating with the polysaccharide structural types, namely those containing a 1,3 linked acetamido sugar (HA, CH-4-S, CH-6-S, DS) on the one hand and those containing a 1,4 linked acetamido residue (H, HS, KS) on the other. From the monosaccharide c.d., the higher intensity of the N-acetyl chromophore $n \longrightarrow \pi^*$ transition at around 210-215 nm will make it the predominating influence on the spectra, although this will be modified by the influence of the corresponding carboxyl transition which

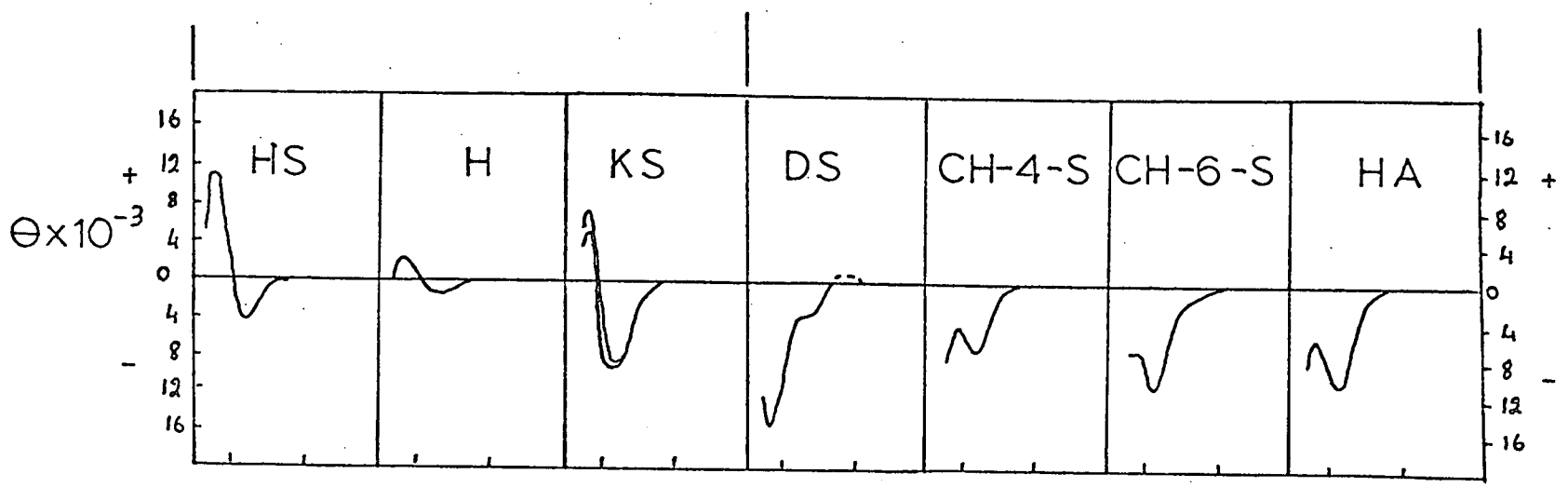

Fig. 10 c.d. spectra of the mucopolysaccharides

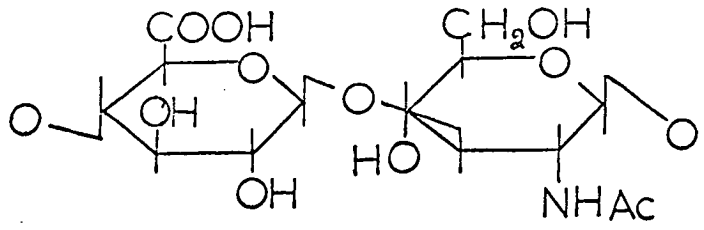

Hyaluronic acid

H A

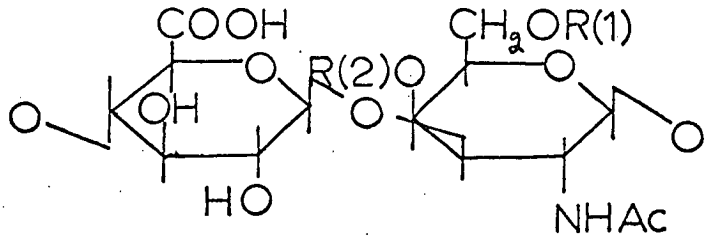

CHondroitin-6-sulphate

CH-6-S

R(1) = SO_3^- R(2) = H

CHondroitin-4-sulphate

CH-4-S

R(1) = H R(2) = SO_3^-

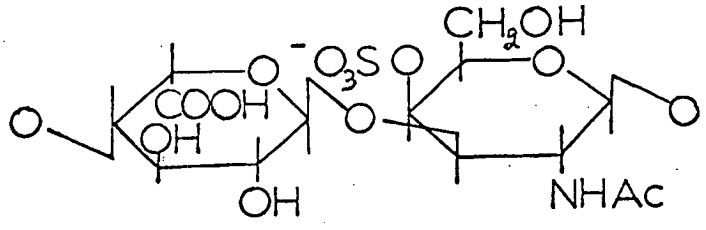

Dermatan sulphate

D S

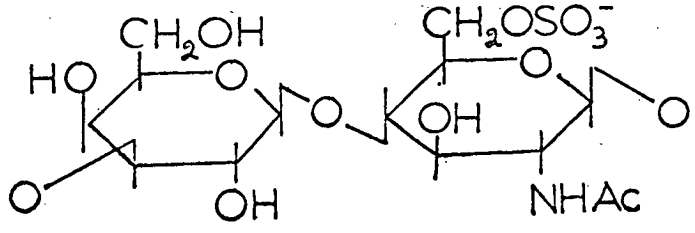

Keratan sulphate

K S

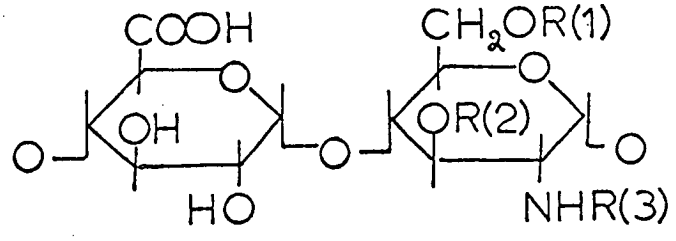

Heparin H

R(1) = R(2) = H

R(3) = Ac or SO_3^-

Heparitin sulphate H S

R(1) = R(2) = SO_3^-

R(3) = Ac or SO_3^-

Table 3. Basic idealised disaccharide repeat units of the mucopolysaccharides.

also takes place in this region.

The mucopolysaccharide chiroptical spectra depend on the local environment of the chromophore and hence on the structure around the group and the overall polysaccharide conformations which are, in turn, determined by the anomeric configurations and linkage positions of the individual sugar residues, along with their particular ring conformations. D-Glucuronic acid, N-acetyl-D-glucosamine and N-acetyl-D-galactosamine exist in the C1 conformation and examination of the disaccharide repeat units in table 3 shows that HA, CH-4-S and CH-6-S are likely to have similar conformations. DS would, however, be expected to have a different conformation, because of the presence of the L-iduronic acid residues, which have been shown[41] to prefer the alternative 1C conformation, and this is borne out by its slightly different c.d. spectrum. However, the chondroitins and dermatan sulphate are probably idealised extremes of a spectrum of closely related structures differing in sulphate content and the nature of the uronic acid group since dermatan sulphates, from different sources, may contain significant amounts of D-glucuronic acid as well as L-iduronic acid[42]. It has already been shown in heparin that although the drawn disaccharide repeat is a significant structural feature the main uronic acid residue is the α-linked L-iduronic acid[43,44] in the 1C conformation and this residue is also partly sulphated.

Further studies into the structural and conformational aspects of these molecules would be useful and c.d. could play a significant part in these, since it is non-destructive and requires only small amounts of material. The use of c.d., coupled with a mild method for the removal of N-acetyl groups and the existing mild method for sulphate

removal[45], could indicate the effect of these on the polysaccharide solution conformations. Moreover, the study of de-N-acetylated mucopolysaccharides, from different sources, might clarify the possibility of differences in uronic acid composition in addition to those found for heparin.

Polysaccharide Derivatives

It is unfortunate that most polysaccharides, unlike those above, do not possess a chiroptically accessible chromophore. Substitution of the hydroxyl groups on the sugar residues, with suitable derivatives such as acetates, carbanilates and xanthates can overcome this difficulty but it must always be remembered that this may have a large effect on the preferred solution conformations of the polymers.

The carbanilates of β-1,4 and α-1,4 linked glycans have been studied, comparatively, by Bittiger and Keilich[46], emphasising cellulose and amylose in particular, along with their corresponding disaccharide building units. Very recently, the corresponding acetates and xanthates of these polymers, plus dextran have been similarly compared[47,48]. The conclusions drawn were very similar and are summarised below. In all cases the advantage of c.d. over o.r.d., for examining single chromophores, was evident.

(a) α-1,6 Linkages: From the symmetry and position of the ellipticity maxima in the c.d. spectra of the dextran acetate series[48], a completely random solution conformation is indicated, as might have been expected from the flexibility conferred on the oligomers, by the presence of the extra bond in these linkages.

(b) β-1,4 Linkages: Both types of derivative[46,47] spectra show a simple negative Cotton effect for cellulose and its related oligo-

saccharides and the position and symmetry of the transition is similar for the xylan series. Thus there is no evidence for preferred conformations in solution. This is in agreement with the rotational flexibility available to both the parent dimers (cellobiose and xylobiose)[49], even in the presence of acetate groups[47], as shown by conformational analyses.

(c) α-1,4 Linkages: The c.d. spectra of the acetates of amylose and its oligomers[48] show completely different features from those above. Glucose penta-acetate and β-maltose octa-acetate give simple positive c.d. spectra but for maltotriose hendeca-acetate the positive c.d. maximum is shifted to longer wavelength and a more pronounced negative band appears. Amylose tri-acetate gives a similar spectrum and a similar type of behaviour is observed for the α-glycan carbanilate derivatives[46]. These dramatic spectral changes have been attributed to interaction of the acetate and carbanilate groups, of the type that may be present in helical systems. In such an arrangement interaction of the chromophores results in an exciton type splitting of the c.d. band associated with transitions such as the carbonyl $\pi \longrightarrow \pi^*$. Thus the negative band in the acetate symmetric exciton spectrum appears in the low wavelength region accessible to the instrument, partly obscuring the weaker $n \longrightarrow \pi^*$ band and apparently shifting its maximum to longer wavelengths.

The interpretation of this splitting as indicative of long-range helical ordering must, however, be questioned, since Nakanishi and his co-workers[50,51] have shown that such an effect can be caused by chromophores suitably arranged in pairs. Thus for vicinal bis p-chlorobenzoates on sugar residues[51], an antiparallel arrangement of the two groups gives rise to a single Cotton effect whereas, when they are gauche-disposed the two groups interact to give a split

pattern in the c.d.; the two maxima of opposite sign being situated on either side of the normal absorption maximum. The signs of the maxima are related to the chirality of the screw pattern defined by the two aroyloxy groups on looking along the connecting C–C bond (c.f. Brewster's conformational assymmetry) and quantitative variations in intensities are extremely sensitive to minor deviations in the dihedral angle between the aroyloxy groups.

SECTION A

MEASUREMENTS OF OPTICAL ROTATION AT A SINGLE WAVELENGTH

CHAPTER 1

THE INFLUENCE OF SOLVENT AND TEMPERATURE ON THE OPTICAL ROTATION OF MONOSACCHARIDES IN THE PYRANOSE RING FORM

INTRODUCTION

A comprehensive understanding of the ordered structures of polysaccharides and their biological function requires a detailed knowledge of the conformations adopted by their constituent sugar units. Similarly, to make full use of single wavelength measurements of optical rotation in studies of these structures by the methods described in the General Introduction, one needs to know the influence of solvent and temperature on the optical rotations of the monosaccharide units which make up the polymers. The studies described here were made on the methyl pyranosides since the mutarotation of the unsubstituted monosaccharides are affected by the temperature and the nature of the solvent, and this will complicate the changes in optical rotation.

The conformational analysis of the pyranose ring forms of carbohydrate monomers is based on the principles established for cyclohexane[10] since only slight changes in the ring geometry will be caused by the substitution of two slightly shorter carbon-oxygen bonds. The conclusion[52] that the "chair" shape is thermodynamically more stable than either the "boat" or the more flexible "skew boat" form was experimentally justified by the pioneering work of Reeves[53]. He used the previously determined, stereochemical requirements for the formation of a complex between cuprammonium reagent and two hydroxyls on a pyranose ring to determine the predominant solution conformations of many methyl pyranosides.

Most of Reeves' assignments have been confirmed by later physical measurements[54], in particular by nuclear magnetic resonance spectroscopy (n.m.r.) which can be used, in favourable cases, to determine the composition of the solution and the conformation of each component. This information may be obtained by consideration of the two kinds of data provided by n.m.r.

(a) Studies of the relationship between the chemical shift of a proton and its environment[55] have shown that the anomeric hydrogen atom, being on a carbon atom attached to two oxygen atoms, is strongly deshielded and usually resonates at a lower field than other protons. Also axially attached protons usually resonate at higher field than equatorial protons in chemically similar environments.

(b) The vicinal spin-spin coupling constants have been shown[55] to vary with the dihedral angle and Karplus[56] rationalised this using the relationship:

$$J = J_o \cos^2 \Phi + K$$

where J is the coupling constant between two hydrogen atoms attached to neighbouring carbon atoms at a dihedral angle of Φ and J_o and K are constants. Although this simplified equation does not take account of the nature and exact geometrical relationship of the substituents[57], it can often distinguish between two possible conformations e.g. trans diaxial (7-10 Hz) and trans diequatorial (2-4 Hz) hydroxyl groups in a pyranose ring.

The conformations of aldohexopyranoses in solution are determined mainly by the tendency of the bulky hydroxymethyl group at C(5) to assume an equatorial orientation. Hence all β-D-anomers exist predominantly in the Reeves' C1 chair ring form[53] because the alternative 1C form is highly destabilised by the repulsive interactions

between syn-diaxial hydroxymethyl and anomeric hydroxyl groups. These steric interactions are not present for α-D 1C ring conformations but most of these also adopt the C1 conformation. The formation of the methyl glycosides of the sugars, by increasing both the repulsive interactions involving the C(1) substituent and the anomeric effect, will increase this relative stability of the C1 form over the alternative 1C form. In the absence of a hydroxymethyl at C(5) the conformations of the aldopentopyranoses are governed by the relative configurations of the hydroxyl groups. Thus α and β-D-arabinopyranoses favour the 1C conformation, α-D-lyxopyranose and α-D-ribopyranose are each conformational mixtures and the other aldopentopyranoses are predominantly in the C1 ring form.

Although the precise calculation of the relative free-energy of each conformation is not possible, approximate calculations are extremely useful in the prediction of the preferred ring conformation. All of these assume that the free energies of conformational isomers are additive functions of the energy terms arising from non-bonded interactions and that interactions of this type do not distort the shape of the ring. The most quantitative of these has been proposed by Angyal[58] and considers not only interactions between axial groups but also gauche interactions between groups attached to contiguous carbon atoms, along with a contribution from the "anomeric effect". The values used for the non-bonded interactions were determined, in aqueous solution at room temperature, from the equilibria of cyclitols with their borate complexes[59] and from the anomeric equilibria of the pyranose ring forms of sugars[58,59,60].

Anomeric Effect

Apart from the steric interaction energies another factor must

be considered in the calculation of the relative free energies of pyranoses. Most 1-substituted derivatives of α-D-glucopyranose (and many other sugars) are more stable than the corresponding β-D-anomers, although the former has the substituent at C(1) axially attached. This predisposition of a polar substituent to assume an axial orientation contrary to pure steric considerations was first referred to by Edward[61] and was named the "anomeric effect" by Lemieux[62]. This phenomenon was attributed[61] to an unfavourable dipole-dipole interaction between the carbon-oxygen bonds and the bond from the anomeric carbon atom to the equatorial substituent since these dipoles form a small angle when the substituent is equatorial but a large one when it is axial (fig. 1.1). This explanation has been extended[62,63,64] and the effect attributed

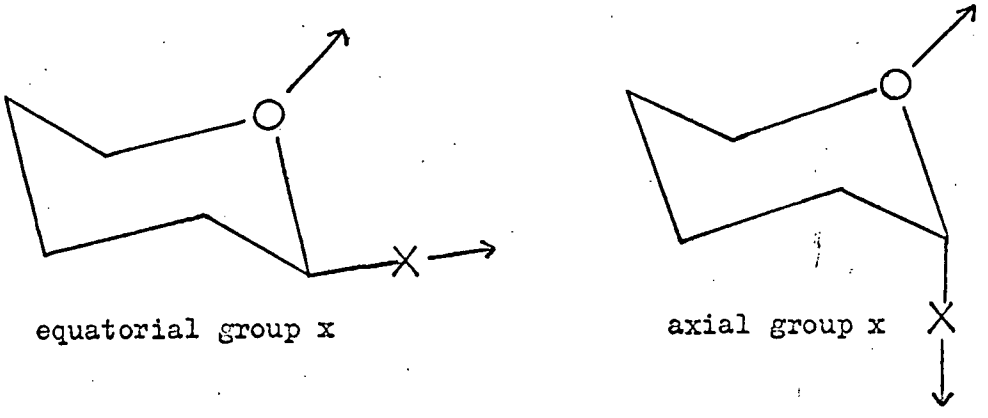

Fig. 1.1

to the tendency of the molecule to adopt that conformation which minimises the number of repulsive interactions between opposing unshared pairs of electrons on the ring oxygen and the aglycone X. In accordance with these theories the magnitude of the anomeric effect

decreases as the polarity of the solvent increases, although Lemieux has suggested[64] that hydrogen bonding of the solvent with the acetal oxygen atoms has a more pronounced effect. Also the anomeric effect is greatest when the effective charge density on the C(1) substituent is high[65].

More recent theoretical considerations[66] show that the anomeric effect represents the balance between attractive and repulsive dominant interactions and suggest that the attractive make the greater contributions. This would indicate that the anomeric effect does not increase the free energy of the anomer with the equatorial anomeric group, by dipole repulsion, but actually decreases, by dipole attraction, the free energy of the axial anomer. The ^{13}C chemical shift data for sugars and their methyl glycosides appear[67] to be consistent with this hypothesis.

The evaluation of the anomeric effect is the least satisfactory part of the free energy calculations because it varies considerably not only with the nature of the solvent but also with the presence and configuration of substituents in other parts of the pyranose molecule. Thus a value of 0.55 k cal mole^{-1} must be attributed[58] to the anomeric effect when the hydroxyl group on C(2) is equatorial but an increased value of 1.0 k cal mole^{-1} must be taken when this hydroxyl is axial and a value of 0.85 k cal mole^{-1} is attributed to the effect when there is no substituent on C(2). The anomeric effect has also been shown[68] to increase with the extent of methylation of the hydroxyl groups. At equilibrium in aqueous solution, D-mannose contains 67% of the α-pyranose form, 2-O-methyl-D-mannose 75%, 2,3 di-O-methyl-D-mannose 80% and 2,3,4,6-tetra-O-methyl-D-mannose 86%. Perlin[68] has also shown that a similar change

(67 - 86%) takes place for D-mannose on changing the solvent from water to dimethyl sulphoxide although no such change is observed for D-glucose. For D-galactose the main effect of this change of solvent is a large increase in the proportion of the furanose ring forms in the equilibrium mixture. Similar effects are observed[68] for the equilibria of the methyl pentosides in methanol[69] and any explanation of these effects must involve not only the increased anomeric effect in less polar solvents but also specific solvent effects by water which favour the pyranose ring forms, and in particular those with equatorial anomeric substituents, over the furanose ring forms.

EXPERIMENTAL

1. Preparation of Samples

Methyl α-D-glucopyranoside, methyl β-D-glucopyranoside, methyl α-D-mannopyranoside and methyl β-D-galactopyranoside were all samples obtained from a commercial source (Koch-Light, Colnbrook, Bucks, England). Methyl β-L-arabinopyranoside was a sample previously prepared at Edinburgh University. These samples were recrystallised twice from ethanol and possessed melting points and specific rotations in close agreement with those in the literature.

The styracitol (1,5 anhydro mannitol) was a gift from Dr J.C.P. Schwarz of the University of Edinburgh and had a melting point and specific rotation very close to the literature value. This sample was used without recrystallisation.

1(a) Preparation of Anhydrous Methyl α-D-Galactopyranoside

Methyl α-D-galactopyranoside monohydrate was purchased from Koch-Light and had m.p. 82-85°C: lit. m.p. for the monohydrate 111°C (Micheel[70]).

The crystals were dissolved in ethanol, a small volume of benzene added and the solvent removed using a rotary evaporator. This was repeated twice and was followed by twice repeating the process using ethanol alone. The sample was recrystallised from ethanol, dried overnight in a vacuum desiccator and stored tightly sealed: m.p. 117-119°C: lit. m.p. for the anhydrous form 114-116°C (Micheel).

1(b) Preparation of Methyl 3,6 Anhydro α-D-Galactopyranoside

This was prepared from a previously made sample of methyl 6-O-toluene-p-sulphonyl-α-D-galactopyranoside[71] using the method of Haworth, Jackson and Smith[72] and had m.p. 137-141°C: lit. m.p. 140°C (Micheel).

1(c) Preparation of Methyl α and β-D-Xylopyranoside by a Fischer Synthesis

Acetyl chloride (4 ml) was added dropwise to anhydrous methanol (200 ml) to give a 1% solution of hydrogen chloride in methanol. D-Xylose (20 g) was boiled under reflux with this solution for six hours and then the acid neutralised overnight with silver carbonate. The solution was decolourised by filtration through a pad of active charcoal and concentrated to a thick syrup. Paper chromatography, using double development with solvent (b) and detection using the periodatocuprate spray, showed the presence of three spots one of which was undetected xylose.

1(d) Preparation of Methyl β-D-Xylopyranoside by Fractional Precipitation

Ethyl acetate was carefully added to the syrup and a white oily semi-solid separated out which was filtered off. This was the methyl β-D-xylopyranoside and it was crystallised by a careful precipitation from ethanol using ethyl acetate. The crystals had m.p. 150-158°C and two recrystallisations from ethanol did not improve this.

A column of Dowex 1 anion exchange resin, in the hydroxide form, was prepared as described in the General Methods section. The crude methyl β-D-xylopyranoside (1.5 g) was dissolved in water (5 ml) and carefully put on to the column using a pipette. This was run on to the column and washed in with a further 5 ml of water added in the same way. The column was eluted with carbon dioxide free water at a constant flow rate ($\sim$ 20 ml hr^{-1}) and the eluate was collected as 10 ml fractions. The amount of carbohydrate in each fraction was determined by the phenol-sulphuric acid test and gave one sharply defined peak between fractions 45-62.

These fractions were combined and concentrated, the last traces of water being removed by the addition of a small amount of benzene. The sample was recrystallised twice from an ethanol-ethyl acetate mixture: m.p. 156-159°C: lit. m.p. 156-157°C (Micheel).

1(e) Preparation of the Methyl α-D-Xylopyranoside by Separation on a Basic Ion Exchange Column[73]

The ethyl acetate mother liquor from the separation of the methyl β-D-xylopyranoside was concentrated to a thick syrup (15.5 g). Paper chromatography using solvent (b) and the periodatocuprate spray gave the same three spots as mentioned above. One of these was the unchanged xylose, one was the methyl β-D-xylopyranoside and the other more prominent spot was attributed to the methyl α-D-xylopyranoside.

The anion exchange column was reconverted to the hydroxide form as described in the General Methods section. The mixture of the D-xylopyranosides (5 g) was dissolved in the minimum amount of water ($\sim$ 10 ml) and carefully transferred to the column and washed in as previously described. The column was again eluted with carbon dioxide free water ($\sim$ 20 ml hr^{-1}) and fractions (10 ml) collected. Approximately 110 fractions were collected and the elution pattern was determined using the phenol-sulphuric acid test for carbohydrate material (fig. 1.2). Paper chromatograms, using solvent (b) and the periodatocuprate spray, were used to determine the extent of overlap of the peaks and the results of these are also shown in fig. 1.2.

Fractions 35-44 were combined and concentrated, the last amounts of water being removed by the addition of a small volume of benzene. The sample was dissolved in ethyl acetate and reconcentrated to give white crystals of methyl α-D-xylopyranoside which were recrystallised from ethyl acetate: m.p. 89-91°C: lit. m.p. 91-92°C (Micheel[70]).

Fig. 1.2 Elution pattern for the separation of the methyl xylopyranosides on an anion exchange column.

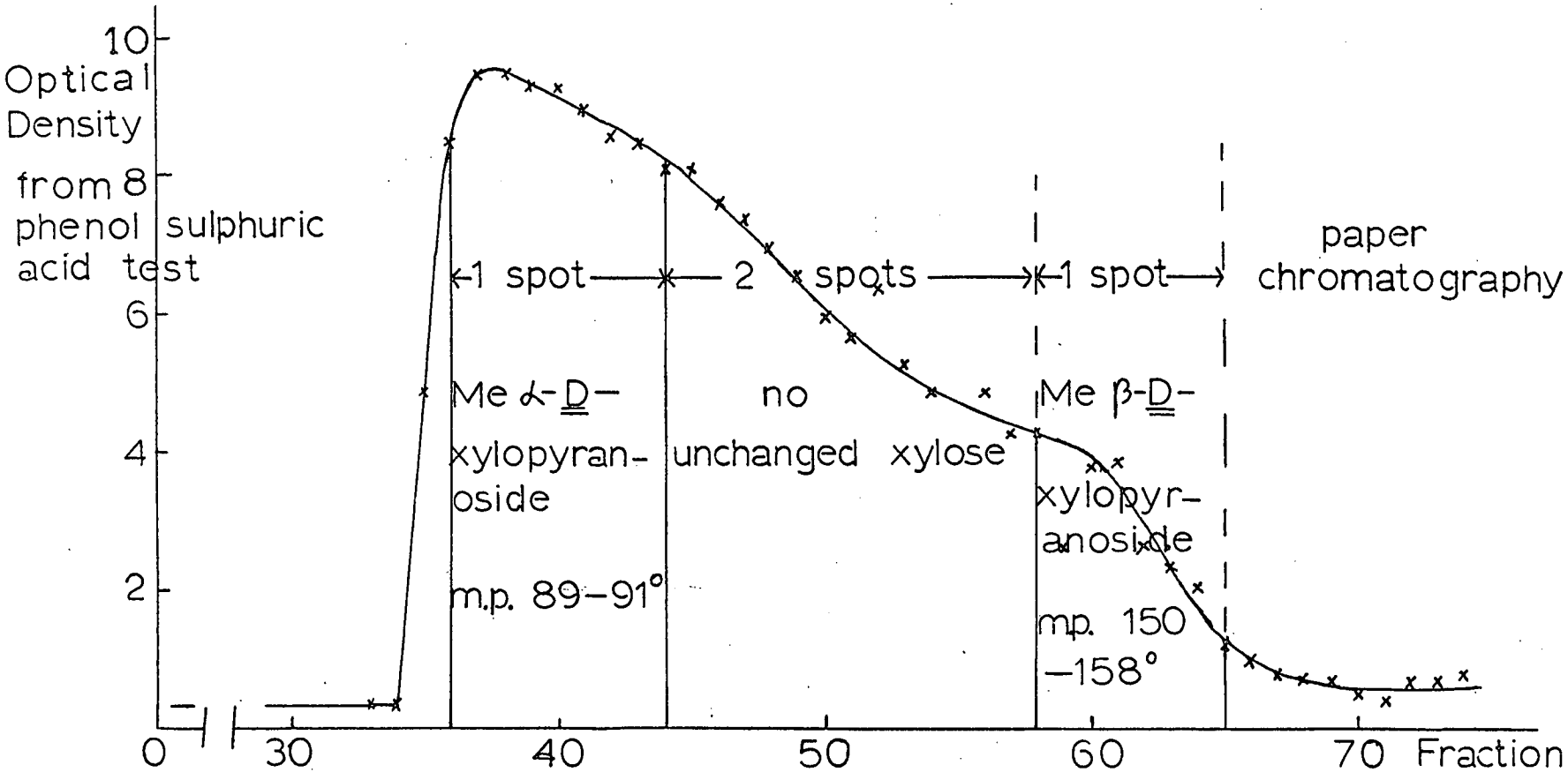

Fractions 58-65 were also combined, concentrated and crystallised in the same way. The resulting crystals had m.p. 150-158°C proving the effectiveness of the separation on the column of anion exchange resin. However only a small quantity of this material was obtained and it was not further purified. The unchanged D-xylose was retained on the column and was not eluted.

2. Solvents Used in the Optical Rotation Measurements

The measurement of the optical rotation against temperature was carried out in three solvents: distilled water, dioxan and dimethyl sulphoxide. The analar dioxan (B.D.H., Poole, England) was redistilled before use and was stored in a dark bottle away from the light. The dimethyl sulphoxide (B.D.H.) was used either directly from a new bottle which had been shown by infra-red spectroscopy to contain very little water or it was dried by vacuum distillation over calcium hydride, having refluxed over calcium hydride for four hours. It was stored, tightly sealed, over molecular sieve (4A) in a vacuum desiccator.

3. Preparation of Sample Solutions

The solutions used for the optical rotation measurements were made up in volumetric flasks by weighing out a quantity of the sample calculated to give a final solution reading on the polarimeter close to 1°. For the dioxan solutions this was normally not possible and the maximum amount which could be dissolved was used. These solutions were left to stand overnight to make sure none of the material settled out. All solutions were millipore filtered and transferred to the polarimeter cell in one operation using a syringe.

4. Measurement of the Optical Rotation against Temperature

The optical rotation measurements were made on a Perkin Elmer

141 polarimeter fitted with an automatic digital readout. The measurements were noted at two wavelengths.

(a) At the wavelength of the sodium D line, 589 nm, for comparison with the empirical theories described in the General Introduction.

(b) At 546 nm, the wavelength of the mercury lamp which has the highest intensity and gives more accurate readings with opaque or absorbing solutions.

The solution measurements were all recorded in the same 1 dm polarimeter cell equipped with an envelope through which water was circulated by a Haake thermocirculator to thermostat the cell. The deviation from the thermostatted temperature was $\pm$ 0.25°C. The average ($\pm$ 0.001°) of four recordings of the optical rotation was noted, for both wavelengths, at temperature intervals of 7-8°C from 20-90°C and at three points when the cell was recooled. The cell was allowed 20 minutes to equilibrate when it reached each new temperature. All readings were corrected for the cell blank of the cell containing the appropriate solvent which was determined for each solvent as indicated in the General Methods section.

The molecular rotations of the sample solutions at each wavelength and temperature were calculated using the formulae detailed in the General Introduction. These were normalised for comparison with the value at 25°C, in the same solvent, by compensating for the change in refractive index and density with temperature using the following equation[74]:

$$(\text{Normalised Molecular Rotation})_S^T = \left[M\right]_S^T \cdot \frac{(n_S^{25°C})^2 + 2}{(n_S^{T°C})^2 + 2} \cdot \frac{p_S^{25°C}}{p_S^{T°C}}$$

$\left[M\right]_S^T$ is the molecular rotation measured at the temperature T°C in a solvent(S) of refractive index (n_S^T) and density (p_S^T) at T°C and

($n_S^{25°C}$) and ($p_S^{25°C}$) are the refractive index and density of the solvent at 25°C.

RESULTS AND DISCUSSION

The normalised molecular rotations were plotted against temperature and the best curves drawn through the points. In all cases the change in this molecular rotation was either linear with temperature or could be best fitted by a shallow curve. An example of the magnitude of the changes at 589 nm and the shape of the curves is shown in fig. 1.3 for three of the methyl α-D-glycopyranosides in water. The magnitude of the changes with temperature in dimethyl sulphoxide and dioxan are similar but the dioxan values are slightly more scattered about the best curve because of errors in measurement caused by the limited solubility of the glycosides in dioxan. To compare the values in dimethyl sulphoxide and dioxan with those in water the normalised molecular rotations were compensated for the change in solvent refractive index according to the equation[74]:

$$\text{c.m.r.} = (\text{normalised mol. rot.})_S^{T\,^\circ C} \cdot \frac{(n_{H_2O}^{25^\circ C})^2 + 2}{(n_S^{25^\circ C})^2 + 2}$$

The normalised molecular rotation at temperature T °C in the solvent (S), which has the refractive index ($n_S^{25^\circ C}$) at 25°C, was taken from the best curve drawn through the points and ($n_{H_2O}^{25^\circ C}$) is the refractive index of water at 25°C. The compensated molecular rotation (c.m.r.) is therefore the normalised molecular rotation referred to the refractive index of water at 25°C.

The variation of compensated molecular rotation with temperature in distilled water, dimethyl sulphoxide and dioxan is given in table 1.1 for all the methyl glycosides (and styracitol) studied. Only the results obtained at the sodium D line (589 nm) are reproduced in table

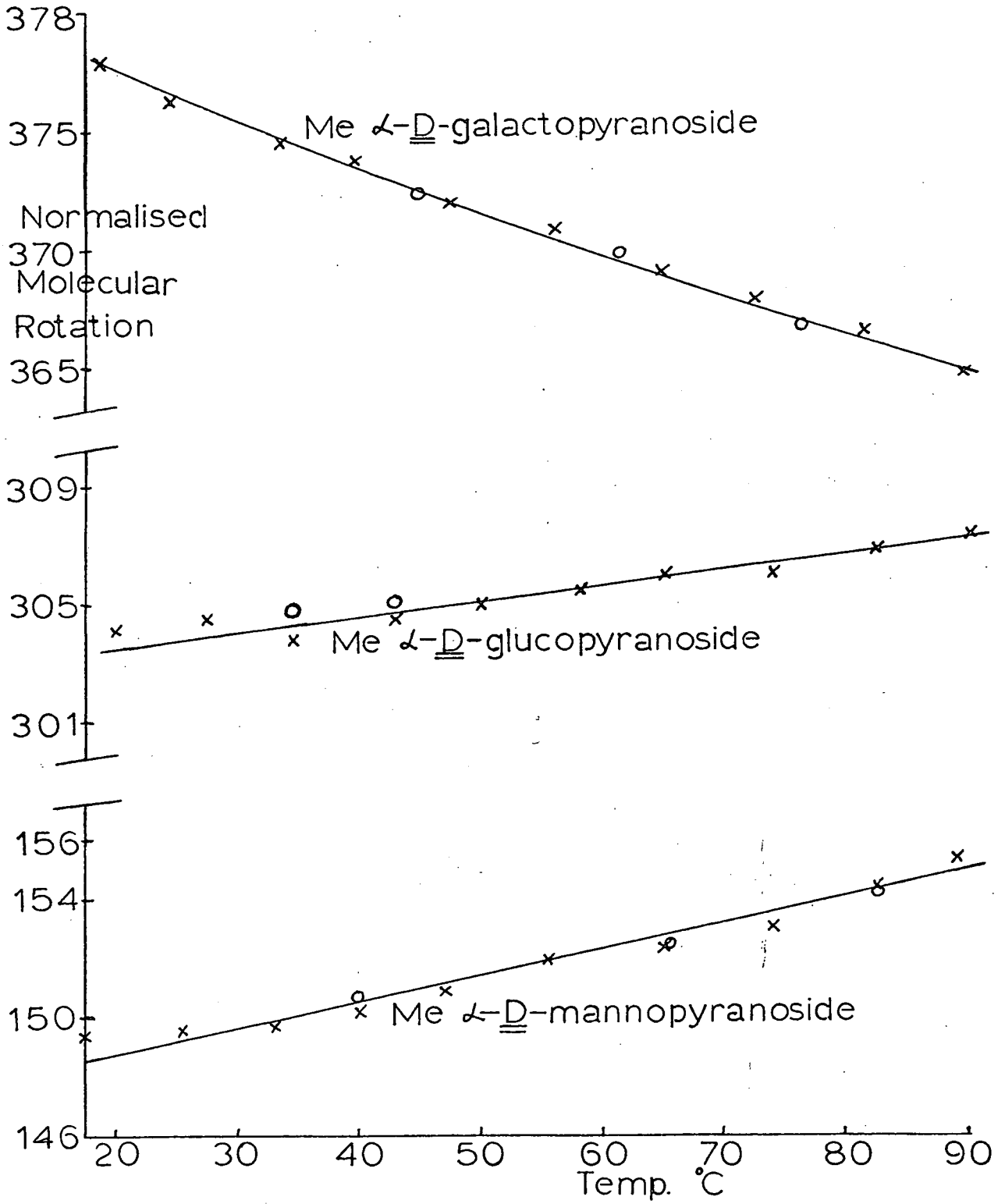

Fig. 1.3 Graph of normalised molecular rotation v temperature for some methyl-α-D-glycopyranosides in H_2O at 589 nm.

1.1 since these can be correlated with previous measurements and also with the empirical rotational perameters used to estimate the molecular rotation of such glycopyranosides (General Introduction). The results obtained at the most intense mercury lamp radiation, 546 nm, are given in Appendix 2.

From table 1.1 it can be readily seen that the variations in the c.m.r. with temperature are small and would be swamped by those caused by any large conformational effects such as a complete alteration in the conformation of the sugar ring or the change in the glycosidic angles, ϕ and ψ, associated with a cooperative polysaccharide transition of the type described in the General Introduction for the carrageenans. The exact magnitude of the variations with temperature are recorded in table 1.2 where the change in the compensated molecular rotation (Δ c.m.r.), at 589 nm, on altering the temperature from 25°C to 80°C is given by:

$$(\Delta \text{ c.m.r.})_{25^\circ C}^{80^\circ C} = (\text{c.m.r.})_D^{80^\circ C} - (\text{c.m.r.})_D^{25^\circ C}$$

The change in the compensated molecular rotation which arises from a change in the solvent can be much larger, although still small compared with that expected for a complete alteration in the conformation of the pyranose ring. These are recorded in table 1.3, again for measurements at 589 nm, where;

$$(\Delta \text{ c.m.r.})_{\text{solvent B}}^{\text{solvent A}} = (\text{c.m.r.})_D^{\text{solvent A}} - (\text{c.m.r.})_D^{\text{solvent B}}$$

The $(\Delta \text{ c.m.r.})_{H_2O}^{NaOH}$ values calculated from Reeves' measurements[75] of the effect of sodium hydroxide upon the optical rotation of methyl pyranosides are included in table 1.3. As shown these have very similar relative magnitudes to those obtained in this study and are consistent with the general treatment developed below. Reeves[75] carried out his measurements at 27.5 $\pm$ 2.5°C and checked

TABLE 1.1

The Variation of the Compensated Molecular Rotation (c.m.r.) with Temperature at λ_{589}

Sample	Solvent	Value of c.m.r. at the temperature indicated (degrees)							
		20	25	30	40	50	60	70	80
Me α-D-glucopyranoside	H_2O	303.7	304.0	304.2	304.7	305.2	305.7	306.2	306.8
	DMSO	298.8	298.8	298.7	298.6	298.5	298.3	298.0	297.6
	Dioxan	306.0	306.8	307.6	308.6	309.3	309.6	309.7	309.8
Me α-D-xylopyranoside	H_2O	248.6	248.7	248.9	249.2	249.4	249.7	250.0	250.3
	DMSO	241.0	241.0	240.9	240.8	240.5	239.9	239.2	238.3
	Dioxan	266.8	266.8	266.7	266.5	266.1	265.8	265.2	264.5
Me α-D-mannopyranoside	H_2O	148.8	149.3	149.7	150.5	151.4	152.2	153.1	153.9
	DMSO	138.8	140.3	141.8	144.6	147.1	149.3	151.2	153.0
	Dioxan	212.8	212.2	211.3	209.0	205.8	201.7	196.6	190.6
Me α-D-galactopyranoside	H_2O	374.4	373.3	372.1	370.3	368.6	367.2	366.2	365.3
	DMSO	336.6	335.6	334.7	333.1	331.5	330.2	328.9	328.0
	Dioxan	303.3	304.1	304.8	306.3	307.7	309.1	310.4	311.4

TABLE 1.1 (Continued)

Sample	Solvent	Value of c.m.r. at the temperature indicated (degrees) 20	25	30	40	50	60	70	80
Me β-L-arabinopyranoside	H_2O	390.7	390.0	389.3	308.0	386.6	385.2	383.9	382.5
	DMSO	332.4	331.1	329.8	327.2	324.8	322.5	320.1	318.1
	Dioxan	333.8	333.9	334.0	334.1	333.8	332.9	331.5	330.0
3,6 Anhydro-me-α-D-galacto-	H_2O	138.8	138.0	137.3	135.8	134.3	132.8	131.4	129.9
pyranoside	DMSO	128.8	128.9	129.0	129.2	129.4	129.6	129.8	130.0
	Dioxan	148.2	147.9	147.6	147.1	146.7	146.3	145.9	145.5
Me β-D-glucopyranoside	H_2O	-62.2	-62.0	-61.7	-61.1	-60.6	-60.1	-59.7	-59.4
	DMSO	-64.5	-63.4	-62.4	-60.7	-59.1	-57.6	-56.5	-55.3
	Dioxan	-67.9	-67.4	-66.8	-66.0	-65.5	-65.3	-65.2	-65.2
Me β-D-xylopyranoside	H_2O	-106.3	-105.9	-105.5	-104.9	-104.4	-103.9	-103.6	-103.3
	DMSO	-95.0	-94.7	-94.3	-93.7	-93.5	-93.4	-93.5	-93.8
	Dioxan	-112.5	-113.2	-114.0	-115.5	-117.0	-118.4	-119.9	-121.4
Me β-D-galactopyranoside	H_2O	-0.7	-1.2	-1.7	-2.6	-3.6	-4.6	-5.6	-6.6
	DMSO	-23.2	-23.2	-23.2	-23.2	-23.2	-23.2	-23.3	-23.3

TABLE 1.1 (Continued)

Sample	Solvent	Value of c.m.r. at the temperature indicated (degrees)							
		20	25	30	40	50	60	70	80
Me β-D-galactopyranoside(Continued)	Dioxan	-48.2	-47.7	-47.5	-47.0	-46.9	-47.0	-47.1	-47.4
Styracitol (1,5 anhydro mannitol)	H_2O	-82.8	-82.8	-82.9	-82.9	-82.9	-83.1	-83.2	-83.2
	DMSO	-85.4	-84.6	-83.7	-82.2	-80.9	-79.8	-78.7	-77.7
	Dioxan								

EDINBURGH EX BIBL UNIV.

TABLE 1.2

The Change in the Compensated Molecular Rotation (Δ c.m.r.) on Changing the Temperature from 25°C to 80°C: Measured at 589 nm

Sample	$(\Delta \text{ c.m.r.})_{25°C}^{80°C}$ in the solvent indicated (degrees)		
	Water	DMSO	Dioxan
Me α-D-glucopyranoside	3	-1	3
Me α-D-xylopyranoside	2	-3	-2
Me α-D-mannopyranoside	5	13	-22
Me α-D-galactopyranoside	-8	-8	7
Me β-L-arabinopyranoside	-8	-13	-4
3,6 Anhydro-me-α-D-galacto-pyranoside	-8	1	-2
Me β-D-glucopyranoside	3	8	2
Me β-D-xylopyranoside	3	1	-8
Me β-D-galactopyranoside	-5	0	0
Styracitol (1,5 anhydro mannitol)	0	7	

TABLE 1.3

The Change in the Compensated Molecular Rotation (Δ c.m.r.) with Change of Solvent: Measured at 589 nm

Sample	$(\Delta \text{ c.m.r.})^{\text{Dioxan}}_{\text{DMSO}}$		$(\Delta \text{ c.m.r.})^{\text{Dioxan}}_{H_2O}$		$(\Delta \text{ c.m.r.})^{\text{DMSO}}_{H_2O}$		$(\Delta \text{ c.m.r.})^{\text{N.NaOH}}_{H_2O}$	
Me α-D-glucopyranoside	8	(26)	3	(18)	-5	(-8)	0	(-3)
Me α-D-xylopyranoside	26		18		-8		-3	
Me α-D-mannopyranoside	72	(90)	63	(78)	-9	(-12)	1	(-2)
Me α-D-galactopyranoside	-32	(3)	-69	(-56)	-38	(-59)	-16	(-16)
Me β-L-arabinopyranoside	3		-56		-59		-16	
3,6 Anhydro-me-α-D-galactopyranoside	19		10		-9		-	
Me β-D-glucopyranoside	-4	(-19)	-5	(-7)	-1	(11)	3	(-2)
Me β-D-xylopyranoside	-19		-7		+11		-2	
Me β-D-galactopyranoside	-25	(10)	-47	(-34)	-22	(-43)	-19	(-19)
Styracitol (1,5 anhydro mannitol)					-2			
Me β-D-mannopyranoside							19	(16)

The values in the brackets are the group contributions mentioned in the text.

that the observed differences in optical rotation, in neutral and alkaline aqueous solutions, were not due to differences in the solution ionic strengths by also observing the optical rotations in sodium chloride solution.

A quantitative explanation of the results listed in the tables 1.1 - 1.3 is not possible with the present limited empirical approaches to an understanding of the optical rotation of sugars but two hypotheses have been considered in an attempt to gain a qualitative insight.

a) The Δ c.m.r. values with solvent and temperature are related to changes in the conformational equilibria in different solvents, as suggested by Lemieux[12,13,64], and that effects due to direct spectroscopic perturbations by the solvent environment are unimportant.

b) The solvent and temperature effects can be explained by changes in the magnitudes of the empirical parameters used to estimate the molecular rotations of saturated pyranoid carbohydrates when the solvent environment is altered. This assumes that the extent of perturbation of the chromophores by dissymmetric features of the molecule is directly influenced by the physical properties of the solvent.

Neither of these hypotheses is likely to account for all the observed changes on its own but the relative importance of the two effects can be indicated. The Δc.m.r. when water is replaced by the non-polar solvents dioxan, carbon tetrachloride or chloroform will be considered in most detail since these are the solvent extremes but the similarities and differences on making the other changes in the solvent environment will also be mentioned.

Hypothesis (a): Changes in the Conformational Equilibria Due to Changes in the Solvent Environment

Reeves and Blouin[75] suggested that the observed changes in the optical rotations of some methyl glycosides was caused by the ionisation

of hydroxyl groups resulting in a change from chair to flexible boat ring forms, due to increased repulsions, particularly where the boat conformation allows bulky substituents to become "equatorial". However the present knowledge of the free energy difference between chair and flexible boat forms makes this explanation very unlikely and more recent n.m.r. evidence[76] has confirmed that the conformations of sugars substituted at C(1) are the same in aqueous and alkaline solutions. All the methyl glycosides are therefore taken to be in the chair form in alkaline solution and it is also considered that the methyl pyranosides do not alter their ring chair conformation when water is replaced by the other simple solvents studied here. The fact that the conformationally rigid compounds studied by Lemieux (table 1.4 and ref. 13) and the methyl 3,6 anhydro α-D-galactopyranoside (table 1.3) give Δ c.m.r. values of similar magnitude to the methyl pyranosides supports this view. The observed Δ c.m.r. values must therefore be due to solvent dependent changes in the conformational equilibrium around the C(5) - C(6) and C(1) - OCH_3 bonds if this hypothesis is to be valid.

The change in the contribution to the c.m.r. which arises from solvent dependent alterations in the orientation of the hydroxymethyl group about the C(5) - C(6) bond can be approximately assessed by comparing the α- and β-D-glucopyranosides with the corresponding D-xylopyranosides and the α-D-galactopyranoside with the β-L-arabinopyranoside. The three possible staggered orientations are shown in fig. 1.4 along with the values which can be assigned to their contribution to the molecular rotation in aqueous solution, using the empirical parameters suggested by Lemieux[12]. The observed effect of introducing the primary hydroxyl group at C(6) into a 6-deoxy-D-hexopyranose structure is to increase the molecular

Fig. 1.4 Staggered orientations around the C(5) - C(6) bond

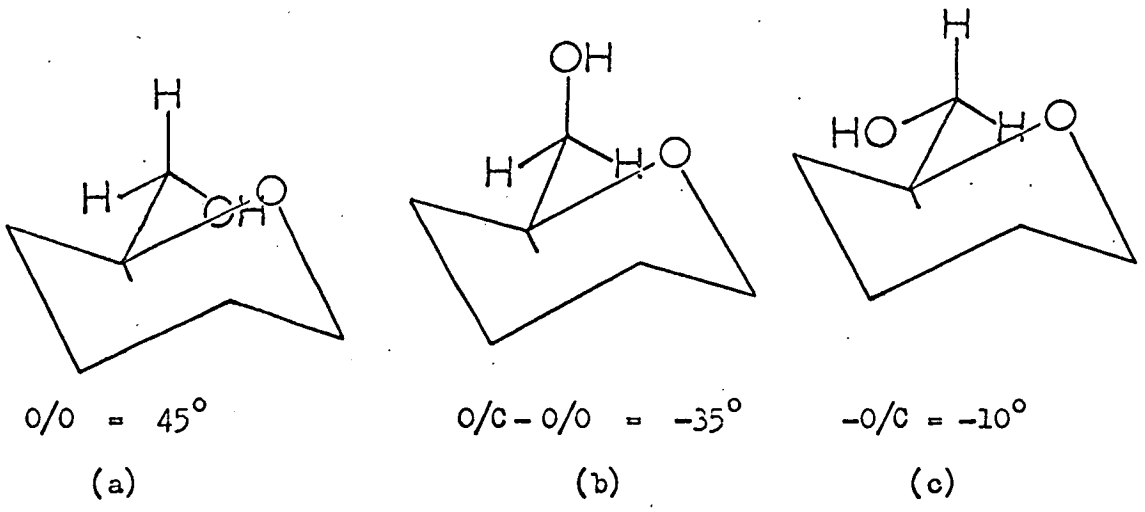

O/O = 45° O/C - O/O = -35° -O/C = -10°

(a) (b) (c)

rotation, in aqueous solution, by about 25°. This indicates that the conformation 1.4(a) is preferred in aqueous solution, whether the hydroxyl group at C(4) is axial or equatorial. On replacing a polar strongly hydrogen bonding solvent such as water by dioxan one would expect an increase in the contributions from 1.4(b) and 1.4(c) for galactopyranosides and glucopyranosides respectively due to the presence of a weak intramolecular hydrogen bond, between O(6) and O(4), in the non-polar solvent. This reasoning is supported by the negative contribution to the c.m.r. from the hydroxymethyl groups in methyl α-D-glucopyranoside and galactopyranoside on making this solvent change. As mentioned in the General Introduction, a similar hydrogen bonded conformation of the carboxyl group with O(4) has been suggested to explain the small higher wavelength band observed in the c.d. of methyl uronosides which have an equatorial hydroxyl group

at C(4) and the size of this band increases when water is replaced by non-polar solvents. However it is difficult to explain on this basis why no effect of this type is observed for the methyl β-D-glucopyranosides and why heating the aqueous solutions from 25°C to 80°C or making the solution alkaline gives no indication of a contribution to the Δc.m.r. from this source.

To test this hypothesis an approximate assessment was made of the contribution by the hydroxymethyl group to the Δc.m.r. (tables 1.2 and 1.3). The assumptions made were those mentioned above with the further assumptions that the hydroxymethyl group will make the same contribution in methyl α-D-mannopyranoside as in methyl α-D-glucopyranoside and its contribution in methyl β-D-galactopyranoside will be identical to that in methyl α-D-galactopyranoside. The contribution of the hydroxymethyl group can then be deducted from the observed Δc.m.r. values and these adjusted values are given in brackets in table 1.3. It can be seen that although the contribution from the hydroxymethyl group may in some cases, e.g. for the methyl α and β-D-glucopyranosides, be the dominant effect, in general the observed Δc.m.r. values in table 1.3 cannot be rationalised simply in terms of changes in the c.m.r. arising from solvent dependent changes in the orientation of the hydroxymethyl group about the C(5) - C(6) bond.

The final conformational equilibrium which may be solvent dependent and hence contribute to the Δ c.m.r. when the solvent environment is altered is that involving rotation about the C(1) - OCH_3 bond. Lemieux[13,64] has studied the effect of solvent on the optical rotation of the conformationally rigid methyl 2,3 dideoxy-4,6-O-ethylidene -α-D-hexopyranoside (1.4(d)) and its β-anomer (1.4(e)) to determine the effect of this. His results, approximately compensated for the change in

solvent refractive index using the refractive indices listed, are shown in table 1.4. It was found that water had a relatively large special effect on the molecular rotation of the α-anomer. This special effect of water is consistent with the results obtained in this study and will be discussed later in this chapter.

Lemieux suggested[13,64] that the special effect of water on the molecular rotations could arise from its unique possibility, because of its dihydric nature, to stabilise the conformation 1.5(b) which has parallel and opposing orbitals for the unshared pairs of electrons on its ring oxygen and glycosidic oxygen. The conformer 1.5(c) which has the CH_3 group antiparallel to the anomeric hydrogen atom is considered so highly strained as to have negligible existence. This theory, by consideration of the empirical rules for the prediction of optical rotation, gives an explanation consistent with the sign of the Δc.m.r. values when water is replaced by any other solvent. However the empirical theories[7,8], whose parameters were calculated from the measured rotations in water, obtain very good agreement between the observed and calculated values by assigning parameters of identical magnitude to both α- and β-anomers on the assumption that they are exclusively in the conformations 1.5(a) and 1.5(d) respectively. This is incompatible with the explanation suggested by Lemieux and it is felt that this effect cannot offer a full explanation of the results in table 1.4. This is discussed more fully under hypothesis (b). Moreover, even when coupled with the estimated contributions to the $(\Delta \text{ c.m.r.})^{\text{solvent}}_{H_2O}$ from the hydroxymethyl group, the changes in the c.m.r. with solvent due to an alteration in the conformational equilibrium around the C(1) - OCH_3 bond cannot fully account for the magnitude of the observed $(\Delta \text{ c.m.r.})^{\text{solvent}}_{H_2O}$. For example, if we examine the $(\Delta \text{ c.m.r.})^{\text{Dioxan}}_{H_2O}$ values adjusted for the

TABLE 1.4

The effect of solvent on the compensated molecular rotation of some 4,6-O-ethylidene-D- hexopyranosides[a] and related compounds.

Solvent	$n^{20°C}$ 77	(c.m.r.)$^{solvent}_{H_2O}$	1.4(a)[b]	1.4(b)[b]	1.4(c)[b]	1.4(d)[b]	1.4(e)[b]
$CHCl_3$	1.4459	(c.m.r.)$^{CHCl_3}_{H_2O}$	2	+8	+3	+20	+1
CCl_4	1.4601	(c.m.r.)$^{CCl_4}_{H_2O}$	2	+9	–	+21	+9
CH_3COCH_3	1.3588	(c.m.r.)$^{(CH_3)_2CO}_{H_2O}$	2	+6	–	+29	–8
CH_3OH	1.3288	(c.m.r.)$^{CH_3OH}_{H_2O}$	–	+5	+19	+40	–15
CH_3CN	1.3442	(c.m.r.)$^{CH_3CN}_{H_2O}$	2	+6	+39	+33	–8
CH_3SOCH_3	1.4783	(c.m.r.)$^{(CH_3)_2SO}_{H_2O}$	2	+12	–17	+17	+13
H_2O	1.3330	$[M]^{25°}_{H_2O}$	+0.2	–43	+246	+218	–141

(a) From ref. 13 approximately corrected for the solvent refractive index using the above values.

(b) The compounds have the structures shown.

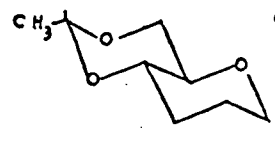

1.4.(a)

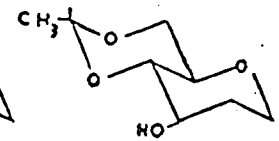

1.4.(b)

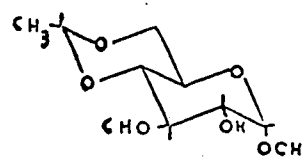

1.4.(c)

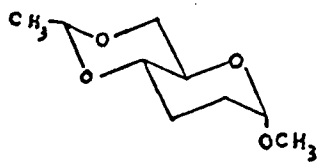

1.4.(d)

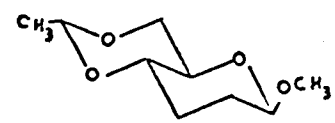

1.4.(e)

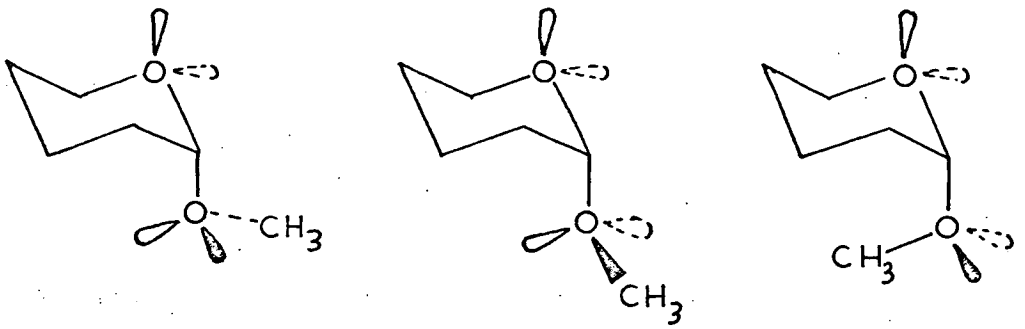

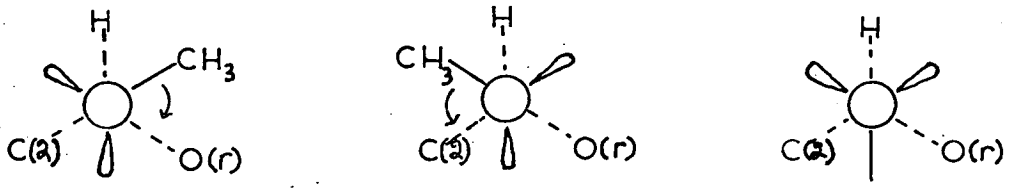

dextro
1.5.(a)

laevo
1.5.(b)

1.5.(c)

Methyl ∝-D-glycopyranoside

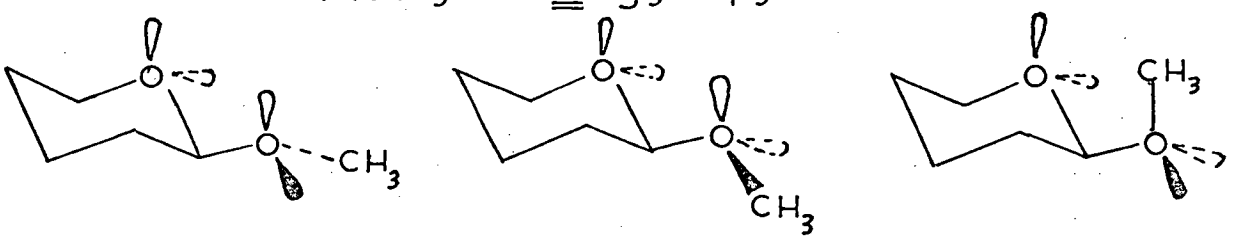

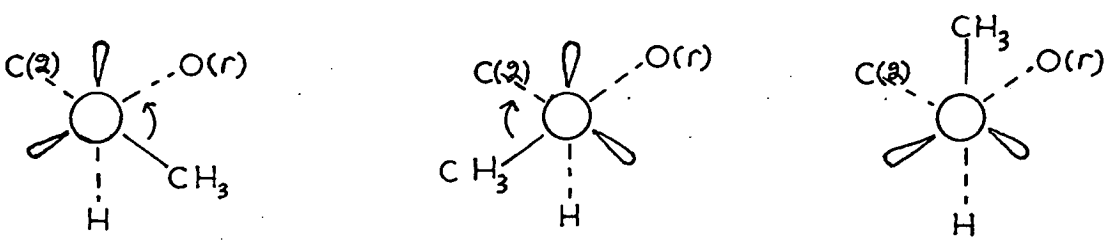

laevo
1.5.(d)

dextro
1.5.(e)

1.5.(f)

Methyl β -D-glycopyranoside

Fig. 1.5 Staggered conformations about the C(1)-OCH_3 bond for ∝ and β-D-glucopyranosides.

contribution of the hydroxymethyl group and given in brackets in table 1.3, then a large discrepancy is apparent between those such as methyl α-D-mannopyranoside ($+78^{\circ}$) and methyl β-D-galactopyranoside (-34°) and those given in table 1.4 for the $(\Delta \text{ c.m.r.})^{\text{non-polar solvent}}_{H_2O}$ of the methyl 2,3 dideoxy-4,6-O-ethylidene α-D-hexopyranoside ($\sim +20^{\circ}$) and its β-anomer ($\sim 0^{\circ}$) respectively.

It is, therefore, considered that changes in the compensated molecular rotations due to changes in the conformational equilibria in the methyl pyranosides when the solvent environment is altered are, by themselves, insufficient to explain the changes in the compensated molecular rotations observed here.

Hypothesis (b): Solvent Dependent Changes in the Magnitude of the Rotational Parameters

In this section an attempt is made to rationalise the Δc.m.r. values that are observed on changing the solvent or the solution temperature in terms of the influence of the solvent environment on the magnitude of the rotational parameters derived in the empirical theories. Such variation could conceivably occur as a result of changes in the wavelengths of the far ultra-violet o.r.d. extrema and/or in the intensity of their Cotton effects, as indeed have been directly observed for the carbonyl group[3,25]. Such solvent dependent group increments have been found[78] to be important in the study of the influence of solvents upon the Cotton effects of rigid ketones and it was suggested[78] they may even be the dominant factor when the chromophores are not in an excessively hindered steric environment.

The hypothesis has been examined by considering in detail the Δc.m.r. values observed when water is replaced by the non-polar solvents dioxan, carbon tetrachloride and chloroform, in which solvent-solute

association will be very limited, but similar relative Δ c.m.r. values are observed (tables 1.2 and 1.3) for the other changes in the solvent environment. The empirical parameters suggested by Brewster[8] are used here since it is felt that they are slightly more consistent with the general theoretical basis of the phenomenon and they also allow the carbohydrates to become part of a wider series of compounds. As shown in table 1.5 the symbols Δa to Δf represent the change in Brewster's rotational constants which are given in more detail in Appendix I.

TABLE 1.5

Rotation constants for use with carbohydrates

Rotation		Brewster's	Present Change
Brewsters[8]	Present	Values(degrees)	in these Values (degrees)
k (O-H)(O-H)	Δa	+45	-15
k (C-H)(O-H)	Δb	+50	0
Permolecular effect C(1)/C(5) (XXXIX)	Δc	+100	+20
Permolecular effect C(2)/C(4) (XL)	Δd	+60	-25
C(6) hydroxymethyl (XLII)	Δe	+25	not applic.
C(1) -O-methyl (XLV)	Δf	+ or - 105	0

The analysis of the methyl pyranosides and the 4,6 ethylidene-D-hexopyranosides in terms of these empirical parameters is given in table 1.6 along with the Δc.m.r. observed when the solvent is changed from water to the non-polar solvents. For the hydroxymethyl group at C(6) it is impossible to distinguish between the magnitude of the

Δc.m.r. caused by solvent dependent changes in the conformational equilibria around the C(5) – C(6) bond and that caused by the effect

TABLE 1.6

Compound	Analysis	$(\Delta \text{c.m.r.})^{\text{solvent}}_{H_2O}$ obs(degrees)	Δc.m.r. calc. (degrees)
Me α-D-glucopyranoside Me α-D-xylopyranoside	+Δa +Δc +Δf	+18[b]	+5
Me α-D-mannopyranoside	−2Δa +Δc −Δd +Δf	+78[b]	+75
Me α-D-galactopyranoside Me β-L-arabinopyranoside	+3Δa +Δc +Δd +Δf	−56[b]	−50
Me β-D-glucopyranoside Me β-D-xylopyranoside	−Δa −Δf	−6[b]	+15
Me β-D-galactopyranoside	+Δa +Δd −Δf	−34[b]	−40
1.4(b)[a]	−Δa +Δb	+9[c]	+15
1.4(c)[a]	+Δa +Δb +Δc +Δf	+3[d]	+5
1.4(d)[a]	+Δc +Δf	+21[c]	+20
1.4(e)[a]	−Δf	+5[c]	0

(a) The structures of these compounds are shown above table 1.4.

(b) $(\Delta \text{ c.m.r.})^{\text{Dioxan}}_{H_2O}$

(c) Average value of $(\Delta \text{ c.m.r.})^{CHCl_3}_{H_2O}$ and $(\Delta \text{c.m.r.})^{CCl_4}_{H_2O}$

(d) $(\Delta \text{ c.m.r.})^{CHCl_3}_{H_2O}$

of the solvent on the contribution from each of the possible orientations (fig. 1.4) of this group. The total contribution from the hydroxymethyl group, from both effects, has therefore been assessed, using the same

assumptions and values described under hypothesis (a)and the $(\Delta c.m.r.)^{Dioxan}_{H_2O}$ values listed in brackets in table 1.3 are used here. This treatment means that the changes in the rotational constants, Δb and Δe, which differentiate between the hexopyranosides and the pentopyranosides are not considered for the methyl pyranosides listed in tables 1.3 and 1.6. Similarly it is impossible to distinguish between the contributions to Δf, the change in the rotation constant XLV (Appendix I) due to changes in the conformational equilibria around the C(1) - OCH_3 bond and those due to solvent influenced changes in the value of the contribution from each of the individual orientations (fig. 1.5). The parameter Δf therefore represents the sum of both these effects.

By equating the observed Δ c.m.r. values with the totals of the rotational parameters used to express the change in the molecular rotations of the compounds (table 1.6) a numerical value can be derived for each of the rotational parameters and these are given in table 1.5. The values, rounded to the nearest five degrees, have been deduced using the values obtained from the minimum no. of compounds as a guide and adjusting them to give the best overall fit with the experimental values. They indicate the change in the numerical value of Brewster's rotation constants required to fit the Δ c.m.r. when the solvent is changed from water to non-polar solvents and a comparison of the calculated and observed Δ c.m.r. values (table 1.6) shows that this treatment is generally very satisfactory.

This approach also gives a very simple explanation of the observed differences in the $(\Delta c.m.r.)^{solvent}_{H_2O}$ for methyl 2,3 dideoxy-4,6-O-ethylidene-α-D-hexopyranoside and its β-anomer (table 1.4 and ref. 13) which is more consistent with the empirical theories[7,8] for the

estimation of carbohydrate molecular rotations. The $(\Delta c.m.r.)_{H_2O}^{solvent}$ for the β-anomer leads to a very small value for Δf, the parameter associated with C(1) - OCH_3, and a numerical value of zero (table 1.5) has been assigned to it. This suggests that when water is replaced by the less polar solvents there is no change from the most favoured conformation 1.5(d) (fig. 1.5) and the influence of solvent on the magnitude of the contribution from this orientation is very small. It is of course possible that a change in the conformational equilibrium of the type suggested by Lemieux[13,64] is equally balanced by the difference resulting from alterations in the contributions from each orientation. Brewster's parameter that corresponds to Δf (table 1.5 and Appendix I) is, according to his method, supposed to have the same magnitude in α and β anomers and the greater observed $(\Delta c.m.r.)_{H_2O}^{solvent}$ for the α anomer can, therefore, be attributed to Δc the change in the rotational constant (XXXIX) which arises from the permolecular effect of the axial C(1) - OCH_3 bond.

General Considerations of the Effect of the Solvent Environment

When all of the Δ c.m.r. values (in brackets in table 1.3) obtained in this study, after subtraction of the hydroxymethyl contribution as previously indicated, are examined along with those of Lemieux, it is noticeable that the observed Δc.m.r. values on replacing water by any other simple solvent are almost invariably greater than those observed on interchanging any of these other simple solvents. This large effect of water on the optical rotation of these pyranosides can be considered in the light of the theoretical description of dilute aqueous solutions of simple carbohydrates.

In water the oxygen atom of each molecule is tetrahedrally coordinated by means of hydrogen bonds to the oxygen atoms of adjacent

water molecules. At 25°C X-ray diffraction detects[79] a high concentration of water molecules 4.9Å apart which is compatible with the distance of an oxygen atom from its co-planar, second nearest neighbour in the ice-like arrangement suggested for water[79,80]. The distance between equatorial hydroxyl groups on the same side of a glucose ring, e.g. hydroxyl groups attached to C(2) and C(4), is 4.86Å [81] and Kabayama and Patterson[82] proposed that the equatorial hydroxyl groups on opposite sides of a monosaccharide ring could form strong hydrogen bonds to two layers of water molecules, in the tridymite water structure, one above and one below the plane of the ring (fig. 1.6). From the study of models the hydration of axial hydroxyl groups is expected to be considerably less than that of equatorial hydroxyl groups because they cannot form strong hydrogen bonds with this "lattice water". These suggestions are consistent with more recent thermodynamic[83], dielectric and n.m.r.[84] studies of aqueous solutions of simple carbohydrates and may contribute substantially to the observed predominance of pyranose over furanose ring forms of reducing sugars in aqueous solution, as mentioned in the Introduction to this Chapter.

A possible explanation of the large effect of water can now be suggested. The strong hydrogen bonding of the equatorial hydroxyl groups on opposite sides of the pyranose ring to different layers of the lattice water will not only restrict the rotation of the hydroxyl groups but also may resist any tendency to flatten the ring arising from steric effects. When this special effect of the water is removed, the steric repulsions between ring atoms and, for example, between an axial hydroxyl group and the lone pair orbitals of the ring oxygen, may flatten the ring slightly as it does in the solid state[85]. This would be expected to

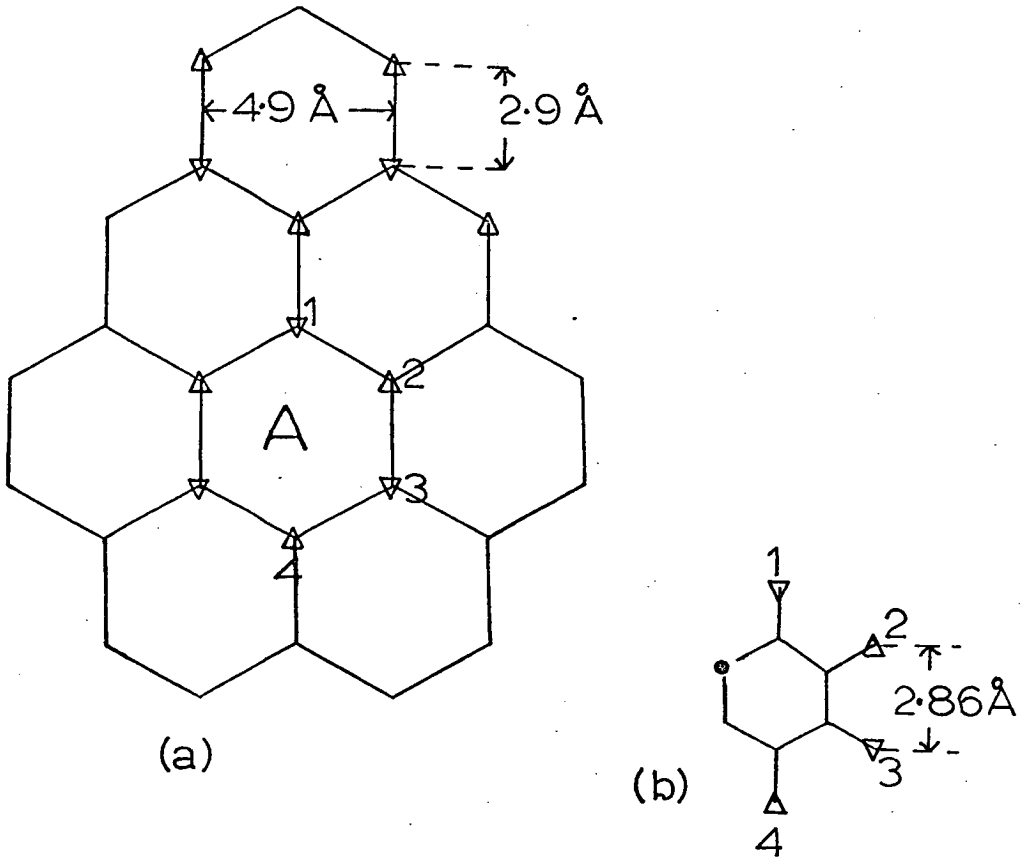

Fig. 1.6 A possible model for the hydration of monosaccharides[82].

(a) A plane of the oxygen atoms in the tridymite structure of water. The atoms marked △ and ▽ are joined by straight hydrogen bonds to the atoms directly below and above respectively.

(b) The β-D-glucose molecule, which can replace the hexagon marked A, showing the direction of possible perpendicular hydrogen bonds.

decrease the C(2)/C(4) permolecular effect (Appendix I) and also the k(O-H)(O-H) contribution by diminishing the exocyclic angle θ of the O-C-C-O conformational units (fig. 2 in the General Introduction; where both u and x are oxygen atoms). This is consistent with the sign of the changes in the rotational constants required to fit the observed results. Also, in water, as the temperature is raised the X-ray diffraction pattern shows[86] that there is a decreasing probability of water molecules being spaced 4.5 - 5.3Å apart. This breakdown of the "lattice water" with the removal of the special solvation would be expected, on the basis of the above suggestion, to give $(\Delta c.m.r.)_{25^oC}^{80^oC}$ values in water which have the same relative magnitude as the $(\Delta\ c.m.r.)_{H_2O}^{Dioxan}$ and this is generally observed.

As previously mentioned the $(\Delta c.m.r.)_{H_2O}^{NaOH}$ values measured by Reeves (table 1.3 and ref. 75) also have the same relative (but not absolute) values as those reported in this study, apart from those methyl glycosides which have vicinal diaxial hydroxyl or hydroxyl/C(1) - OCH_3 groups. This alkali sensitivity of the glycosides, where the effect of the alkaline water solvent may be thought of as being equivalent to that expected from a water/dimethyl sulphoxide hybrid (table 1.3), could possibly be due to the large structure-breaking capacity of the highly solvated hydroxyl ions on bulk water[87] coupled with increased repulsions of the axial hydroxyl group with the ring oxygen lone pair orbitals under ionising conditions. The breakdown of the "lattice water" would be expected to diminish the special solvent effect of water although the unstructured alkaline water solvent would still be strongly hydrogen bonding, c.f. dimethyl sulphoxide. Similar effects are observed on the optical rotation of methyl-β-maltoside and amylose when water is replaced by

aqueous alkali or dimethyl sulphoxide and this will be discussed in Chapter 2. From the results of this study given in table 1.3 it is apparent from the small $(\Delta \text{c.m.r.})^{DMSO}_{H_2O}$ value and the large $(\Delta \text{c.m.r.})^{Dioxan}_{H_2O}$ that methyl α-D-mannopyranoside is inconsistent with the explanation developed above but is consistent with the small $(\Delta \text{c.m.r.})^{NaOH}_{H_2O}$ observed by Reeves[75] for this compound. Thus for methyl α-D-mannopyranoside aqueous alkali and dimethyl sulphoxide show anomalous behaviour giving optical rotation values very close to those of the water value and similar effects are observed[75] for methyl α-D-lyxoside, altroside and guloside and methyl α-L-rhamnoside, in aqueous alkali.

In conclusion, just as a wide range of rotational constants can be employed[7,8,12] in the determination of the molecular rotations of carbohydrates, a similar wide range is possible for the postulated change in the value of these with variations in the solvent or temperature. Moreover, this approach is also subject to all the limitations[10] caused by considering only one type of interaction. However, it is felt that the evidence presented here indicates that the concept of solvent dependent changes in the magnitude of these interactions (hypothesis b) can be at least as important as that of solvent induced changes in the conformational equilibria (hypothesis a). The evidence presented here also suggests that in the sugar residues which are important in biological systems there could be small, solvent dependent changes in the rotational equilibrium of the hydroxymethyl group around the C(5) - C(6) bond. Also the suggested explanation of the observed changes in the compensated molecular rotation when the solvent environment is altered involves small solvent induced changes in the ring chair conformation. This makes hypothesis (b) equivalent to hypothesis (a)

and a fuller understanding of the effect of solvent environment would have to consider both the direct and the indirect influences of any change in the solvent environment on the optical rotation of the residues which constitute the biological molecules.

CHAPTER 2

THE CHARACTERISATION OF THE LINKAGE ROTATIONS OF SOME DI, OLIGO AND POLYSACCHARIDES BY OPTICAL ROTATION MEASUREMENTS AT A SINGLE WAVELENGTH

INTRODUCTION

The overall shape of di, oligo and polysaccharides is determined by two factors.

a) The conformation of the individual monosaccharide residues.

b) The relative conformations of pairs of these residues around their glycosidic linkage.

The sugar residues in the carbohydrate oligomers and polymers which have been subjected to detailed conformational analysis exist in the expected ring chair conformations. Thus if a reasonable value (usually around 117°) is assumed for the C-O-C bond angle associated with the glycosidic linkage only two more variables require to be defined to determine the conformation of a disaccharide unit. These are the torsional angles, ϕ and ψ, around the glycosidic linkage and are illustrated in fig. 2.1 for cellobiose.

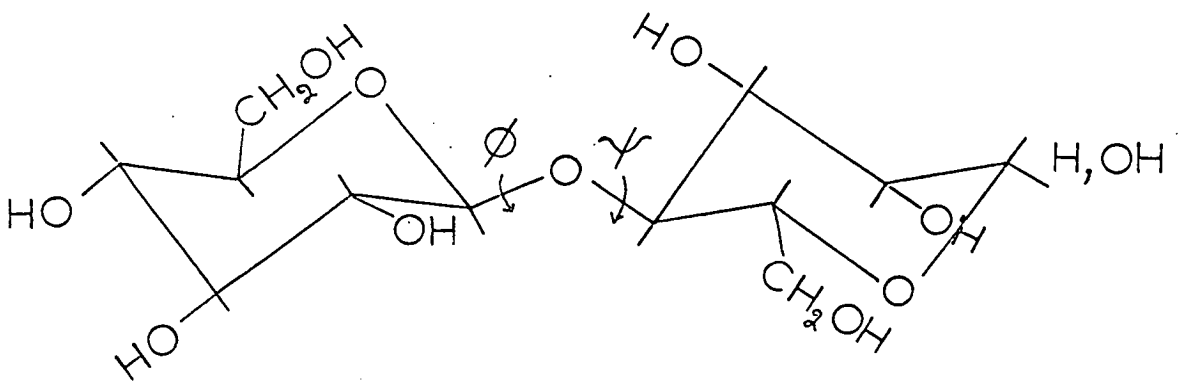

Fig. 2.1

The definition of the conformation with $\phi = \psi = 0$ is an arbitrary one and as yet no standard definition has been agreed. In this study Rees'[15] notation, $\Delta\phi$ $\Delta\psi$, is used for which the angles are measured from the positions which bisect the reflex angles O(5) - C(1) - C(2) and C(3) - C(4) - C(5) respectively (for a 1,4-linkage) and have the positive directions given in Appendix 1.

The methods now in use for the calculation of the conformational energies of polysaccharides have recently been assessed[88] and it was concluded that even though the energy functions remain incompletely developed and tested, conformational analysis can still make useful predictions for polysaccharides. Despite uncertainties about the energies arising from polar, torsional and hydrogen bonding interactions the interatomic distances at which van der Waals repulsion becomes intolerably severe are well known for most pairs of atoms and can be used as a first approximation to the assessment of conformational stabilities[89]. Conformations are said to be "fully allowed" if all pairs of atoms are separated by greater distances than the sum of their van der Waals radii and "marginally allowed" if some separation distances are closer than this sum but no closer than 0.9 of this sum. All possible conformations may be sampled by using a computer to step through $\Delta\phi$ and $\Delta\psi$ and the results are normally plotted as a conformational map. More than 90% of the conformations on the map are disallowed[16], as shown in fig. 2.2 for α-1,2; α-1,3 and α-1,4 linked glucobiose residues. It is also noticeable that the maps are rather similar when the convention for ϕ and ψ which is used in this Chapter is employed and this similarity is also apparent when energy functions are used[90].

For α-1,4 and β-1,4 linked polysaccharides it is possible to evaluate these energy calculations by comparing them with model

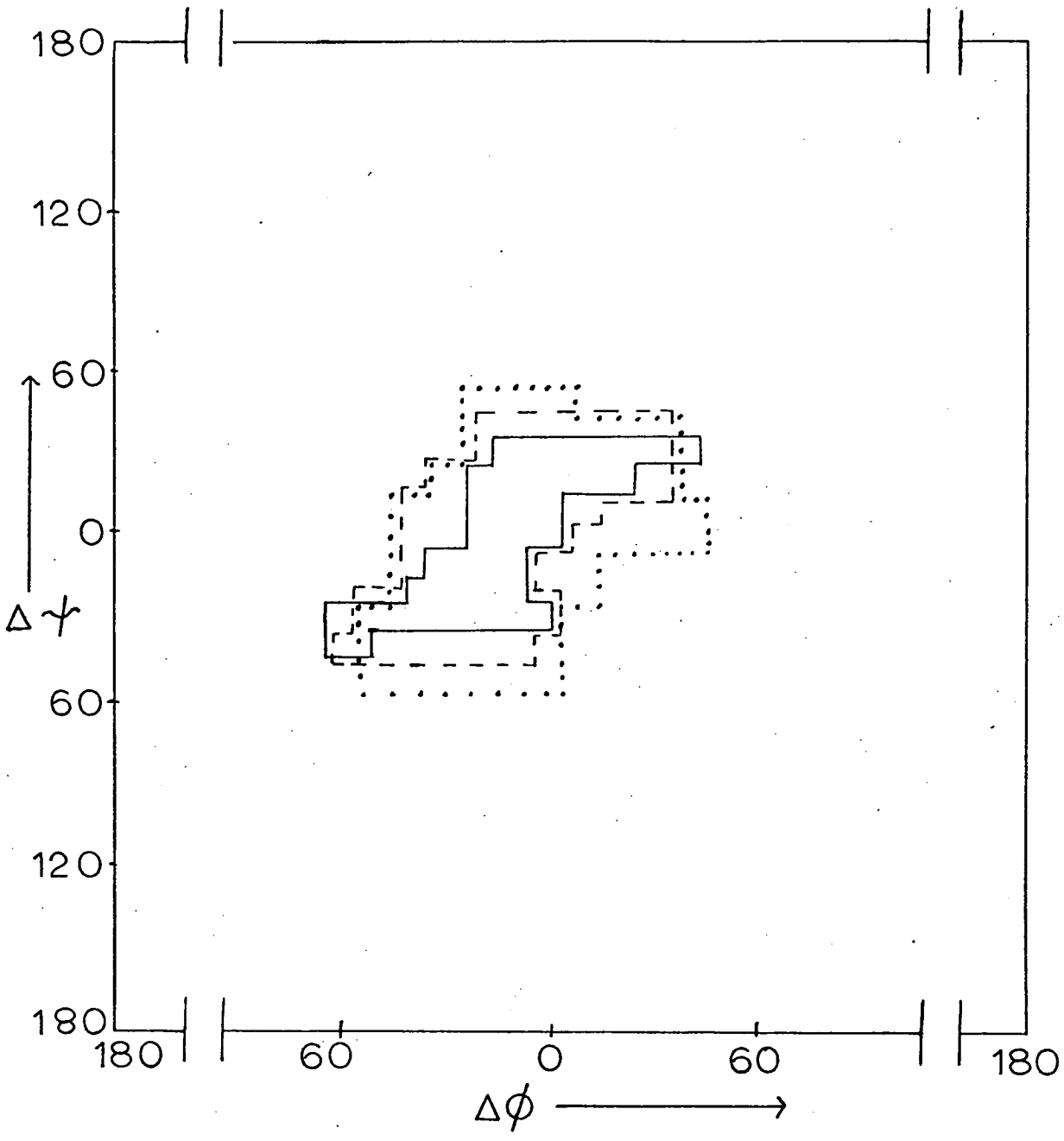

Fig. 2.2 Conformational map for α-1,4, α-1,3 and α-1,2 glucans; the allowed conformations are enclosed by continuous, broken and dotted lines respectively. The map is a corrected version of the one in ref. 14.

crystal structures. Fig. 2.3 shows the energy maps derived for β-1,4[49] and α-1,4[91,97] linkages by stepping the angles $\Delta\phi$ and $\Delta\psi$ through small increments and computing the van der Waals energy at each stage. The most likely hydrogen bond across the β-1,4 linkage is between O(3′) and O(5) (fig. 2.4(a)) and across the α-1,4 linkage it is between O(3′) and O(2) (fig. 2.4 (b)). The boundaries of these hydrogen bonds as determined by the O...O distances are shown in fig. 2.3 by the dotted lines.

The β-1,4 linked disaccharides β-cellobiose[92] and methyl β-cellobioside[93] have slightly different crystal conformations but both lie in that region of the map which offers the best compromise between van der Waals energy and hydrogen bonding. For comparison

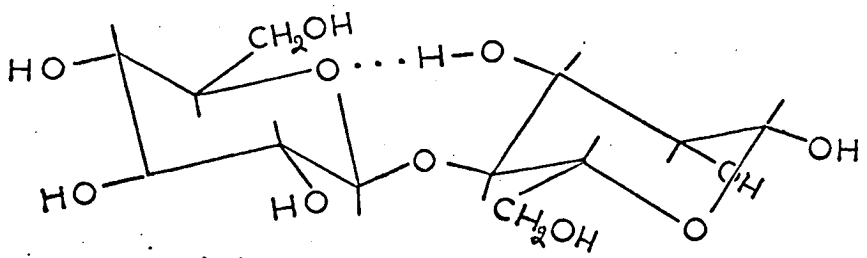

(a) Cellobiose

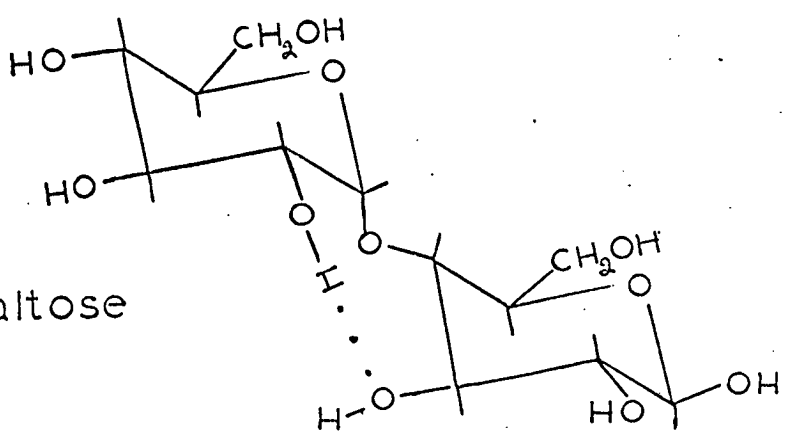

(b) Maltose

Fig. 2.4

the "bent chain" conformation of cellulose is also shown and it lies in the same region as the established disaccharide conformations and appears to be stabilised in the same way. For the α-1,4 linkages similar correlations emerge that only a narrow band of the map allows

Fig. 2.3 Comparison of the conformations of glycosidic linkages in di and oligosaccharide crystals with conformational energies and with possible polysaccharide conformations. The limits of the possible hydrogen bonds described in the text are indicated by the dotted lines. The van der Waals energies are shown by the contours of constant energy and are in k cal. (1 k cal. = 4.2 kJ). When the results were given in terms of other conventions for ϕ and ψ they were converted to $\Delta\phi$ and $\Delta\psi$ using the approximate relations given in ref. 15.

(a) β-1,4 Linkage; the symbols are ●, β-cellobiose[92]; □, methyl β-cellobioside[93]; O, the "bent chain" conformation for cellulose. The map is adapted from ref. 49..

(b) α-1,4 Linkage; the symbols are ●, β-maltose[94]; ▲, cyclohexa-amylose[95], □, methyl β-maltoside[96]; O, left handed v-amylose; △, left handed hollow helix model for B-amylose.

The map is adapted from refs. 91 and 97.

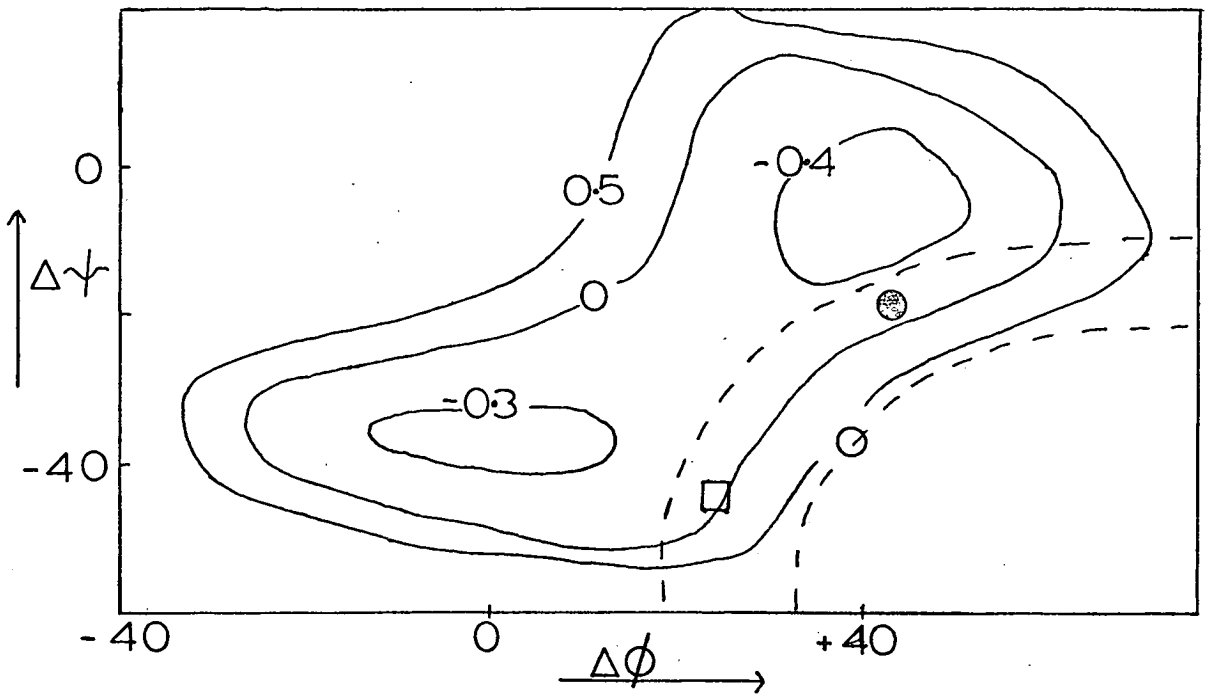

(a)

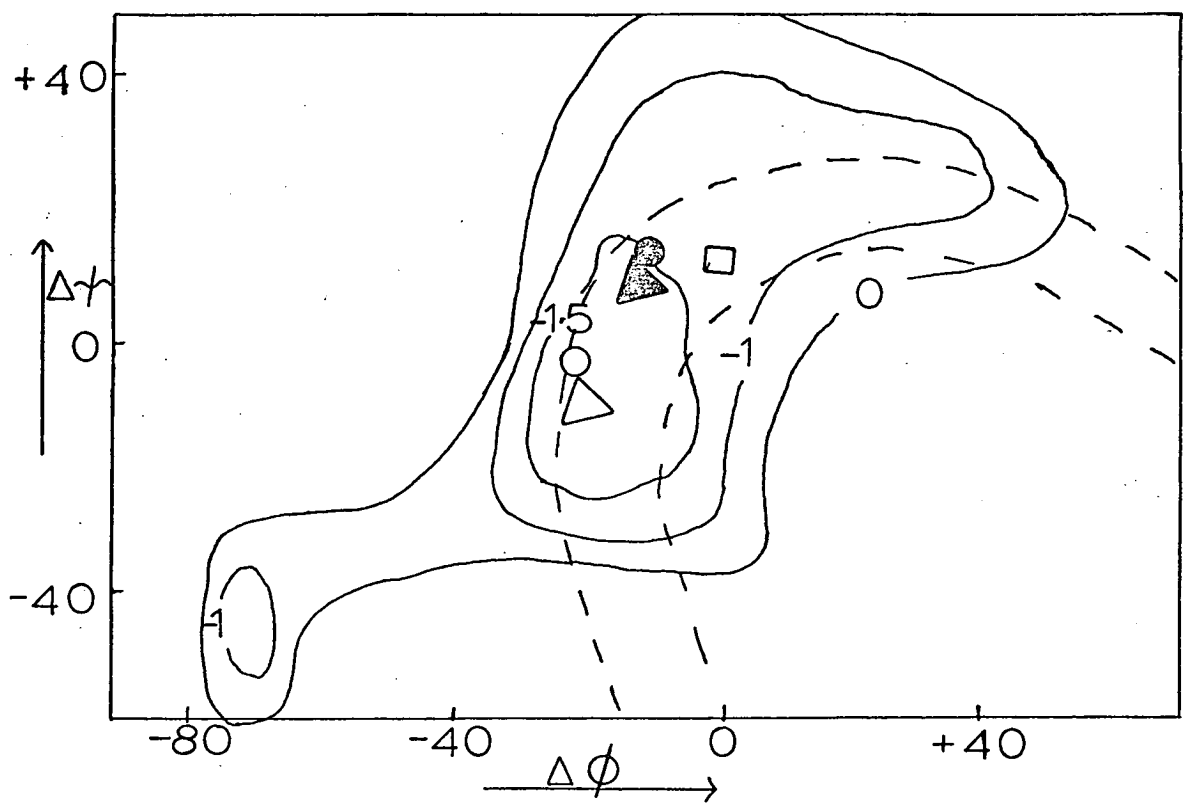

(b)

Fig. 2.3 The legend is given opposite

simultaneous hydrogen bonding and low van der Waals energy and all the experimentally established conformations of small molecules lie in this. The left handed V-amylose and the "hollow helix" β-amylose conformations relate to the model compounds in the same way cellulose did to its own series.

Investigation of the Linkage Conformation in Solution

Although ordered conformations of polysaccharides are likely to be found in the solid state due to cooperative effects between chains as well as within them, in a typical polymer conformational entropy is likely to offset this in solution, because of the possibility of rotation about a large number of bonds in the molecule with very little change in its internal energy, and thus a random coil is normally to be expected. It is presumed that the fluctuations in $\Delta\phi$ and $\Delta\psi$ at each linkage will be confined to values within the allowed area of the conformational map for most of the time. Thus the populations of particular conformations could be calculated from the Boltzman distribution law and an average $\Delta\phi$ and $\Delta\psi$ derived from this to specify an "average linkage conformation".

The first and one of the most elegant methods for experimentally investigating linkage conformation was by ^{1}H n.m.r. spectroscopy in dimethyl sulphoxide solution using the observable hydroxy proton resonances. These resonances show a downfield shift when they are involved in intra-molecular hydrogen bonding. For example the presence of the O(3′)...O(2) hydrogen bond in α-1,4 di and oligosaccharides and amylose could be demonstrated in this way[98]. The proportion of conformers having this hydrogen bond was found to diminish in the order cyclodextrins > amylose > maltodextrins > maltose and this is consistent with the evidence from optical rotation

measurements which will be discussed later in this Chapter. For β-1,4 glucans the spectra were consistent[98,99] with the presence of the O(3′)...O(5) hydrogen bond. The influence of competition and steric effects that may alter the solvent-solute hydrogen bonding must also be considered when this method is used but these complications appear to be readily predictable[100].

A rough correlation also exists between the chemical shift of H(1) and the value of $\Delta\phi$ presumably due to the diamagnetic shielding by the aglycone bond[100,101]. Although only $\Delta\phi$ can usually be estimated and the effects are small the method can, in principle, be applied in any solvent including water and is, therefore, more versatile than the method described above. More recently ^{13}C n.m.r.[102] has also been used to gain information about linkage conformations in aqueous solution. This method shows great promise and the results will be discussed later in this Chapter.

Finally it has been shown[15,16,22] that the optical rotation of di, oligo and polysaccharides can be empirically related to the linkage conformation in solution and this treatment has been discussed in the General Introduction. As already mentioned this one parameter is insufficient to determine $\Delta\phi$ and $\Delta\psi$ but it can be used to determine whether the crystal conformations of di and oligosaccharides dominate in solution and an example of this is given in Appendix 1 for methyl-β-cellobioside. Similarly the linkage rotations of the conformations suggested by n.m.r. measurements or by conformational analyses can be compared with the experimentally observed values. Moreover conformational principles and the shift in the linkage rotation $[\Lambda_{obs}]_D$ can show[16] how the linkage conformation is influenced by structural change and by attractions and repulsions such as van der Waals interactions, dipolar interactions and inter-residue hydrogen bonding.

In this Chapter the effect of solvent and temperature on the linkage rotations of a few disaccharide glycosides has been studied. Using the results of this study, along with conformational analysis, a suggested explanation is given for the observed anomalous linkage rotation of cyclohexa-amylose in aqueous solution. The implications of this hypothesis on the solution conformations of the larger cyclodextrins, the maltodextrins and amylose, as indicated by their optical rotation, are also discussed.

EXPERIMENTAL

1. Preparation of Samples

Methyl β-cellobioside was a gift from Dr I.C.M. Dea and had m.p. 187-191°C; $[\alpha]_D^{25°C}$ = -18.1°; lit. value m.p. 193°C; $[\alpha]_D$ = -19.1 (Micheel). The methyl α-sophoroside was prepared by W.G. Blann and had m.p. 251-255°C; $[\alpha]_D^{25°C}$ = 63.7°.

1. (a). Preparation of Anhydrous 1-O-(α-D-Glucopyranosyl)-O-α-D-Glucopyranoside (α,α-Trehalose)

α,α-Trehalose crystals from a commercial source (Nutritional Biochemicals Corporation, Cleveland, Ohio) were dissolved in ethanol and a small volume of benzene was added before removal of solvent using a rotary evaporator. This was repeated twice and was followed by twice repeating the process using ethanol alone. The sample was recrystallised from ethanol, dried overnight in a vacuum desiccator and stored tightly sealed: m.p. 207-211°C; lit. value m.p. = 203°C (Micheel).

1. (b). Preparation of Methyl β-Maltoside Monohydrate[103]

(i) Preparation of Methyl Hepta-O-acetyl-β-Maltoside

Finely powdered maltose (50 g) was suspended in acetic acid (250 ml) and acetic anhydride (125 ml). Perchloric acid (1.5 ml) was added to the cooled, stirred mixture and the flask was stirred for 90 minutes. The clear solution was cooled to 0°C and a 40% w/v solution of hydrogen bromide in glacial acetic acid (200 ml) added. The mixture was allowed to warm to room temperature and was then poured into 1.5 litres of ice-cold water and stirred for 15 minutes. The sticky precipitate was filtered off, washed twice with water and dissolved in chloroform. The chloroform solution was washed once with water, once with aqueous sodium bicarbonate and once more with water before being dried overnight over anhydrous magnesium sulphate. The chloroform solution was filtered and concentrated to a thick syrup.

This amorphous hepta-o-acetyl-α-maltosyl bromide was shaken in benzene (225 ml) and methanol (45 ml) in the presence of mercuric cyanide (45 g) for 3 hours. 1,2 Dichloroethane (750 ml) was added and the resulting solution washed with water until the washings gave no precipitate with silver nitrate solution. The solution was dried over anhydrous magnesium sulphate, filtered and concentrated to a syrup which crystallised on the addition of ethanol. The crystals were recrystallised twice from ethanol and had m.p. 125 - 128°C; lit. value 128 - 129°C (Micheel). The yield was 21 g ($\sim$ 22% overall from maltose).

(ii) Preparation of Methyl β-Maltoside Monohydrate

The methyl, hepta-o-acetyl-β-maltoside (21 g) was refluxed for 5 hrs in anhydrous methanol (150 ml) containing n-butylamine (4 ml). The solution was concentrated to a thick syrup which was dissolved in ethanol, a small amount of benzene added and the solvent taken off on a rotary evaporator. A white amorphous solid (10.8 g) was obtained and infra red showed no sign of the acetate carbonyl peak at 1750 cm^{-1} but gave a peak at 1660 cm^{-1} and a large broad hydroxyl stretching peak centred at 3750 cm^{-1}. The sample was recrystallised twice from ethanol and dried in a vacuum desiccator: m.p. 107 - 110°C; $[\alpha]_D^{25°C} = 77.1°$; lit. value m.p. 110 - 111°C; $[\alpha]_D = 78.8$ (Micheel).

1.(c). Preparation of 1,5 Anhydro 4-(O-β-D-Glucopyranosyl)-D-Sorbitol

(i) Preparation of Thiophenyl, Hepta-o-Acetyl β-Cellobioside[104]

Octa-o -acetyl cellobiose (30 g) was suspended in chloroform (50 ml) and 45% w/v hydrogen bromide in glacial acetic acid (150 ml) added. The mixture was shaken for 10 minutes and the resulting solution allowed to stand for a further 90 minutes before being

poured into ice-cold water. The chloroform layer was separated and the water layer twice more extracted with chloroform. The combined extracts were washed with water and concentrated to ~ 100 ml.

This chloroform solution was added, without drying, to ~0.45N alcoholic caustic potash (100 ml), prepared by dispersing potassium hydroxide (2.5 g) in ethanol to which thiophenol (4.8 ml) had been added. The condensation was completed by warming the mixture (45 - 50°C) for 1 hr. The clear liquor with its crystalline deposit of potassium bromide was repeatedly washed in a separatory funnel with dilute aqueous sodium bicarbonate until the odour of the thioalcohol became faint. The chloroform solution was finally washed with water and dried over anhydrous calcium chloride. The solution was then concentrated to a thin syrup and the phenyl-1-thio, hepta-o-acetyl-β-cellobioside precipitated by the careful addition of light petroleum. The crystals were twice recrystallised by dissolving them in warm chloroform (100 ml) and precipitating them by the addition of hot absolute alcohol: m.p. 220 - 223°C; lit. value 225 - 226°C; yield 17.5 g.

(ii) Preparation of Hepta-o-Acetyl 1,5 Anhydro 4-(O-β-D-Glucopyranosyl)-D-Sorbitol[105]

The phenyl-1-thio, hepta-o-acetyl-β-cellobioside (17.5 g) was suspended in absolute alcohol (150 ml) and to this was added Raney-nickel (150 g) in absolute alcohol, which had been freshly prepared as indicated in the General Methods section. The mixture was refluxed gently for 1 hr and, after cooling, the supernatant solution was decanted and the nickel washed by decantation with three successive portions (150 ml) of boiling absolute alcohol. The combined

decantates were filtered through a scintered glass funnel and concentrated to ~ 800 ml where crystallisation was spontaneous as a mass of fine needle shaped crystals. These were filtered off and dried in a vacuum desiccator; yield 6.8 g. The product was twice recrystallised from ethanol and had m.p. 190 - 193°C; lit. value 194 - 195°C[105].

(iii) Preparation of 1,5 Anhydro 4-(O-β-D-Glucopyranosyl)-D-Sorbitol

The hepta-o-acetyl 1,5 anhydro 4-(O-β-D-glucopyranosyl)-D-sorbitol was dissolved in anhydrous methanol (60 ml). To this was added 5 ml of a freshly prepared solution of sodium methoxide (0.1 g sodium in 20 ml anhydrous methanol). The reaction mixture was allowed to stand at room temperature overnight and after checking it was still alkaline to phenolphthalein an equal volume of water was added. The solution was neutralised by stirring it with I.R. 120 Amberlite resin (25 ml) in the hydrogen form and the resin filtered off. The clear solution was evaporated to dryness, anhydrous methanol (50 ml) added and the solution again evaporated to dryness. This was repeated before the product was recrystallised twice from ethanol; yield, 2 g; m.p. 167 - 170°C; lit. value 172°C[105].

2. Solvents Used in the Optical Rotation Measurements

The measurement of the optical rotation against temperature was carried out in distilled water, dimethyl sulphoxide and, for the methyl β-maltoside, dioxan. It was not possible to dissolve a sufficient quantity of the other samples in dioxan to measure the variation of their optical rotation with temperature. The dimethyl sulphoxide and dioxan were redistilled before use as described in Chapter 1.

3. Preparation of Sample Solutions

The solutions used for the optical rotation measurements were

made up in volumetric flasks and had accurately recorded concentrations of the order of 1 - 1.5 g/100 ml. For α,α-trehalose a smaller concentration, which gave a reading on the polarimeter close to 1°, was used. For the solution of methyl β-maltoside in dioxan the maximum amount which could be dissolved ($\sim$ 0.1 g/100 ml) was used. All solutions were millipore filtered and transferred to the polarimeter cell in one operation using a syringe.

4. Measurement of Optical Rotation against Temperature

The optical rotation measurements were carried out as described in Chapter 1 and the readings were corrected for the cell blank of the cell containing the appropriate solvent as described in the General Methods section. The specific and molecular rotations of the sample solutions at each wavelength and temperature were calculated using the formulae given in the General Introduction. These were normalised for comparison with the values at $25^{\circ}C$, in the same solvent, by compensating for the change in refractive index and density using the equation given in the Experimental section of Chapter 1.

RESULTS AND DISCUSSION

As described in Chapter 1, the normalised molecular and specific rotations were plotted against temperature and the best curves drawn through the points. As for the monosaccharide methyl glycosides the change in the molecular rotation with temperature was small and either linear or could be best fitted by a shallow curve. The points on the graph lie very close to the best curve for the measurements made in distilled water and dimethyl sulphoxide but the measurements for methyl β-maltoside in dioxan are more scattered about the best curve because of errors in these measurements caused by the very limited solubility. As in Chapter 1 to compare the values in dimethyl sulphoxide and dioxan with those recorded in water the normalised molecular and specific rotations were compensated for the change in the solvent refractive index using the equation:[74]

$$\left.\begin{matrix}\text{c.m.r.}\\ \text{c.s.r.}\end{matrix}\right\} = \left.\begin{matrix}(\text{normalised mol. rot.})_S^{T^\circ C}\\ (\text{normalised specific rot.})_S^{T^\circ C}\end{matrix}\right\} \cdot \frac{(n_{H_2O}^{25^\circ C})^2 + 2}{(n_S^{25^\circ C})^2 + 2}$$

The normalised molecular and specific rotations at $T^\circ C$ in the solvent (S) which has the refractive index ($n_S^{25^\circ C}$) at $25^\circ C$, were taken from the best curves drawn through the points on their respective graphs and ($n_{H_2O}^{25^\circ C}$) is the refractive index of water at $25^\circ C$. These compensated rotations are, therefore, the normalised molecular or specific rotations referred to the refractive index of water at $25^\circ C$ and they are given in table 2.1; the compensated specific rotations are given in the brackets. Only the results obtained at the sodium D line, 589 nm, are recorded in table 2.1 the results obtained at 546 nm being given in Appendix 3.

The values for the compensated molecular rotation (c.m.r.) of the disaccharide glycosides, at 589 nm, can now be used, along

TABLE 2.1

The Variation of the Compensated Molecular and Specific (in brackets) Rotations with Temperature at λ_{589}

Sample	Solvent	Value of c.m.r. and c.s.r. (in brackets) at the temperature indicated							
		20	25	30	40	50	60	70	80
Methyl β-cellobioside	H_2O	-65.3	-64.6	-63.9	-62.6	-61.5	-60.7	-60.0	-59.5
		(-18.3)	(-18.1)	(-17.9)	(-17.7)	(-17.4)	(-17.1)	(-16.9)	(-16.8)
	DMSO	-69.2	-67.8	-66.5	-64.2	-63.2	-60.7	-59.3	-58.2
		(-19.6)	(-19.2)	(-18.7)	(-18.0)	(-17.4)	(-17.0)	(-16.6)	(-16.3)
Methyl β-maltoside	H_2O	288.2	288.3	288.4	288.6	288.9	289.1	289.4	289.7
Monohydrate		(77.1)	(77.1)	(77.1)	(77.2)	(77.3)	(77.4)	(77.4)	(77.4)
	DMSO	214.6	216.7	218.8	222.5	225.8	229.0	231.8	234.4
		(57.5)	(58.0)	(58.5)	(59.5)	(60.4)	(61.2)	(62.0)	(62.7)
	Dioxan	213.6	216.6	219.5	224.5	228.5	231.8	233.9	235.5
		(57.1)	(58.0)	(58.8)	(60.3)	(61.4)	(62.2)	(62.7)	(63.0)
Methyl α-sophoroside	H_2O	226.9	227.0	227.1	227.3	227.5	227.7	227.7	227.7
		(63.7)	(63.7)	(63.8)	(63.9)	(63.9)	(64.0)	(63.9)	(63.9)
	DMSO	225.2	225.6	226.0	226.6	227.2	227.1	226.5	225.8
		(63.1)	(63.3)	(63.4)	(63.7)	(63.8)	(63.8)	(63.6)	(63.4)

TABLE 2.1 (Continued)

Sample	Solvent	Value of c.m.r. and c.s.r. (in brackets) at the temperature indicated							
		20	25	30	40	50	60	70	80
α,α-Trehalose	H_2O	626.5	626.3	626.1	625.7	625.3	624.9	624.5	624.1
		(183.0)	(183.0)	(182.9)	(182.9)	(182.8)	(182.7)	(182.5)	(182.4)
	DMSO	579.3	580.2	581.1	582.4	584.3	585.3	586.1	586.6
		(169.3)	(169.6)	(169.8)	(170.3)	(170.6)	(170.9)	(171.2)	(171.4)
1,5 Anhydro 4-(O-β-D-glucopyranosyl)	H_2O	94.9	94.8	94.6	94.2	93.8	93.2	92.4	91.4
		(29.1)	(29.0)	(29.0)	(28.9)	(28.7)	(28.6)	(28.3)	(28.0)
D-sorbitol	DMSO	78.7	78.3	78.0	77.1	76.2	75.2	74.1	72.8
		(24.1)	(24.0)	(23.9)	(23.6)	(23.3)	(23.0)	(22.7)	(22.3)

TABLE 2.2

The Variation of the Di saccharide Linkage Rotation $[\Lambda obs.]$ with Temperature at 589 nm

		Value of $[\Lambda obs.]$ at the temperature indicated							
Sample	Solvent	20	25	30	40	50	60	70	80
Methyl β-cellobioside	H_2O	59.1	59.4	59.5	59.6	59.7	59.5	59.4	59.3
	DMSO	59.8	58.6	58.3	57.2	55.0	54.5	53.7	52.4
Methyl β-maltoside	H_2O	46.7	46.3	45.9	45.0	44.3	43.5	42.9	42.3
Monohydrate	DMSO	-19.7	-18.9	-17.5	-15.4	-13.6	-11.7	- 9.7	- 7.9
	Dioxan	-24.5	-22.8	-21.3	-18.1	-15.3	-12.5	-10.6	- 9.1
Methyl α-sophoroside	H_2O	-14.6	-15.0	-15.4	-16.3	-17.1	-17.9	-18.8	-19.7
	DMSO	- 9.1	-10.0	-10.3	-11.3	-12.2	-13.6	-15.0	-16.5
α, α-Trehalose	H_2O	+19.1	+18.3	+17.7	+16.3	+14.9	+13.5	+12.1	+10.5
	DMSO	-18.3	-17.4	-16.3	-14.4	-12.7	-11.3	- 9.9	- 8.6

with the c.m.r. values of the methyl α and β-D glucopyranosides given in table 1.1, to calculate the observed linkage rotation $[\Lambda_{obs}]_D$ for the disaccharides by using equation (1) given in the General Introduction. The empirical method is also given in more detail in Appendix 1 and an example of the calculation of $[\Lambda_{obs}]_D$ is also given for methyl β-cellobioside in aqueous solution. The variation of the linkage rotation of the disaccharides with temperature in the solvents studied is given in table 2.2. This type of approach means that the variation of $[\Lambda_{obs}]_D$ with temperature contains no contribution from the monosaccharide residues which make up the disaccharide and no contribution from any possible change in the rotational equilibrium around the C(1) - OCH_3 bond. Moreover the use of the monosaccharide and disaccharide glycosides in the determination of $[\Lambda_{obs}]_D$ avoids any possible errors due to differences in the mutarotation equilibria of the parent mono and disaccharides.

β-Linked Disaccharides

The graph of the linkage rotation $[\Lambda_{obs}]_D$ against temperature for the β-linked disaccharides, methyl β-cellobioside and methyl α-sophoroside, in water and dimethyl sulphoxide is given in fig. 2.5. For methyl β-cellobioside it can be seen that the $[\Lambda_{obs}]_D^{25°C}$ are very similar in both solvents although the values do diverge at higher temperatures. This indicates that at room temperature the preferred conformations of methyl β-cellobioside in both these solvents may be very similar. Moreover, the values of ϕ and ψ which have been calculated[49] from the crystal coordinates for β-cellobiose[92] correspond to $\Delta\phi = 42°$, $\Delta\psi = -18°$, i.e. $[\Lambda_{calc}]_D = 62°$, which is in remarkably good agreement with the observed values in both solvents (fig. 2.5 and table 2.2). Independent confirmation that

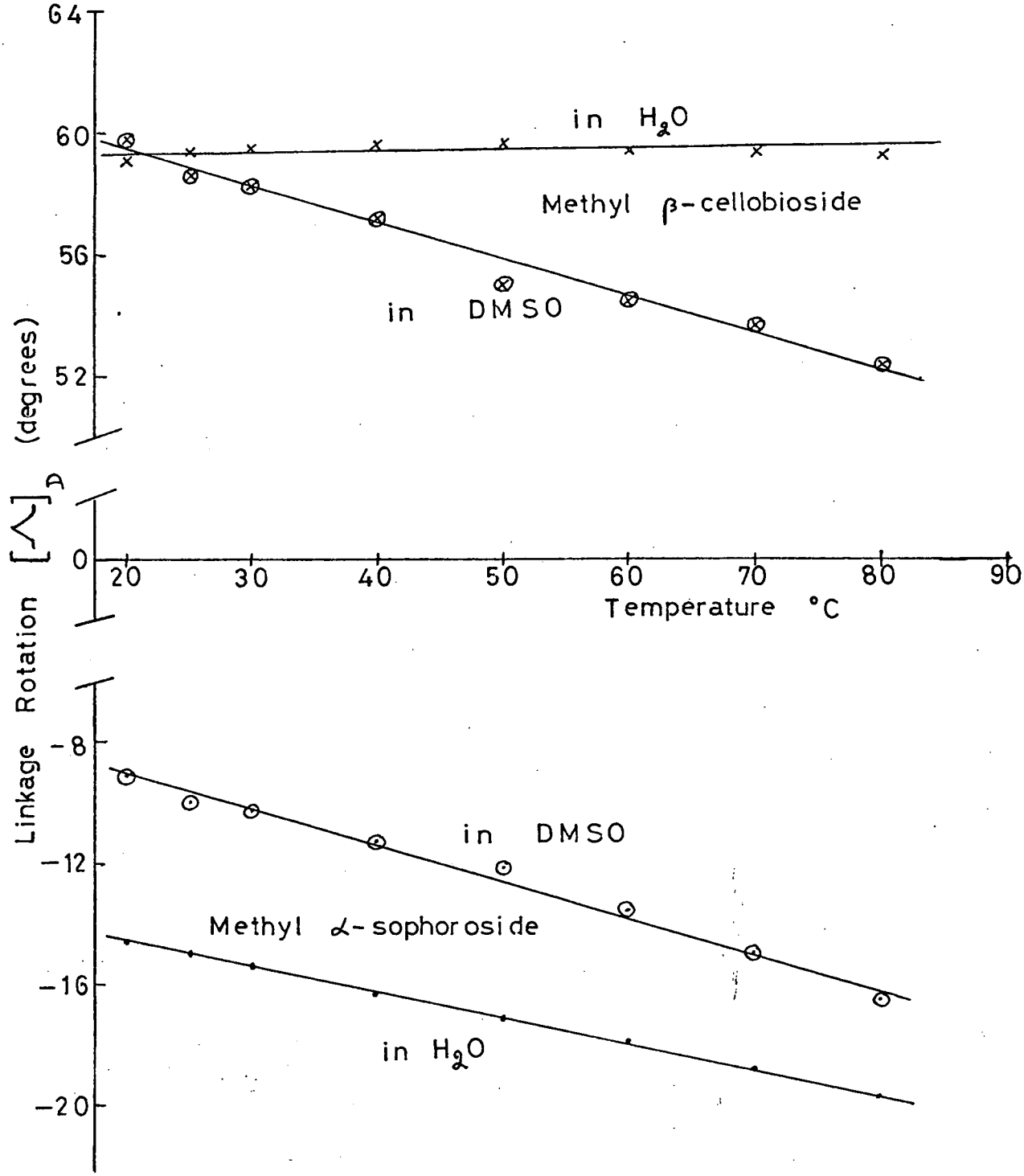

Fig. 2.5 Graph of the linkage rotation $[\Lambda]_D$ against temperature for β-linked disaccharides.

the crystal and solution conformations are similar comes from the ^{1}H n.m.r. of cellobiose in dimethyl sulphoxide (Introduction to this Chapter and ref.98) which shows that there is a hydrogen bond to O(5) which is likely the O(3') ... O(5) bond observed in the crystal.

This agreement between the observed and calculated rotations does not suggest that the disaccharide is locked in its crystal conformation in solution but rather than the intramolecular energy is near the minimum in the crystal conformation and indeed calculations indicate that the cellobiose crystal conformation is very close to the minimum of van der Waals and hydrogen bond energy (Introduction to this Chapter). In solution it is expected that $\Delta\phi$ and $\Delta\psi$ will fluctuate about this minimum energy conformation but the observed agreement between $[\Lambda_{obs}]_D$ and $[\Lambda_{calc}]_D$ suggests that this oscillation is probably of very small amplitude at room temperature. From the Boltzmann distribution law the population of conformations with intramolecular energies greater than the minimum will be increased when the temperature is raised. The fact that the $[\Lambda_{obs}]_D$ in dimethyl sulphoxide decreases with increasing temperature while very little variation is observed in aqueous solution therefore suggests that either, in contrast to the aqueous solution, the energy well is not symmetrical in dimethyl sulphoxide or that the minimum energy conformation is stabilised by some additional factor when water is the solvent. One possibility for the latter suggestion comes from the work of Kobayama and Patterson[82] who have shown that the "bent chain" conformation of cellulose can be fitted into the tridymite water structure (discussed in Chapter 1) without undue distortion. This conformation is very similar (fig. 2.3) to the cellobiose crystal conformation and it is possible that in

aqueous solution compatibility with the "lattice water" may increase the relative stability of the minimum energy conformation.

For methyl α-sophoroside the $[\Lambda_{obs}]_D^{25°C}$ in water and dimethyl sulphoxide also have very similar magnitudes although their absolute values are very different from those observed for methyl β-cellobioside. As discussed in the General Introduction, Rees has shown that for di-equatorial glycosidic linkages the numerically averaged values of $\Delta\phi$ and $\Delta\psi$ ($\overline{\Delta\phi}$ and $\overline{\Delta\psi}$) are almost independent and that glucosyl oligomers may be assigned the cellobiose $\overline{\Delta\phi}$ value (42°). If this is done for methyl α-sophoroside we can therefore calculate the $\overline{\Delta\psi}$ value from the $[\Lambda_{obs}]_D$ given in table 2.2 using equation (3) given in the General Introduction. This has been done for the $[\Lambda_{obs}]_D^{25°C}$ in water and the $\overline{\Delta\psi}$ value is compared with that of methyl β-cellobioside in fig. 2.6. Examination of molecular models shows that replacement of the equatorial substituents adjacent to the glycosidic oxygen by smaller substituents allows much more freedom around the glycosidic linkage in methyl α-sophoroside than is possible for methyl β-cellobioside. This is in agreement with Rees' first rule[16]. Considering now the second rule the results obtained here suggest that replacement of the bulky hydroxymethyl group at R_3 in methyl β-cellobioside by a hydroxyl group in methyl α-sophoroside has a larger effect than the replacement of the hydroxyl group at R_2 by a hydrogen atom and leads to the observed shift of $\overline{\Delta\psi}$ to the right in methyl α-sophoroside. Another contributing factor may be that in addition to the possibility of an O(3') ... O(5) hydrogen bond similar to that suggested for methyl β-cellobioside an O(2) ...O(3') hydrogen bond is also possible for methyl α-sophoroside (fig. 2.7). A study of molecular models shows that $\overline{\Delta\psi} = 18°$ for methyl

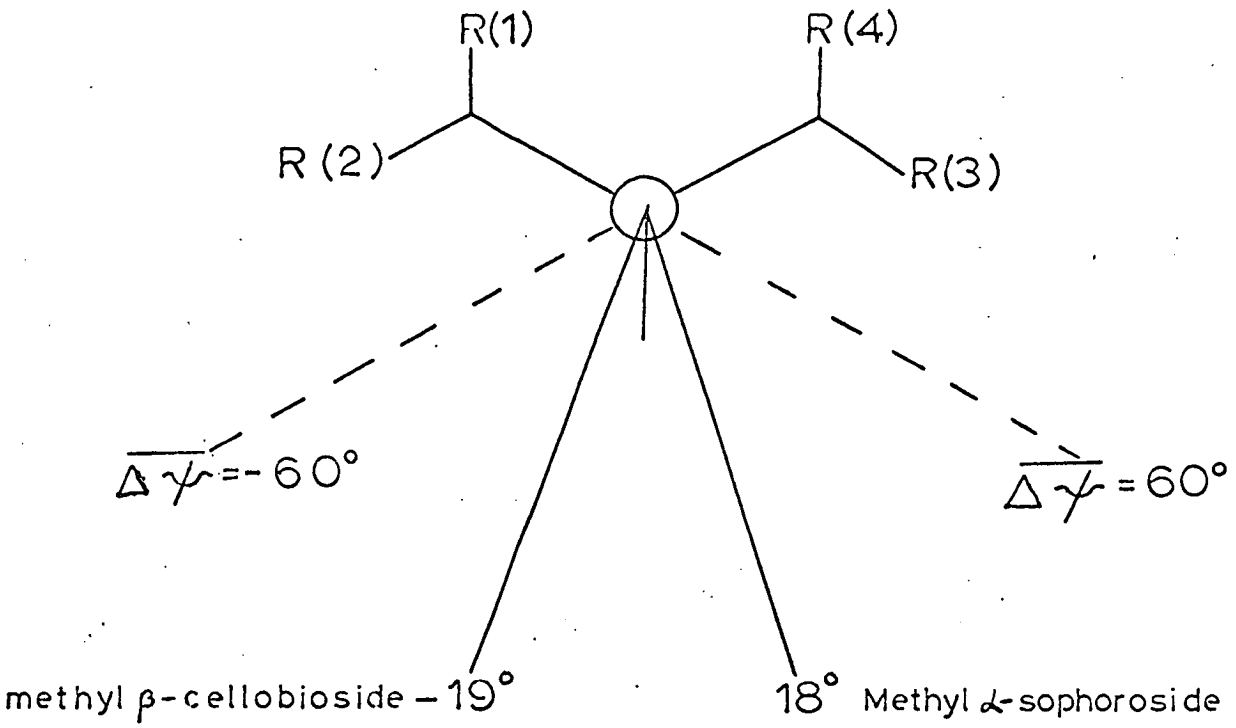

	R_1	R_2	R_3	R_4	$[\overline{\Delta\psi}]^{25°C}_{H_2O}$
Methyl β-Cellobioside	H	OH	CH_2OH	H	−19°
Methyl α-Sophoroside	OCH_3	H	OH	H	+18°

Fig. 2.6 Values of $\overline{\Delta\psi}$ calculated from the optical rotations of methyl β cellobioside and methyl α-sophoroside as described in the text. The stereochemistry about the aglycone bond is shown as a Newman projection down the bond, viewing from the glycosidic linkage.

Rees[16] has indicated how this method of plotting allows the results to be easily translated into models: i.e.

> a framework or Dreiding model of the disaccharide with $\Delta\phi$ fixed according to the assumption used (see text), is held so that the glycosidic oxygen is at the apex of the diagram, the aglycone bond is perpendicular to and pointing behind the diagram, and C–H is eclipsed by the line shown for $\Delta\psi = 0$; C(1) is then rotated about the aglycone bond until O(1)–C(1), projected onto the diagram and produced, passes through the point which is plotted for the compound.

Fig. 2.7 Possible O(2) ... O(3') hydrogen bond for methyl α-sophoroside

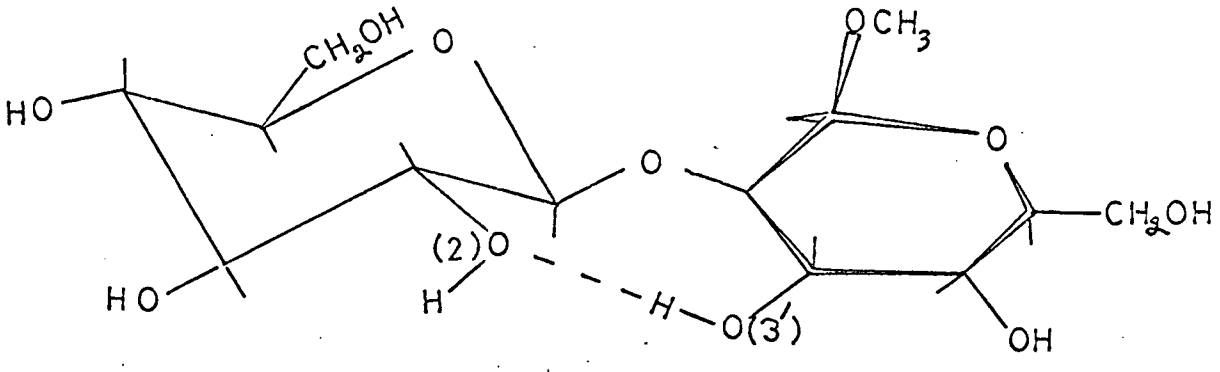

α-sophoroside is compatible with this latter hydrogen bond but indicates that it is unlikely that the molecule spends much of its time in the O(3') ... O(5) hydrogen bonded conformation since this has a very much larger $\Delta\psi$ value ($> +60^{\circ}$). When the solutions of methyl α-sophoroside are heated the $[\Lambda_{obs}]_D$ become more negative, as shown in fig. 2.5, and the $\overline{\Delta\psi}$ values more positive. This variation of the $[\Lambda_{obs}]_D$ values with temperature, in both solvents, again suggests that the energy well is shallow and unsymmetrical for this compound, the variation in dimethyl sulphoxide being only slightly greater than it is in water.

α-Linked Disaccharides

The graph of the linkage rotation $[\Lambda_{obs}]_D$ against temperature for the α-linked disaccharides, methyl β-maltoside and

α,α-trehalose, in the solvents studied is given in fig. 2.8 and it is immediately obvious that some additional factor must be considered in order to rationalise these observed linkage rotations. Thus, although the $[\Lambda_{obs}]_D$ of methyl β-maltoside in dimethyl sulphoxide and dioxan are very similar at room temperature and also give only small differences in the magnitude of their variation with temperature, the $[\Lambda_{obs}]_D$ in aqueous solution is grossly different both in its magnitude at room temperature and in the sign of its variation with temperature. A similar but smaller effect is also apparent for the observed linkage rotation of α,α-trehalose in dimethyl sulphoxide and water.

A comparison of the linkage rotations observed for methyl β-maltoside in this study with the calculated value, $\Delta\phi = -11^\circ$, $\Delta\psi = 13^\circ$, i.e. $[\Lambda_{calc}]_D = -109^\circ$, indicates that in all the solvents studied the crystal conformation[95] does not exist in solution. This is probably because in the crystal the linkage conformation is very close to the eclipsed position for both bonds and although the O(2) ... O(3') hydrogen bond could offset these repulsions in the crystal this is unlikely to occur in strongly hydrogen bonding solvents such as water or dimethyl sulphoxide. The van der Waals minimum is at $\Delta\phi = -30^\circ$, $\Delta\psi = -10^\circ$, i.e. $[\Lambda_{calc}]_D = -24$ [91]. Comparison of other calculations (fig. 2.3 and ref. 97) suggest an additional minimum which has been estimated at $\Delta\phi = -70^\circ, \Delta\psi = -30^\circ$, i.e. $[\Lambda_{calc}]_D = 68^\circ$ but could be in the region up to $\Delta\phi = -70^\circ, \Delta\psi = -50^\circ$. For the purposes of this discussion a value of $\Delta\phi = -70^\circ$, $\Delta\psi = -40^\circ$, i.e. $[\Lambda_{calc}]_D = 85^\circ$ will be used.

Rees[15] has suggested that methyl β-maltoside in dimethyl sulphoxide solution ($[\Lambda_{obs}]_D^{25^\circ C} = -18.9^\circ$ in this study) could be a

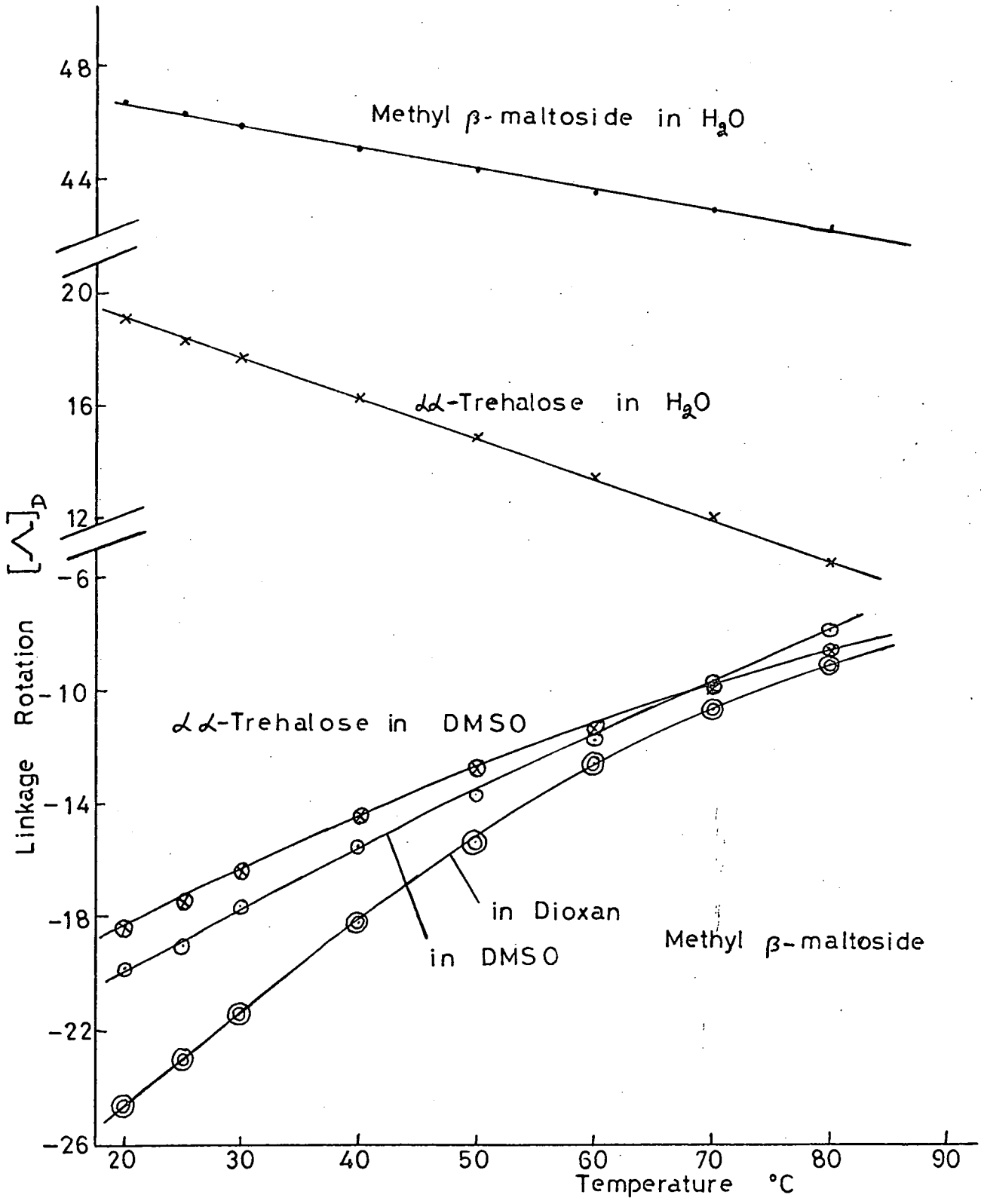

Fig. 2.8 Graph of the linkage rotation $[\Lambda]_D$ against temperature for α-linked disaccharides.

mixture of both of these conformations which minimise van der Waals repulsion with the hydrogen bonded crystal conformation. This is consistent with the evidence from ^{1}H n.m.r. spectroscopy where (i) the chemical shift of the anomeric proton suggests that the C(1) - H bond is on average further from the eclipsed position ($\Delta\phi = 0$) than the corresponding bond in cyclohexa-amylose[98,100,101](discussed later in this Chapter) and (ii) the downfield shift of O(2) and O(3) proton resonances of cycloamyloses, caused by hydrogen bonding of the type found in the crystal, is also observed for maltose but is less pronounced[98] showing that the molecule spends less of its time in a hydrogen bonded conformation. The shift is large enough, however, to suggest that the conformation with $[\Lambda_{calc}]_D = 85^\circ$ must make an appreciable contribution to the conformation. In the non polar solvent, dioxan, where there will be only weak solvent-solute association the methyl β-maltoside would be expected to spend more of its time in the hydrogen bonded conformation and consequently the $[\Lambda_{obs}]_D$ should be more negative than it is in dimethyl sulphoxide. This is in fact observed, $[\Lambda_{obs}]_D^{25^\circ C} = -22.8^\circ$, but the effect is very small. When both these solutions are heated the $[\Lambda_{obs}]_D$ become more positive as might have been expected since the effect of raising the temperature is to break down the hydrogen bond and increase the population of the other (more positive) conformations. Consistent with this the slope of the curve (fig. 2.8) is greater in dioxan than in dimethyl sulphoxide but again the effect is very small.

In aqueous solution the observed linkage rotation ($[\Lambda_{obs}]_D^{25^\circ C} = 46.3^\circ$) suggests that the molecule must spend a much larger proportion of its time in the conformation with $[\Lambda_{calc}]_D = 85^\circ$. Such a conformation has also been independently suggested[106] to account for

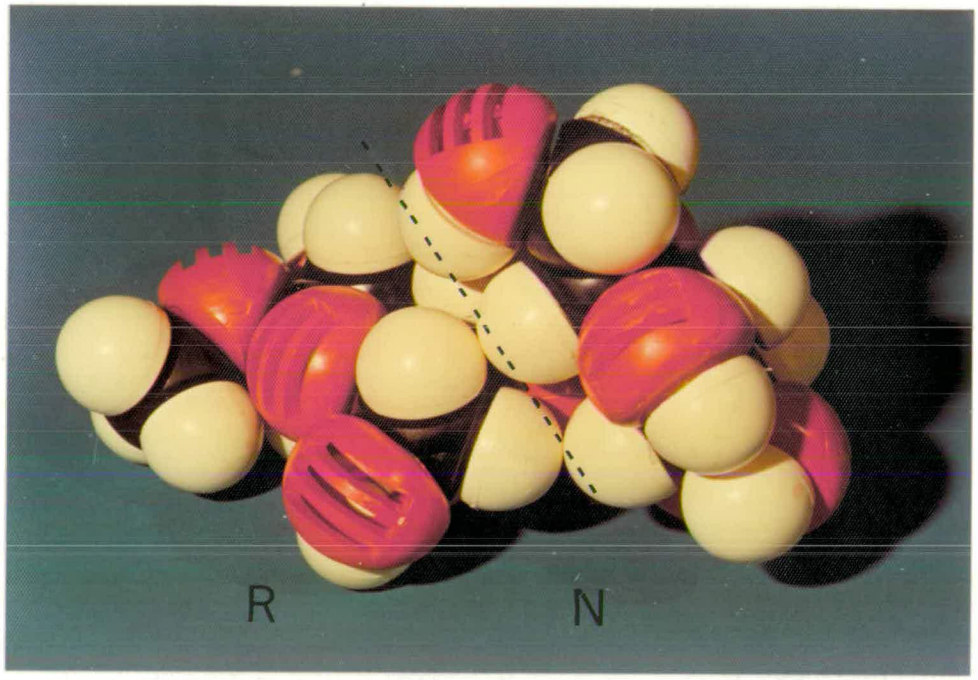

Fig. 2.9 A Corey-Pauling-Koltun (CPK) space filling model of methyl β-maltoside in the "folded" conformation. The hydrogen atoms H(4) and 2H(6) on the R residue are in contact with H(3) and H(5) on the N residue. It is not possible to arrange β-1,4 linked disaccharides into a similar conformation.

Table 2.3

The specific and linkage rotation of methyl β-maltoside in aqueous and 5 N NaOH solution.

Sample	Solvent	Specific Rot^n(589nm) $[\Lambda_{obs}]_D$		
Methyl α-D-glucopyranoside	H_2O	158.6°	a	
	5 N NaOH	155.5°	a	
Methyl β-D-glucopyranoside	H_2O	-32.8°	b	
	5N NaOH	-31.1°	b	
Methyl β-maltoside	H_2O	82.2°	a	
	5 N NaOH	66.0°	a	5°

a From ref. 107

b From ref. 75. The NaOH value was measured at 1 N but it does not change much with the strength of the alkaline solution and hence would introduce very little error into $[\Lambda_{obs}]_D$.

when the aqueous solution is made alkaline[76]. If the linkage rotation is calculated for this solvent change then it can be seen that, analogous to the results given in Chapter 1, the alkaline solution behaves like a water/dimethyl sulphoxide hybrid. This might have been expected on the basis of the above hypothesis since, as indicated in Chapter 1, the strongly solvated hydroxyl ion acts as a very effective structure breaker and creates considerable disorder in water. This would break down any water structure which may be the cause of the increased population of the conformation with $[\Lambda_{calc}]_D = 85°$ and this would be expected to lead to an increase in the population of the other conformations mentioned above, thus explaining the

observed negative shift of the $[\Lambda_{obs}]_D$ in 5 N NaOH. This hypothesis is also supported by ^{13}C n.m.r. to the extent that preliminary studies in alkaline solution show that the spectra have large differences from those in aqueous solution[102] and this should yield more information about the favoured conformations. Moreover, the observed negative shift in the linkage rotation in aqueous solution when the solution is heated is also consistent with the above theory since the effect of raising the temperature will again be (see Chapter 1) to break down the water structure.

Cyclohexa-amylose

In the potassium acetate complex of the looped hexasaccharide cyclohexa-amylose[95] each segment is locked in a hydrogen bonded conformation similar to fig. 2.4(b) and has $\Delta\phi = -9^\circ$, $\Delta\psi = 9^\circ$, i.e. $[\Lambda_{calc}] = -105^\circ$. In dimethyl sulphoxide solution the linkage rotation ($[\Lambda_{obs}]_D = -99^\circ$) is in very good agreement with the above value and this conformation is consistent with the observed ^1H n.m.r. results given earlier in this Chapter. In aqueous solution, however, the linkage rotation ($[\Lambda_{obs}]_D = -65^\circ$) is in very poor agreement with the value for the crystal structure. It has been pointed out[15] that, whereas dimethyl sulphoxide can form V-amylose complexes[107] and is therefore probably capable of solvating the cavity in the torus shaped molecule, in water the undistorted cavity would probably represent a source of high free energy due to the inherent shape of the hole coupled with the hydrophobic nature of the interior of the ring where the hydrogen atoms on C(3) and C(5) point towards the centre. This latter fact is also suggested by the tendency of the molecule to form inclusion complexes in aqueous solution[109]. When small amounts of alkanoic acids are

added shifts in the optical rotation are observed[110] which increase as the chain length of the non-polar paraffin chain increases and are caused by the alkyl chain rather than the carboxy-chromophore since they show no variation with wavelength down to 248 nm. The molecular rotation levels off at high alkyl chain length and corresponds to $[\Lambda_{obs}]_D = -90^\circ$. This value is in good agreement with conformational analysis but is rather lower than predicted from the crystal structure which suggests that in the crystal conformation hydrogen bonding occurs at the expense of angle strain. In aqueous solution this intramolecular hydrogen bonding would be very much weaker and the relief of the angle strain leads to a new conformation around $\Delta\phi = -20^\circ, \Delta\psi = 11^\circ$, i.e. $[\Lambda_{calc}]_D = -87^\circ$ on the conformational map given in fig. 2.3(b) and ref. 97 or given as $\Delta\phi = -15^\circ$ to -25°, $\Delta\psi = 11^\circ$ to 18°, i.e. $[\Lambda_{calc}]_D = -94^\circ$ [111]. Rees[15], therefore, concluded that the formation of an inclusion complex in aqueous solution relieves conformational distortion of an unknown kind in the cyclohexa-amylose molecule.

The results of this study, coupled with the indications from a very recent X-ray study of the structure of cyclohexa-amylose hexahydrate[112], may be used to suggest a possible explanation of this distortion. It was shown that, in contrast to the potassium acetate complex where the residues are located around a two fold axis, in the hexahydrate only four of the O(4) linking oxygens lie in a plane; the O(4) atom from one glucose residue being displaced from the plane by 0.71Å while the O(4) atom of the adjacent residue is displaced by -0.98Å. It, therefore, appears that in the hexahydrate the strain which is apparent in a model of the hexagonally symmetrical conformation is relieved by the rotation of a single

residue rather than a symmetrical puckering of the whole molecule. The angles $\Delta\phi$ and $\Delta\psi$ for all the linkages can be calculated from the crystal coordinates[113] and are given in table 2.4 along with their contribution to the average linkage rotation. Four of the

Table 2.4

The glycosidic angles for the cyclohexa-amylose hexahydrate crystal conformation.

Linkage	$\Delta\phi$	$\Delta\psi$	$[\Lambda_{calc}]_D$	Average $[\Lambda_{calc}]_D$
1,2	-8°	15°	-119.4°	
2,3	-18°	9°	-86.7°	
3,4	-16°	3°	-78.2°	-85.4°
4,5	-34°	-4°	-29.5°	
5,6	-33°	46°	-126.0°	
6,1	-20°	4°	-72.3°	

values of $\Delta\phi$ and $\Delta\psi$ are seen to be very similar but the other two are significantly different from these. However, when the linkage rotations are calculated from these using equation (3) given in the General Introduction it is seen that the differences in $\Delta\phi_{5,6}$ and $\Delta\psi_{5,6}$, from the four values which are reasonably close together, tend to cancel each other out and the $[\Lambda_{calc}]_D$ is not much changed from the $[\Lambda_{calc}]_D$ for the 1,2 linkage. In the case of the 4,5 linkage $\Delta\phi$ and $\Delta\psi$ are significantly different from the other values and the differences reinforce each other when the $[\Lambda_{calc}]_D$ is determined. Moreover, these values are tending towards the values for the "folded" conformation ($\Delta\phi = -70, \Delta\psi = -40$) of methyl β-maltoside and this is reflected by the fact that the calculated average linkage rotation of this crystal structure, $[\Lambda_{calc}]_D = -85°$, is closer to the observed linkage rotation, $[\Lambda_{obs}]_D = -65°$, in aqueous solution.

Using space filling molecular models and extrapolating from the above results it can be seen that one glucose residue in cyclohexa-amylose may rotate about its glycosidic linkages to approach a "folded" conformation. This would give an "intramolecular inclusion complex" for cyclohexa-amylose as shown in the photograph fig. 2.10 and in such a conformation the internal hydrogen atoms of the ring are juxtaposed thus increasing the net hydrophilic character of the ring and increasing its compatibility with the "lattice" water. Thus if the value $\Delta\phi = -70^\circ$, $\Delta\psi = -40^\circ$, i.e. $[\wedge_{calc}]_D = 85^\circ$ is substituted for the 4,5 linkage in table 2.4 and the other values remain unchanged then the average $[\wedge_{calc}]_D$ becomes -66.3° which is in very good agreement with the observed value (-65°) in aqueous solution. Alternately if one linkage is assumed to have the value $[\wedge_{calc}]_D = 85^\circ$ and all the others are assumed to be in the hydrogen bonded conformation, $[\wedge_{calc}]_D = -105^\circ$, the average linkage rotation $[\wedge_{calc}]_D = -73^\circ$ whereas if all the others are assumed to have the conformation calculated from conformational energy studies, $[\wedge_{calc}]_D = -90^\circ$, which is probably more likely in aqueous solution, the average $[\wedge_{calc}]_D = -61^\circ$, again in very good agreement with the observed value.

It is, therefore, considered that in aqueous solution cyclohexa-amylose may exist as an "intramolecular inclusion complex", with one linkage in the "folded" conformation previously suggested for methyl β-maltoside, thus making the molecule more compatible with the "lattice structure" of water. As shown in the photograph (fig. 2.10), in such a conformation the C(6) - OH group of the residue which has been rotated about its glycosidic linkage will also be in the correct position to form a strong hydrogen bond with the hydroxymethyl group on the residue on the opposite side of the ring and will give this structure

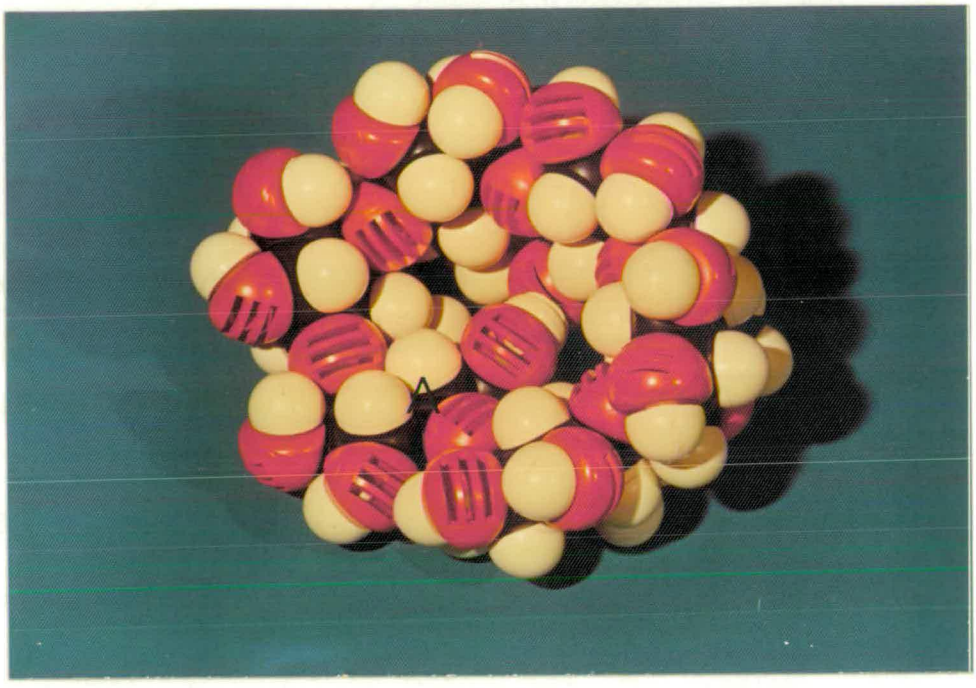

Fig. 2.10 A CPK space filling model of the suggested "intramolecular inclusion complex" formed by cyclohexaamylose in aqueous solution. In such a conformation one glucose residue (A) has rotated about its glycosidic linkage to approach the "folded" conformation previously suggested for methyl β-maltoside. In such a conformation the internal hydrogens of the ring are juxtaposed thus increasing the net hydrophilic character of the ring. The C(6)-OH group of the residue which has been rotated about its glycosidic linkage can also form a strong hydrogen bond with the hydroxymethyl group of the residue on the opposite side of the ring.

additional stability. There is no reason why this conformation should remain static and it may rotate around the ring with different linkages adopting the folded conformation. It is, however, impossible in cyclohexa-amylose to have more than one linkage in this conformation at any given moment. The hexahydrate crystal conformation may not completely adopt this conformation because of crystal packing considerations or, and perhaps more likely, because only small amounts of water are present and there is no effect from the structuring of the solvent which is present in aqueous solution.

Oligosaccharides and Amylose

The present suggestions about the possible conformation of methyl β-maltoside and cyclohexa-amylose in aqueous solution, as indicated by their optical rotations, can be extended to α-1,4 linked oligosaccharides and amylose. The $[\Lambda_{obs}]_D$ for the cyclodextrins, the maltodextrins and amylose are given in table 2.5.

In the cyclodextrin series the $[\Lambda_{obs}]_D$ increases from cyclohexa-amylose through the series to cyclododeca-amylose. This might have been expected since, as the molecules become larger, the glycosidic linkages gain more freedom to relieve torsion and van der Waals strain and to make themselves more compatible with the water structure. Thus the "folded" conformation might be expected to make a larger contribution to $[\Lambda_{obs}]_D$ as the series is ascended which is consistent with the observed increase in its value beyond that of methyl β-maltoside in dimethyl sulphoxide solution and beyond the $[\Lambda_{calc}]_D$ for the first van der Waals minimum (-24°). However, this increase in the $[\Lambda_{obs}]_D$ levels off at cycloundeca-amylose and cyclododeca-amylose at a value very close to that of amylose. A possible reason for this is discussed below.

Table 2.5

Linkage rotations for α-1,4 oligomers and amylose.

Compound	H_2O		DMSO		5 N NaOH	
	$[\alpha]_D$	$[\Lambda_{obs}]_D$	$[\alpha]_D$	$[\Lambda_{obs}]_D$	$[\alpha]_D$	$[\Lambda_{obs}]_D$
Cyclohexa-amylose	150.5°	-65° [a]	129.0°	-99° [a]		
Cycloheptа-amylose	162.0°	-48° [a]				
Cycloocta-amylose	177.4°	-21° [a]				
Cyclonona-amylose	191.0°	+1° [a]				
Cyclodeca-amylose	197.0°	+11° [a]				
Cycloundeca-amylose	200.0°	+16° [a]				
Cyclododeca-amylose	201.0°	+17° [a]				
Maltodextrins						
Maltose	130.4°	+69.0° [b]				
Maltotriose	158.4°	+46.4° [b]				
Maltotetraose	168.5°	+37.2° [b]				
Maltopentaose	177.6°	+38.6° [b]				
Maltohexaose	180.0°	+32.2° [b]				
Maltoheptaose	184.0°	+17.0° [b]				
Amylose	200.0°	+16.0° [a]	158°	-52° [a]	140°	-75°

a. Values from ref. 15 and the references quoted there. The values in dimethyl sulphoxide solution have been corrected for the change in the solvent refractive index.

b. The values are the average of those calculated from the optical rotation values of C.T. Greenwood and D.J. Hourston[114] and those given by Bailey[115]. The values were calculated by subtracting the molecular rotation of the monosaccharide from that of the maltodextrins, dividing the result by the number of glycosidic linkages in the molecule and subtracting the molecular rotation of methyl α-D-glucopyranoside (305.1°).

c. Valuon from ref. 107; calculated by subtraction of the molecular rotation of methyl α-D-glucopyranoside in 5 N NaOH from that of the "residue molecular rotation" (i.e. $[\alpha]_D$ x 162/100) for amylose.

In the maltodextrin series the $[\Lambda_{obs}]_D$ for the disaccharide suggests that, as for methyl β-maltoside, the molecule spends a very large portion of its time in the "folded" conformation. However, on ascending the series the $[\Lambda_{obs}]_D$ rapidly converges on the amylose value suggesting that there is some interaction present which reinforces the O(2) ... O(3) hydrogen bond between neighbouring residues. It has been suggested[15] that this is most probably due to the possibility of consecutive hydrogen bonds due to the dipole interactions shown in fig. 2.11.

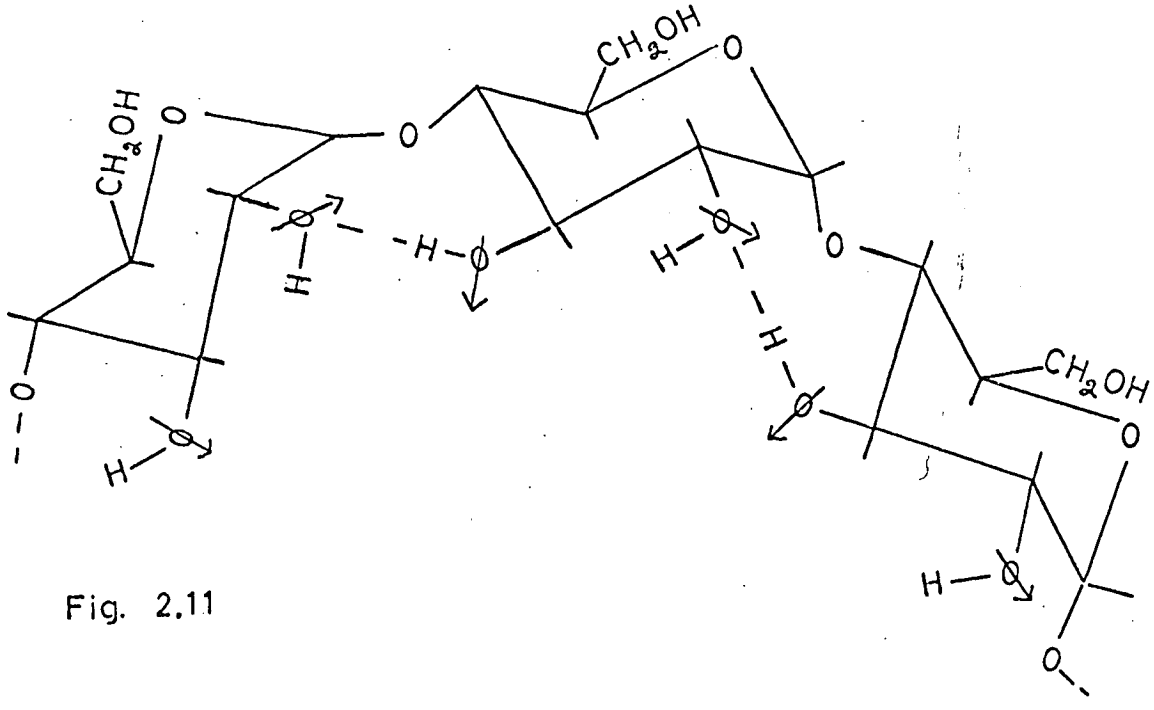

Fig. 2.11

The linkage rotations for the large cyclodextrins (n $\geqslant$ 11 or 12), the large maltodextrins (n $\geqslant$ 7) and amylose in aqueous solution suggest that for each linkage there is a dynamic equilibrium between

the hydrogen bonded conformation or consecutive hydrogen bonded conformations, the van der Waals minimum conformation and the "folded" conformation with the last named conformation making the largest contribution, possibly because it is more compatible with water structure. In dimethyl sulphoxide there will be no effect due to structuring of the solvent and the intramolecular hydrogen bonding will also be slightly stronger than in water. Each linkage would therefore be expected to spend more of its time in the hydrogen bonded conformation and the $[\Lambda_{obs}]_D = -52^\circ$ for amylose is consistent with this. However, since the hydrodynamic data indicate that in dimethyl sulphoxide[116] amylose exists as a random coil and not as a rigid rod, this increased hydrogen bonding does not pull the chain into the correct symmetry to initiate helix growth. Reeves[107] also measured the optical rotation of amylose in NaOH solution and the $[\Lambda_{obs}]_D$ from these results become more negative as the concentration of NaOH is increased, again consistent with the theory that the effect of hydroxyl ions is to break up the water structure thus removing its stabilising effect on the "folded" conformation. For amylose in NaOH, however, the results indicate that an additional effect may be present since the $[\Lambda_{obs}]_D$ does not in this case indicate that the alkaline solution acts like a water/dimethyl sulphoxide hybrid but becomes even more negative than the $[\Lambda_{obs}]_D$ in dimethyl sulphoxide. Reeves was also unable to make measurements in solutions stronger than 5 N NaOH because the solutions gelled before mixing could be completed, possibly because of polyelectrolyte effects of the type described by Rees[34]. The extra large decrease in the $[\Lambda_{obs}]_D$ in alkaline solution may therefore be caused by a further conformational change at the glycosidic linkage when the chains interact in this way.

The results and deductions of this study are also very difficult to fit in with the "hollow helix" model[97] for B-amylose since they suggest that water is unlikely to form a hydrogen bonded system within the helix core which can give the observed stability of the crystalline B-amylose. The ideas presented here can be much more easily reconciled with the "double helical" model[117] for this crystalline compound, where the hydrophobic regions of each chain will be juxtaposed in the centre of the helix. The respective merits of these two suggested structures have been thoroughly reviewed by Rees[88] and will not be covered here. It is sufficient to say that the evidence is, as yet, inconclusive and it is not possible to make a definite decision about the structure of B-amylose.

α,α-Trehalose

α,α-Trehalose is a non-reducing disaccharide composed of two α-D-glucopyranose units linked by a glycosidic oxygen bridge between their two anomeric carbon atoms C(1) and C(1'). The molecule is thus symmetrical about the glycosidic oxygen and by extending the treatment suggested by Rees (Appendix I and ref. 15) we may deduce that for α,α-trehalose:

$$[\Lambda_{obs}] = [M_{\alpha,\alpha\text{-trehalose}}] - 2[M_{Me\ \alpha\text{-D-gluc}}]$$

The $[\Lambda_{obs}]_D$ values in water and dimethyl sulphoxide are given in table 2.2. Similarly the $[\Lambda_{calc}]_D$ is given by:

$$[\Lambda_{calc}]_D = -210 - 240 \text{ Sin } \Delta\phi$$

We can, therefore, use these values to calculate the observed $\Delta\phi$ values in water and dimethyl sulphoxide and this has been done for the values at 25°C. This gives $\Delta\phi = -53^\circ$ and -72° for dimethyl sulphoxide and water respectively.

The crystal structure of α,α-trehalose dihydrate has been determined by X-ray analysis in three independent laboratories[118]. The average torsion angles of the three determinations lead to the values $\Delta\phi = -57.7^{\circ}$, $\Delta\phi' = -45.1^{\circ}$ i.e. $\overline{\Delta\phi}$ for the crystal conformation is -51.4°. This is in good agreement with the observed $\Delta\phi$ (-53°) in dimethyl sulphoxide solution suggesting that in this solvent the molecule may predominantly exist in a conformation which produces an almost maximally extended structure similar to that of the crystal. For aqueous solution, however, the results obtained again suggest that an additional interaction is present. Studies of molecular models show that when $\Delta\phi = -73^{\circ}$ the molecule adopts a conformation very close to that shown in the photograph - fig. 2.12. It is noticeable that in such a conformation two sets of hydrogen atoms become juxtaposed. These are H(1) and $H(O_2)$ with H(5') and $H\,(O'_{CH_2OH})$ and H(1') and $H(O'_2)$ with H(5) and $H\,(O_{CH_2OH})$. Such a conformation would therefore be expected to increase the net hydrophilic character of the molecule and to make it more compatible with the structured water in an analogous way to the favoured conformation suggested for methyl β-maltoside. This is supported by shifts in the $[\Lambda_{obs}]_D$ on raising the temperature of the α,α-trehalose solutions which are very similar in both sign and magnitude to those observed for methyl β-maltoside (fig. 2.8).

In conclusion it is felt that the results given in this study indicate that the structured nature of water plays a large part in determining the preferred conformation of α-1,4 linked di and oligosaccharides and amylose in aqueous solution. It is also noticeable that the "folded" conformation ($\Delta\phi = -70^{\circ}$, $\Delta\psi = -40^{\circ}$), which has been suggested to be the conformation most compatible with

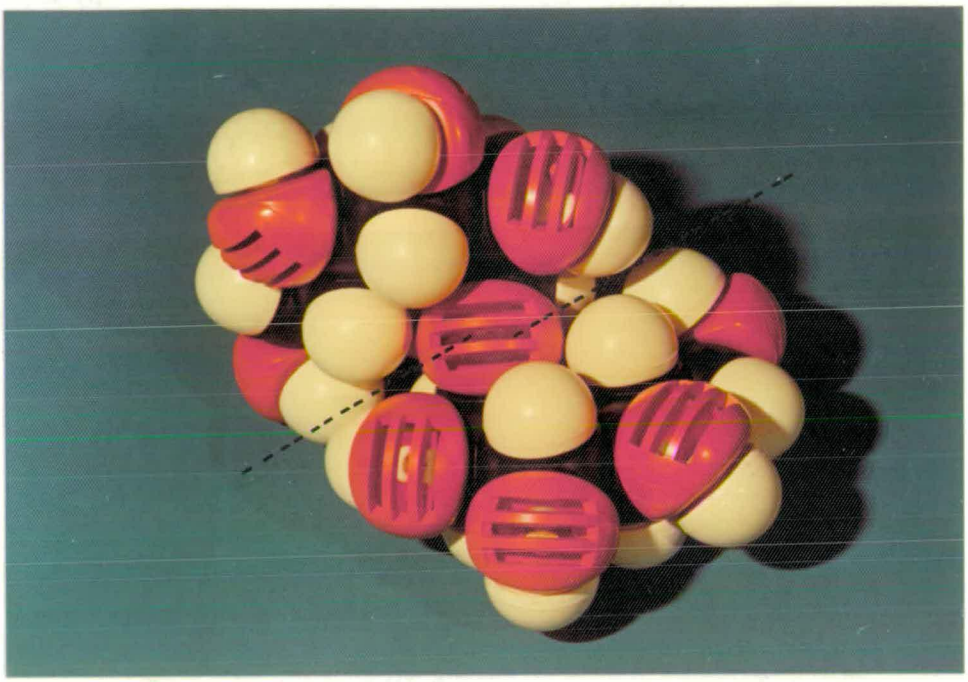

Fig. 2.12 A CPK space filling model of α,α-trehalose in the suggested conformation in aqueous solution. Two sets of hydrogen atoms are juxtaposed: H(1) and H(O(2)) with H(5′) and H(O′(CH_2OH)) and H(1′) and H(O(2′)) with H(5) and H(O(CH_2OH)). In such a conformation the net hydrophilic character of the molecule will be increased.

the "lattice" water, has a $\Delta\phi$ value very close to the value ($\Delta\phi = -60^{\circ}$) required before an intelligible trend can be observed in the average linkage conformations of α-linked oligosaccharides in aqueous solution when only van der Waals repulsions are considered[16]. As mentioned in the General Introduction such an approach gave excellent internally consistent conclusions when applied to β-linked oligosaccharides. This $\Delta\phi$ value (-60°) was suggested to be favoured by the exo-anomeric effect but the results of this study indicate that the structured nature of water may be at least as significant in determining the predominant conformation of α-linked oligosaccharides in aqueous solution.

SECTION B

CIRCULAR DICHROISM

CHAPTER 3

THE DETERMINATION OF THE URONIC ACID COMPOSITION AND SEQUENCE IN ALGINATES USING CIRCULAR DICHROISM

INTRODUCTION

Alginic acid is a high molecular weight polysaccharide found originally in one of the major groups of benthonic algae, the Phaeophyceae (brown seaweed), which still provide the main source for it. A structurally similar polysaccharide has also been isolated from Azoto bacter vinelandii[119] and Pseudomonas aeruginosa[120] but the bacterial polymer is usually also partly o-acetylated.

Structural Studies

Until 1955 it was thought that alginic acid contained only D-mannuronic acid but Fischer and Dorfel[121] showed that different samples of the polysaccharide contained various proportions of both D-mannuronic acid and its C(5) epimer L-guluronic acid (fig. 3.1)

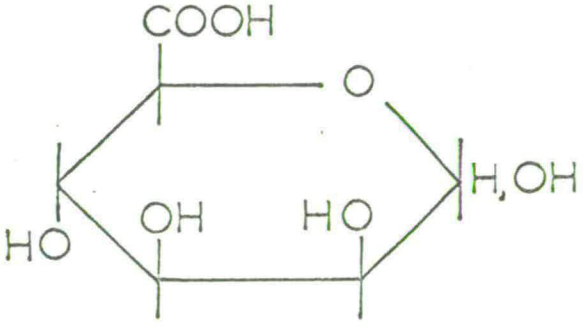

D-mannuronic acid

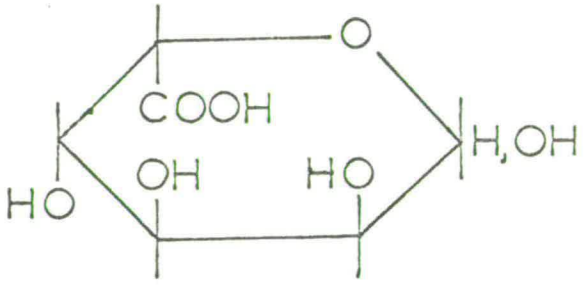

L-guluronic acid

Fig. 3.1

and this has been confirmed by other authors[122]. After methylation, reduction of the carboxyl groups and hydrolysis, derivatives of 2,3

di-o-methyl-D-mannose and 2,3 di-o-methyl-L-gulose were apparently the only products[123] from a number of samples[124] indicating that both these units are 1,4-linked. This conclusion has been substantiated by other methods of structural investigation[122(b)] and the results of earlier work are also consistent with this[125]. When sodium alginate is oxidised with periodate over 40% of the hexuronic acid residues fail to react with the reagent. The implication that these periodate resistant linkages arise from 1,3-linkages has been shown to be incorrect since methylation of the unattacked portion of the molecule has shown that only 1,4-linkages are present[119,124]. This anomaly has been convincingly explained[126] by the suggestion that aldehyde functions of oxidised residues form stable, six-membered, cyclic acetals with the residues adjacent, so blocking further oxidation.

Isolation of 4(-O-β-D-mannopyranosyl)-D-mannopyranose[127] from a partial hydrolysis of the reduced polysaccharide indicates that the mannuronic acid residues in alginic acid are linked through their C(4) positions by a β-linkage and that the linkage is 1,4-pyranosyl rather than 1,5-furanosyl. This anomeric configuration for the D-mannose residue is consistent with the strongly negative optical rotation and on this basis the L-gulose residue was generally assumed to have the α-L-configuration. This has been shown to be correct by x-ray diffraction studies of poly-D-mannuronic acid and poly-L-guluronic acid[128] which indicate that the D-mannuronic acid residues are β-linked in the C1 conformation and the L-guluronic acid residues are α-linked in the 1C conformation. Very recent n.m.r. evidence[129] suggests that the residues are also in these conformations in solution. Partial fractionation of alginate samples into fractions

that are enriched with respect to mannuronic and guluronic acid, respectively, has been achieved[130] but repeated fractionations failed to indicate the existence of homopolysaccharides. Proof that the two types of residue can occur in the same chain in at least some of the molecules was supplied by the isolation of oligouronic acids[131] containing both residues and of a crystalline mannosyl-gulose[127], from partial acid hydrolysis and its reduction products respectively.

Haug et al[132,133] have obtained information about sequence from an elegant method based on heterogeneous hydrolysis. The results showed that a certain amount of the alginate passed rapidly into solution but that even prolonged hydrolysis did not significantly increase this concentration of carbohydrate in the solution. The acid resistant material could be fractionated into two components having degrees of polymerisation of about twenty and containing predominantly L-guluronic acid and D-mannuronic acid respectively. No fraction with an intermediate uronic acid composition could be prepared from the insoluble material. The soluble fraction has been shown[132,134] to consist predominantly of the two monomers and a mixed disaccharide. It has therefore been suggested that this fraction may approximate closely to an alternating arrangement of D-mannuronic and L-guluronic acid residues. The alginic acid molecule may thus be represented as shown in fig. 3.2 where the homopolymeric blocks of at least 20 residues are separated by blocks of a similar length which are primarily alternating in structure. The homopolymeric blocks probably resist hydrolysis because they form crystalline regions and are therefore inaccessible to reagents.

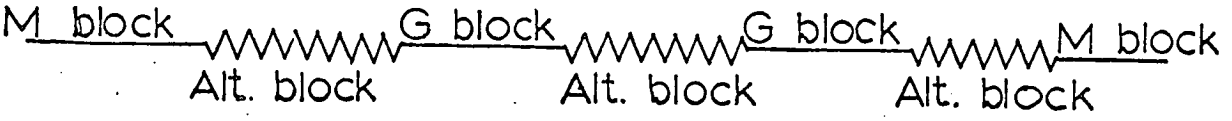

Alginic acid

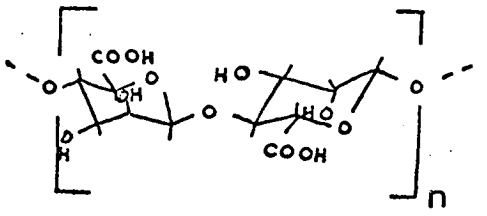

M block

4(-O-β-D-mannosyluronate)-β-D-mannuronate

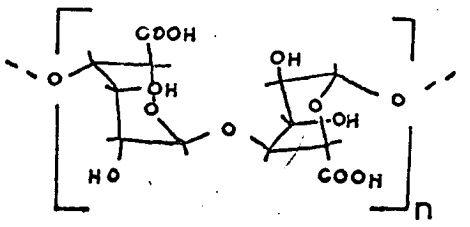

G block

4(-O-α-L-gulosyluronate)-α-L-guluronate

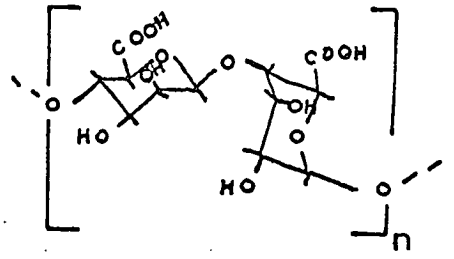

Alt. block

4(-O-β-D-mannosyluronate)-α-L-guluronate

Where the minimum value of n is approximately 10

Fig. 3.2 Schematic representation of alginic acid.

Methods Available for the Determination of the Uronic Acid Composition and Block Structure of Alginates

Alginates are widely used in industry due to their ability to form strong gels with polyvalent metal ions and, in particular, with calcium ions. As discussed in Chapter 4 of this thesis, the gelling characteristics of an alginate are strongly influenced by its uronic acid composition, i.e. the ratio of mannuronic to guluronic acid residues (M/G ratio). This work also suggests that a more important parameter is the block structure of the alginate, i.e. the proportion of mannuronic acid blocks (M blocks), guluronic acid blocks (G blocks) and alternating blocks (M/G blocks), since these blocks differ in their ability to form junction zones. It is thus important to have a reliable method for determining the M/G ratio and the block structure of alginates.

The M/G ratio of an alginate can be determined by complete acid hydrolysis and separation of the uronic acids using chromatography on an anion exchange column[135]. The amounts of the two uronic acids may subsequently be determined colorimetrically[136]. The standard method of determining alginate block structures involves heterogeneous partial acid hydrolysis and separation of the various fragments by acid precipitation[132], followed by determination of their uronic acid compositions by complete acid hydrolysis as described above. These methods give reliable results which can be correlated with the physical properties of the alginates[133] but they are very time consuming and are not suitable for the routine characterisation of large numbers of samples. Moreover, a factor correcting for the different rates of breakdown of L-guluronic acid and D-mannuronic acid during the complete acid hydrolysis must be used and this may introduce a

systematic error into the method.

The carbazole reaction[137] gives very different colour intensities for mannuronic and guluronic acids and a method for determining M/G ratios of alginates has been suggested which is based on analysing alginates by the carbazole method applied under two different reaction conditions[138]. There is evidence, however, that this method consistently overestimates guluronic acid[129] when applied to alginates, although it works well on mixtures of mannuronic and guluronic acid monomers and it is possible that the carbazole reagent reacts differently with the acids in the polymeric and monomeric forms. Moreover, unless one is experienced in the use of this method, it is difficult to obtain reproducible results.

Spectroscopic Techniques

More recently spectroscopic techniques have been applied to the determination of the M/G ratio and block structure of alginates. Mackie[139] has noted that infra-red spectroscopy on films of the alginic acids can be used to give a very fast, semi-quantitative estimation of alginate M/G ratios using the areas of the bands at 808 and 797 cm^{-1} for mannuronic and guluronic acids respectively. However, these bands do overlap and the estimation of the baseline is difficult making the method not very accurate or reproducible, as indeed was recognised by the author. Moreover, there is evidence[140] that this method may overestimate mannuronic acid. Penman and Sanderson[129] have determined the uronic acid sequence of several alginate samples by splitting the alginates into alternating and homopolymeric fractions using partial acid hydrolysis. They estimated the relative proportions of M blocks and G blocks in the homopolymeric fraction by n.m.r. spectroscopy making use of the

fact that the more shielded axially oriented H(1) in the β-linked mannuronate residues in polymannuronate sequences resonates at higher field (5.34 τ) than the equatorially oriented H(1) of the α-linked guluronate residues in polyguluronate sequences (4.96 τ). The concentration of alginate in the soluble and insoluble fractions was determined by the phenol-sulphuric acid reaction making the assumption that the ratio of mannuronate to guluronate residues (M/G ratio) in the soluble fraction was 1. This method is much faster than the completely chemical analysis described above and it can be carried out on much less material. The method does, however, destroy the sample used. Moreover, the work of Haug et al[132,133] suggests that the partial acid hydrolysis may not completely separate the homopolymeric and alternating blocks and this may introduce errors into the determination of the alginate concentration in the soluble fraction.

As indicated in the General Introduction uronic acids show Cotton effects around 210 nm typical of the $n \rightarrow \pi^*$ transitions of carboxyl groups. Moreover, as shown in fig. 3.3 the c.d. spectra of (methyl β-D-mannopyranosid)-uronate and (methyl α-L-gulopyranosid)-uronate, each as its sodium salt, have been shown[33] to be quite different. The sodium methyl α-L-guluronate gives a single broad negative trough in the spectral region from 250 to 190 nm whereas the sodium methyl β-D-mannuronate has a positive peak and a much smaller negative trough, at higher wavelength, in addition to the onset of a negative trough below 195 nm. The effect of two overlapping gaussian peaks of opposite sign is to increase the separation of the observed peak maxima and this means that the main peaks observed in the two uronate spectra occur at different wavelengths. This difference suggested

Fig. 3.3 The c.d. spectra of sodium methyl β-D-mannopyranosyluronate (dashed line) and methyl α-L-gulopyranosyluronate (continuous line); the summation curve is shown by the dotted line.

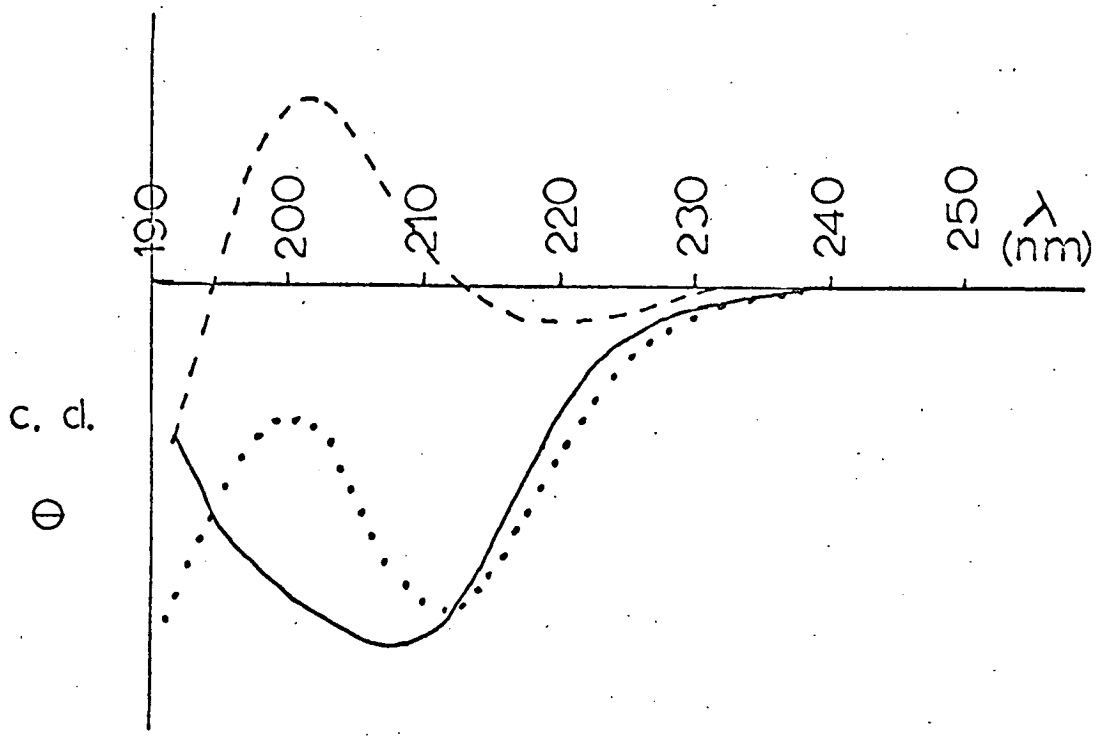

that it might be possible to use circular dichroism to obtain a simple method for the analysis of alginate composition and this is illustrated much more clearly, as shown in fig. 3.3, by the summation curve of the sodium β-D-mannuronate spectrum and the sodium α-L-guluronate spectrum. This Chapter describes the development of rapid, sensitive and non-destructive techniques for the determination of alginate composition (M/G ratio) and block structure.

Experimental

1. Materials

The alginate samples coded 5-10 were all from commercial sources; these coded 5-9 were supplied by Alginate Industries Ltd. while sample 10 was obtained from Alginates Australia Ltd. All the above samples are of seaweed origin and had been characterised by Dr A.Penman and Dr G. Sanderson by the n.m.r. and/or chemical methods described in ref. 129. In the chemical determination of the compositions of the alginates the results were corrected[135] for the different rates of breakdown of mannuronic and guluronic acid on complete acid hydrolysis. Three alginate fragments, which were a gift from Dr A.Penman,were also examined. These had been prepared by the partial acid hydrolysis of alginate sample 7 (using a very similar method to that described by Haug, Larsen and Smidsrød[133]) into three types of short chain segments containing; (a) mainly guluronic acid (1); (b) a large proportion of mannuronic acid residues (3) and (c) a sequence in which the two types of residue are primarily alternating (2). These blocks have a degree of polymerisation of approximately 20 and samples 1 and 3 have been characterised by both the n.m.r. and chemical methods. The alternating blocks have been characterised by the chemical method only. Two bacterial alginate samples (11,12), which were kindly supplied by Dr C.J. Lawson of Tate and Lyle, were also studied.

All the samples were purified as described in the General Methods section.

1(a) Preparation of the Mannuronate Block Sample (4)[133,141]

Sodium alginate (sample 8: 30 g) was hydrolysed heterogeneously in 0.3 N hydrochloric acid (1 l.) at 100°C. After 20 minutes the solution was removed from the insoluble material by filtration and

washing with 0.3 N acid. The insoluble material was suspended in water and neutralised with N sodium hydroxide. The resulting solution was made up to 850 ml, 2 N hydrochloric acid (150 ml) was added to make the solution up to 0.3 N and the heterogeneous hydrolysis was continued for 20 hr. The solution was removed by filtration and discarded. The insoluble material was suspended in water and solubilised by the addition of sodium hydroxide to pH 7.0. Sodium chloride was added to 0.1 M and the polysaccharide was precipitated by the addition of ethanol.

The dried precipitate was redissolved in water to give a 0.5% solution, sodium chloride was added to 0.1 M and the pH was adjusted to 2.85 using 0.025 N hydrochloric acid. The resulting suspension was centrifuged (2.5×10^3 r.p.m.: 30 min). The solution was decanted, neutralised with N sodium hydroxide and the high M fragment isolated precipitation with ethanol. The precipitate was washed with ethanol (twice) and ether (twice) and dried by leaving it to stand at room temperature.

This material was hydrolysed heterogeneously for a further six hours in 0.3 N hydrochloric acid and the insoluble material was separated from the solution by filtration as previously described. A fragment containing a very high proportion of mannuronic acid was isolated from this insoluble material, as its sodium salt, by fractional precipitation at pH 2.85 (as described above) followed by neutralisation of the solution and precipitation with ethanol. The sample was purified as described in the General Methods Section.

A small amount of this mannuronate block sample (100 mg) was deuterated by dissolving it three times in D_2O (1.5 ml), the

solvent being removed each time by evaporation under reduced pressure. The deuterated sample was taken up in D_2O (0.5 ml) and its n.m.r. spectrum was recorded at 80°C and a sweep width of 250 Hz on a Varian HA 100 high resolution spectrometer using tertiary butanol as internal standard. The relative proportions of the two types of residue were obtained from the areas of the low field signals due to sodium mannuronate (H(1) : 5.33 τ) and guluronate (H(1) : 4.90 τ) and these are given in table 3.2.

2. Determination of the Purity of the Freeze-Dried Alginate Samples

This work was carried out in conjunction with the Analytical Department, Unilever Research Laboratory, Colworth House. Several methods for the determination of the amount of water in the freeze-dried alginate samples were compared using two purified alginate samples and the results are shown in table 3.1.

TABLE 3.1

Comparison of the methods for the quantitative determination of the sodium uronate content of purified freeze-dried alginate samples

Alginate Code	% Solids from Oven Drying at 105°C	Karl Fischer	% Alginate from Conductiometric Titration	(a)Ash	Ashing (b)Titre	(c)Na
7	90-93%	86%	63%	78.5%	76.5%	80.5%
9	90-91%	84.7%	56%	75.0%	70.5%	77.6%

(a) Oven Drying at 105°C

A weighed amount of the samples was heated in a vacuum oven at 105°C overnight. The samples were allowed to cool in a vacuum desiccator before they were reweighed. The results shown in table 3.1 suggest that this did not remove all the water from the samples.

(b) Conductiometric Titration

This procedure is based on a standard method for the determination of the salts of weak acids. A 0.1% (w/v) solution of the purified alginate (50 ml) was titrated with standard 0.1 N hydrochloric acid, the conductance being measured after each addition. In this type of measurement it is not necessary to get readings in the region of the equivalence point, but it is necessary to have several well spaced points before and after for extrapolation. The method was tested with a standard sodium acetate solution and this gave an accurate sharp equivalence point. The results for sodium alginate were expected to be less sharp and this proved to be the case. However, as shown in table 3.1, this method also considerably underestimates the purity of the alginate samples. The alginates precipitate at a point just past the apparent equivalence point and it is thought that this may reduce the accessibility of the acid to the carboxyl groups and prevent their complete titration. This method was therefore abandoned.

(c) Karl Fischer Moisture Determination[142,143]

The extraction with anhydrous methanol was carried out for $\frac{1}{2}$, 1 and 2 hours but no increase in the amount of water which could be extracted from the samples was found. This method was experimentally more difficult than the ashing technique described below since the freeze-dried alginate sample absorbed the methanol and expanded to occupy the whole volume of the flask. It was decided that the complete ashing method gave more accurate results and, therefore, this method was not used.

(d) Ashing

A known weight of the alginate samples ($\sim$100 mg) was

ashed at 550°C until the weight of the ash remained constant. From the weight of sodium carbonate the percentage of sodium alginate in the original sample was calculated.

The ash was dissolved in deionised water (100 ml) and two aliquots (25 ml) of this solution were titrated with 0.1 N hydrochloric acid. The average titration was used to check the amount of carbonate in the ash and from this a second estimate of the percentage of sodium alginate in the sample was calculated. Finally atomic absorption spectrometry was used to determine the sodium content of the solution of the ash. From this the amount of sodium in the ash was calculated and a third estimate of the amount of alginate in the original sample was obtained.

As shown in table 3.1 this method gave very consistent results. The complete ashing method was therefore used to determine the total amount of sodium uronate in the purified freeze-dried alginate samples; the average of all three estimates described above was taken in each case.

3. Preparation of Sample Solutions

The freeze-dried alginate samples (~60 mg) were weighed into a small flask, the weight was noted accurately and deionised water (20 ml) was added using a pipette. The solutions were magnetically stirred until the alginate dissolved. The pH of ~15 ml of this solution was adjusted to 7.0 using a small amount of N sodium hydroxide added by means of a syringe. Any overshoot in the pH was brought back using the extra 5 ml of the original solution. The solutions were millipore filtered (3 μ) and transferred to the c.d. cell in one operation using a syringe.

4. Measurement of Circular Dichroism

The c.d. spectra were recorded on a Cary 61 C.D. Spectropolarimeter

in a 1 mm pathlength cell and using a 10 second integration period. A base line was recorded, for the cell containing deionised water, for each sample solution. All measurements were made at 25°C; the temperature being regulated using a Haake thermocirculator and a thermostattable cell holder.

For the analysis of alginate block structure the c.d. spectra were measured up at every 2.5 nm from 260 nm to 192.5 nm and were corrected at each point for the value of the base line. Now using the weighed concentrations of the alginate solutions, plus the total amount of sodium uronate actually contained in the purified freeze-dried samples, the spectra were converted to molecular ellipticities ($[\theta]$) using the formula;

$$[\theta] = \frac{\theta \; M}{10 \; l \; x \; c} \quad \text{degree} - \text{cm}^2 \; \text{decimole}^{-1}.$$

M is the gram-molecular weight of a sodium uronate residue; c is the uronate concentration (g/cm^3) of the solution and l is the pathlength of the cell (cm). To make the figures easier to handle all molecular ellipticities were divided by 10^3 in this study.

5. Determination of Uronate Sequence in Alginates by Computer Curve Fitting

All computer programmes were written by Dr E.R. Morris. The language used was Fortran II and the programmes were run on a Honeywell time-sharing computer terminal. The final computer programme "Algfit" is given in Appendix 4.

The spectra of the three types of sequences found in alginates, plus those of the four alginate samples 5, 7, 8 and 10, were fed into the computer. All spectra were expressed in molecular ellipticity ($[\theta]$) x 10^{-3}. The computer was asked to synthesise the best fit of the alginate spectra using combinations of fractions of the three

block spectra. A weighting factor for each point in each spectrum, which depended upon the slope of the spectral curve between that point and the previous one, is incorporated into the programme. This means that the computer attaches more importance to the match at the spectral extrema and is less concerned about achieving a perfect fit where the spectral curve is changing rapidly and the errors in measurement are consequently greater.

Five choices were incorporated into the programme.

(a) The computer can either compare the spectrum synthesised from given fractions of the block spectra with that of the alginate or, by an iterative procedure, it can adjust the given fractions of the block spectra until it obtains the best possible fit for the alginate spectrum.

(b) A table, comparing the original alginate spectrum with that of the fitted spectrum at every measured point and also listing the difference between the two spectra at every point, can be obtained if desired.

(c) A graph comparing the original alginate spectrum with that of the synthesised spectrum can be obtained if requested. The computer prints a $\circ$ for the original alginate spectrum, a + for the synthesised spectrum and if the spectra are within 0.1×10^{-3} degree of each other a * is printed out.

(d) Since the sum of the fractions of the blocks must equal unity, an option is incorporated into the programme whereby the computer ensures that the total of the proportion of M blocks, G blocks and alternating blocks sums to one. An unconstrained fit means that the computer can alter the proportion of all three block spectra whereas in a fit forced to 1.0 only the proportions of the spectra of two

of the block samples are varied; the other being automatically determined.

(e) A facility was incorporated into the programme whereby the computer lists the proportion of M blocks, alternating blocks and G blocks after a set number of iterations (usually 25). The computer can then be told to continue its iterative procedure or, if it is not changing the proportions of the three blocks, it can be told to stop and list the requested table or graph.

RESULTS AND DISCUSSION

Estimation of Alginate Composition (M/G ratio)

All sodium alginate c.d. spectra show a trough centred around 212 nm and a peak around 200 nm which are thought, by comparison with the methyl uronoside spectra (fig. 3.3), to arise from the $n \rightarrow \pi^*$ transitions of the carboxyl groups on the two different residues. All spectra also show the onset of a large negative band below 195 nm which is considered to be due to the $\pi \rightarrow \pi^*$ transitions of the carboxyl groups. The spectra of the samples approximating to the three different block types are shown in fig. 3.8. While the spectra of the homopolymeric sodium polymannuronate and polyguluronate blocks broadly resemble the corresponding methyl glycoside spectra, there are appreciable second order differences showing the sensitivity of the uronic acid c.d. to neighbouring residues in the alginate chain. These can be used to give a method for the determination of alginate block structure and this will be discussed later in this Chapter. However, inspection of the alginate spectra, as shown by the examples in fig. 3.4 which compares the spectra of alginates with different compositions of the constituent uronic acids, indicates that they may also be used to give a rough measure of alginate composition. To a first approximation the depth of the trough appears to be related to sodium guluronate content and the peak height to sodium mannuronate content. Thus the parameter Peak Height/Trough Depth (fig. 3.4) increases with increasing M/G ratio and hence with an increasing content of sodium mannuronate in the sample. This ratio has been calculated for the alginate samples studied and this is given in table 3.2 along with the estimates of alginate composition obtained from the chemical and n.m.r. methods[129].

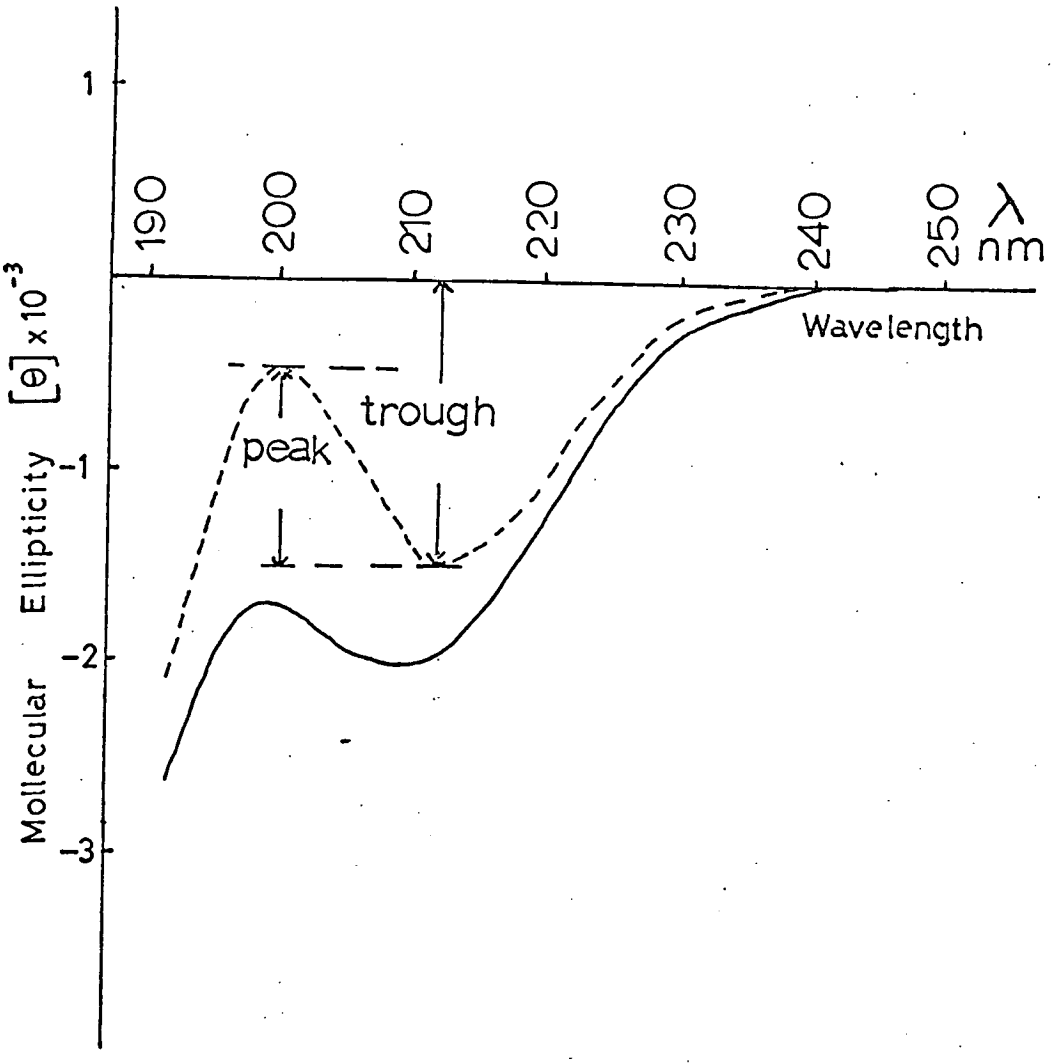

Fig. 3.4 Circular dichroism spectra for alginate samples 5 (continuous line) and 8 (dashed line) having mannuronate and guluronate residues in the ratio 29.5:70.5 and 58:42 respectively (table 3.2). There is a direct correlation between the ratio of the two residues and the ratio of the amplitudes marked "Peak" and "Trough".

Using the given values for the samples marked with a * in table 3.2 a standard curve of c.d. (Peak/Trough x 100) against composition can be drawn and this is shown in fig. 3.5. Using this standard curve the composition of the alginates shown in table 3.3 has been estimated and compared with the results obtained by other methods. The results demonstrate that the estimates of alginate composition obtained from the c.d. spectra are in very good agreement with those obtained using other techniques. It was expected that, since the alginate block spectra show the sensitivity of the uronic acid c.d. to neighbouring residues, the alternating block sample might show the largest deviation from the standard curve. However, the results in table 3.3 indicate that the difference between the calculated value from c.d. measurements and that observed from the chemical analysis is also small in this case. It is, therefore, concluded that circular dichroism gives a rapid, simple and sensitive method for the estimation of alginate composition. The normal sample requirement is of the order of one hundredth of a gram but analysis of rare samples can be carried out on less than a thousandth of a gram if necessary. Moreover, the method is non-destructive and the sample can be recovered if necessary.

It should be noted that the alginate samples 5 and 6 and 8 and 9, which are high and low viscosity fractions of the same alginates, give extremely similar c.d. spectra while the blocks which are around twenty units in length also give spectra which fit in well with those of the polymers as shown in figure 3.5. It, therefore, appears that this method is independent of molecular weight. The spectra do, however, change

TABLE 3.2

Correlation of alginate composition and c.d.

Alginate Code	Source	% M	% G	C.D. at 25°C (Peak/Trough x 1
1. Polyguluronate block*	Partial hydrolysis of 7	0	100[a]	8.1
2. Alternating block	"	60	40[b]	71.1
3. High mannuronate*	"	77.5	22.5[a]	143.8
4. Polymannuronate block*	Partial hydrolysis of 8	93	7[c]	194.9
5. *	Laminaria hyperborea	29.5	70.5[a]	15.4
6. *	"	31	69[a]	17.7
7. *		37	63[a]	23.4
8. *	Ascophyllum nodosum	58	42[a]	70.2
9. *	"	54.5	45.5[a]	69.6
10.	Macrocystis pyrifera	61	39[c]	75.0
11.	Azotobacter vinelandii	51	49[d]	54.4
12.	"	High	M[d]	187.7

(a) Average of chemical and n.m.r. determinations[129].

(b) Chemical determination only.

(c) N.m.r. determination only.

(d) Value supplied with the sample.

(e) The alginate samples marked with a * were used to give a standard curve of c.d. (Peak/Trough x 100) at 25°C against composition. This is shown in fig. 3.5.

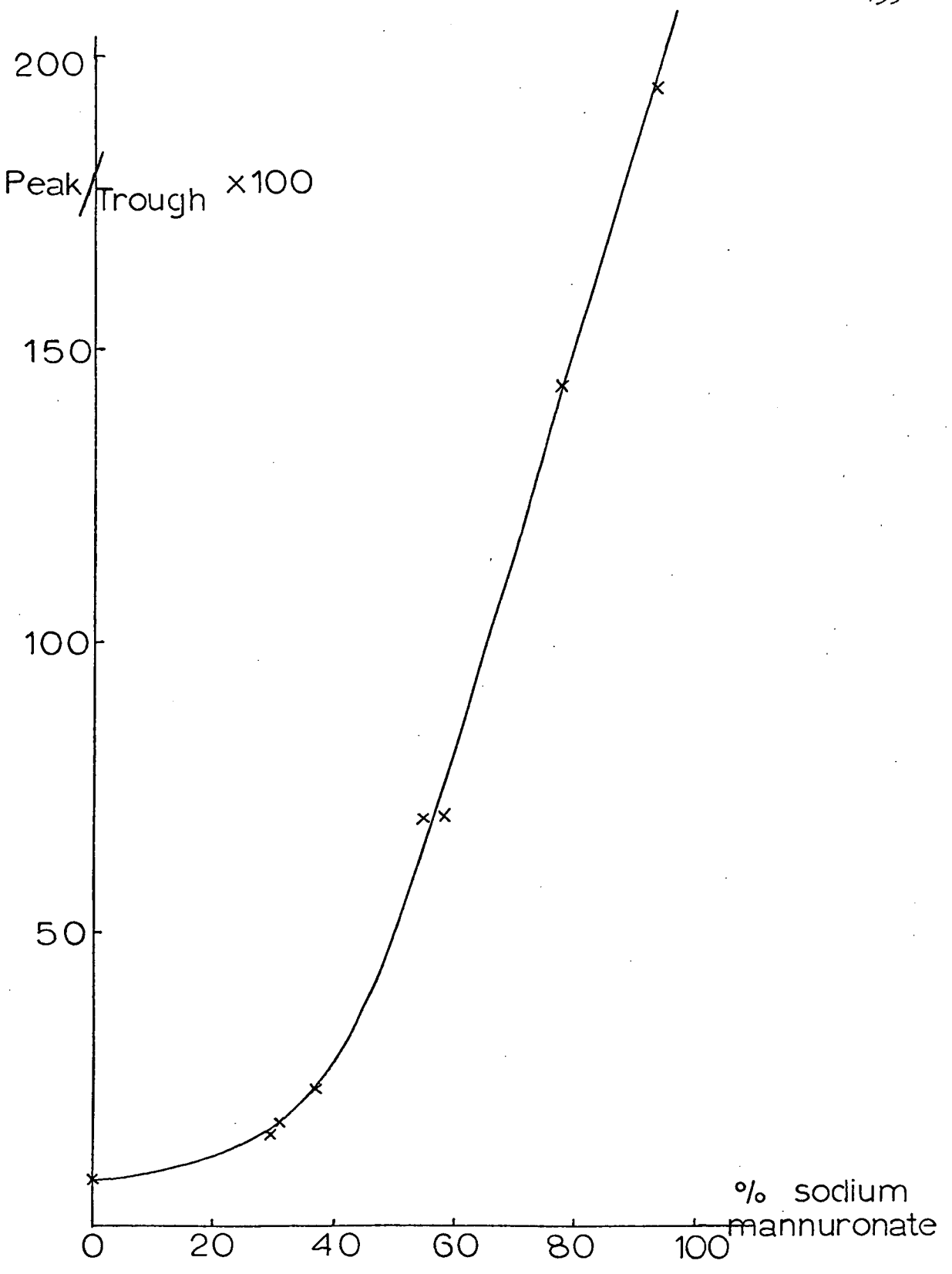

Fig. 3.5 Standard curve of c.d. (Peak/Trough x 100) against the percentage of sodium mannuronate in the alginate samples.

TABLE 3.3

Estimation of alginate composition using c.d.

Alginate Code	Estimated by c.d.		Observed[a]	
	% M	% G	% M	% G
2 Alternating block	56	44	60	40
10	57.5	42.5	61	39
11	51	49	51	49
12	90	10	High M	

(a) From table 3.2.

with temperature with the spectral features becoming less pronounced as the temperature is increased. All the spectra in this study were measured at 25°C. Alginate c.d. is also extremely sensitive to pH as shown in fig. 3.6 for the polyguluronate block sample and fig. 3.7 for the high mannuronate fragment sample. The spectra used here were all recorded on sodium alginate solutions at pH 7.0.

Determination of Alginate Block Structure by Computer Curve Fitting

The spectra of the alginate block samples used to determine the block structure of the four alginate samples are given in molecular ellipticity x 10^{-3} in table 3.4 and are shown in fig. 3.8. From table 3.2 it can be seen that the "poly(β-D-mannuronate)" sample (4) contains 7% of sodium α-L-guluronate residues. It is also apparent that the "poly(β-D-mannosyluronate-α-L-guluronate)" sample (2) is not completely alternating in structure but, as shown by chemical analysis, contains 60% of sodium β-D-mannuronate residues. The spectra listed in table 3.4 have been compensated for these deficiencies making the following assumptions.

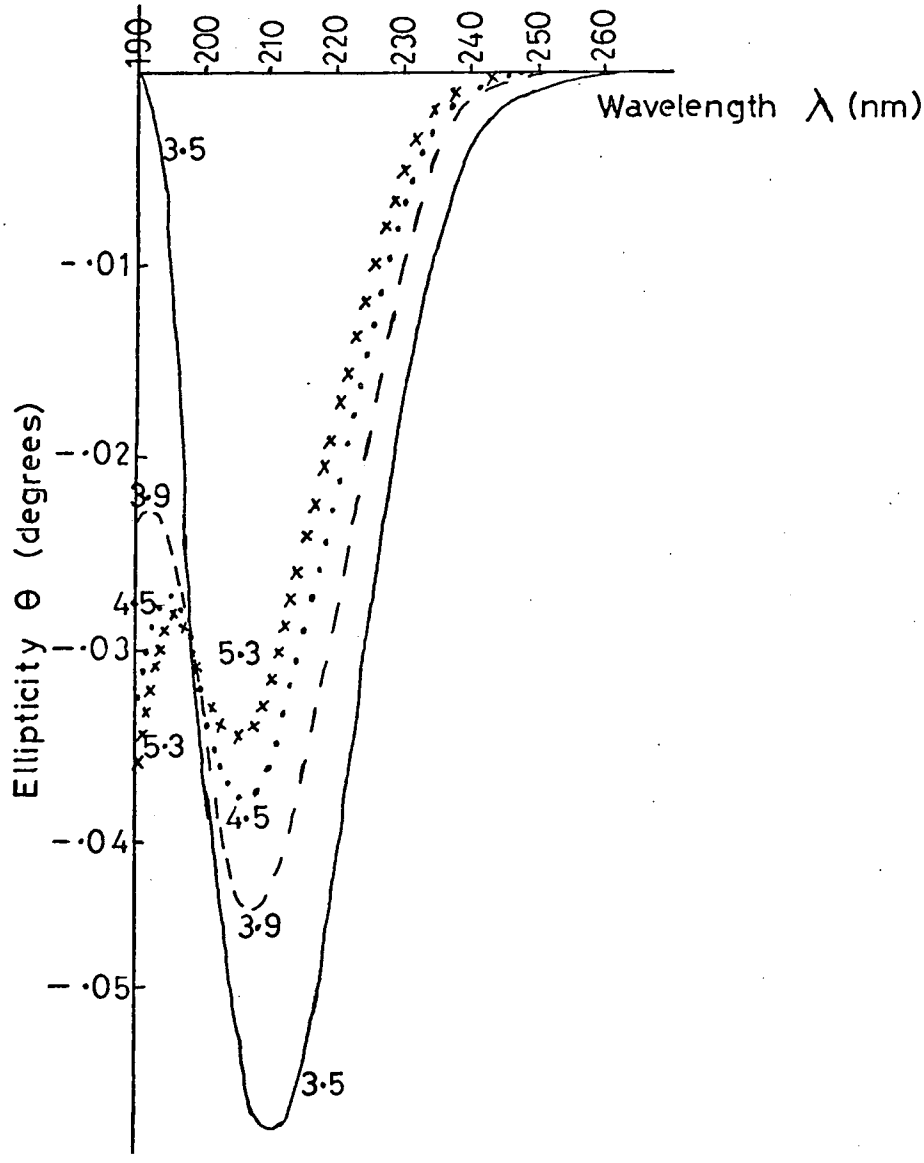

Fig. 3.6 pH dependence of the polyguluronate block (1) spectrum at 10°C; the pH of the solutions is marked on the curves.

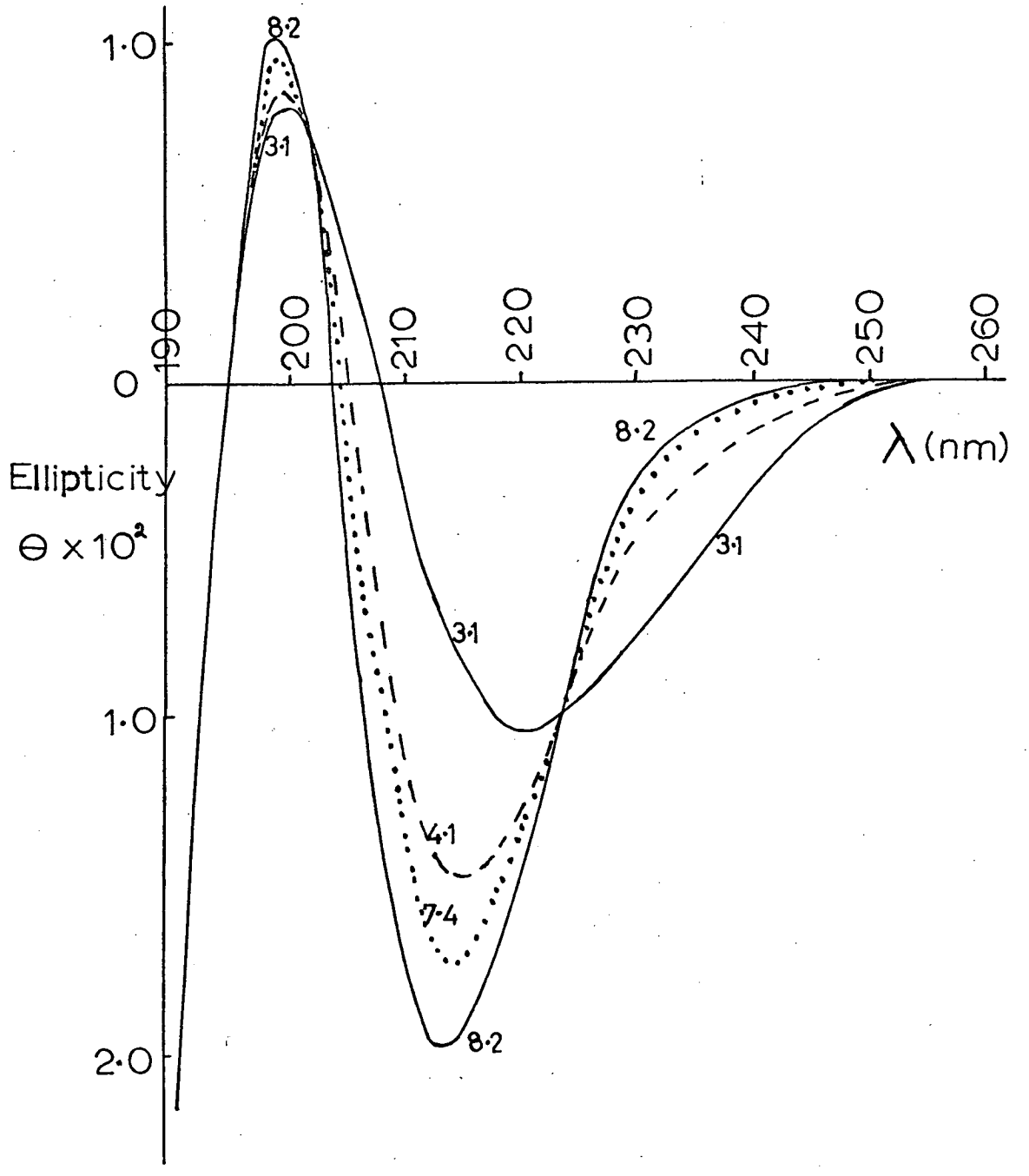

Fig. 3.7 pH dependence of the high mannuronate fragment (3) spectrum - at 10°C; the pH of the solutions is marked on the curves.

TABLE 3.4

Alginate block spectra

Wavelength (nm)	C.D. ($[\theta] \times 10^{-3}$)		
	M-blocks	Alternating blocks	G blocks
260.00	.00	.00	-.0055
257.50	.01	-.0025	.0109
255.00	.00	.00	.00
252.50	.0163	.0184	.0219
250.00	.0163	.0184	.0055
247.50	.0191	8.43045E-04	.0164
245.00	.009	.0034	-.0274
242.50	-.0012	-.0222	-.0219
240.00	.0019	-.0117	-.0438
237.50	-.0093	-.0314	-.0602
235.00	-.0469	-.067	-.1805
232.50	-.0662	-.096	-.2462
230.00	-.1676	-.1832	-.4049
227.50	-.3054	-.312	-.662
225.00	-.5179	-.4558	-.8972
222.50	-.7657	-.619	-1.2474
220.00	-1.0502	-.8518	-1.6194
217.50	-1.2648	-1.012	-1.986
215.00	-1.2889	-1.1298	-2.3088
212.50	-1.1282	-1.1418	-2.6316
210.00	-.6567	-1.0514	-2.8285
207.50	.0149	-.9492	-2.9981
205.00	.6981	-.7992	-3.0419
202.50	1.2536	-.7523	-2.9598
200.00	1.5309	-.8893	-2.8832
197.50	1.3833	-1.2238	-2.7957
195.00	.8836	-2.0275	-3.0255
192.50	.1334	-3.0667	-3.6984

(a) The 7% of α-L-guluronate residues in the poly(β-D-mannuronate) sample (M blocks) is all in alternating sequences, i.e. this sample contains 86% of M blocks and 14% of alternating blocks.

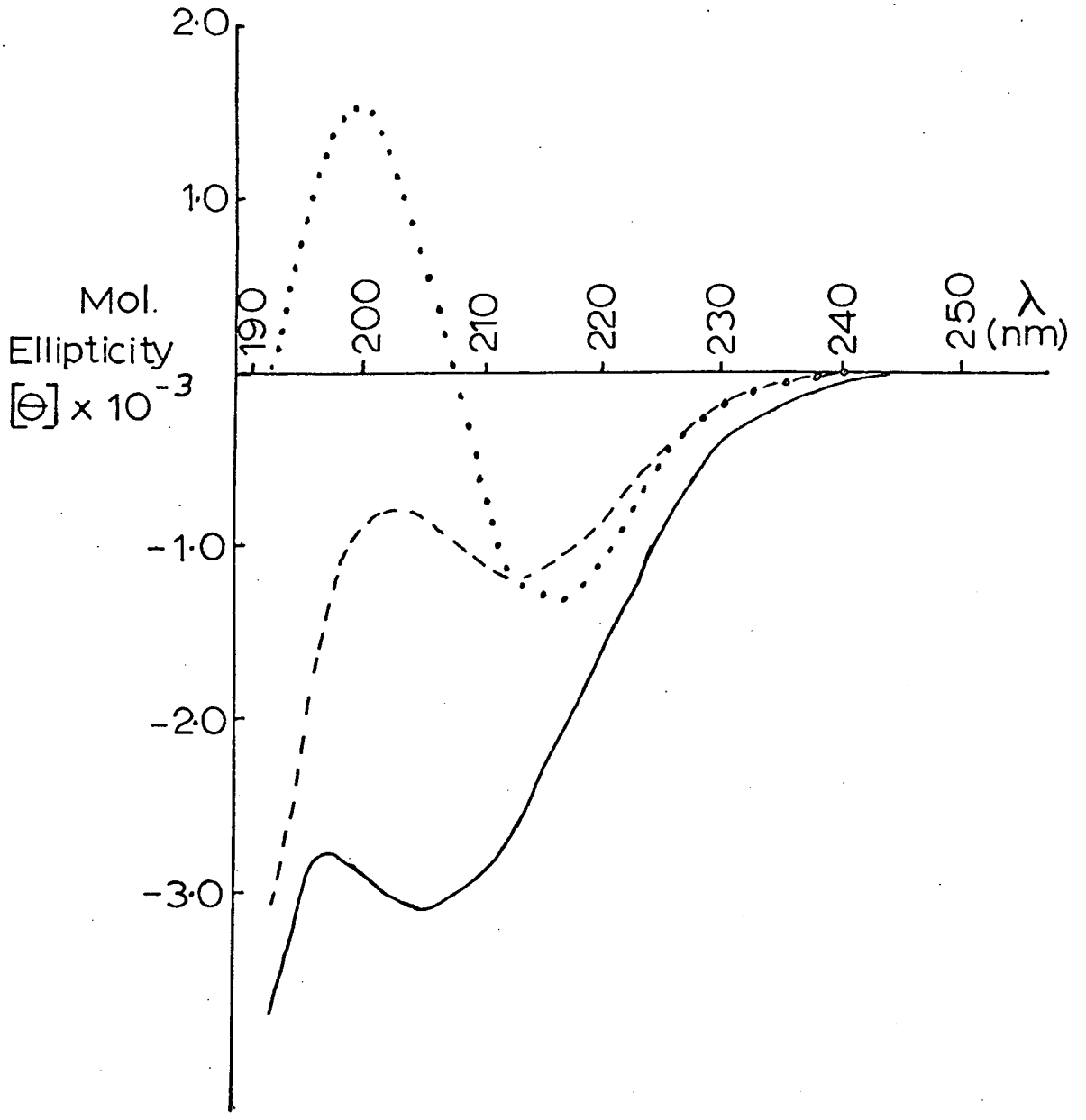

Fig. 3.8 Circular dichroism spectra of the poly(α-L-guluronate), poly(β-D-mannuronate) and poly(β-D-mannosyluronate-α-L-guluronate) block samples in molecular ellipticity ($[\theta]$ x 10^{-3}): the spectra are given by the continuous, dotted and dashed lines respectively.

(b) The 20% excess of β-D-mannuronate residues in the poly(β-D-mannosyluronate-α-L guluronate) sample (alternating blocks) will all behave spectroscopically as poly(β-D-mannuronate), i.e. this sample contains 80% of alternating blocks and 20% of M blocks. As shown in table 3.2 the poly(α-L-guluronate) sample (G blocks) contains only α-L-guluronate residues.

Using the block spectra the computer was asked to compare the spectrum obtained from an equal mixture of the M and G blocks with that of the alternating block and this is shown in fig. 3.9. The spectra show appreciable differences in detail confirming the sensitivity of the c.d. of the uronate residues to neighbouring units

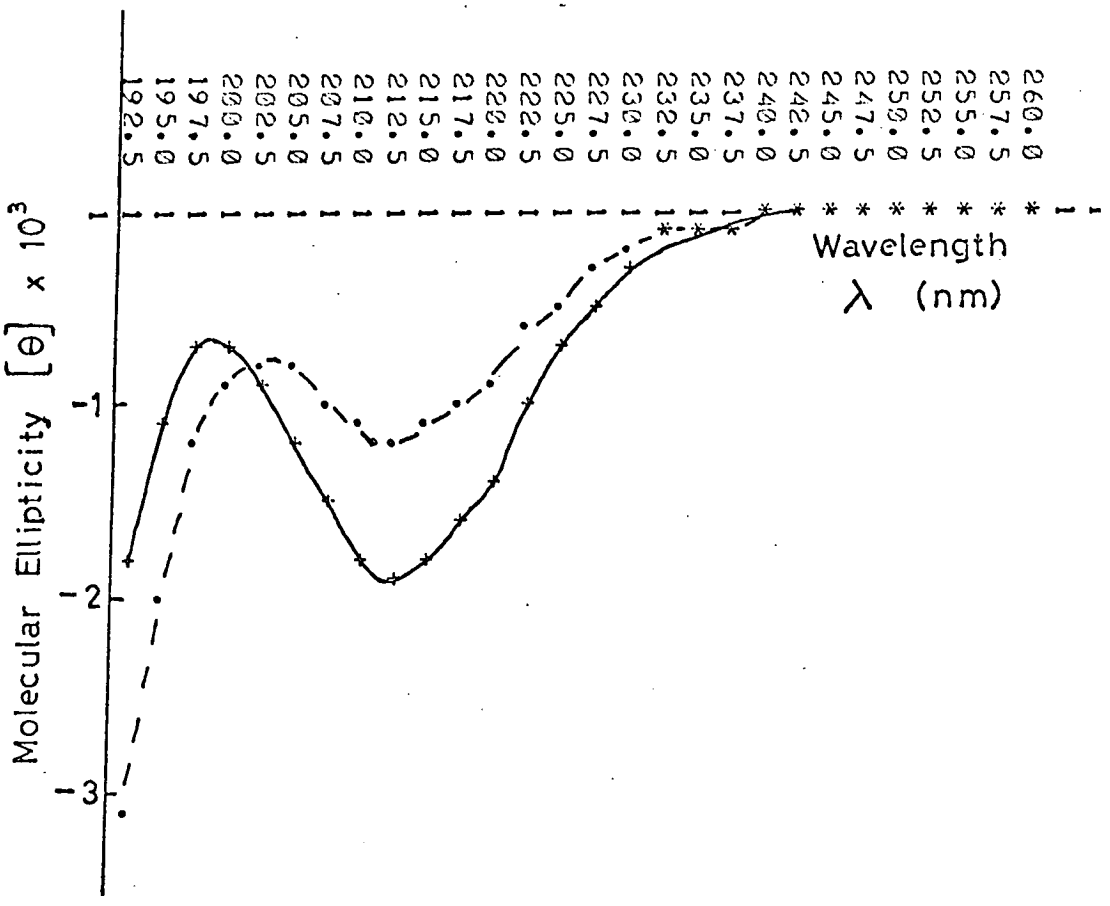

Fig. 3.9 Comparison of the Alt. block spectrum (.- - .) with a 0.5:0.5 mixture of the M block + G block spectra (*——*).

in the alginate chain. The alternating block spectrum has a smaller separation in the wavelength of the peak and trough extrema from that of the mixture and it is also noticeable that the alternating block spectrum is much smaller than that of the mixture. Since increased optical activity is often associated with a locking of conformation[6,10] this is consistent with conformational energy calculations which indicate that the alternating sequences have much greater flexibility about the glycosidic linkages[144] than the homopolymeric sequences. The Peak/Trough ratio of the two spectra in fig. 3.9 can also be measured and from this the percentage of sodium mannuronate determined from the standard curve in fig. 3.5. The alternating block sample (44.5% M) and the mixture of the homopolymeric blocks (54% M) straddle the correct value (50% M) but they remain in reasonable agreement with it considering that these are the extremes of samples which may be encountered. This increases the confidence felt about the accuracy of the c.d. method for the determination of alginate composition.

The computer was given the three block spectra plus the four spectra of the alginate samples 5, 7, 8 and 10; all spectra being expressed in molecular ellipticity $[\theta] \times 10^{-3}$. The computer was asked to determine the best unconstrained fit of the alginate sample spectra by the block spectra as explained in the Experimental section of this Chapter. For all four samples the agreement between the experimental and computer synthesised spectra was extremely good and an example of this agreement for sample 5 is shown in fig. 3.10. However, from the results listed in table 3.5 it can be seen that the proportions of the block spectra required to obtain this agreement do not sum to unity and hence a fundamental condition of

Fig. 3.10. Example of the agreement between the observed and unconstrained computer synthesised spectra for alginate sample 5

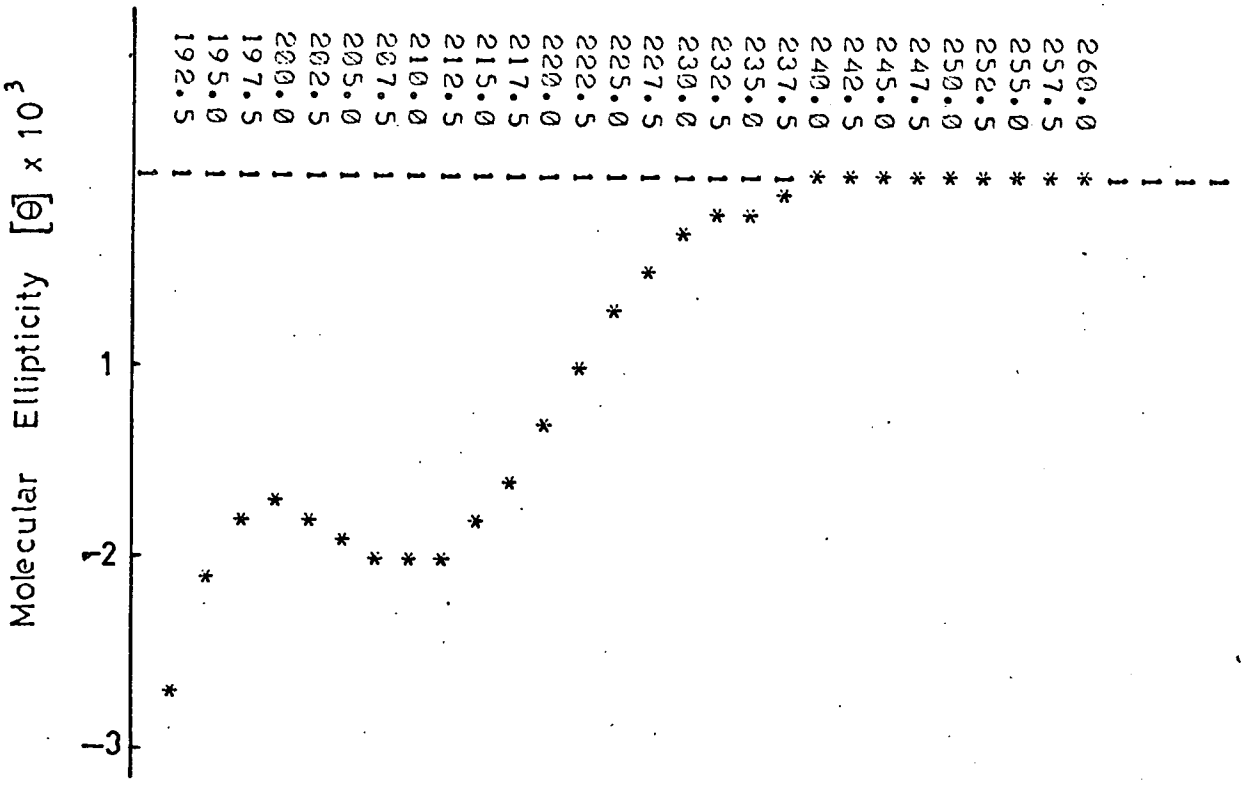

the method is not fulfilled. As indicated below, the spectral agreement obtained when the computer is given this additional piece of information is still very good and these unconstrained results give an indication of the "slackness" of the fit.

TABLE 3.5

Unconstrained computer synthesis of alginate spectra

Alginate Code	Fraction of Block Type			Total
	M	Alternating	G	
5	0.139	0.184	0.601	0.924
7	0.151	0.340	0.464	0.955
8	0.336	0.448	0.207	0.991
10	0.341	0.556	0.162	1.059

The computer was now asked to obtain the best correlation between the observed and synthesised alginate spectra which gave a sum of the proportions of the block spectra equal to one. As explained in the Experimental section of this Chapter this is equivalent to allowing the computer to vary the proportions of two of the block spectra with the third proportion being automatically defined by the sum of the two proportions. For each alginate spectrum a single combination of the block spectra was obtained irrespective of the initial proportions of the block spectra fed into the computer. The observed and synthesised spectra along with the difference between them are shown, for the four alginate samples considered, in figures 3.11 to 3.14 at the end of this Chapter and a graph of the two spectra for each alginate is also included there. It can readily be seen that for all four alginate samples considered the deviation of the synthesised spectrum from the observed spectrum is still very small and well within the acceptable limits for this method. The results obtained giving the computer this additional piece of information are therefore considered to give the detailed analysis of the alginate block structure for the samples studied. In table 3.6 the results are compared with those obtained by the n.m.r. method[129].

TABLE 3.6

Comparison of alginate block structure as determined by c.d. and n.m.r. methods:

Alginate	Proportion of Block Type					
	C.D.			N.M.R.[129]		
Code	M	Alternating	G	M	Alternating	G
5	0.16	0.27	0.57	0.19	0.23	0.59
7	0.16	0.40	0.44	0.20	0.30	0.49
8	0.34	0.46	0.20	0.38	0.41	0.21
10	0.33	0.48	0.19	0.41	0.42	0.18

It can be seen that the c.d. and n.m.r. methods give very good agreement on the amount of poly(α-L-guluronate) in the alginate samples but differ in the amounts of poly(β-D-mannuronate) and poly(β-D-mannosyluronate-α-L-guluronate). A difference in the proportions between the two methods might have been expected since there is no apparent reason why the spectroscopic behaviour of the uronate sequences should coincide exactly with their behaviour under the partial acid hydrolysis which is the basis of the n.m.r. method. It is, therefore, slightly surprising that the agreement between the methods on the amount of G blocks in the alginate samples is so good. This is, however, consistent with the observation[140] that it is easier to prepare pure G blocks by partial acid hydrolysis than it is to obtain pure M blocks or completely alternating blocks, and hence this may be expected to be the most accurately determined proportion by the n.m.r. method.

The proportions of the three block types given in table 3.6 can be used to calculate the sodium uronate composition of the alginates. The compositions calculated in this way are compared in

table 3.7 with those calculated from the n.m.r. method[129] and those determined by other methods. The results show that the composition calculated from the c.d. block structure analysis gives very good

TABLE 3.7

Comparison of alginate compositions calculated from c.d. and n.m.r. block structure with those determined by other methods

Alginate Code	Source	Calculated				Found	
		C.D.		N.M.R.[129]			
		% M	% G	% M	% G	% M	% G
5	Laminaria hyperborea	29.5	70.5	30	70	29	71[(a)]
7		36	64	36	64	38	62[(a)]
8	Ascophyllum nodosum	57	43	60	40	56	44[(a)]
10	Macrocystis pyrifera	57	43	61	39	57.5	42.5[(b)]

(a) By Chemical Analysis (Experimental section of this Chapter).

(b) By c.d. estimation (table 3.3).

agreement with the values determined by chemical means and that this agreement is slightly better than that found between chemical analysis and that calculated from the n.m.r. determination of block structure. The alginate sample 10 also shows that the composition calculated from the alginate block structure analysis agrees very well with that previously determined by the c.d. Peak/Trough method for estimating alginate composition.

Table 3.6 shows that as expected the alginates from different

sources have very different block structures. The sample isolated from Laminaria hyperborea has a high percentage of G blocks with an intermediate amount of alternating blocks and a small amount of M blocks. The samples from Ascophyllum nodosum and Macrocystis pyrifera contain a small amount of G blocks with much larger amounts of M and alternating blocks. As discussed in Chapter 4, this difference in block structure has very important consequences when alginate solutions are gelled, by the controlled introduction of divalent ions, due to the differing abilities of the blocks to form the microcrystallite junction zones which are the basis of the gel.

It is thus concluded that circular dichroism gives a sensitive method for the determination of alginate block structure in addition to that described for the determination of composition (M/G ratio). Three possibilities for improving the technique may be suggested.

(a) If pure samples of poly(β-D-mannuronate) and poly(β-D-mannosyluronate-α-L-guluronate) can be obtained the assumptions listed at the beginning of this section need not be applied.

(b) The Cary 61 can be equipped to record the alginate spectrum directly on to tapes which can be fed into the computer. This would speed up the analysis by making it unnecessary to measure the spectra manually. Moreover, since the spectra could be recorded at every nm (or less), the accuracy of the spectra, and hence the final analysis, would be increased.

(c) If an exact method for determining the concentration of sodium uronate in solution can be obtained the alginate concentration may be determined directly on the solution used to record the c.d. spectrum. This would greatly speed up the analysis and would lead to a quick, sensitive, non-destructive method for the determination of

alginate block structure analogous to that which is possible for the determination of alginate composition.

CORRELATION BETWEEN OBSERVED AND COMPUTER SYNTHESISED ALGINATE SPECTRA USING THE CONDITION :

M BLOCK + ALTERNATING BLOCK + G BLOCK = 1

Fig. 3.11. Alginate sample 5 ($[\theta] \times 10^{-3}$)

calculated proportions M: Alt: G .158: .270: .571

WAVELENGTH	ALGINATE	FITTED	DIFFERENCE
192.50	-2.723	-2.9187	.1957
195.00	-2.0834	-2.1354	.052
197.50	-1.7448	-1.7082	.0366
200.00	-1.6696	-1.6445	.0251
202.50	-1.7495	-1.6951	.0544
205.00	-1.8718	-1.8424	.0294
207.50	-1.9612	-1.9658	.0046
210.00	-1.98	-2.0027	.0227
212.50	-1.9376	-1.9892	.0516
215.00	-1.7824	-1.827	.0446
217.50	-1.5567	-1.6071	.0504
220.00	-1.3027	-1.3206	.0179
222.50	-.9923	-1.0004	.0081
225.00	-.7102	-.7172	.007
227.50	-.5079	-.5105	.0026
230.00	-.301	-.3071	.0061
232.50	-.1834	-.177	.0064
235.00	-.1458	-.1286	.0172
237.50	-.0611	-.0443	.0168
240.00	-.0282	-.0279	3.31400E-04
242.50	-.0141	-.0187	.0046
245.00	-.0141	-.0133	7.94600E-04
247.50	.0094	.0126	.0032
250.00	.0094	.0107	.0013
252.50	.0141	.02	.0059
255.00	-.0047	.00	.0047
257.50	.0094	.0071	.0023
260.00	.0047	-.0031	.0078

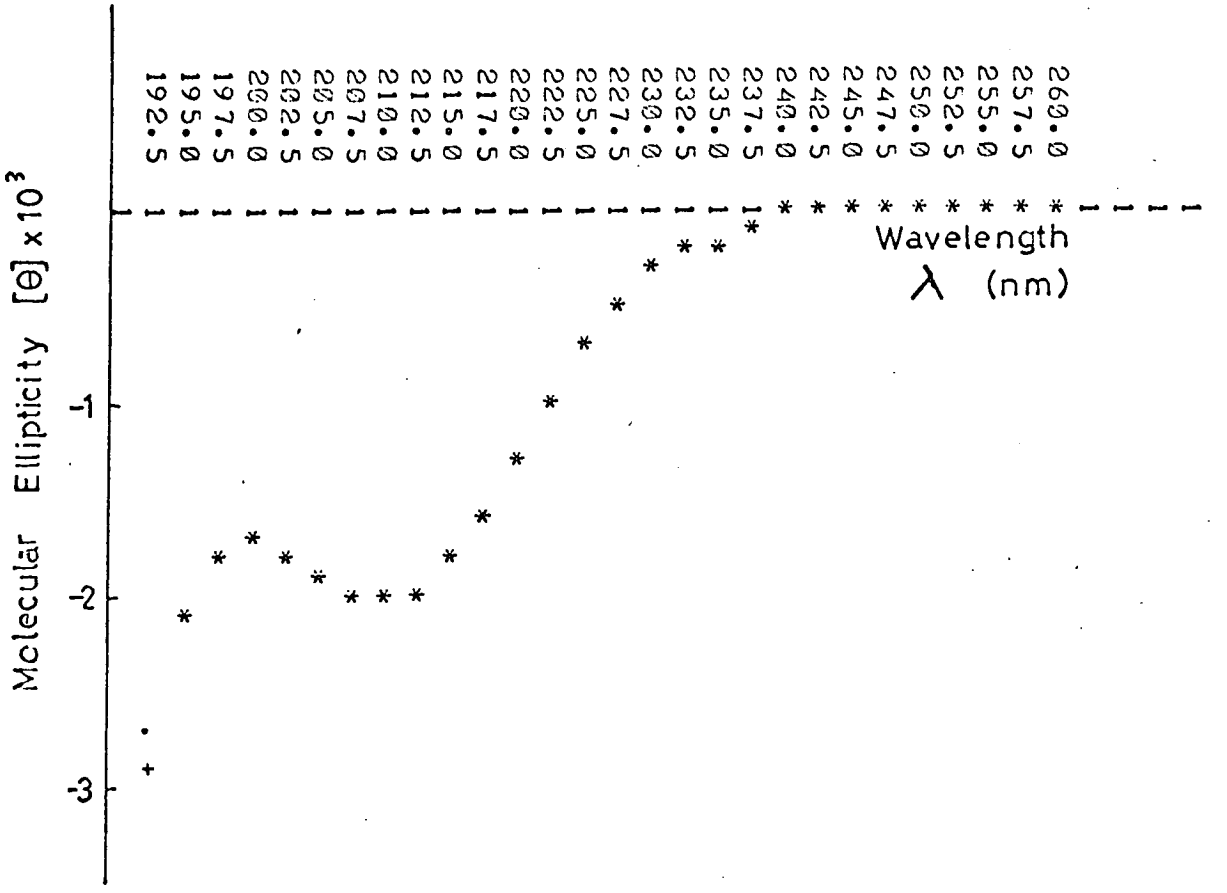

Fig. 3.12. Alginate sample 7 ($[\theta] \times 10^{-3}$)

calculated proportions M: Alt: G .160: .395: .444

WAVELENGTH	ALGINATE	FITTED	DIFFERENCE
192.50	-2.77	-2.8321	.0621
195.00	-1.9765	-2.0028	.0263
197.50	-1.4764	-1.5034	.027
200.00	-1.3609	-1.3865	.0256
202.50	-1.4908	-1.4107	.0801
205.00	-1.5918	-1.5546	.0372
207.50	-1.7072	-1.7037	.0035
210.00	-1.7697	-1.7762	.0065
212.50	-1.7649	-1.80	.0351
215.00	-1.6495	-1.6776	.0281
217.50	-1.4667	-1.4839	.0172
220.00	-1.183	-1.2235	.0405
222.50	-.9137	-.9209	.0072
225.00	-.6492	-.6613	.0121
227.50	-.4472	-.466	.0188
230.00	-.2693	-.279	.0097
232.50	-.1731	-.1578	.0153
235.00	-.0962	-.1141	.0179
237.50	-.0529	-.0406	.0123
240.00	-.0289	-.0238	.0051
242.50	-.0048	-.0187	.0139
245.00	.0048	-.0094	.0142
247.50	.0048	.0107	.0059
250.00	.00	.0123	.0123
252.50	.0096	.0196	.01
255.00	-.0048	.00	.0048
257.50	.0048	.0055	6.52100E-04
260.00	.0096	-.0024	.012

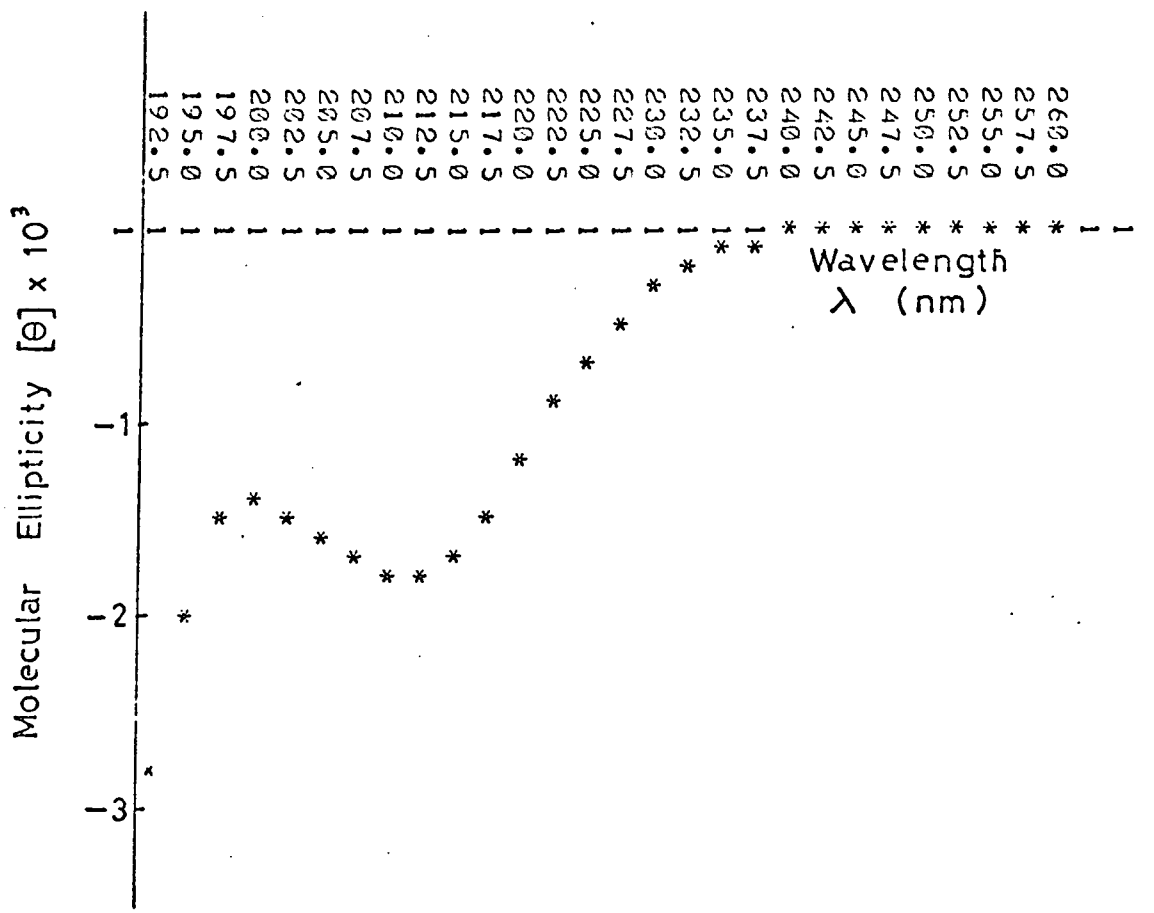

Fig. 3.13. Alginate sample 8 ($[\theta] \times 10^{-3}$)

calculated proportions M: Alt: G .338: .460: .202

WAVELENGTH	ALGINATE	FITTED	DIFFERENCE
192.50	-2.0667	-2.1127	.046
195.00	-1.2505	-1.2451	.0054
197.50	-.6825	-.6601	.0224
200.00	-.4678	-.474	.0062
202.50	-.5441	-.5202	.0239
205.00	-.7398	-.7461	.0063
207.50	-1.0214	-1.0372	.0158
210.00	-1.2744	-1.277	.0026
212.50	-1.4367	-1.4381	.0014
215.00	-1.4224	-1.4217	6.66201E-04
217.50	-1.2935	-1.2942	6.94400E-04
220.00	-1.0692	-1.0739	.0047
222.50	-.8019	-.7955	.0064
225.00	-.5537	-.566	.0123
227.50	-.3818	-.3805	.0013
230.00	-.2243	-.2227	.0016
232.50	-.1146	-.1163	.0017
235.00	-.0859	-.0831	.0028
237.50	-.0334	-.0297	.0037
240.00	-.0143	-.0136	7.12600E-04
242.50	-.0048	-.015	.0102
245.00	.0048	-9.28800E-04	.0057
247.50	.0095	.0102	6.56401E-04
250.00	.0048	.0151	.0103
R52.50	.0239	.0184	.0055
255.00	.00	.00	.00
257.50	.00	.0044	.0044
260.00	-.0095	-.0011	.0084

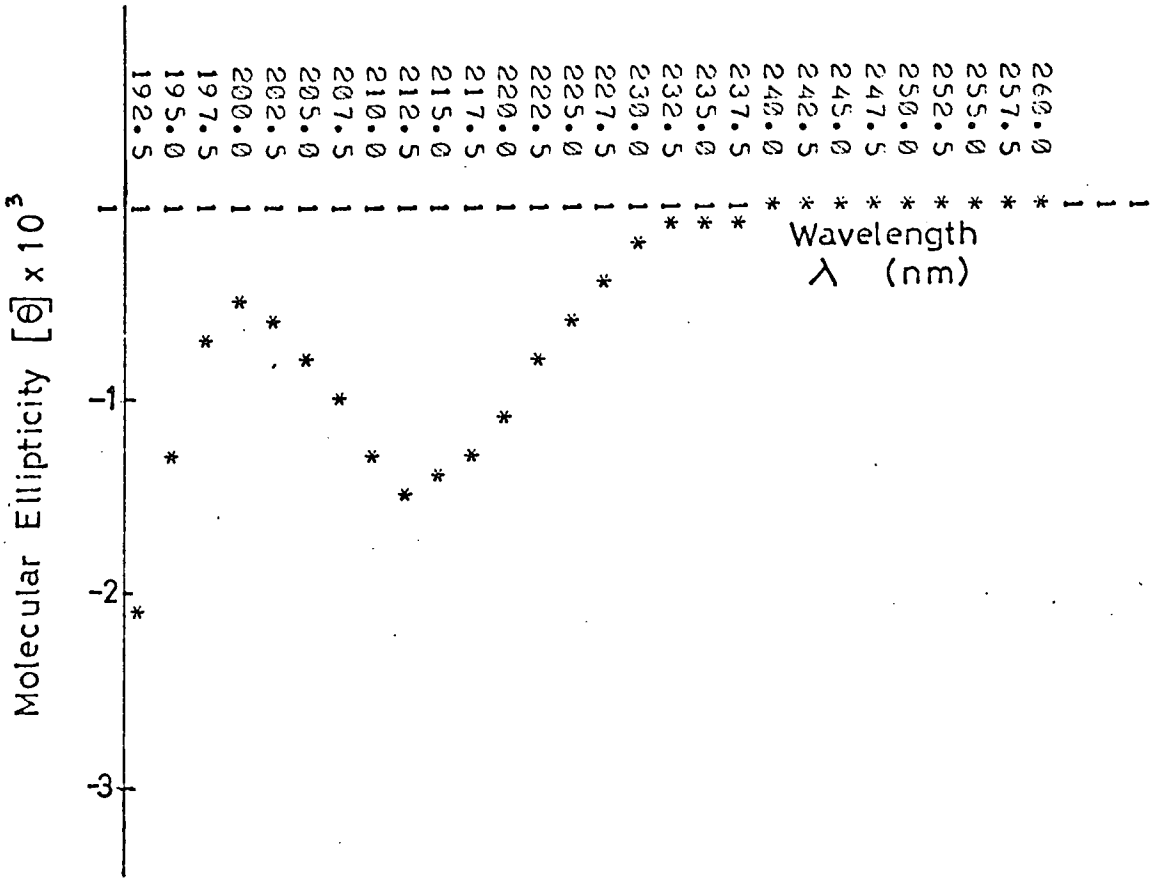

Fig. 3.14. Alginate sample 10 ($[\theta] \times 10^{-3}$)

calculated proportions M: Alt: G .332: .476: .192

WAVELENGTH	ALGINATE	FITTED	DIFFERENCE
192.50	-2.2765	-2.1256	.1509
195.00	-1.3557	-1.2526	.1031
197.50	-.6246	-.66	.0354
200.00	-.3887	-.4686	.0799
202.50	-.5367	-.5102	.0265
205.00	-.6987	-.7327	.034
207.50	-1.0133	-1.0225	.0092
210.00	-1.2632	-1.2616	.0016
212.50	-1.439	-1.4233	.0157
215.00	-1.4436	-1.409	.0346
217.50	-1.3094	-1.2829	.0265
220.00	-1.0781	-1.065	.0131
222.50	-.8282	-.7884	.0398
225.00	-.5691	-.5612	.0079
227.50	-.3748	-.377	.0022
230.00	-.2267	-.2206	.0061
232.50	-.1249	-.1149	.01
235.00	-.0648	-.0821	.0173
237.50	-.0278	-.0296	.0018
240.00	-.0139	-.0133	5.52000E-04
242.50	-.0046	-.0152	.0106
245.00	-.0046	-6.54400E-04	.0039
247.50	.0046	.0099	.0053
250.00	.0278	.0152	.0126
252.50	.0046	.0184	.0138
255.00	.00	.00	.00
257.50	.0093	.0042	.0051
260.00	.00	-.0011	.0011

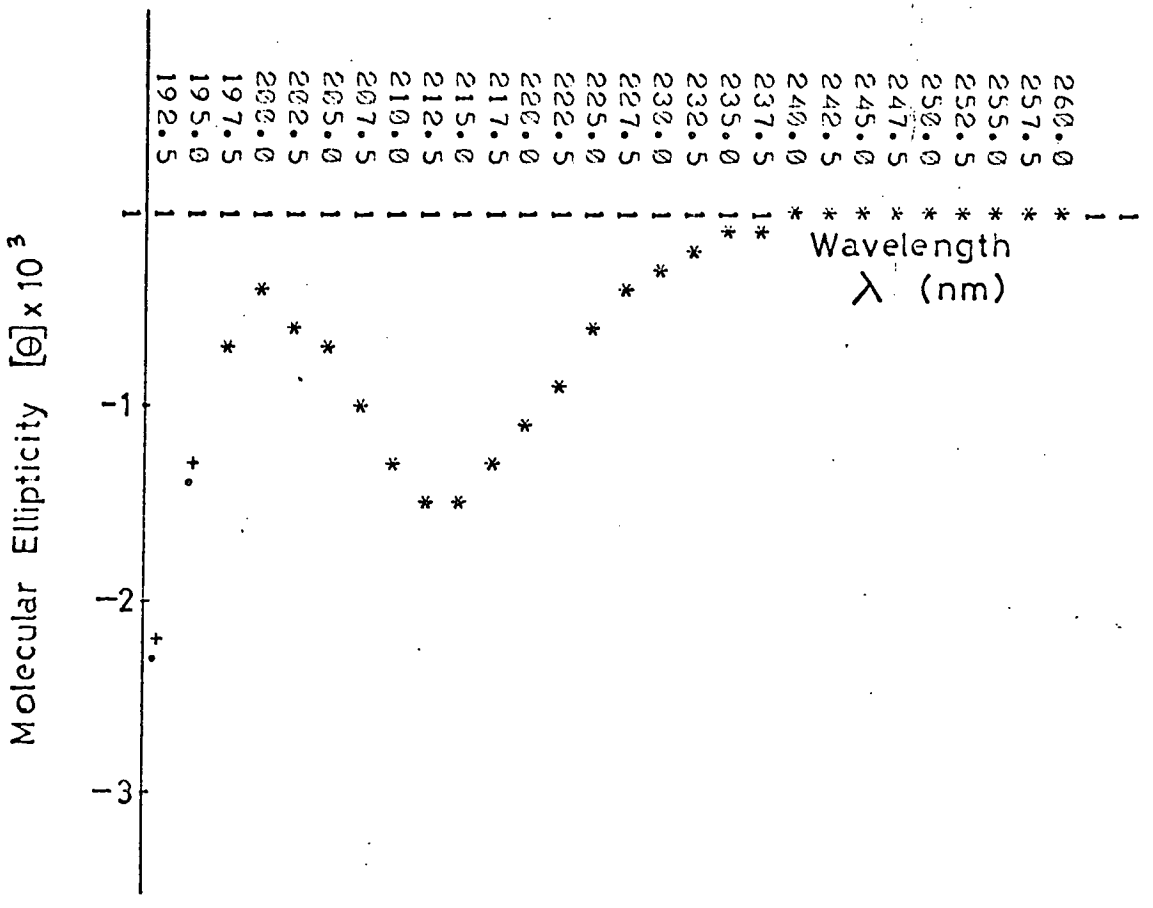

CHAPTER 4

THE CHARACTERISATION OF THE JUNCTION ZONES IN AN ALGINATE GEL USING CIRCULAR DICHROISM

INTRODUCTION

When divalent or trivalent (but not magnesium) metal ions are added to a solution of sodium alginate in a controlled manner firm, reversible gels are formed. The properties of these gels and in particular those prepared using Ca^{++} ions, have been extensively studied and the gels are widely used in industry. Unlike agar or carrageenan gels, they cannot be "melted" and reformed by heat but may be liquefied by ion exchange with an alkali metal cation such as Na^{+} or by sequestering the gelling cation. The general explanation of gel formation of this type is that chain segments associate to form a 3-dimensional framework with solvent in the interstices. The associated regions are called "junction zones" and may be formed from two or more chains. The basic aim of the work described in this Chapter is to understand the precise molecular arrangements in these junction zones and the forces which hold molecules together in them. This study indicates that circular dichroism is a powerful tool for obtaining this kind of information about the specific interactions between polysaccharide polyelectrolytes and inorganic cations.

Gelation Studies

The gels formed by diffusion of divalent metals into solutions of polyuronates have been shown to be birefringent[145] and the presence of X-ray crystallinity[146] after gentle drying of the gel has also been demonstrated. Since the polyuronates in solution behave like random coils[147] the divalent metal ions must have this ordering effect

on the macromolecule. If the proportion of Ca^{++} ions added to the polyuronates is increased the gels have an increased tendency to synerese which suggests that the ordered framework is becoming more and more tightly cross-linked. The final products are the precipitated calcium salts which have been shown to be crystalline[148]. From fibre diffraction of polymannuronic and polyguluronic acid, coupled with supporting i.r. dichroism evidence[128], the chains are seen to be ribbon-like and extended and they pack together like planks in a timber yard. The chains have two fold screw symmetry. For calcium polyguluronate the X-ray evidence[149] suggests that the two fold axis is retained and that the residues remain in the Reeves 1C ring form. Calcium polymannuronate on the other hand exists in a three fold helix with the monosaccharide units in the C1 ring form[149]. This evidence is consistent with model building calculations[16] which show that the only ordered conformations of polyuronates which are stable enough to exist are of the extended type.

The gross properties of polyuronate gels such as strength, texture and appearance under a polarising microscope[145] depend on the method of preparation of the gel. Moreover, on being left to stand the gels exhibit syneresis although this may not begin for several hours after the preparation of the gels. These facts suggest that the networks are not equilibrium states but are changing too slowly to be observed on a laboratory time-scale. This also implies that on this time-scale the frameworks are not continuously breaking and reforming otherwise they would quickly approach the true equilibrium position. Using the above evidence Rees[34,150] suggested that the junction zones are "microcrystallites" held together by cooperative attractions between the chains and the divalent cations which are bound into the chain bundles and

must make a large contribution to the packing energy. At the same time he also refuted the idea of "point cross linking", whether by simple ionic bridging of the negative charges on polyuronates by a divalent metal ion or by chelation of single ions by suitably arranged hydroxyl and carboxyl groups[151]. It is probable, though not essential, that each junction zone is formed from covalent blocks of the same type and that each chain is caused to leave the association at the appropriate block terminus. These termini would then have an equivalent role to the D-galactose-6-sulphate units in carrageenan[150] or the L-rhamnose units contained in the chain in pectate[152] which act as "kinks" in the chain and have a large influence on the cross-linking interactions. Similar views have also been expressed, more recently, by other authors[153,154] and the effect of structural variation of polyuronates is also consistent with this hypothesis. Thus, partial acetylation of polyuronates prevents gel formation[151] and also the selectivity of pectate for calcium in the calcium-potassium ion-exchange reaction (see below) decreases strongly with increasing degree of esterification[155]. This is probably because the irregularly substituted molecules cannot pack together to give a strong, regular lattice.

Ion Binding by Polyuronates

The ion exchange properties of alginates and pectates have attracted considerable attention in recent years and they have been investigated from several different viewpoints. The activities of the counterions have been measured with permeselective membranes[156], osmotic and Donnan equilibria[157] and cation sensitive electrodes[158]. The relative capacities of divalent cations to cause gelation of alginates has been studied by several authors[151,159,160] and the

relative affinities of the divalent cations to alginates have also been determined[161]. The sequence of divalent metals based on gel forming ability and on affinity are significantly different[159] and also depend upon the uronic acid composition of the sample[161]. Ion-exchange reactions between monovalent and divalent cations indicate that the affinity of the alginate for the divalent cations increases with increasing content of guluronic acid residues[162]. A more detailed study[163] also suggests that for the ion-exchange reactions Ca^{++}-Sr^{++}, Sr^{++}-Mg^{++}, Ca^{++}-Mg^{++} and Co^{++}-Ca^{++} the selectivity of alginates is associated solely with the guluronic acid units present. Moreover, it has also been found that polyguluronate and polygalacturonate have a much higher selectivity for calcium ions for the calcium-potassium ion exchange equilibrium than has polymannuronate[164].

The above evidence prompted Haug and Smidsrød[165] to compare the ion binding properties of polyuronates with those of some other polyanions. In general they found that the cases where a significant selectivity is observed fall into two groups.

(a) The selectivity for copper compared to calcium, which seems to be a characteristic feature of all carboxylate containing polymers and of polyphosphate while no such selectivity is observed for sulphated polysaccharides. The main characteristic of these reactions is the lack of importance of the detailed stereochemistry of the polyanion.

(b) The selectivity of polyuronates in exchange reactions between alkaline earth ions; these exchange reactions depend very much on the detailed structure of the polymer and any selectivity is completely destroyed by acetylation. In all cases where a

significant selectivity within the alkaline earth ions is observed, the larger ion is preferentially bound. The three polyuronates, however, seem to behave quite differently with respect to the different alkaline earth ions. Polymannuronate distinguishes only between the large Ba^{++} ions and the other three, pectate between the small magnesium ion and the other three and polyguluronate is unique in distinguishing between the alkaline earth ions with intermediate sizes, namely Ca^{++} and Sr^{++} ions. Polyguluronate, however, has no significant selectivity in the Ba^{++}-Sr^{++} exchange reaction.

All the ion-binding studies mentioned above were carried out on polyuronate samples in the gel state but it has also been noticed[163] that the high selectivity in the alkaline earth exchange reactions appears to be dependent on the existence of the alginate molecules in this insoluble gel state. This has been confirmed by a more detailed study of the ion exchange reactions involving Ca^{++} and Mg^{++} ions for an alginate fragment containing 90% L-guluronic acid residues[153]. Results of experiments with cross-linked fragments, with fragments contained in an agarose gel and with fragments cross-linked to a large excess of dextran show that the selectivity increases with increasing possibility of the fragments forming inter-chain linkages. By comparison of the results with a theoretical model for cooperative ion binding, it has been suggested that the calcium ions are indeed selectively bound in long sequences between polysaccharide chains.

Very recently Kohn and Larsen have also prepared soluble calcium oligo and polyuronates by a very elegant method[166] and they have studied the calcium activities of solutions of these using

tetramethylmurexide as auxilliary ligand. The activity coefficient ($\gamma_{Ca^{++}}$) in solutions of calcium monouronates is close to that of a corresponding solution of calcium chloride. With increasing degree of polymerisation (DP) of oligo and polyuronates the activity coefficients decrease as shown in fig. 4.1. For calcium mannuronates

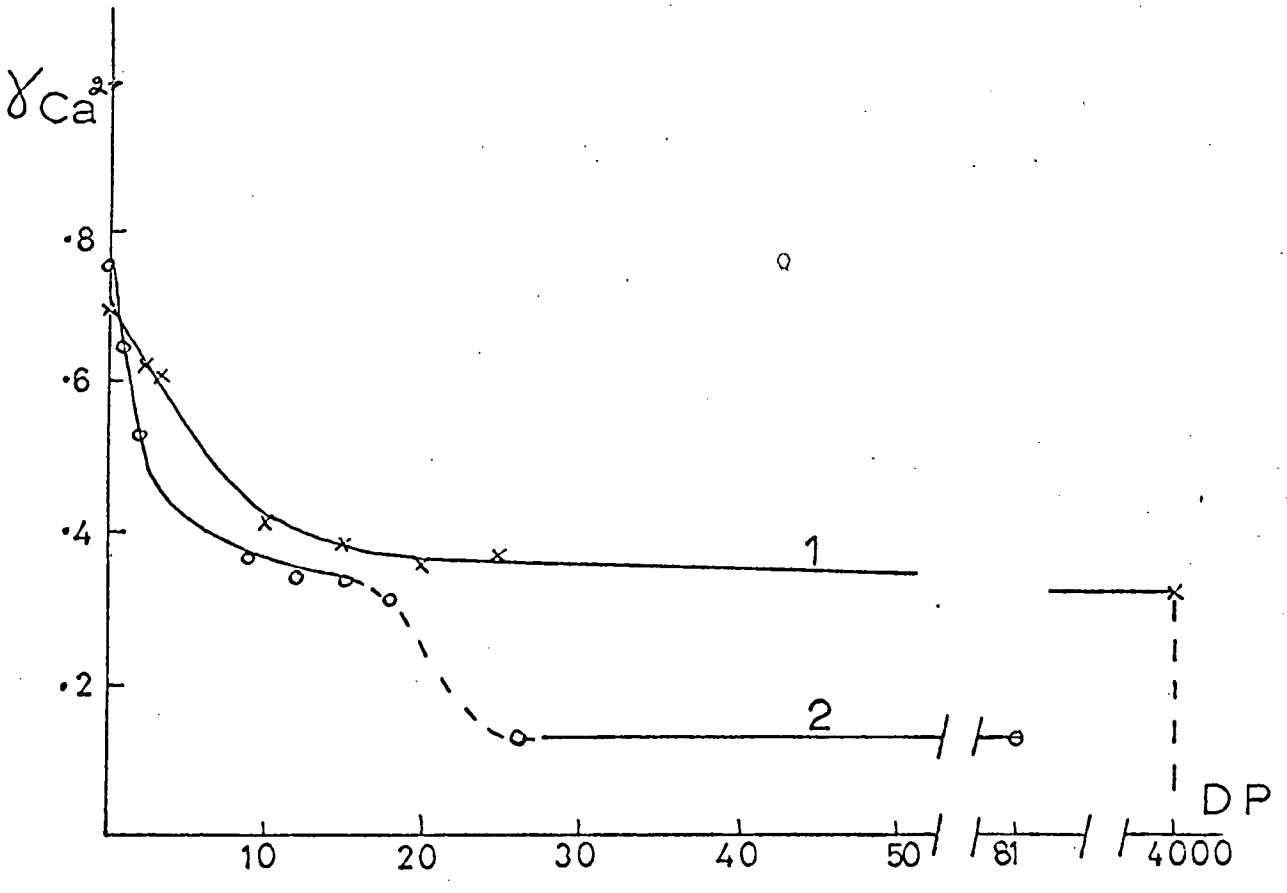

Fig. 4.1 Graph of the activity coefficient (γCa^{2+}) in solutions of calcium oligo and polyuronates against the degree of polymerisation (DP)

1 .. Calcium oligo and polymannuronates

2 .. Calcium oligo and polyguluronates

there is a steady decrease in the calcium activity coefficient with increasing DP up to a chain length of about 30. This type of behaviour can be explained by simple polyelectrolyte effects[34,167]. For calcium guluronates on the other hand there is a much more complicated dependence on molecular weight. Initially the calcium activity shows a steady decrease which is greater than that observed for the mannuronate case. This would have been expected from the higher linear charge density on the buckled polyguluronate chains where each residue has the Reeves 1C conformation. However, calcium guluronates also show a pronounced drop in the activity coefficient in the DP region between 18 and 26 which gives the graph a two step appearance. Kohn and Larsen offered no explanation of this "second step" but such a sigmoidal shaped curve is typical of a cooperative process and may be due to the cooperative association of polyguluronate chains to form soluble aggregates which would be expected to have enhanced ion binding.

EXPERIMENTAL

1. Materials

The alginate samples coded 5, 6, 8 and 9 in Chapter 3 were used in the gelation experiments and the same coding is used in this Chapter. All of the samples had been purified as described in the General Methods section and their purity had been determined by the complete ashing method described in Chapter 3. Analytical grade metal chlorides were used in all the dialysis experiments and all solutions were prepared with deionised water. Dialysis experiments were carried out against solutions of the following ions; K^{+}, Mg^{++}, Ca^{++}, Sr^{++} and Cu^{++}.

2. Measurement of Circular Dichroism

The c.d. spectra were recorded on a Cary 61 C.D. Spectropolarimeter in a 10 mm pathlength cell and using a 10 second integration period. For the solution spectra a base line was recorded on the cell containing deionised water. For the gelation spectra a base line was recorded on the dialysate after the experiment had been terminated. All measurements were made at $25^{\circ}C$ as described in Chapter 3.

To obtain the difference spectra the gelation and solution spectra were measured at every 2.5 nm from 260 nm to 192.5 nm and were corrected at each point for the value of their respective base lines. The corrected gelation spectrum was then subtracted from the corrected solution spectrum. Also, to compare the corrected gelation spectra with the spectra given by the fractions of the three types of blocks which are contained in the alginate the corrected gelation spectra were converted to molecular ellipticities using the formula given in Chapter 3. The molecular ellipticities were again divided by 10^{3} to make the values easier to handle.

3. Measurement of Optical Density

An indirect measure of the optical density of solutions and gels was obtained by measuring their dynode voltage, on the Cary 61 C.D. Spectropolarimeter, with the slit width kept constant. The dynode voltage provides a measure of the light intensity incident on the photomultiplier, higher voltages indicating lower light levels, and thus provides an indication of the sample absorbance.

4. Study of Gelation by Circular Dichroism

A 0.1% solution of the freeze-dried sodium alginate sample was prepared as described in Chapter 3. The solution was millipore filtered (3 μ) and transferred to a dry c.d. cell (on which a base line had been recorded) in one operation using a syringe. The c.d. spectrum of the solution was recorded.

The cell was topped up with more of the solution and a piece of dialysis membrane was stretched over the neck and held in place using a polythene circlip. This is shown in the photograph fig. 4.2. Care was taken that no air bubbles were trapped behind the membrane. The cell was suspended in a large volume(1.5 l) of a 6mM solution of the divalent metal ion and this solution was stirred slowly using a magnetic stirrer. The large excess of the dialysate was used to keep the concentration of the cation in the dialysate at 6mM.

After 4 days the cell was removed from the solution and its exterior dried. The end plates of the cell were cleaned with a tissue impregnated with ethanol. The cell was equilibrated at 25°C in the spectropolarimeter for 15 minutes before the c.d. spectrum of the sample was recorded. After recording the spectrum the cell was resuspended in the solution of the divalent metal chloride. During all these operations the cell was handled as gently as possible to avoid destroying any gel network which was formed.

Fig. 4.2 10 mm c.d. cell as used in the dialysis experiments.

This procedure was repeated after 10 days and further repeated at intervals of 5 to 6 days until no further change in the c.d. spectrum was observed. The cell was removed from the dialysate at this point and its contents examined to see if a gel had been formed. Finally a base line was recorded on the cell filled with the dialysate.

5. Study of the Optical Density on Gelation

This was carried out exactly as described above for the study of gelation by c.d. but in addition every time the c.d. was recorded the dynode voltage was also recorded as described above.

RESULTS AND DISCUSSION

The figures showing the results of this study of alginate gelation using circular dichroism are given at the end of this Chapter. As indicated in Chapter 3, the alginate sample 5 has mannuronate and guluronate residues in the ratio 29:71 and will be referred to as a "high G" alginate. The alginate sample 8 has mannuronate and guluronate residues in the ratio 58:42 and will be referred to here as a "high M" alginate. Moreover, as discussed in Chapter 3, the alginate samples 5 and 6 and 8 and 9 are high and low viscosity fractions of the same alginates. The results obtained in this study will be discussed under several subheadings and the figures referred to as necessary.

1. Gelation of the High G Alginate Sample 5 by Diffusion of Ca^{++} Ions

When Ca^{++} ions are diffused into a 0.1% solution of the high G alginate sample 5 dramatic spectral changes are observed as shown in fig. 4.5. No further spectral changes are observed after 10 days. Examination of the contents of the cell after the dialysis has taken place also shows that a clear, firm, homogeneous gel has formed which occupies all the cell. This simultaneous gelation and large spectral change suggests that the c.d. is monitoring the interaction between the alginate chains and the Ca^{++} ions which causes the chains to become cross-linked to form a 3-dimensional network. This is supported by the results of two other dialysis experiments.

(a) When K^{+} ions are diffused into solutions of both the high G alginate sample 5 and the high M alginate sample 8 only small changes in the c.d. spectra are observed (fig. 4.3 and fig. 4.9). The changes are completed in 4 days and the spectra after diffusion are also slightly increased in amplitude in both cases, in contrast to the

effects with Ca^{++} or Sr^{++} ions. Because of the large excess of the dialysate the alginate must be completely converted to the potassium salt. As expected no gel was formed with this monovalent cation and the alginate solution was clear and free-flowing.

(b) When Mg^{++} ions are diffused into solutions of both the high G alginate sample 5 and the high M alginate sample 8 the spectral changes are again small (fig. 4.4 and fig. 4.10) and again as expected no gel is formed. In this case, however, the amplitude of the spectra decreases as diffusion proceeds, i.e. it changes in the same direction as is observed on diffusion of Ca^{++} and Sr^{++} ions. This is consistent with suggestions[154,168] that magnesium alginate forms soluble aggregates in solution (although no gelation is observed with magnesium ions) but the effect, as observed under the conditions employed here, is extremely small.

At first sight the spectral changes caused by the diffusion of Ca^{++} ions appear to be caused by the removal of the negative contribution to the spectrum from the guluronate residues (which occur predominantly in the form of consecutive sequences in this sample) with the spectrum changing to a more M block type spectrum (c.f. fig. 3.8). The difference spectrum obtained by subtracting the corrected 10 day gelation spectrum from that of the corrected solution spectrum is also shown in fig. 4.5. It is a single sharp trough which is centred on 206 nm and is mathematically gaussian. The position and shape suggest that this component is part of the $n \rightarrow \pi^*$ band and that no alteration takes place in the $\pi \rightarrow \pi^*$ region. A closer examination of the magnitude of the difference spectrum also quickly reveals that it cannot be explained simply in terms of the disappearance of the guluronate contribution to the solution spectrum. The difference

spectrum is very much larger than the solution spectrum and this suggests that not only must a negative contribution be disappearing but also that a positive contribution must be replacing it. This is also shown in fig. 4.6 where the solution and 10 day gelation spectra are compared with the spectra of the proportions of the three types of block which make up the solution spectrum (table 3.6 in Chapter 3). It can readily be seen that there is no way in which a simple disappearance of the contribution from the proportion of one type of block can give the 10 day gelation spectrum. Any explanation must, therefore, involve the appearance of a positive peak.

Two pieces of evidence argue against the possibility that the spectral changes described above are caused by distortions due to light scattering or stress birefringence artefacts.

(a) The difference spectra (fig. 4.14) indicate that the spectral changes are confined to the $n \longrightarrow \pi^*$ region and that very little alteration takes place in the $\pi \longrightarrow \pi^*$ region.

(b) Measurement of the absorbance (dynode voltage) of the low viscosity high G and high M alginate samples (6 and 9 respectively) were carried out in conjunction with the measurements of c.d. In all cases, as shown in figs. 4.19 and 4.22, there was no significant difference between the solution and the 4 and 10 day gelation spectra. These experiments were carried out for the diffusion of Ca^{++} and Sr^{++} ions into solutions of both alginates.

It, therefore, appears that there is a selective perturbation of carboxylate n-orbitals by their proximity to bound Ca^{++} ions and that this causes a reversal in sign of the optical activity of the corresponding $n \longrightarrow \pi^*$ transition. From the evidence presented in the Introduction to this Chapter and the evidence gained from model

building using physical and mathematical methods (discussed later in this Chapter), coupled with the observed extent of the spectral change and the fact that this sample is very rich in G blocks, it may be suggested that c.d. spectroscopy observes a cooperative molecular process which predominantly involves poly(α-L-guluronate) sequences in the alginate structure. The "second step" observed in the ion-binding studies of guluronate oligomers[166] would, therefore, represent the onset of this process observed by circular dichroism.

The guluronate residues in consecutive sequences each have $n \longrightarrow \pi^*$ transitions associated with both carboxylate oxygens and it can be concluded that at least one of these transitions (for each carboxyl group) is initially negative and converts to positive in this region of the spectrum when Ca^{++} ions are cooperatively bound. This explanation is supported by the model building studies (discussed below) which show the likely coordination site of the Ca^{++} ion. Relative to the symmetry planes of the chromophore the ion is in the same region of space as O(4) and O(5) which, in solution, determine the sign of the $n \longrightarrow \pi^*$ band[33]. It may, therefore, be suggested that the positive charge induces optical activity which is more pronounced and in the opposite sense to that induced by the electronegative oxygen atoms. A similar dependence of the sign and magnitude of induced optical activity on the nature of the inducing substituent has been clearly demonstrated[169] for the closely related but more fully understood ketone $n \longrightarrow \pi^*$ transition.

2. Gelation of the High G Alginate Sample 5 by Diffusion of Sr^{++} Ions

When Sr^{++} ions are diffused into a solution of the high G alginate sample 5 large spectral changes are again observed which are similar to those obtained on diffusion of Ca^{++} ions. However,

as shown in fig. 4.7, the final diffusion spectrum is more positive on dialysis of Sr^{++} ions and, moreover, the spectral changes are not complete in 10 days but continue, although at a much slower rate, up to $\sim$25 days. Examination of the cell contents after the spectrum had stopped changing again showed that a clear, homogeneous gel had formed which occupied all the cell. The differences in the gelation processes using Sr^{++} and Ca^{++} ions are much more easily studied by comparing the difference spectra and these are given in figs. 4.14 and 4.15. The increased magnitude of the final difference spectrum for the strontium gelation is readily observed and it can also be seen that the sharp, negative trough has moved to lower wavelength and now has its minimum at 204 nm. The difference spectra also emphasise again that when Sr^{++} ions are diffused into the high G alginate solution instead of Ca^{++} ions, although a larger change has taken place after 4 days, the complete change takes longer to occur.

As mentioned in the Introduction to this Chapter, ion-binding studies[163,165] show that alginate has a much greater affinity for Sr^{++} ions than for Ca^{++} ions and this applies particularly to poly(α-L-guluronate) sequences. Two possible explanations for the differences in the difference spectra may, therefore, be suggested which are consistent with the observed ion-exchange properties.

(a) It may be considered that when Ca^{++} ions are diffused into the high G alginate solution all of the polyguluronate sequences are not completely associated because of constraints imposed by the formation of the 3-dimensional network. It may then be suggested that when Sr^{++} ions are diffused into the alginate solution the increased affinity of the chains for the large Sr^{++} ions leads to a greater amount of chain association and a more tightly bound network. The larger initial

change which is observed (after 4 days) may be due to the increased affinity of the chains for Sr^{++} ions while the slowing up of the spectral change thereafter is consistent with the idea that the network constraints will begin to play an ever-increasing part in hindering association.

(b) It is possible that the amount of polyguluronate sequences associated is the same in both diffusion cases. The preference of the chains for the large Sr^{++} ions which is shown by the ion binding studies may then be due to these ions being a better "fit" for the coordination sites than the Ca^{++} ions and this is consistent with the model building calculations discussed later in this Chapter. From the above statements it may be suggested that the larger observed difference spectrum arises from a more specific positioning of the Sr^{++} ion, with respect to the coordinating atoms and the symmetry planes of the chromophore, which enhances the optical activity induced in the chromophore by the presence of the positively charged ion. Such an explanation is consistent with the observed shift of the difference spectrum minimum to slightly lower wavelengths.

It is also possible that both these processes are occurring simultaneously and that the observed differences in the difference spectra arise from the sum of the effects described above.

3. Gelation of the High G Alginate Sample 5 by Diffusion of Cu^{++} Ions

As shown in fig. 4.8, diffusion of Cu^{++} ions into a solution (0.1%) of the high G alginate sample 5 also produces large spectral changes but these are completely different from the effects observed on diffusion of Ca^{++} and Sr^{++} ions. In this case the spectrum after 4 days is considerably broadened and flattened and this trend is accentuated in the 10 day spectrum. The 10 day spectrum is also

very noisy in the spectral region below 220 nm. The dialysis experiment was terminated at this point. Although the gel formed after 4 days appeared to be perfectly clear, that observed after 10 days diffusion was definitely not homogeneous but had a striated, stringy appearance. It is, therefore, considered that in the 10 day spectrum there is probably some distortion due to light scattering or stress birefringence artefacts and this is possibly also true for the 4 day spectrum.

The spectra do, however, give a dramatic illustration that the binding mechanism of the high G alginate for Cu^{++} ions is very different from that involved for Ca^{++} and Sr^{++} ions. The single, sharp, negative, gaussian troughs of the difference spectra for Ca^{++} and Sr^{++} diffusion suggest that a specific binding site must be involved. In contrast, the broad, flattened spectra on diffusion of Cu^{++} ions indicate that a large number of non-specific binding sites are probably involved which absorb at different wavelengths. This is in agreement with the ion-binding studies mentioned in the Introduction to this Chapter. Moreover, it has also been found[165] that the higher affinity of such polyanions for copper relative to calcium is not destroyed by acetylation and is, therefore, independent of the presence of hydroxyl groups. A very recent paper also indicates[170] that coordination to copper ions can be sufficiently strong, in carboxylate containing sugar molecules, to cause distortion of the pyranose chair conformation.

In conclusion, the ion-binding studies coupled with the evidence from circular dichroism suggest that the alginate molecules are tightly bound to Cu^{++} ions in a very large number of different ways which are independent of the detailed stereochemistry around the carboxyl groups, unlike the specific site binding suggested for Ca^{++} and Sr^{++} ions.

4. Gelation of The High M Alginate Sample 8 by Diffusion of Ca^{++} and Sr^{++} Ions

As shown in figs. 4.11 and 4.13, large spectroscopic changes are again observed when Ca^{++} and Sr^{++} ions are diffused into a 0.1% solution of the high M alginate sample 8. As for the high G alginate, diffusion of these ions produces very similar spectral changes although there are some secondary differences which are discussed below. For solutions of this alginate all spectral changes are completed after 10 days diffusion of the ions and examination of the cell contents shows that clear, firm gels had been formed in both cases.

The maximum of the $n \longrightarrow \pi^*$ peak at $\sim$ 200 nm in the solution spectrum of the high M alginate is initially negative because of the contribution from the guluronate residues in this sample. On diffusion of Ca^{++} ions, this maximum becomes positive as is seen from the 4 day spectrum (fig. 4.11). This is most probably due to spectral changes, of the type described above, which are caused by the cooperative binding of the Ca^{++} ions by association of poly(α-L-guluronate) sequences. In a subsequent step, however, the spectrum swings back to become less positive and this can be seen from the 10 day spectrum. It therefore appears that an additional effect takes place in this case. This reasoning is supported by considering the difference spectra obtained by subtracting the corrected gelation spectra from the corrected solution spectrum. As shown in fig. 4.16(a), these difference spectra are not gaussian, unlike those for the high G alginate, and the peak minimum has also shifted to higher wavelength ($\sim$ 211 nm). By considering the spectra which would be given by the proportions of the block samples which make up this alginate structure,

(fig. 4.12), coupled with the results from the model building calculations discussed later, the most probable explanation is that some association of poly(β-D-mannuronate) sequences can occur which has a similar type of effect to that shown by the polyguluronate sequences when they form junction zones. For polymannuronate a reduction in size of both the positive and negative peaks might be expected if this were the case and this is consistent with the observed effects.

It is now possible to give two interpretations of the observed spectral changes for alginate sample 8.

(a) Hypothesis 1: in the first stage the cooperative binding of Ca^{++} ions by polyguluronate proceeds with its characteristic spectroscopic change until the available binding sites are saturated and the concentration of Ca^{++} is able to rise. Binding by polymannuronate can then occur, when the threshold for this process is passed, and this causes a shift in the negative direction which stops when chain association is constrained by the network.

(b) Hypothesis 2: polymannuronate chains can associate very quickly but their affinity for calcium ions is very much less than that of polyguluronate chains because of the much poorer coordination sites for the cations (discussed below). It may now be imagined that when the polyguluronate chains associate they can rupture any association of polymannuronate blocks which is hindering this process. The polymannuronate blocks will, therefore, be continually associating and dissociating as the polyguluronate junctions form. On complete association of the polyguluronate chains the polymannuronate chains which are not already associated will try to do so as best they can although they will be hindered by the constraints of the network. These two explanations of the gelation of alginate sample 8 could be

distinguished by monitoring the gelation of the alginate continuously, by carrying out the diffusion process in the c.d. spectropolarimeter, and hence observing the initial stages of gelation. Both of these theories do, however, imply that, although polymannuronate sequences can play a role in alginate gelation, the strength and texture of the gels is predominantly influenced by the cooperative binding of ions by polyguluronate sequences.

Similar but less detailed conclusions were already indicated by the evidence presented in the Introduction to this Chapter and, more recently, by evidence that gel stiffness is a function of the guluronate residues[171,172]. On the other hand the rate of gelation is greater[172] for alginates having lower contents of guluronic acid residues. This is also indicated by comparison of the difference spectra for the diffusion of Ca^{++} into the high G and high M alginates (fig. 4.14 and fig. 4.16(a)). It can be seen that after 4 days the high M alginate has almost completed its spectral changes whereas the high G alginate shows a very much greater difference between the 4 and 10 day spectra. This can be readily explained in the terms already postulated. In high M alginates the longer lengths containing mannuronate residues have much less tendency to associate (or to remain associated in hypothesis 2) and they retain a greater flexibility as the polyguluronate blocks associate and the system as a whole becomes increasingly constrained. This allows more freedom for the movement of polyguluronate binding sites within the developing network so that the final gel is established more quickly.

On diffusion of Sr^{++} ions into the high M alginate solution the $n \rightarrow \pi^*$ maximum again goes from negative to positive from the solution spectrum to the 4 day spectrum. The positive peak is

greater in magnitude (fig. 4.13), than is the case for Ca^{++} diffusion but the residual trough is also bigger. The spectra also show a decrease in the size of this peak after 10 days diffusion of Sr^{++} ions. To compare the results of diffusion of Sr^{++} and Ca^{++} it is better to examine the difference spectra (fig. 4.16). For the diffusion of Sr^{++} it is seen that the difference spectrum is broader than for Ca^{++} diffusion and it also has its minimum at lower wavelength ($\sim$ 207 nm). This is consistent with there being a contribution from the poly (α-L-guluronate) sequences which behaves analogously to the effects observed for the high G alginate, i.e. for Sr^{++} diffusion its minimum is at lower wavelength and may be greater in magnitude. However, it is obvious that an additional effect is also seen, when Sr^{++} ions are diffused into high M alginate, which appears to be very similar to that observed on diffusion of Ca^{++} ions.

5. Gelation of the "Low" Viscosity Samples of the High G (sample 6) and High M (sample 9) Alginates by Diffusion of Ca^{++} and Sr^{++} Ions

Gelation experiments were also carried out in which Ca^{++} and Sr^{++} ions were dialysed into 0.1% solutions of the "low" viscosity forms of the high G and high M alginates (samples 6 and 9 respectively). The results are shown in figs. 4.17 and 4.18 and figs. 4.20 and 4.21. It can be readily seen that these samples give spectral changes which are extremely similar to those shown by the "high" viscosity samples and the dialysis was, therefore, stopped after 10 days. As already mentioned indirect optical density measurements were made on the solutions and gels (fig. 4.19 and 4.22) but no significant differences were observed. Using the thermostattable cell holder on the Cary 61 the cell containing the gels formed after 10 days diffusion of Ca^{++} were also heated at 80°C for 1 hr and then recooled and the spectrum

re-recorded. As shown in figs. 4.20 and 4.17 the spectrum of the high M alginate sample did not change at all after this treatment and the high G sample spectrum only became very slightly more positive

Discussion on the Molecular Arrangements in the Junction Zones of an Alginate Gel

Three main factors must be considered in attempting to understand the binding of cations by these polyuronates[150].

(a) The intramolecular stereochemistry

(b) The polyelectrolyte effect

(c) The ease with which the polysaccharide chains can pack together when chain association is part of the binding mechanism.

In the Introduction to this Chapter it was shown that the D-mannuronate residues in an alginate molecule are β-linked in the Reeves C1 conformation and that the L-guluronate residues are α-linked in the 1C conformation in both the solid state and in solution. The effect of this on the ion-binding due simply to polyelectrolyte effects was also discussed there and will not be considered in this section. This discussion is concerned with the detailed 3-dimensional geometry of the associated polysaccharide chains in the junction zones of an alginate gel.

A close inspection of the buckled chain of guluronate residues in poly (α-L-guluronate) sequences indicates that there is a hydrophilic "nest" formed between each pair of residues (fig. 4.23). This is made up of the carboxyl group and O(5) on one residue with O(2′) and O(3′) on the next residue in the "non-reducing" direction. Using the criterion for optimum binding suggested by Williams[173] that a Ca-O(6) distance of 2.6 ± 0.2 Å is required, with as many as possible other Ca-O distances of 2.7 ± 0.3 Å, Smith[174]

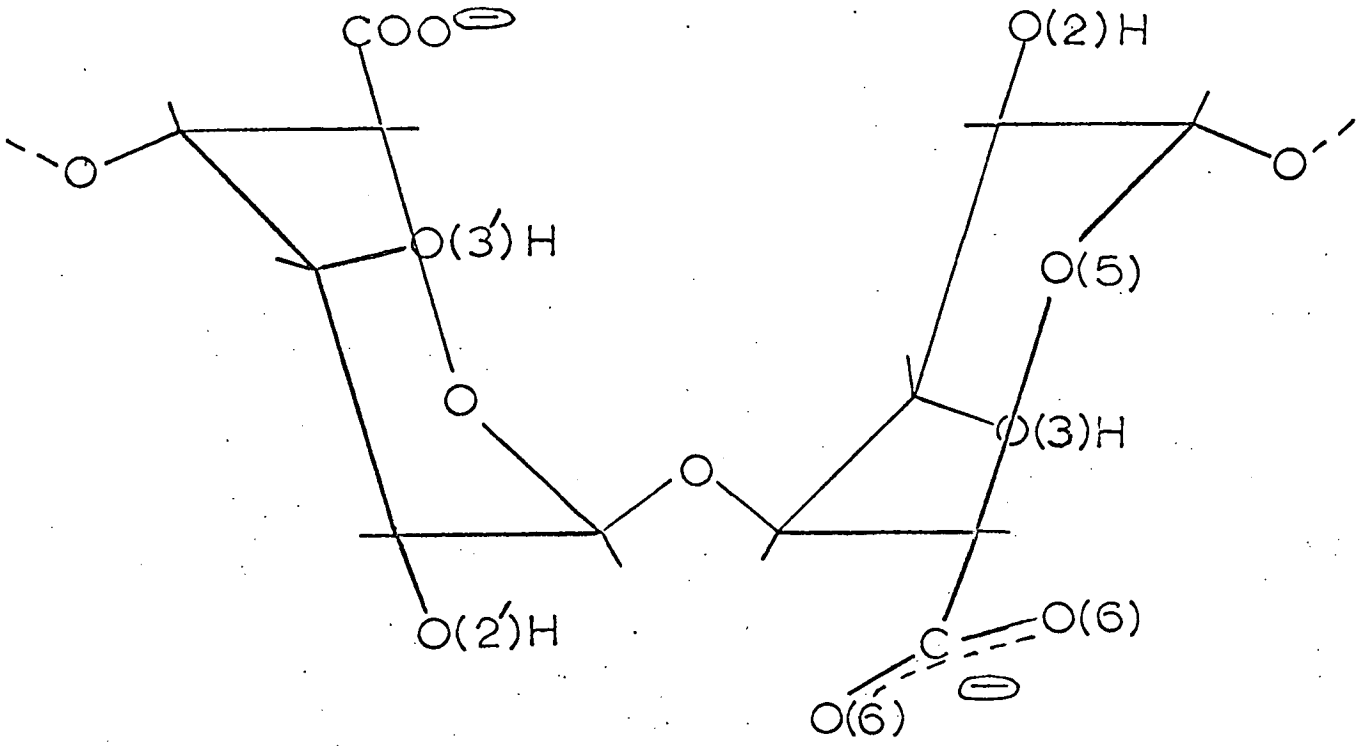

Fig. 4.23 The disaccharide repeat in the buckled chain of a poly(α-L-guluronate) sequence.

investigated the ion-binding ability of polyuronates by computer model building. The angles ϕ, ψ and ω (fig. 4.24) were varied systematically over reasonable ranges and at each stage the ion-binding capacity was assessed in terms of the above criterion.

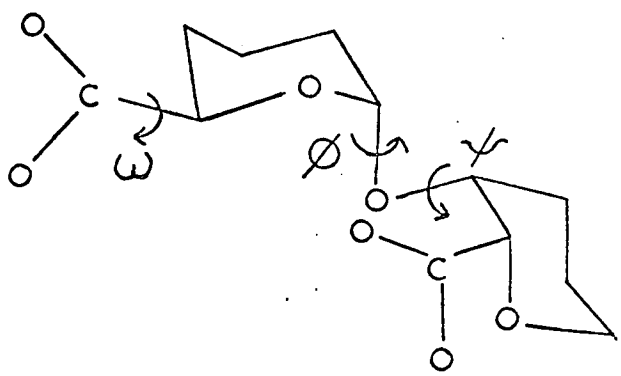

Fig. 4.24

Since the binding phenomenon involves ordered chain conformations, only backbone conformations with integral screw symmetry were considered.

It was shown that polyguluronate could indeed coordinate the Ca^{++} ion using the four oxygen atoms mentioned above and that the chains could have two or three fold symmetry. Using this information a study of molecular models indicated that two polyguluronate chains appear to be able to pack together best if they have two fold symmetry and are antiparallel. This is consistent with the experimentally determined crystal structure[149]. A space filling model of the proposed structure of the microcrystallite junction zones formed from polyguluronate sequences is shown in the photograph - fig. 4.25. Three associated chains are shown. Each chain has two fold symmetry and the centre chain is antiparallel to the other two. The buckled nature of single polyguluronate chains is clearly shown by the line drawn through the bottom chain. The calcium ions bound by the top and centre chains lie towards the top of the model as it is photographed. The ions bound by the centre and bottom chains lie in identical sites but, because of the two fold axis, they are towards the bottom of the model. It can be seen that each calcium ion lies in a well defined site formed from two of the hydrophilic "nests" mentioned earlier. Each calcium ion is completely surrounded by oxygen atoms and is coordinated by two carboxyl groups (balance of charge) and six other oxygen atoms (O(2′) O(3′) and O(5)) on each chain. This gives the calcium ions a coordination sphere of 8 atoms which is the coordination number often found[175] for Ca^{++} and Sr^{++} ions. Examination of the model also shows that the hydrophobic regions of the alginate chains which lie between the hydrophilic nests are also juxtaposed in an

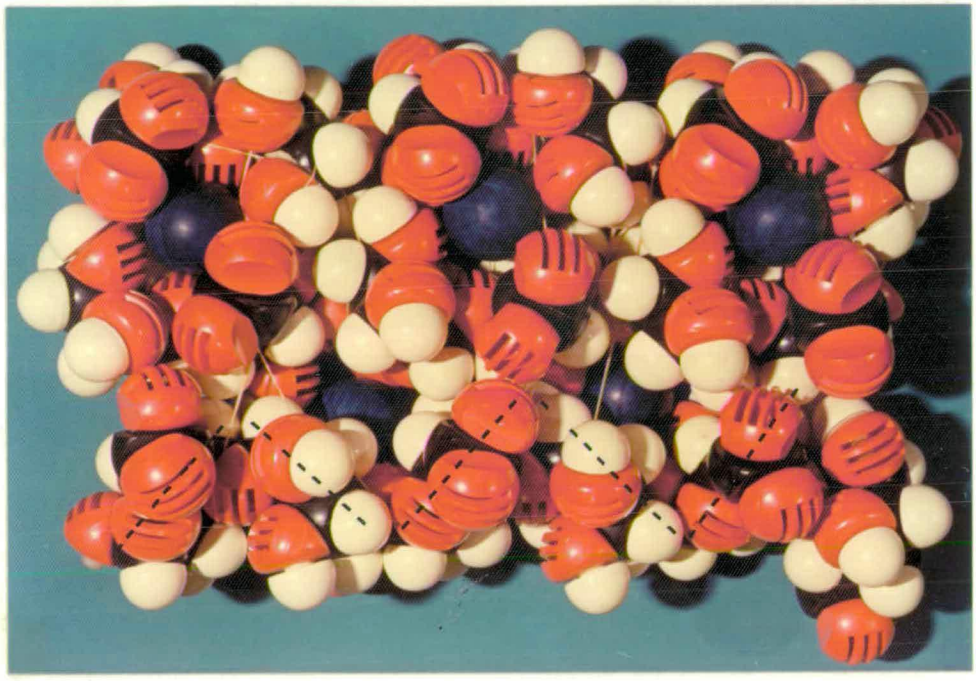

Fig. 4.25 A CPK space filling model of the proposed structure of the microcrystalline junction zones formed from polyguluronate sequences. Three chains are shown. Each chain has 2 fold symmetry and the centre chain is antiparallel to the other two. As explained in the text each calcium ion occupies a specific site in which it is coordinated by a carboxyl group and three oxygen atoms (O(2′) O(3′) and O(5)) on each chain. Examination of the model also shows that the hydrophobic regions of the chain which lie between the hydrophilic "nests" are juxtaposed in this structure and this should help the chains to pack together.

associated structure of this type and this should also increase the ability of the chains to pack together.

The computer calculations also show that polymannuronate chains can form sites with both two and three fold screw symmetry and in fact calcium polymannuronate crystallises with three fold screw symmetry[149]. Inspection of models, however, shows that the equatorial-equatorial linkage, as opposed to the axial-axial linkage in polyguluronate, leads to a much flatter structure which gives much poorer "nests" for the cations to occupy. Moreover, the axial O(2) on each residue protrudes from this flattened structure and would hinder the efficient packing of the chains. This may partly explain the lower tendency of such chains to complex. The calculations also show that when the inherently more flexible chains[144] of alternating mannuronate and guluronate residues are constrained to ordered structures having integral screw symmetry (mainly four fold) they have little ability to complex.

Polygalacturonate has an axial-axial linkage and superficially it has a very similar buckled ribbon shape to that of polyguluronate. The computer calculations show, however, that because of the equatorial hydroxyl on C(3) polygalacturonate has fewer coordination possibilities than polyguluronate and that most of these only involve three oxygen atoms. Two fold symmetry would seem to be preferred. It might, therefore, be expected that polyguluronate would form the strongest complexes and indeed strontium polyguluronate is much more stable than any known complex of polygalacturonate[165]. Moreover, the calculations also show that the spacing of the coordinating oxygen atoms is larger for polyguluronate (3.8 Å rather than 3.4 Å). This may explain why polyguluronate shows a strong selectivity of Sr^{++} for Ca^{++} whereas polygalacturonate does not[165].

In conclusion, the cooperative mechanism for the association of two or more chains in the gelation of alginates by divalent cations can be thought of in terms of an "egg-box" model similar to that shown schematically in fig. 4.26. The buckled chains are shown

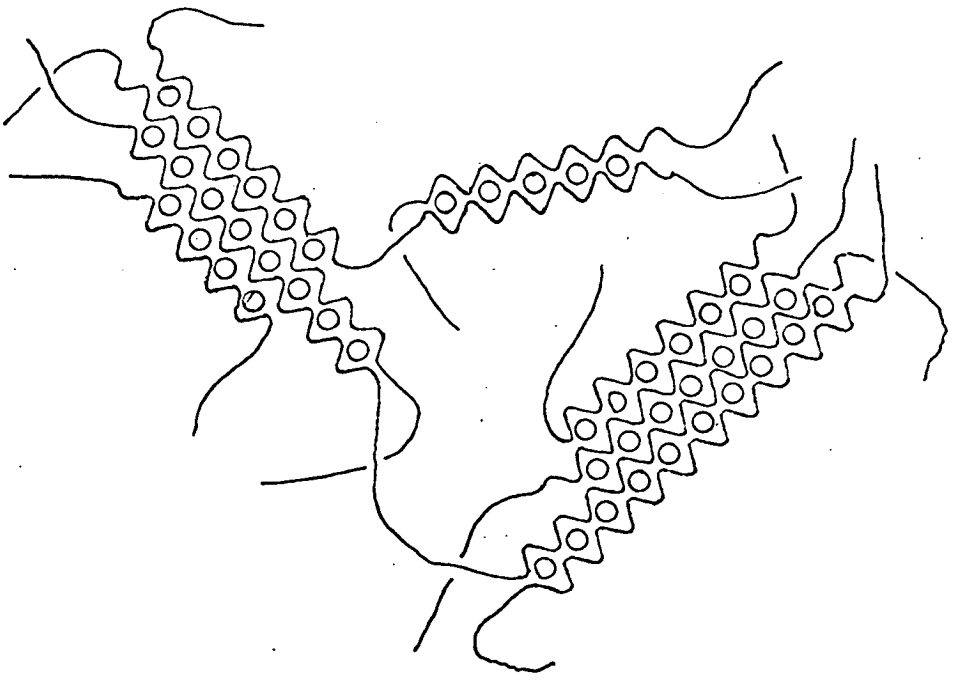

Fig. 4.26 Schematic representation of the "egg-box" model for the junction zones in an alginate gel.

as a two dimensional analogy to a corrugated egg-box in which the ions can pack and be coordinated. For the chains with three fold symmetry the association would probably occur in three dimensions rather than two. Chains with two fold symmetry may conceivably associate in the third dimension but for polyguluronate sequences this is not a necessary

requirement. The analogy is that the strength and selectivity of binding by the cooperative mechanism is determined by the way in which the "eggs" can pack into the "box" and by the way in which the polysaccharide chains forming the box can pack with each other around the eggs.

CIRCULAR DICHROISM SPECTRA

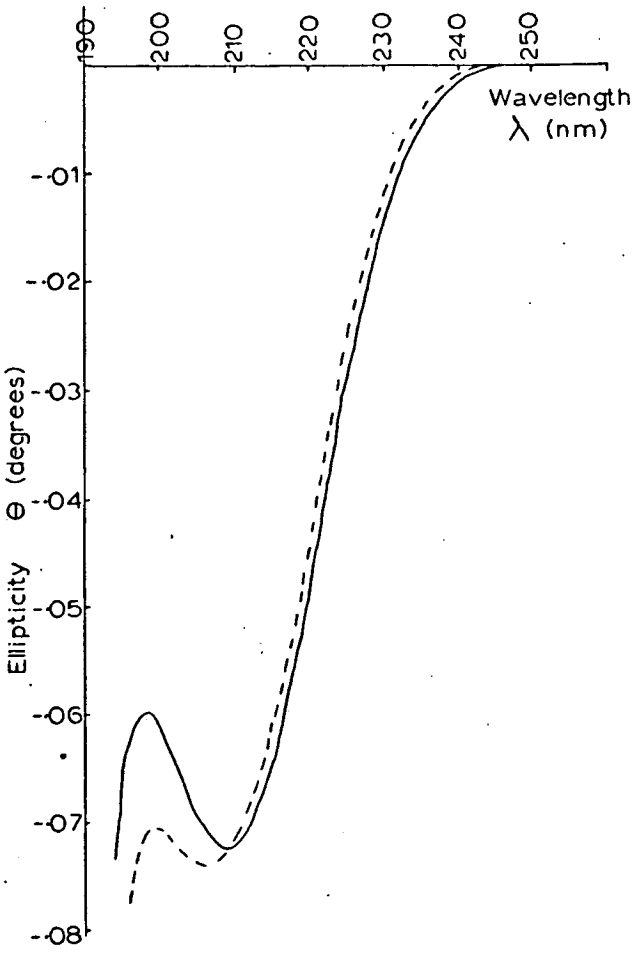

Fig. 4.3 Changes in circular dichroism spectrum with the diffusion of K^+ to a final concentration of 6mM into a solution (0.1%) of the high G alginate sample 5. The solution spectrum is shown by the continuous line and the spectrum after 4 days is shown by the dashed line. No further changes were observed.

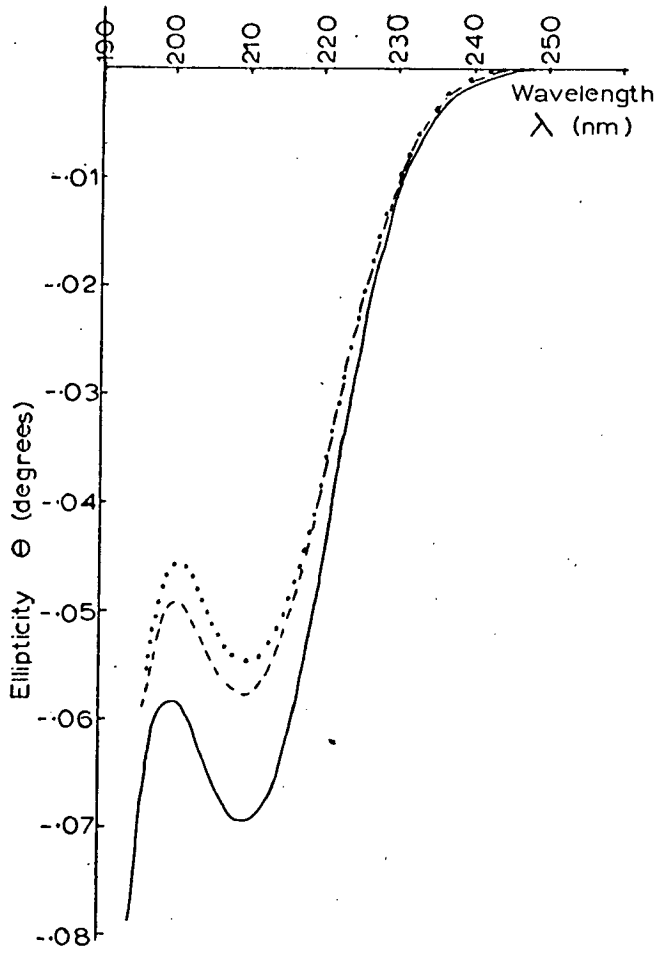

Fig. 4.4 Changes in c.d. spectrum with the diffusion of Mg^{++} to a final concentration of 6mM into a solution (0.1%) of the high G alginate sample 5. The solution spectrum is shown by the continuous line and the 4 and 10 day spectra are shown by the dashed and dotted lines respectively.

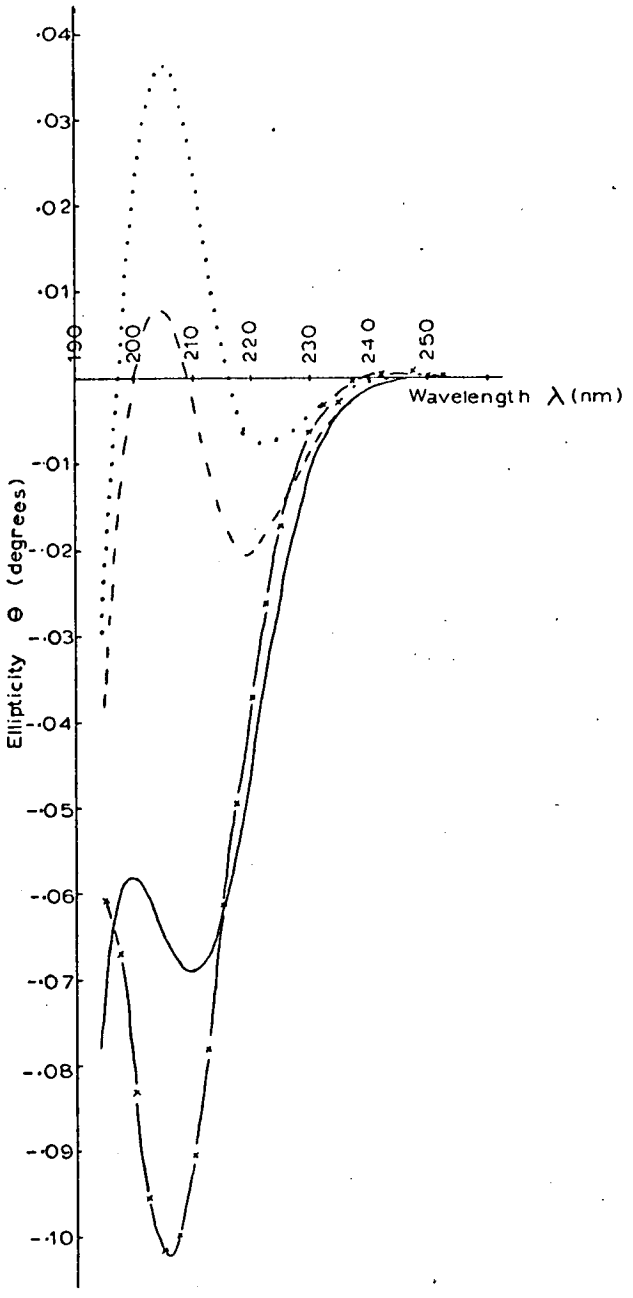

Fig. 4.5 Changes in c.d. spectrum with diffusion of Ca^{++} to a final concentration of 6mM into a solution (0.1%) of the high G alginate sample 5. The solution spectrum is shown by the continuous line and the 4 and 10 day spectra are shown by the dashed and dotted lines respectively. The 10 day difference spectrum is also shown (x——x).

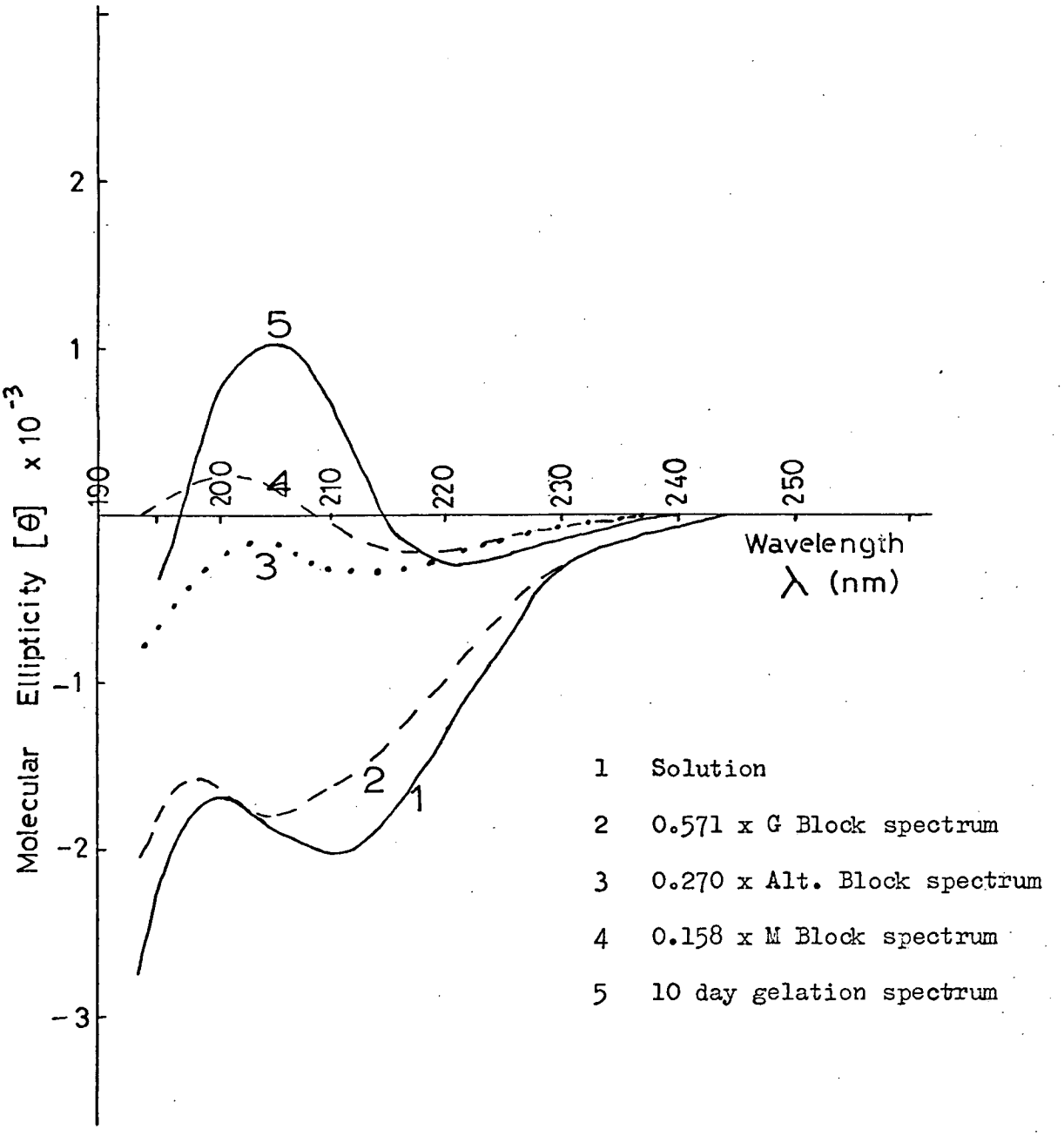

Fig. 4.6 Comparison of the solution and 10 day gelation spectrum, on diffusion of Ca^{++}, with the spectra from the proportions of the three types of blocks which make up the high G sample (table 3.6).

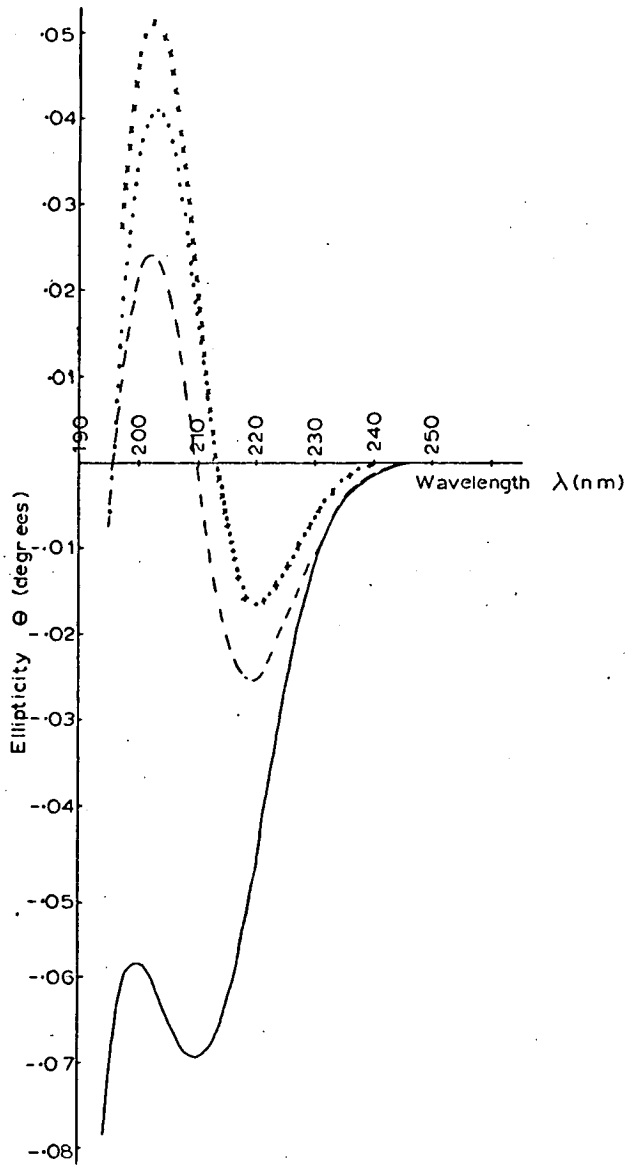

Fig. 4.7 Changes in c.d. spectrum with diffusion of Sr^{++} to a final concentration of 6mM into a solution (0.1%) of the high G alginate sample 5. The solution spectrum is shown by the continuous line and the 4, 10 and 25 day spectra are shown by the dashed, dotted and crossed lines respectively.

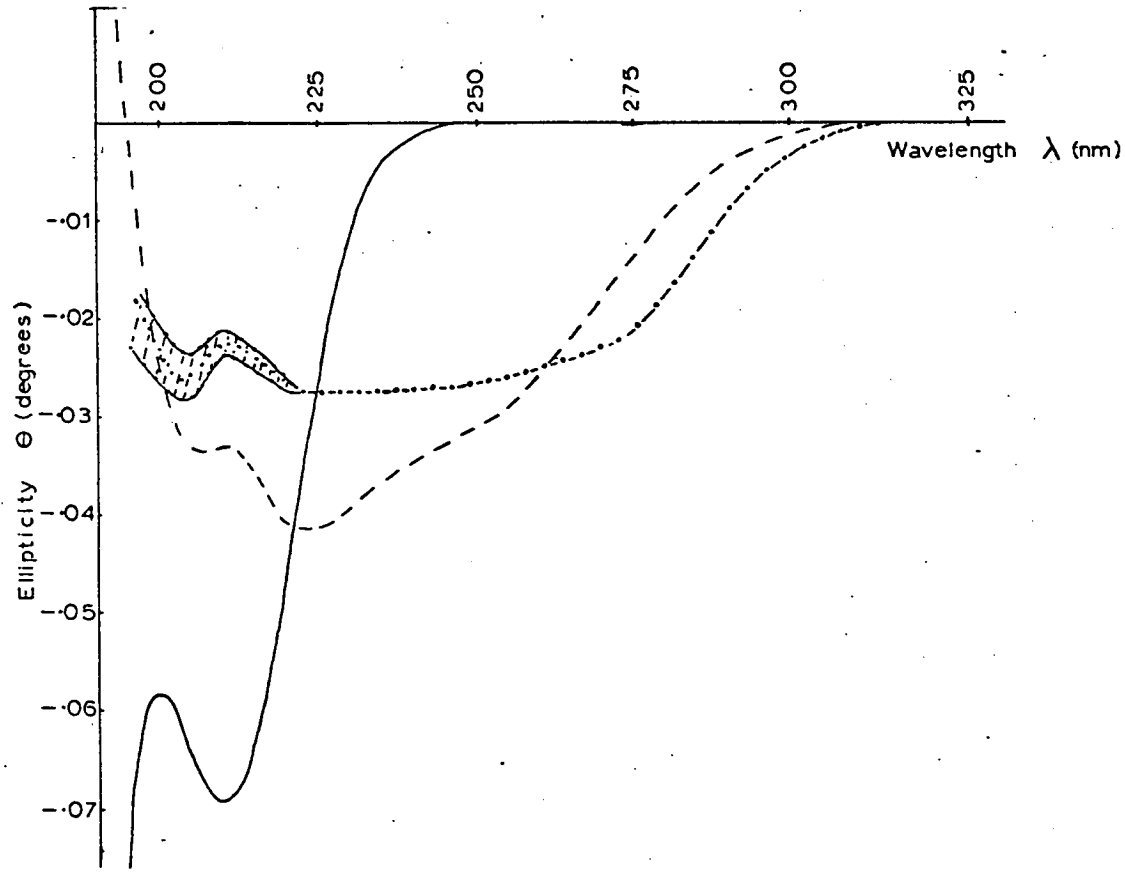

Fig. 4.8 Changes in c.d. spectrum with diffusion of Cu^{++} into a solution (0.1%) of the high G alginate sample 5. The solution spectrum is shown by the continuous line and the 4 and 10 day gelation spectra are shwon by the dashed and (.———.) lines respectively.

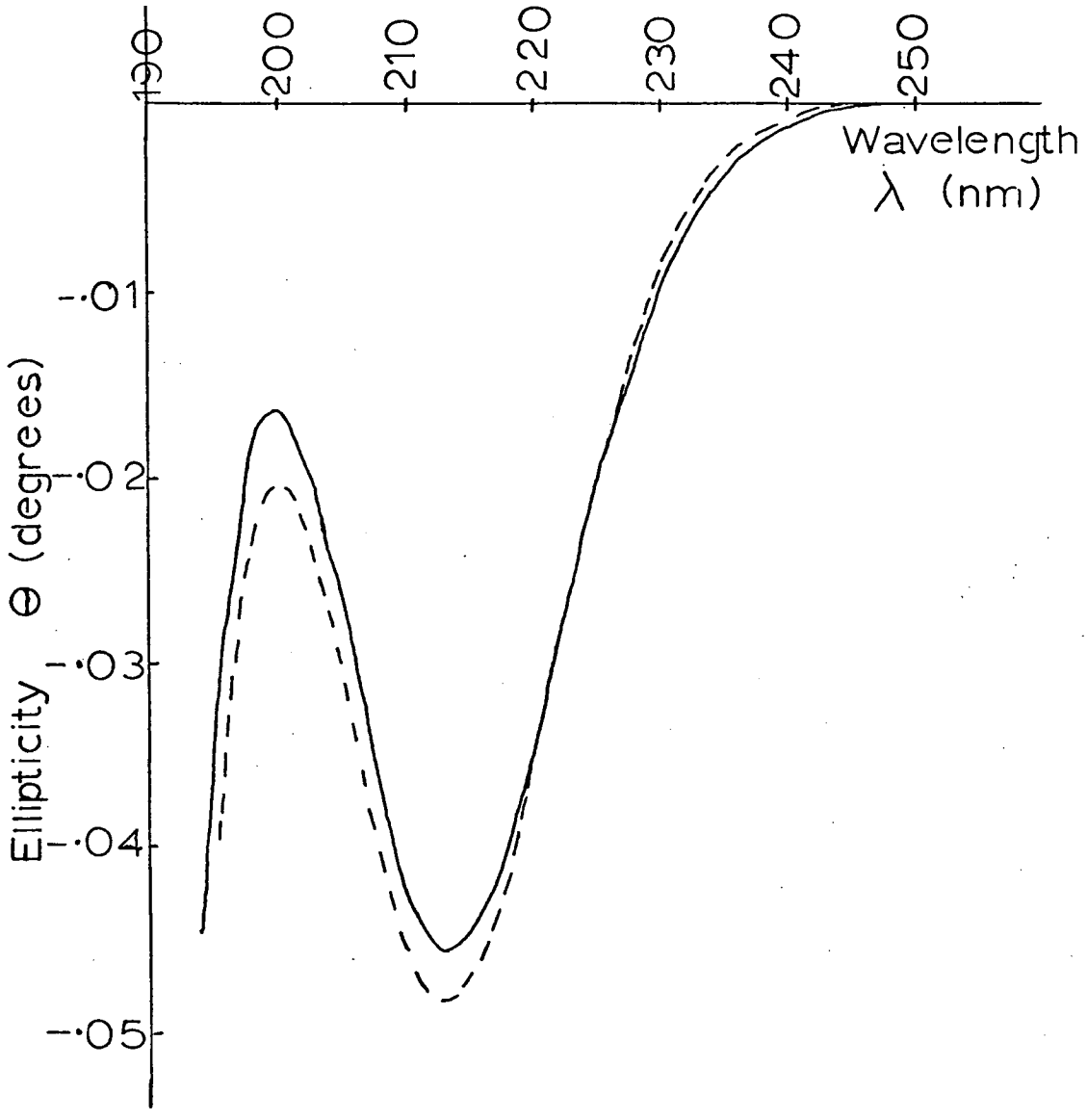

Fig. 4.9 Changes in c.d. spectra with diffusion of K^+ to a final concentration of 6mM into a solution (0.1%) of the high M alginate sample 8. The solution spectrum is shown by the continuous line and the spectrum after 4 days diffusion is shown by the dashed line.

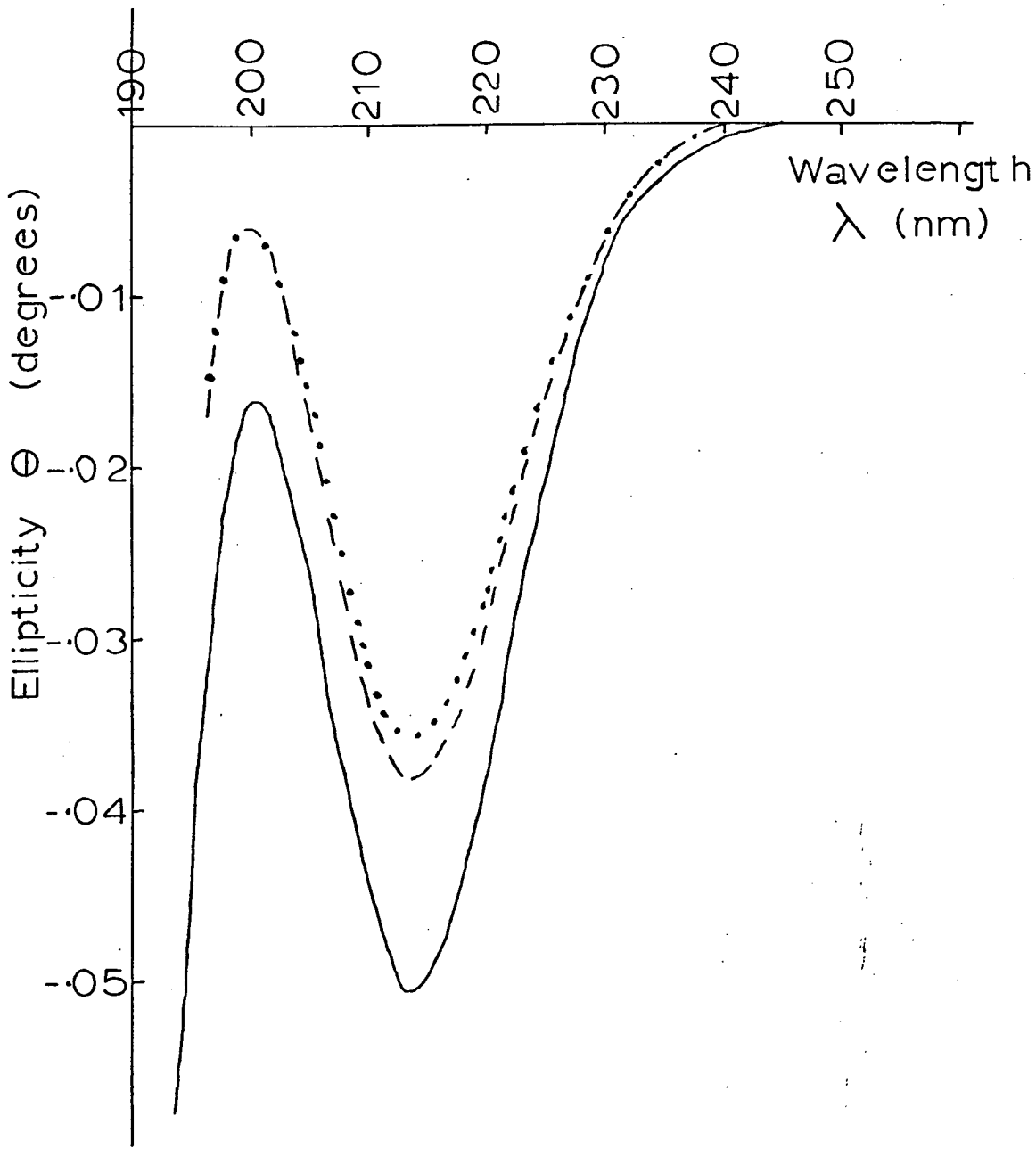

Fig. 4.10 Changes in c.d. spectrum with diffusion of Mg^{++} to a final concentration of 6mM into a solution (0.1%) of the high M alginate sample 8. The solution spectrum is shown by the continuous line and the 4 and 10 day spectra are shown by the dashed and dotted lines respectively.

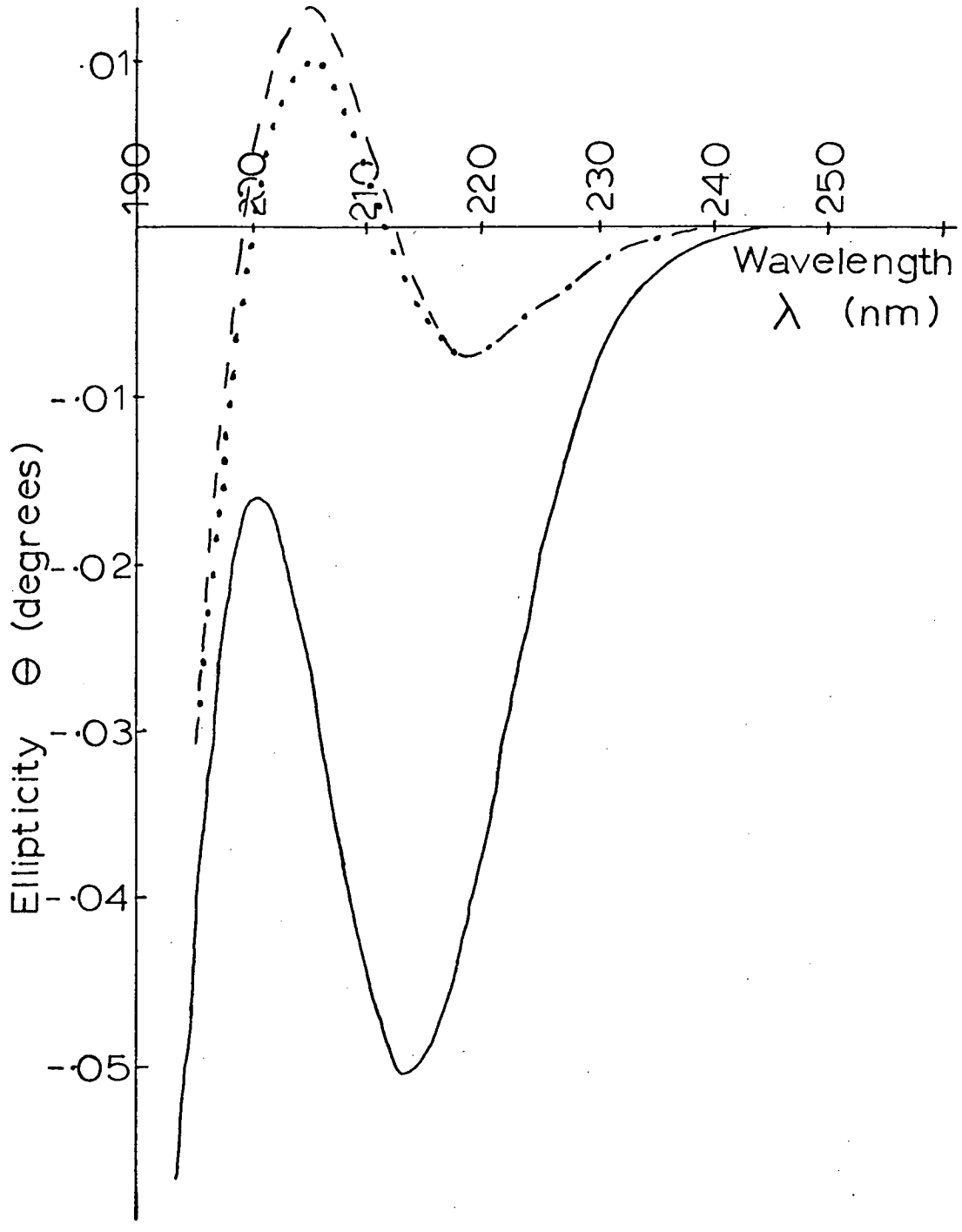

Fig. 4.11 Changes in c.d. spectrum with diffusion of Ca^{++} to a final concentration of 6mM into a solution (0.1%) of the high M alginate sample 8. The solution spectrum is shown by the continuous line and the 4 and 10 day gelation spectra are shown by the dashed and dotted lines respectively.

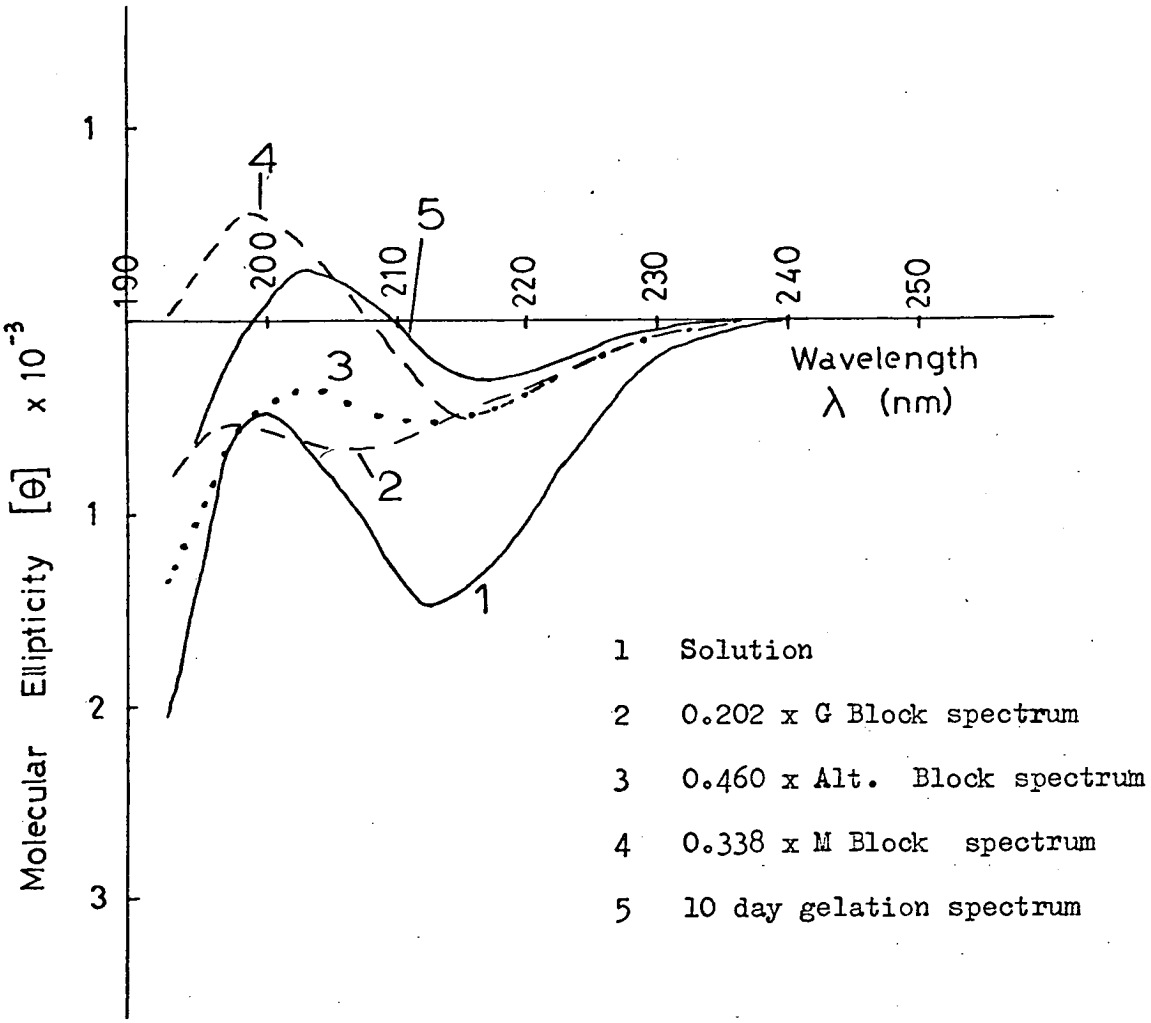

Fig. 4.12 Comparison of the solution and 10 day gelation spectra, for Ca^{++} gelation, with the spectra obtained from the proportions of the three types of blocks which make up the high M alginate sample 8.

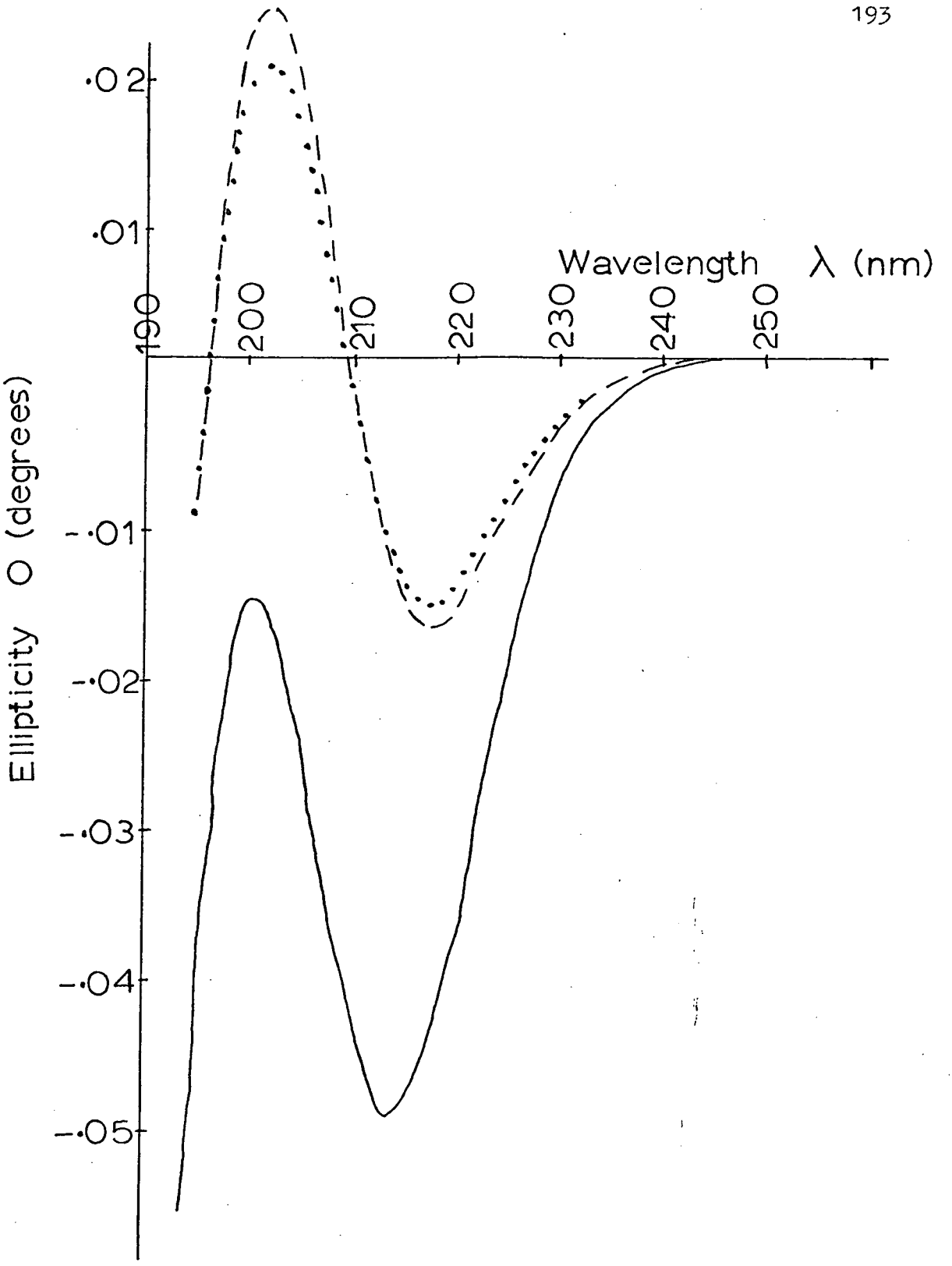

Fig. 4.13 Changes in c.d. spectrum with diffusion of Sr^{++} to a final concentration of 6mM into a solution (0.1%) of the high M alginate sample 8. The solution spectrum is shown by the continuous line and the 4 and 10 day gelation spectra are shown by the dashed and dotted lines respectively.

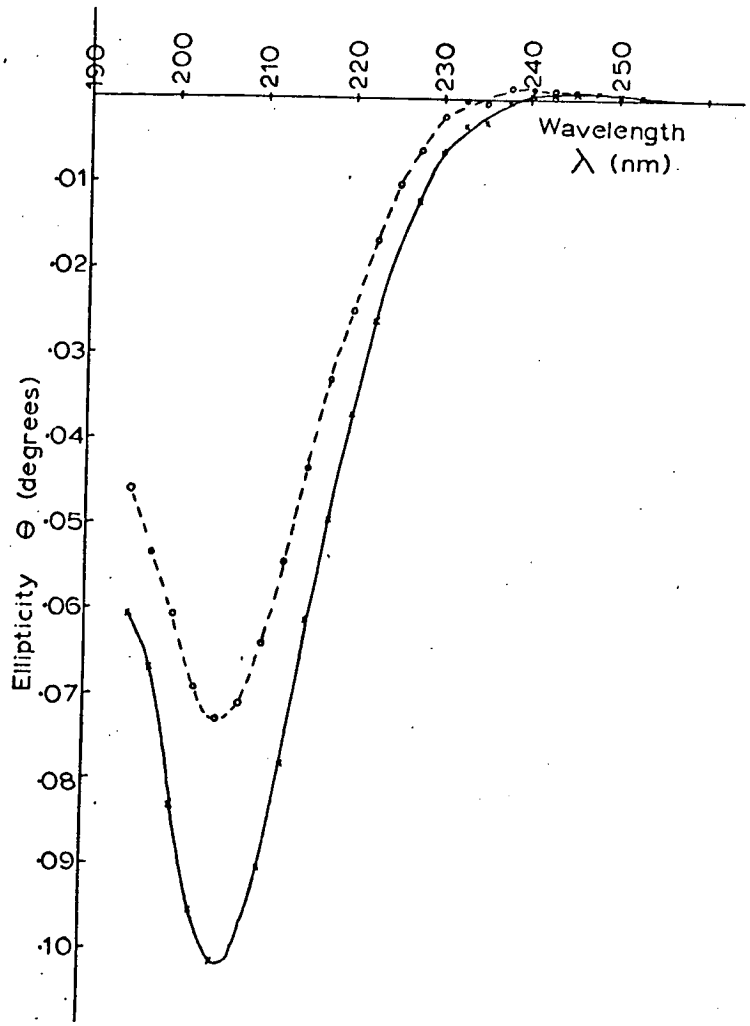

Fig. 4.14 Difference spectra for the diffusion of Ca^{++} into the solution of the high G alginate sample 5. The 10 day difference spectrum is shown by the continuous line and the 4 day difference spectrum is shown by the dashed line.

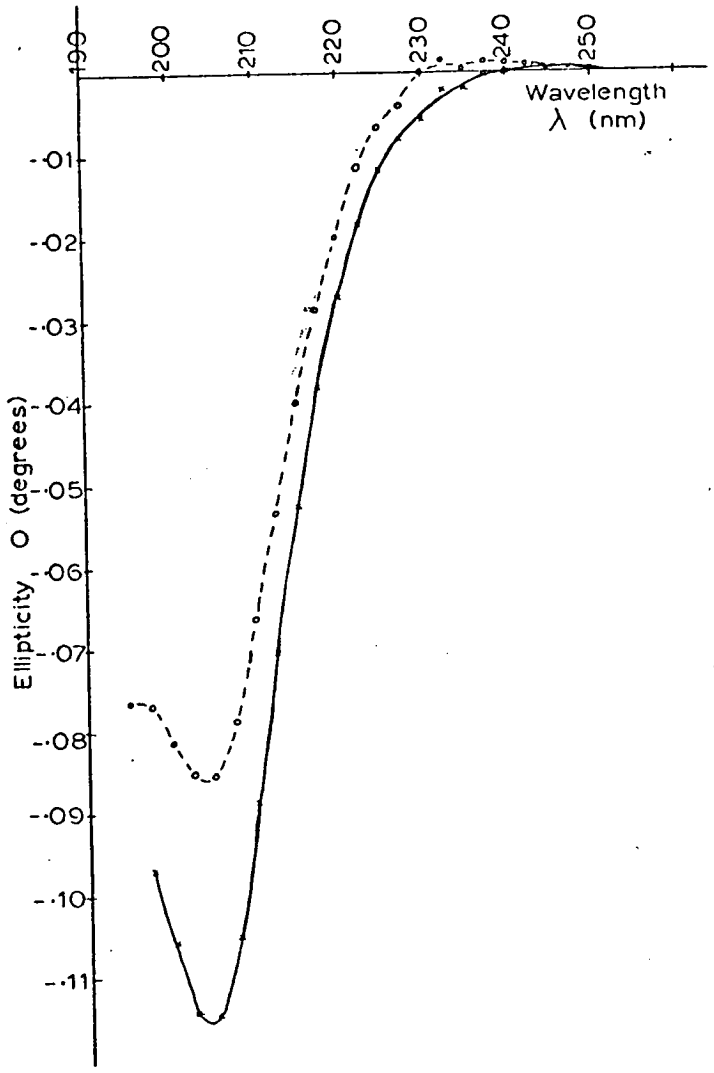

Fig. 4.15 Difference spectra for the diffusion of Sr^{++} into the solution of the high G alginate sample 5. The difference spectrum for the completed change is given by the continuous line. The 4 day difference spectrum is given by the dashed line.

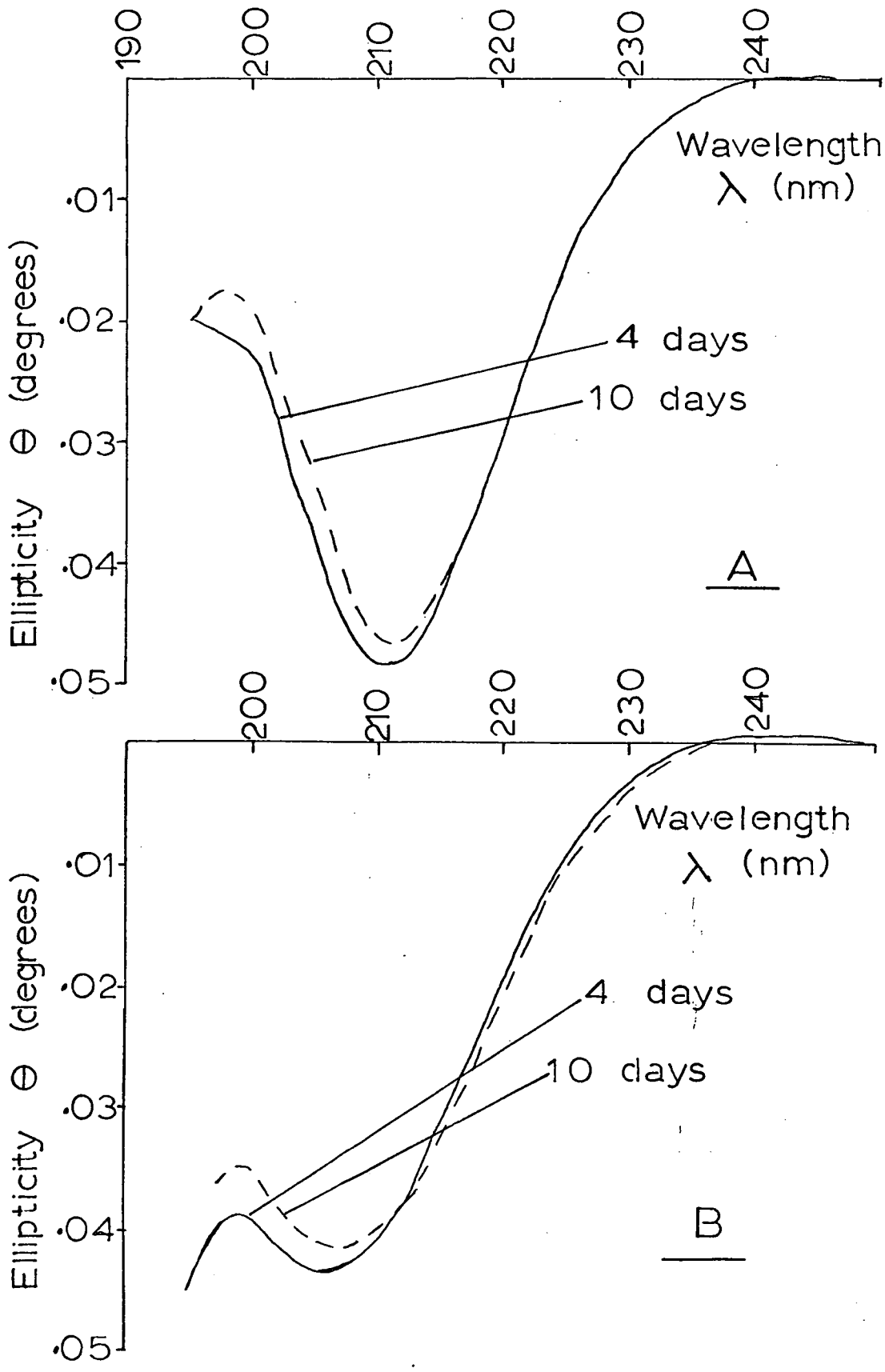

Fig. 4.16 Difference spectra for the diffusion of (A) Ca^{++} and (B) Sr^{++} into solutions of the high M alginate sample 8.

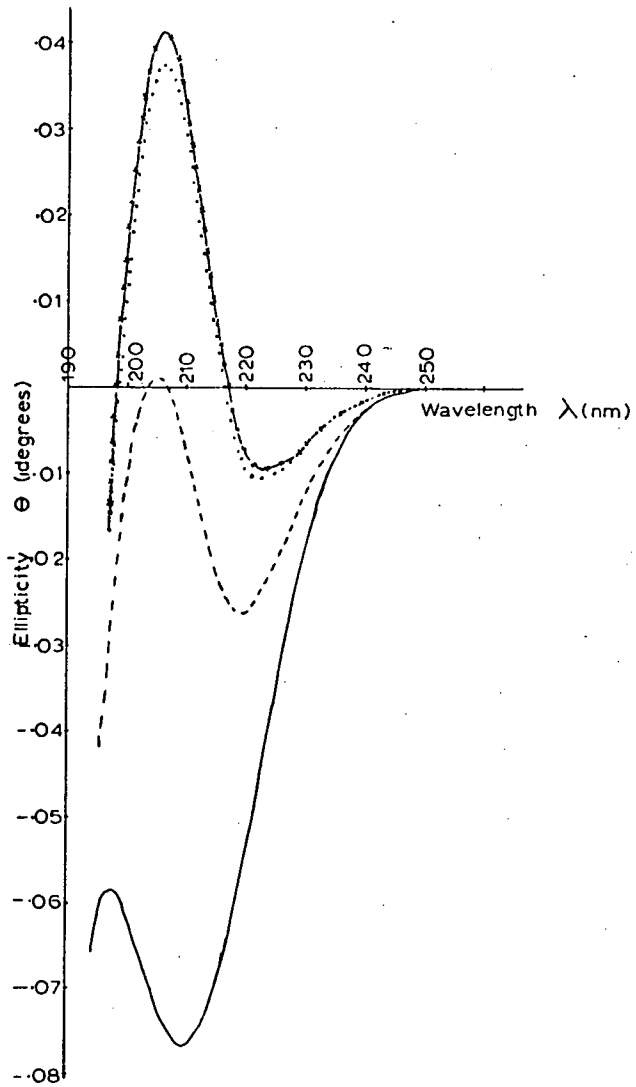

Fig. 4.17 Changes in the c.d. spectrum on diffusion of Ca^{++} to a final concentration of 6mM into a solution (0.1%) of the low viscosity high G alginate sample 6. The solution spectrum is shown by the continuous line and the 4 and 10 day gelation spectra by the dashed and dotted lines respectively. The spectrum after heating the 10 day gel for 1 hr is shown by(x———x).

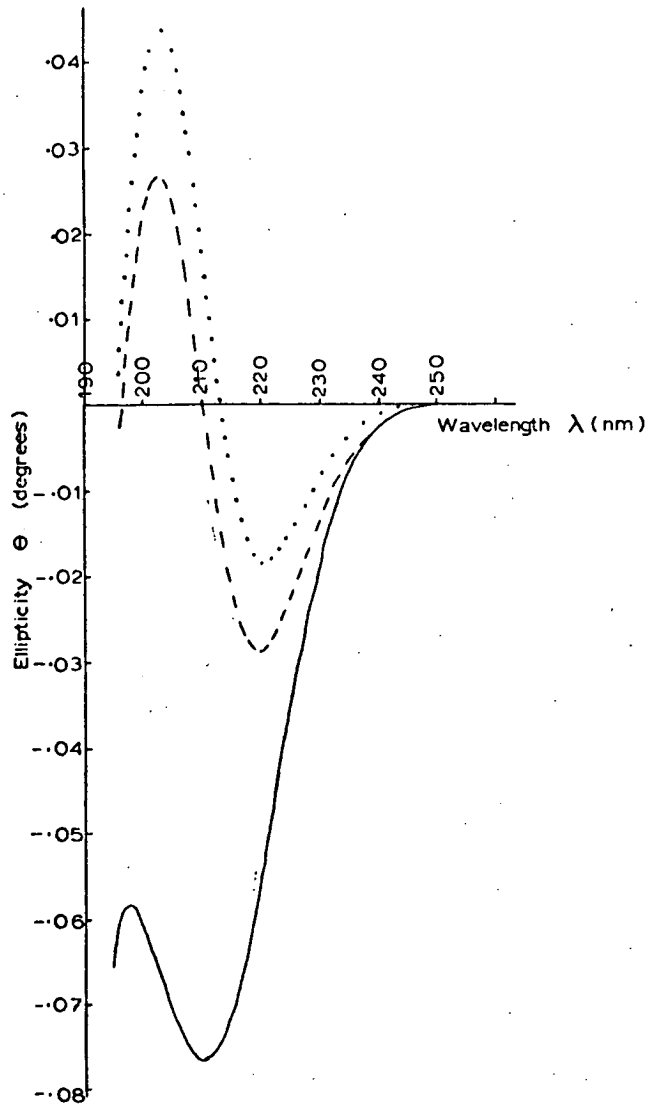

Fig. 4.18 Changes in c.d. spectrum on diffusion of Sr^{++} to a final concentration of 6mM into a solution (0.1%) of the low viscosity high G alginate sample 6. The solution spectrum is shown by the continuous line and the 4 and 10 day spectra by the dashed and dotted lines respectively.

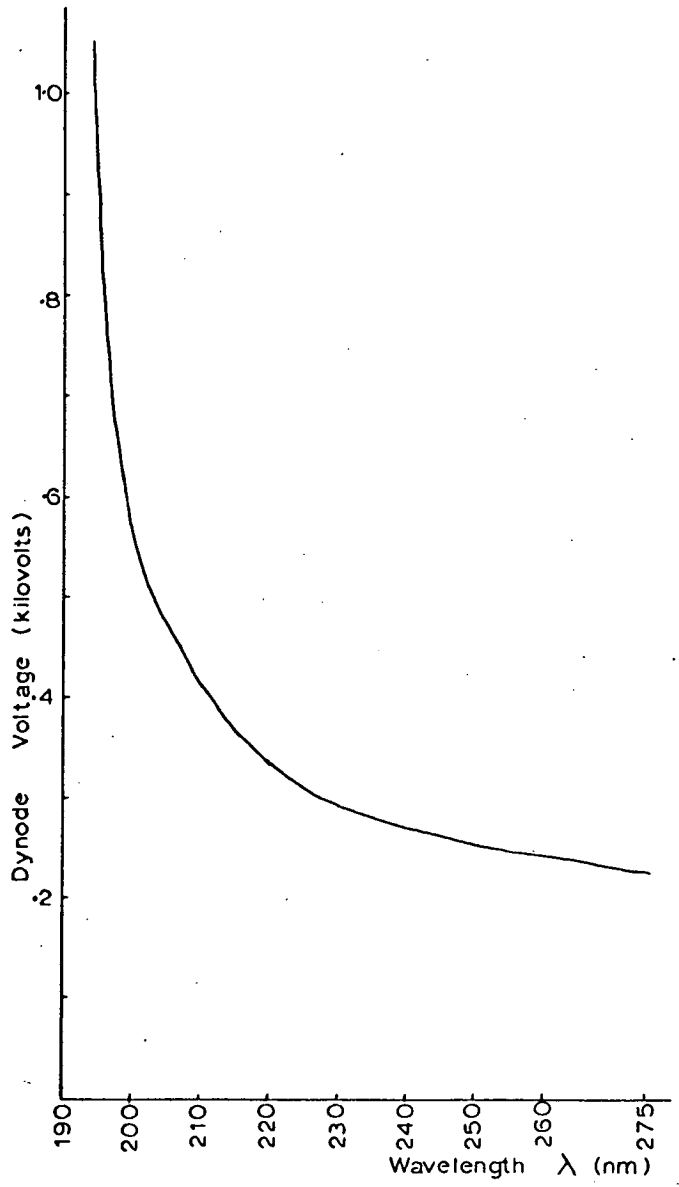

Fig. 4.19 Dynode Voltage spectrum recorded on the low viscosity high G alginate sample 6 solution (0.1%). No significant changes were observed on diffusion of Ca^{++} or Sr^{++} for 4 and 10 days.

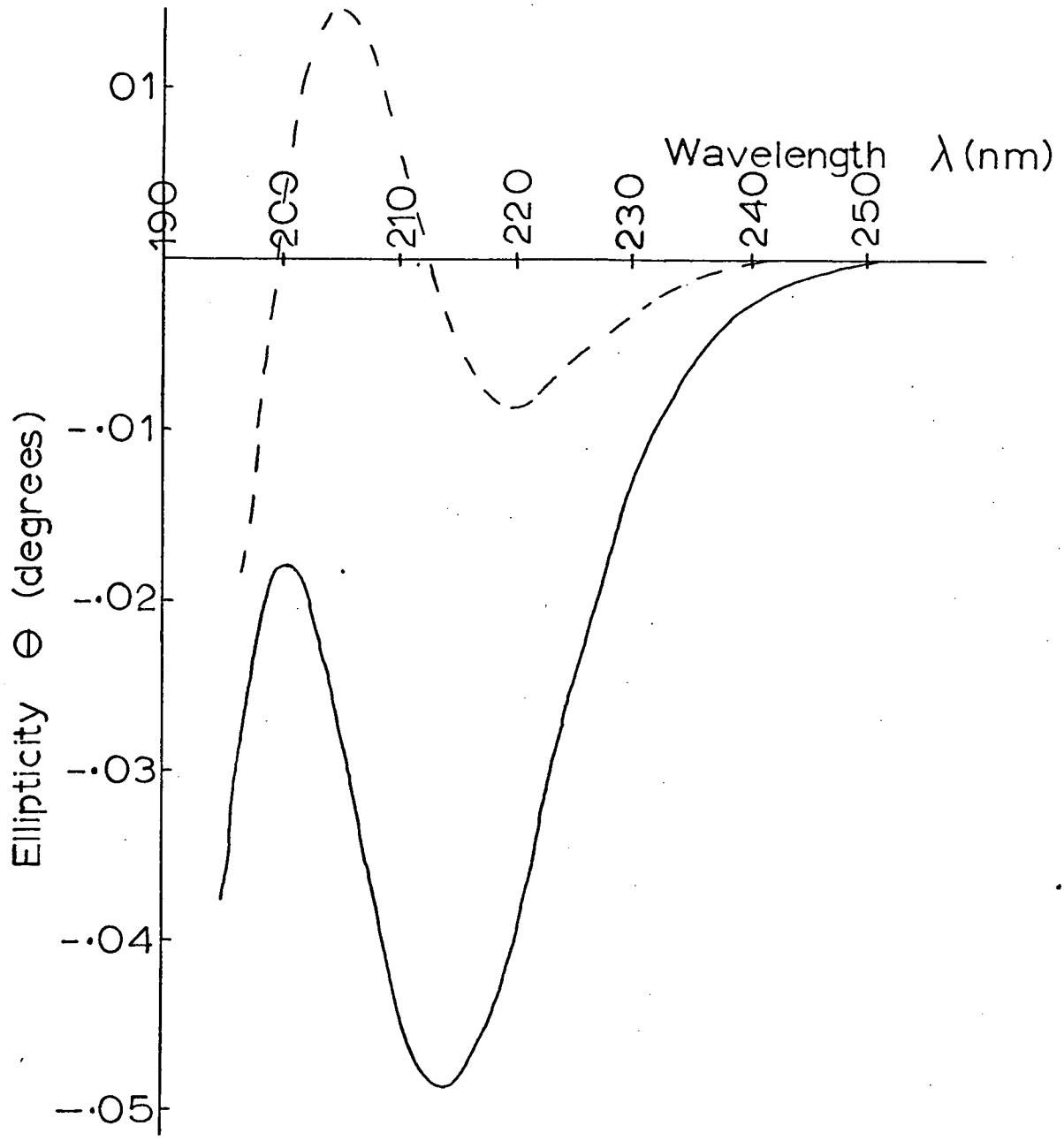

Fig. 4.20 Changes in c.d. spectra with diffusion of Ca^{++} to a final concentration of 6mM into a solution (0.1%) of the low viscosity high M alginate sample 9. The solution spectrum is shown by the continuous line and the 4 day spectrum by the dashed line. No further changes were observed after 10 days diffusion or after heating the 10 day gel at 80°C for 1 hr.

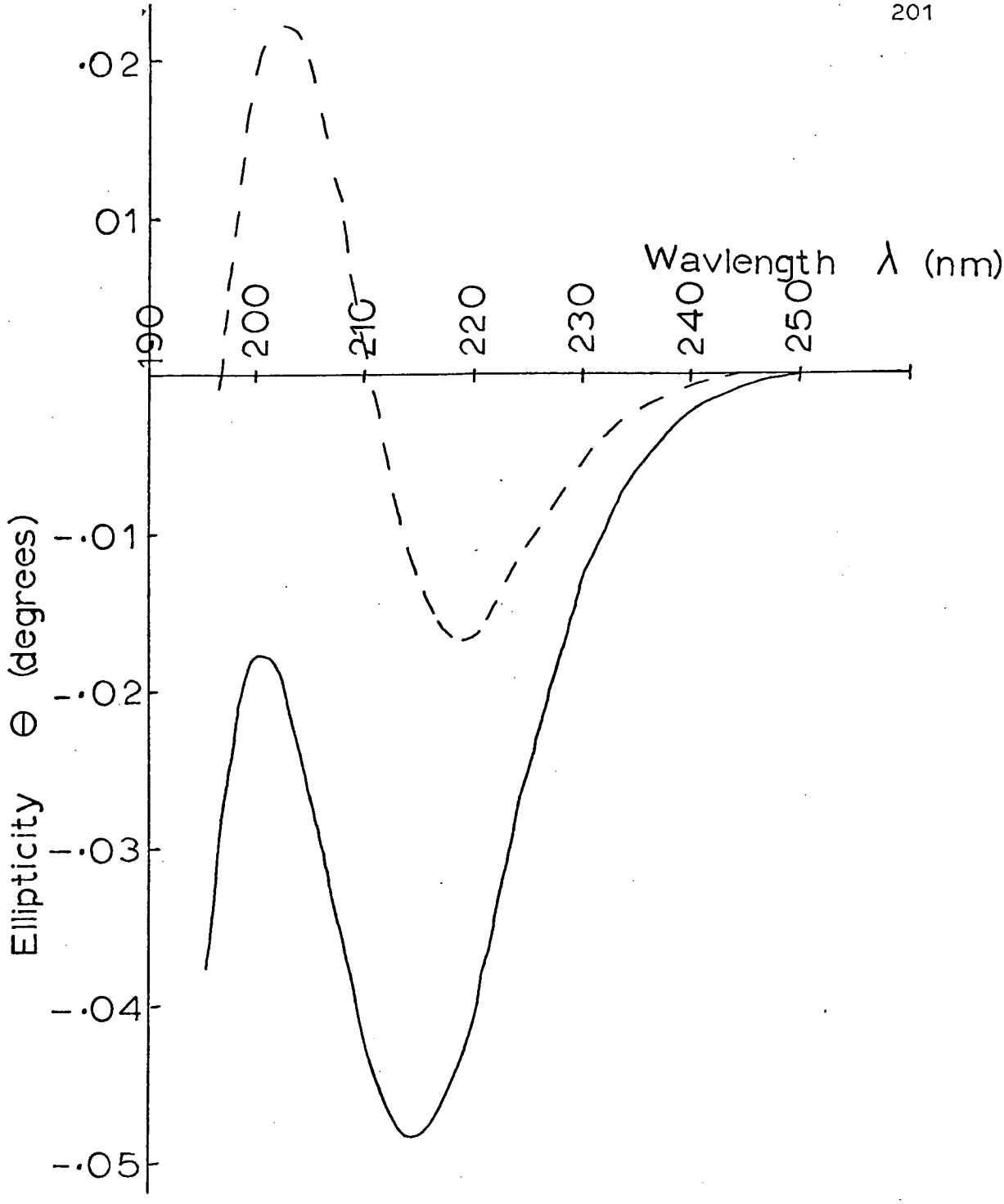

Fig. 4.21 Changes in c.d. spectrum on diffusion of Sr^{++} to a final concentration of 6mM into a solution (0.1%) of the low viscosity high M alginate sample 9. The solution spectrum is given by the continuous line and the 4 day spectrum by the dashed line. No further change was observed after 10 days diffusion.

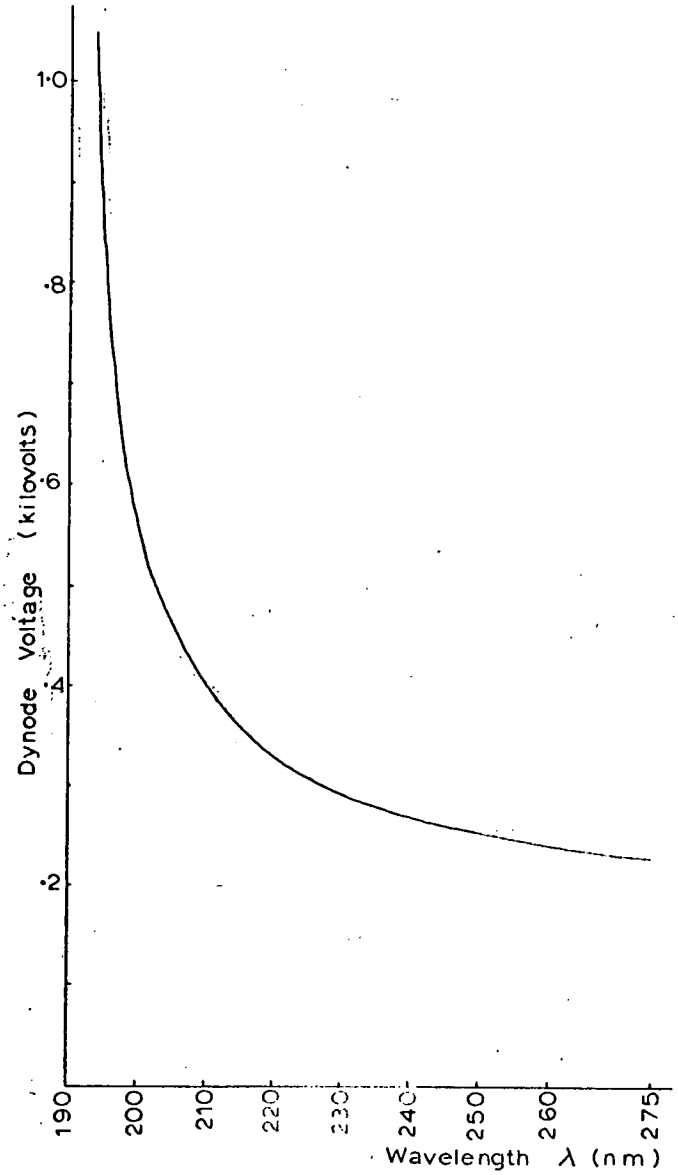

Fig. 4.22 Dynode voltage spectrum recorded on the low viscosity high M alginate sample 9 solution (0.1%). No significant changes were observed on diffusion of Ca^{++} or Sr^{++} for 4 and 10 days.

GENERAL METHODS

GENERAL METHODS

Concentration of Solutions

Solutions were concentrated under reduced pressure using a rotary evaporator. The temperature of the water bath was not allowed to exceed 40°C.

Melting Points

All melting points were determined on a Kofler hot-stage apparatus and are uncorrected.

Paper Chromatography

Chromatograms were developed overnight on Whatman No. 1 paper. The solvent systems used were (v/v):-

(a) n-butanol:ethanol:water (4:1:5)

(b) n-butanol:ethanol:water:ammonia (40:10:49:1)

For the separation of methyl glycosides double development using solvent (b) was found to give the best results.

Detection of the Methyl Glycosides

The reagent used for the detection of methyl glycosides was

Potassium Periodatocuprate (spray)[176]

Copper sulphate pentahydrate (12.5 g) was dissolved in boiling water (400 ml). The heat was turned off and a little potassium periodate was carefully added. A violent reaction took place and a light green precipitate formed. The remainder of the potassium periodate (23 g) was added and a concentrated solution of potassium hydroxide (56 g) in water was added and the solution turned a dark green. Small amounts of potassium persulphate were added to the hot solution at 1 minute intervals until 20 g had been added. The solution was boiled for 20 min and it turned a dark red. The solution was cooled, decanted from the flask and diluted to 500 ml

with water. The solution now contained 0.05 M potassium periodatocuprate in 2 N potassium hydroxide and it could be stored indefinitely in tightly sealed polythene bottles.

The chromatograms were sprayed with the reagent and the compounds were shown up almost immediately as white spots against a yellow-brown background. When sprayed on to paper the background faded quickly but if a permanent record was desired a rosaniline solution could be sprayed on 1 min after the periodatocuprate and this gave red spots against a white background.

Rosaniline (spray)

Rosaniline hydrochloride (0.3 g) was dissolved in acetic acid (100 ml) and made up to 1 l. with acetone.

Phenol-Sulphuric Acid Test for Carbohydrates[177]

The sugar solution (1 ml) was placed in a test tube and aqueous phenol (5% w/v: 1 ml) added. Analar concentrated sulphuric acid (5 ml) was added quickly directly on to the surface of the solution. After 30 minutes, when the solution had cooled, the optical density of the solution was measured with an EEL colorimeter using filter number 623 (maximum transmission at 495 nm).

Preparation of the Column of Dowex-1 Strong Anion-Exchange Resin

The chloride form of the resin was slurried with 2 N sodium hydroxide solution. After 20 minutes the supernatant liquid and fines were decanted. This process was repeated three times and it was accompanied by a large increase in resin volume. The resin was transferred to a column and conversion was completed by passing 2 N sodium hydroxide through the column until the eluate, after neutralisation with nitric acid, gave a negative test for chloride ions.

The resin was removed from the column, slurried with carbon dioxide free water and repacked. It was eluted with water until the eluate was neutral and no further expansion in the volume took place.

Reconversion of the Column of Strong Anion-Exchange Resin

The column was reconverted for use by passing M Na Cl solution down it until the effluent was neutral to litmus, followed by removal of the interstitial chloride ions by washing with water. The column was then converted to the hydroxide form as indicated before.

Preparation of Anhydrous Methanol

This was prepared as described by Vogel[178].

Preparation of Raney-Nickel Catalyst (W-2)[179]

A stirred solution of NaOH (63.5 g) in distilled water (250 ml) was cooled to 10°C and nickel-aluminium alloy (B.D.H.: 50 g) was added in small portions at such a rate that the temperature did not rise above 25°C. When all the alloy had been added the stirrer was stopped and the mixture was allowed to come to room temperature. After the evolution of hydrogen became slow the reaction mixture was allowed to stand on a boiling water bath until the evolution of hydrogen again became slow ($\sim$ 12 hrs). The volume of the solution was kept constant during this period. The nickel was allowed to settle and was washed three times with water, the water being removed by decantation. The nickel was then washed with a solution of NaOH (8.5 g) in water (85 ml) and the solution decanted off. The nickel was washed by suspension in distilled water, as described by Mozengo[179], until the washings were neutral to litmus and then further washed ($\sim$ 80 l. in total) to completely remove all traces of alkali. The nickel was washed three times with 95 % ethanol and three times with absolute ethanol, the solvent being removed each time by decantation.

The catalyst was stored under absolute ethanol in bottles completely filled with absolute ethanol.

Measurement of Cell Blanks for the Optical Rotation Measurements

The cell blanks were recorded on the 10 cm polarimeter cell containing the appropriate solvent. The measurements were made, for both wavelengths (589 nm and 546 nm), at temperature intervals of 7-8°C from 20-90°C and at three points when the cell was recooled. The values were plotted against temperature and the best curve drawn through these in each case. Corrections for the cell blanks at the appropriate temperature were taken from these best curves. The cell blanks, in all solvents, at both wavelengths were very small: of the order of $\pm$ 0.002° up to 50°C and increasing slightly up to 0.006° from 50°C to 90°C.

Refractive Index and Density Measurements of the Solvents

The refractive index and density of water were obtained from the Handbook of Chemistry and Physics[180], those of dimethyl sulphoxide from Schläfer and Schaffernight[181] and the density of dioxan was obtained from the Zeitschrift fur Physicalische Chemie[182].

The refractive index of dioxan was measured on an Abbé refractometer which was thermostatted by circulating water through its water jacket using a Haake thermocirculator. The refractive index was measured at temperature intervals of 7-8°C from 17.5-87.5°C. A graph of the refractive index plotted against temperature gave a straight line.

Purification of the Alginate Samples

The alginate samples were dissolved in deionised water and their pH adjusted to 7.0 using N Na OH added by means of a syringe.

Sodium chloride was added to 0.1 M and the alginate solutions were dialysed in cellophane tubes suspended in deionised water. A small amount of chloroform was added to the solutions to prevent bacterial action. After dialysis the solutions were filtered through scintered glass funnels or glass filter paper and the alginate samples were isolated from the clarified solutions by freeze-drying.

REFERENCES

1. Hudson, C.S. (1909). J. Amer. Chem. Soc., 31, 66.

2. Harris, T.L., Hirst, E.L. and Wood, C.E. (1934). J. Chem. Soc., 1825 : (1935) J. Chem. Soc., 1658.

3. Velluz, L., Legrand, M. and Grosjean, M. (1965). Optical Circular Dichroism : Principles, Measurements and Applications, (Weinheim: Verlag Chemie).

4. Moscowitz, A. (1960). Chapter 12 in Optical Rotatory Dispersion : Applications to Organic Chemistry, by C. Djerassi,(New York : McGraw-Hill).

5. Eliel, E.L., Allinger, N.L., Angyal, S.J. and Morrison, G.A. (1965). Chapter 6 in Conformational Analysis, (New York : John Wiley).

6.(a) Kauzmann, W. and Eyring, H. (1941). J. Chem. Phys., 9, 41.

(b) Kauzmann, W. (1957). Quantum Chemistry, (New York : Academic Press).

7. Whiffen, D.H. (1956). Chem. Ind. (London), 964.

8. Brewster, J.H. (1959). J. Amer. Chem. Soc., 81, 5475, 5483 and 5493.

9. Marker, R.E. (1936). J. Amer. Chem. Soc., 58, 976.

10. Kauzmann, W., Clough, F.B. and Tobias, I. (1961). Tetrahedron, 13, 57.

11.(a) Horton, D. and Wander, J.D. (1967). J. Org. Chem., 32, 3780.

(b) Ibid (1970). Carbohyd. Res., 14, 83.

12. Lemieux, R.U. and Martin, J.C. (1970). Carbohyd. Res., 13, 139.

13. Lemieux, R.U., Pavia, A.A., Martin, J.C. and Watanabe, K.A. (1969). Canad. J. Chem., 47, 4427.

14. Lemieux, R.U. and Pavia, A.A. (1969). Canad. J. Chem., 47, 4441.

15. Rees, D.A. (1970). J. Chem. Soc., B., 877.

16. Rees, D.A. and Scott, W.E. (1971). J. Chem. Soc., B., 469.

17. de Hoog, A.J., Buys, H.R., Altona, C. and Havinga, E. (1969). Tetrahedron, 25, 3365.

18. Rees, D.A., Steele, I.W. and Williamson, F.B. (1969). J. Polym. Sci., Part C., 28, 261.

19. McKinnon, A.A. (1973). Ph. D. Thesis,(University of Edinburgh).

20. McKinnon, A.A., Rees, D.A. and Williamson, F.B. (1969). Chem. Commun., 701.

21. Jones, R.A. and Penman, A. J. Chem. Soc. in press

22. Rees, D.A., Scott, W.E. and Williamson, F.B. (1970). Nature, 227, 390.

23. Anderson, N.S., Campbell, J.W., Harding, M.M., Rees, D.A. and Samuel, J.W.B. (1969). J. Mol. Biol., 45, 85.

24. Dea, I.C.M., McKinnon, A.A. and Rees, D.A. (1972). J. Mol. Biol., 68, 153.

25. Crabbe, P. (1971). An Introduction to the Chiroptical Methods in Chemistry, (Mexico).

26. Listowsky, I. and Englard, S. (1968). Biochem. Biophys. Res. Commun., 30, 329.

27. Listowsky, I., Avigad, G. and Englard, S. (1965). J. Amer. Chem. Soc., 87, 1765.

27.(a)Nelson, R.G. and Johnson, W.C. Jr. (1972). J. Amer. Chem. Soc., 94, 3343.

28. Moffit, W., Woodward, R.B., Moscowitz, A., Klyne, W. and Djerassi, C. (1961). J. Amer. Chem. Soc., 83, 4013.

29. Schellman, J.A. (1968). Accounts Chem. Research, 1, 144.

30.(a)Gratzer, W.B. and Cowburn, D.A. (1969). Nature, 222, 426.

(b)Wellman, K.M., Briggs, W.S. and Djerassi, C. (1965). J. Amer. Chem. Soc., 87, 73.

31. Morris, E.R. and Sanderson, G.R. (1973). in New Techniques in Biophysics and Cell Biology. Vol 1., edited by R. Pain and B. Smith, (London : John Wiley).

32.(a)Listowsky, I., Avigad, G. and Englard, S. (1968). Carbohyd. Res., 8, 205.

(b)Listowsky, I., Englard, S. and Avigad, G. (1969). Biochem., 8, 1781.

33. Morris, E.R., Rees, D.A. and Sanderson, G.R. (1973). in preparation.

34. Rees, D.A. (1969). Advances in Carbohydrate Chem. and Biochem., 24, 267.

35. Rees, D.A. and Wight, A.W. (1971). J. Chem. Soc., B., 1366.

36. Grant, G.T. (1973). Ph.D. Thesis, (University of Edinburgh).

37. Listowsky, I., Avigad, G. and Englard, S. (1968). Carbohyd. Res., 8, 205.

38. Listowsky, I., Avigad, G. and Englard, S. (1970). Biochem., 9, 2186.

39. Brimacombe, J.S. and Webber, J.M. (1964). Mucopolysaccharides, (London : Elsevier).

40.(a)Stone, A.L. (1967). Nature, 216, 551.

(b)Stone, A.L. (1969). Biopolymers, 7, 173.

(c)Stone, A.L. (1971). Biopolymers, 10, 739.

41. Perlin, A.S., Casu, B., Sanderson, G.R. and Tse, J. (1972). Carbohyd. Res., 21, 123.

42.(a)Hoffmann, P., Linkler, A. and Meyer, K. (1956). Science, 124, 1252.

(b)Fransson, L.A. and Roden, L. (1967). J. Biol. Chem., 242, 4161, 4170.

43. Perlin, A.S., Casu, B., Sanderson, G.R. and Johnson, L.F. (1970). Canad. J. Chem., 48, 2260.

44. Perlin, A.S., Mackie, D.M. and Deitrich, C.P. (1971). Carbohyd. Res., 18, 185.

45. Usov, A.I., Adamyants, K.S., Miroshnikova, L.I., Shaposhnikova, A.A. and Kochetkov, N.K. (1971). Carbohyd. Res., 18, 336.

46. Bittiger, H. and Keilich, G. (1969). Biopolymers, 7, 539.

47. Mukherjee, S., Marchessault, R.H. and Sarko, A. (1972). Biopolymers, 11, 291.

48. Mukherjee, S., Sarko, A. and Marchessault, R.H. (1972). Biopolymers, 11, 303.

49. Rees, D.A. and Skerrett, R.J. (1968). Carbohyd. Res., 7, 334.

50. Harada, N. and Nakanishi, K. (1969). J. Amer. Chem. Soc., 91, 3989.

51. Harada, N., Sato, H. and Nakanishi, K. (1970). Chem. Commun., 1691.

52. Hassel, O. and Ottar, B. (1947). Acta Chem. Scand., 1, 929.

53.(a)Reeves, R.E. (1949). J. Amer. Chem. Soc., 71, 215.

(b)Reeves, R.E. (1950). J. Amer. Chem. Soc., 72, 1499.

(c)Reeves, R.E. (1951). Advances Carbohyd. Chem., 6, 107.

54. Durette, P.L. and Horton, D. (1972). Advances Carbohyd. Chem., 26, 49.

55. Lemieux, R.U., Kullnig, R.K., Bernstein, H.J. and Schneider, W.G. (1957). J. Amer. Chem. Soc., 79, 1005; (1958). 80, 6098.

56. Karplus, M. (1959). J. Chem. Phys., 30, 11.

57. Karplus, M. (1963). J. Amer. Chem. Soc., 85, 2870.

58.(a)Angyal, S.J. (1969). Angew. Chem. Int. Ed., 8, 157.

(b)Angyal, S.J. (1968). Aust. J. Chem., 21, 2737.

59. Angyal, S.J. and McHugh, D.J. (1956). Chem. Ind. (London), 1147.

60. Angyal, S.J., Pickles, V.A. and Ahluwahlia, R. (1966). Carbohyd. Res., 1, 365.

61. Edward, J.T. (1955). Chem. and Ind., 1102.

62.(a)Lemieux, R.U. and Chü , N.J. (1958). Abstr. Papers Amer. Chem. Soc. Meeting, 133, 31N.

(b)Lemieux, R.U. (1963). in Molecular rearrangements, edited by P. de Mayo, (New York : Interscience, John Wiley).

63. Hutchins, R.O., Kopp, L.D. and Eliel, E.L. (1968). J. Amer. Chem. Soc., 90, 7174.

64. Lemieux, R.U. (1971). Pure and Appl. Chem., 25, 527.

65. Coxon, B. (1966). Tetrahedron, 22, 2281.

66. Wolfe, S., Rauk, A., Tel, L.M. and Csizmadia, J.G. (1971). J. Chem. Soc., B., 136.

67. Perlin, A.S., Casu, B. and Koch, H.J. (1970). Canad. J. Chem., 48, 2596.

68.(a)Perlin, A.S. (1966). Canad. J. Chem., 44, 539.

(b)Mackie, W. and Perlin, A.S. (1966). Canad. J. Chem., 44, 2039.

69. Bishop, C.T. and Cooper, F.P. (1963). Canad. J. Chem., 41, 2743.

70. Micheel, F. (1956). Chimie der Zucker and Polysaccharide (Leipzig : Geest and Portig K,-G.).

71. Dolan, T.C.S. (1965). Ph.D. Thesis, (University of Edinburgh).

72. Haworth, W.N., Jackson, J. and Smith, F. (1940). J. Chem. Soc., 620.

73. Austin, P.W., Hardy, F.E., Buchanan, J.G. and Baddily, J. (1963). J. Chem. Soc., 5350.

74. Kauzmann, W., Walter, J. and Eyring, H. (1940). Chem. Rev., 26, 339.

75. Reeves, R.E. and Blouin, F.A. (1957). J. Amer. Chem. Soc., 79, 2261.

76. Rao, V.S.R. and Foster, J.F. (1965). J. Phys. Chem., 69, 636.

77. The Handbook of Chemistry and Physics, 52nd Edition, (1971-72). Edited by R.C. Weast (Cleveland: The Chemical Rubber Co.).

78. Kirk, D.N., Klyne, W. and Wallis, S.R. (1970). J. Chem. Soc., C., 350.

79. Danford, M.D. and Levy, H.A. (1962). J. Amer. Chem. Soc., 84, 3965.

80. Pople, J.A. (1951). Proc. Roy. Soc. (London), A, 205, 163.

81. Warner, D.T. (1962). Nature, 196, 1055.

82. Kabayama, M.A. and Patterson, D. (1958). Canad. J. Chem., 36, 563.

83. Franks, F., Ravenhill, J.R. and Reid, D.S. (1972). J. Solution Chem., 1, 3.

84. Tait, M.J., Suggett, A., Franks, F., Ablett, S. and Quickenden, P.A. (1972). J. Solution Chem., 1, 131.

85. Arnott, S. and Scott, W.E. (1972). J. Chem. Soc., Perk. II, 324.

86. Narton, A.H., Danford, M.D. and Levy, H.A. (1967). Disc. Faraday Soc., 43, 97.

87. Good, W. (1967). Electrochimica Acta, 12, 1031.

88. Rees, D.A. (1973). in MTP International Review of Science: Organic Chemistry Series One, Vol. 7: Carbohydrates, Vol. Editor G.O. Aspinall. (London : Butterworth).

89. Ramachandran, G.N., Ramakrishman, C. and Sasisekharan, V. (1963). in Aspects of Protein Structure, edited by G.N. Ramachandran, 121. (New York : Academic Press).

90. Sathyanarayana, B.K. and Rao, V.S.R. (1971). Biopolymers, 10, 1605.

91. Rao, V.S.R., Sundararajan, P.R., Ramakrishman, C. and Ramachandran, G.N. (1967). in Conformation of Biopolymers, edited by G.N. Ramachandran, 2, 721. (London : Academic Press).

92. Chu, S.S.C. and Jeffrey, G.A. (1968). Acta Crystallogr., Sect. B., 24, 830.

93. Ham, J.T. and Williams, D.G. (1970). Acta Crystallogr., Sect. B., 26, 1373.

94. Quigley, G.J., Sarko, A. and Marchessault, R.H. (1970). J. Amer. Chem. Soc., 92, 5834.

95. Hybl, A., Rundle, R.E. and Williams, D.E. (1965). J. Amer. Chem. Soc., 87, 2779.

96. Chu, S.S.C. and Jeffrey, G.A. (1967). Acta Crystallogr., 23, 1038.

97. Blackwell, J., Sarko, A. and Marchessault, R.H. (1969). J. Mol. Biol., 42, 379.

98. Casu, B., Reggiani, M., Gallo, G.G. and Vigevani, A. (1966). Tetrahedron, 22, 3061.

99. Michell, A.J. (1970). Carbohyd. Res., 12, 453.

100. Casu, B., Reggiani, M., Gallo, G.G., and Vigevani, A. (1968). Tetrahedron, 24, 803.

101. Casu, B., Reggiani, M., Gallo, G.G. and Vigevani, A. (1970). Carbohyd. Res., 12, 157.

102. Dorman, D.E. and Roberts, J.D. (1971). J. Amer. Chem. Soc., 93, 4463.

103. Wolfrom, M.L., Hung, Y.L., Chakravarty, P., Yuen, G.U. and Horton, D. (1966). J. Org. Chem., 31, 2227.

104.(a)Freudenberg, K. and Nagai, W. (1932). Ann., 494, 63.

(b)Purves, C.B. (1929). J. Amer. Chem. Soc., 51, 3619.

105. Fletcher, H.G. and Hudson, C.S. (1948). J. Amer. Chem. Soc., 70, 310.

106. Neal, J.L. and Goring, D.A.I. (1970). Can. J. Chem., 48, 3745.

107. Reeves, R.E. (1954). J. Amer. Chem. Soc., 76, 4595.

108. Zobel, H.F., French, A.D. and Hinkle, M.E. (1967). Biopolymers, 5, 837.

109. Thoma, J.A. and Stewart, L. (1965). in Starch: Chemistry and Technology, Vol. 1, edited by E.L. Whistler and E.F. Paschall, 209. (New York : Academic Press).

110. Schlenk, H. and Sand, D.M. (1961). J. Amer. Chem. Soc., 83, 2312.

111. Sundararajan, P.R. and Rao, V.S.R. (1970). Carbohyd. Res., 13, 351.

112. Manor, P.C. and Saenger, W. (1972). Nature, 237, 392.

113. Saenger, W. Personal Communication.

114. Hourston, D.J. (1967). Ph.D. Thesis, (University of Edinburgh).

115. Bailey, R.W. (1965). in International Series of Monographs on Pure and Applied Biology : Biochemistry Division : Vol. 4: Oligosaccharides. London : Pergamon Press).

116. Banks, W. and Greenwood, C.T. (1968). Carbohyd. Res., 7, 414.

117. French, D. (1969). in Symposium on Foods : Carbohydrates and their Roles edited by H.W. Schulz 26. (Westport Connecticutt: A.V.I. Publishing Co.).

118. Brown, G.M., Rohrer, D.C., Berking, B., Beevers, C.A., Gould, R.O. and Simpson, R. (1972). Acta Crystallogr., B28, 3145.

119. Gorin, P.A.J. and Spencer, J.F.T. (1966). Canad. J. Chem., 44, 993.

120.(a)Linker, A. and Jones, R.S. (1964). Nature, 204, 187.

(b)Carlson, D.M. and Matthews, L.W. (1966). Biochemistry, 5, 2817.

121. Fischer, F.G. and Dorfel, H. (1955). Z. Physiol. Chem., 302, 186.

122.(a)Whistler, R.L. and Kirby, K.W. (1959). Z. Physiol. Chem., 314, 46.

(b)Drummond, D.W., Hirst, E.L. and Percival, E. (1962). J. Chem. Soc., 1208.

123. Hirst, Sir E. and Rees, D.A. (1965). J. Chem. Soc., 1182.

124. Rees, D.A. and Samuel, J.W.B. (1967). J. Chem. Soc., C., 2295.

125.(a)Hirst, E.L., Jones, J.K.N. and Jones, W.O. (1939). J. Chem. Soc., 1880.

(b)Chanda, S.K., Hirst, E.L., Percival, E.G.V. and Ross, A.G. (1952). J. Chem. Soc., 1833.

126. Painter, T. and Larsen, B. (1970). Acta Chem. Scand., 24, 813.

127. Hirst, E.L., Percival, E. and Wold, J.K. (1964). J. Chem. Soc.,1493.

128.(a)Atkins, E.D.T., Mackie, W. and Smolko, E.E. (1970). Nature, 225, 626.

(b)Atkins, E.D.T., Mackie, W., Parker, K.D. and Smolko, E.E. (1971). J. Polym. Sci. Part B., 9, 311.

129. Penman, A. and Sanderson, G.R. (1973). Carbohyd. Res., in press.

130. Haug, A. and Smidsrød, O. (1965). Acta Chem. Scand., 19, 1221.

131. Vincent, D.L. (1960). Chem. and Ind., 1109.

132. Haug, A., Larsen, B. and Smidsrød, O. (1966). Acta Chem. Scand., 20, 183.

133. Haug, A., Myklestad, S., Larsen, B. and Smidsrød, O. (1967). Acta Chem. Scand., 21, 768.

134. Haug, A., Larsen, B. and Smidsrød, O. (1967). Acta Chem. Scand., 21, 691.

135. Haug, A. and Larsen, B. (1962). Acta Chem. Scand., 16, 1908.

136. Brown, A.H. (1946). Arch. Biochem., 11, 269.

137. Dische, Z. (1947). J. Biol. Chem., 167, 189.

138. Knutson, C.A. and Jeanes, A. (1968). Anal. Biochem., 24, 470, 482.

139. Mackie, W. (1971). Carbohyd. Res., 20, 413.

140. Penman, A., Personal Communication.

141. Szejtli, J. (1966). Acta Chim. Acad. Scient. Hun., 47, 301.

142. Mitchell, J., Jun. and Smith, D.M. (1948). in Chemical Analysis Vol. 5 : Aquametry. Application of the Karl Fischer Reagent to Quantitative Analyses involving Water, (New York and London : Interscience).

143. Hawkins, A.E. (1964). Analyst., 89, 432.

144. Whittington, S.G. (1971). Biopolymers, 10, 1481, 1617.

145. (a)Thiele, H., Joraschky, W., Plohnke, A., Wiechen, A., Wolf, R. and Wollmer, A. (1964). Kolloid-Z., 197, 26.

(b)Thiele, H. (1954). Discussions Faraday Soc., 18, 294.

146. Sterling, C. (1957). Biochim. Biophys. Acta, 26, 186.

147. (a)Smidsrød, O. and Haug, A. (1968). Acta Chem. Scand., 22, 797.

(b)Smidsrød, O. (1970). Carbohyd. Res., 13, 359.

148. (a)Astbury, W.T. (1945). Nature, 155, 667.

(b)Frei, E. and Preston, R.D. (1962). Nature, 196, 130.

149. Mackie, W. (1971). Biochem. J., 125, 89P.

150. Rees, D.A. (1972). Biochem. J., 126, 257.

151. Schweiger, R.G. (1962). J. Org. Chem., 27, 1789; (1964). Kolloid-Z., 196, 47.

152. Rees, D.A. and Wight, A.W. (1971). J. Chem. Soc. B., 1366.

153. Smidsrød, O. and Haug, A. (1972). Acta Chem. Scand., 26, 2063.

154. Smidsrød, O., Haug, A. and Whittington, S.G. (1972). Acta Chem. Scand., 26, 2563.

155. Kohn, R. and Furda, I. (1967). Collection Czech. Chem. Commun., 32, 1925, 4470.

156. Hardisty, D.R. and Neale, S.M. (1960). J. Polym. Sci., 46, 195.

157. Katchalsky, A., Cooper, R.E., Upadhyay, J. and Wassermann, A. (1961). J. Chem. Soc., 5198.

158. Smidsrød, O. and Haug, A. (1967). J. Polym. Sci., C., 16, 1587.

159. Haug, A. and Smidsrød, O. (1965). Acta Chem. Scand., 19, 341.

160. Thiele, H. and Hallich, K. (1957). Kolloid-Z., 151, 1.

161. Haug, A. (1961). Acta Chem. Scand., 15, 1794.

162. Haug, A. (1964). Report No. 30, Norwegian Institute of Seaweed Research, Trondheim.

163. Smidsrød,O. and Haug, A. (1968). Acta Chem. Scand., 22, 1989.

164. Kohn, R., Furda, I., Haug, A. and Smidsrød, O. (1968). Acta Chem. Scand., 22, 3098.

165. Haug, A. and Smidsrød, O. (1970). Acta Chem. Scand., 24, 843.

166. Kohn, R. and Larsen, B. (1972). Acta Chem. Scand., 26, 2455.

167. Rice, S.A. and Nagasawa, M. (1961). Polyelectrolyte Solutions, (New York : Academic Press).

168. Buchner, P., Cooper, R.E. and Wasserman, A. (1961). J. Chem. Soc., 3974.

169. Bartlett, L., Kirk, D.N., Klyne, W., Wallis, S.R., Erdtman, H. and Thoren, S. (1970). J. Chem. Soc., C., 2678.

170. Delbaere, L.T.J., Higham, M., Kamenar, B., Kent, P.W. and Prout, C.K. in preparation.

171. Smidsrød, O. and Haug, A. (1972). Acta Chem. Scand., 26, 79.

172. Hutchins, J.B. and Wood, F.W. Unpublished observations.

173. Williams, R.J.P. Personal Communication.

174. Smith, P.J.C. (1972). Ph.D. Thesis, (University of Edinburgh).

175. Williams, R.J.P. (1970). Chem. Soc. Quart. Rev., 24, 331.

176. Bonner, J.G. (1960). Chem. and Ind., 345.

177. Dubois, M., Gilles, K.A., Hamilton, J.K., Rebers, P.A. and Smith, F. (1956). Analyt. Chem., 28, 350.

178. Vogel, A.I. (1956). A Textbook of Practical Organic Chemistry, (London : Longmans 3rd Edition) 169.

179. Mozingo, R. (1951). Organic Synthesis : Collected Volume 3, 181 (London : Wiley).

180. Handbook of Chemistry and Physics, 47th Edition, (1966-67). (Cleveland : The Chemical Rubber Co.).

181. Schläfer, H.L. and Schaffernight, W. (1960). Angew. Chem., 72, 618.

182. Herz, W. and Lorentz, E. (1929). Z. Phys. Chem., 140, 407.

APPENDIX 1

SUMMARY OF THE EMPIRICAL METHODS FOR CALCULATING CARBOHYDRATE MOLECULAR ROTATIONS AND LINKAGE ROTATIONS

In this appendix the main features of the empirical methods used to calculate carbohydrate molecular rotations and linkage rotations are reproduced. An example of the application of each method is also given.

A. Calculation of the Molecular Rotations of Monosaccharides

1. Whiffen[7]

A satisfactory empirical theory of optical activity for organic molecules should, therefore, consider the possibility of applying superposition rules to two types of terms: (i) those associated with asymmetric carbon centres and dependent on the nature of the four substituents and their disposition in one or other of the enantiomorphic tetrahedral arrangements; (ii) terms associated with chemical bonds and dependent on the nature of the bond, of the substituents at its constituent atoms, and also on an angular co-ordinate describing the internal twisting of the terminal arrangements about the bond axis.

Terms under the heading (i) are those envisaged by van't Hoff and have often been considered; one of the simplest applications is that of Marker.[8] However, the molecular rotations of his table are all small in comparison with those of most active cyclic compounds, and none of his simple aliphatic hydrocarbons and alcohols has molecular rotations ($[\alpha]_D \times 0{\cdot}01$ M) outside the range ± 15.

Type (ii) terms merit a fuller consideration. The existence of some such contribution is certainly implicit in the theoretical treatments[2–6] and also in some optical activity rules, notably those involved in the cuprammonium complex work of Reeves,[9, 10] and is recognized by Stokes and Bergmann[11] in discussing steroids. These authors concentrate attention on the particular structures in which they are interested and do not consider the additivity of such terms or their transferability to other classes of compounds.

If a general, fully substituted carbon–carbon bond, as in UVWC-CXYZ, were taken as the basic unit for additivity of type (ii) terms, numerical values would have to be associated with the sets of six substituents U, V, W, X, Y, and Z and with a function dependent on the internal rotation angle. A discussion on this basis would seem to be unwieldy, and simplifying assumptions are clearly required. In the present account, which considers only compounds of carbon, hydrogen and oxygen without multiple bonds, the five assumptions designated (A)–(E) are made.

(A) The optical rotation for a bond structure UVWC-CXYZ can be taken as the sum of a term each for the nine constituent structures, UC-CX, UC-CY, UC-CZ, VC-CX, VC-CY, VC-CZ, WC-CX, WC-CY, and WC-CZ. Likewise, for UVWC-OX there are three additive terms for UC-OX, VC-OX, and WC-OX. The optical rotation of the whole molecule is then taken to be the sum of the contributions applicable to each of its bonds.

This assumption provides the major simplification required and is justified chiefly by the results shown in the Tables below.

(B) For compounds containing only carbon, hydrogen and oxygen and no multiple links, type (i) contributions, referring to asymmetric carbon centres, are negligible, i.e., contribute less than 20 to the molecular rotation.

For this restricted class of compounds at least two of the atoms substituted at each carbon must be identical, and the asymmetry arises from the differing natures of the next nearest and more distant atoms. Marker's[8] compilation indicates ± 15 to be the magnitude of these terms, but since his discussion does not exclude type (ii) terms, this is probably an upper limit.

(C) The contribution for UC-CX is independent of the other atoms.

This assumption is relaxed for ring atoms and glycosidic oxygen atoms which are differentiated, but no distinction is made between the carbon atoms of $-CH_3$ and $-CH_2OH$ groups, for instance.

(D) The -OH group may be treated as an O atom and contributions from C-OH bonds omitted.

This can be justified if all three potential minima which arise from rotation about the C-OH bond are of equal depth, or if terms involving hydrogen atoms are small. Both conditions are approximately met.

(E) For acyclic aliphatic compounds and six-membered rings in their normal chair forms, all angles may be taken as those of a regular tetrahedron and the staggered arrangement is present about each bond.

This assumption is not strictly true when oxygen atoms are involved, but it is probably good enough. For three- or five-membered rings, (E) would have to be replaced by a more appropriate assumption.

Before suggesting numerical values and applying these assumptions, it is necessary to discuss the change of the value of the contribution of UC-CX with internal rotation; this rotation is best described by the angle 0 between the planes UCC and CCX. The positive direction is indicated in (I) where U is taken to be projected towards the observer. Restricting 0 to the range $\pi \geqslant 0 > -\pi$ the dependence of the optical rotation of the UC-CX unit on 0 must involve some odd function of 0, such as sin 0, of which the most general is $\sum_{n=0}^{\infty} a_n \sin(n\,0)$. This is not an additional assumption, but a

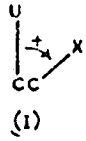

(I)

necessary condition if *dextro* and *laevo* enantiomorphs are to have the same numerical values, but opposite signs, for their rotations. Assumption (E) restricts θ to $\pm\pi/3$ or π. Consequently, if U|X is written as an abbreviation for the contribution of UC–CX when $\theta = +\pi/3$, then $-$U|X is the contribution when $\theta = -\pi/3$, and there is zero contribution when $\theta = \pi$ and the four atoms are coplanar. Consequently, three of the nine terms envisaged under assumption (A) are in fact zero when assumption (E) is also made, and for the remaining six terms a discussion of the explicit angular dependence is not required. The unit of (1) may be rotated in space to bring X forward to the observer, and this cannot affect the optical activity contribution and so $U|X = X|U$. If one of the central atoms is oxygen, the abbreviation for the contribution of UO–CX when $\theta = +\pi/3$ will be written $\bar{U}|X = X|\bar{U}$ which is not the same as $\bar{X}|U$, which must be reserved for the case when X is directly attached to the oxygen atom.

The next logical step would be to express the molecular rotations of a number of compounds in terms of the parameters described, equate these totals to the observed rotations, solve the set of simultaneous equations for individual contributions of the U|X type and finally check these values against further compounds. An attempt to do this shows that only certain sums and differences occur and the individual terms U|X, etc., are not obtainable. This is an inherent property of the problem; it is entirely analogous to the impossibility of obtaining bond dipole moments from measurements on polyatomic molecules and it is known that only bond moment differences are obtainable. Also, it is unwise to obtain numerical values from the minimum requisite number of compounds and better to use such values as a guide and adjust them to give the best overall fit with the experimental values. Table I indicates suitable sum and difference parameters whose use circumvents the first difficulty; the numerical values suggested are those which give closest overall agreement, throughout the tables, with the experimental values of the molecular rotations in water solutions and for the wavelength of sodium D lines.

Table I

Definitions of the rotation parameters and suggested empirical values

Definition	Symbol	Value
$O\|O-2O\|H+H\|H$	F	+45
$O_g\|O-O_g\|H-O\|H+H\|H$	G	+32
$O\|C-C\|H-O\|H+H\|H$	H	+34
$O_r\|O-C_r\|O-O_r\|H+C_r\|H$	I	+43
$\bar{C}_r\|O_g-C_r\|H+C_r\|H-C_r\|O_g+O_g\|H-H\|H$	J	+113
$\bar{C}_r\|C-\bar{C}_r\|H+C_r\|H-C_r\|C+C\|H-H\|H$	K	*ca.* −29

r = ring atom
g = glycosidic oxygen

Example:

Calculated molecular rotation of Methyl α-D-Galactopyranoside in the C1 Conformation

	Contribution from bond
$C_1 - C_2$	$O_r/C_r - C_r/O_g + O_g/O - O/H + H/H - H/O_r$
$C_2 - C_3$	$C_r/H - H/O + O/O - O/H + H/C_r - C_r/C_r$
$C_3 - C_4$	$C_r/C_r - C_r/H + H/H - H/O + O/O - O/C_r$
$C_4 - C_5$	$C_r/H - H/H + H/C - C/O + O/O_r - O_r/C_r$
$C_5 - O_r$	$C_r/C_r - C_r/H$
$O_r - C_1$	$C_r/O_g - C_r/C_r$
Total	$O_g/O - C_r/O_g - 4\,O/H + H/H + 2\,C_r/H + 2\,O/O$
	$- O/C_r + O/O_r - C_r/H + C_r/O_g - H/O_r + H/C - O/C$

$$J = \overline{C}_r/O_g - \overline{C}_r/H + C_r/H - C_r/O_g + O_g/H - H/H$$

$$2F = 2\ O/O - 4\ O/H + 2\ H/H$$

$$G = O_g/O - O_g/H - O/H + H/H$$

$$I = O_r/O - C_r/O - O_r/H + C_r/H$$

$$-H = -O/C + C/H + O/H - H/H$$

$$\underline{\text{Total}} \quad \overline{C}_r/O_g - \overline{C}_r/H + 2\ C_r/H - C_r/O_g + H/H + 2\ O/O - 4\ O/H + O_g/O + O_r/O - C_r/O - O_r/H - O/C + C/H.$$

$\therefore$ Molecular rotation = J + 2 F + G + I − H

= 113 + 90 + 32 + 43 − 34

= 244

Now the empirical value for the hydroxymethyl group for a D sugar = + 30

and the empirical value to give the methyl α-D-glycoside = + 100

$\therefore$ Calculated methyl-α-D-galactoside value = 374

Observed value $[M]^{Na}$ = 380

2. Brewster[8]:

an attempt empirically to relate sign of rotation[4] to structure, conformation and absolute configuration.[5] It has been found that this can be done for many compounds by use of two general rules, a simple method of conformational analysis, and a limited number of empirical rotation constants. Indeed, in many cases, the magnitude of rotation can also be predicted. The general rules are empirical elaborations of the following hypothesis[6] which underlies the whole treatment used here: *A center of optical activity[7] can usefully be described as an asymmetric screw[8] pattern of polarizability.*[9]

This hypothesis will be useful[6] only if centers of optical activity[7] can be described in such a way that there is, empirically, a correlation between assigned screw handedness and observed sign of rotation[4] and also a correlation between the amount of polarizability distributed in a screw sense and the magnitude of rotatory contribution. The empirical rules developed to meet these requirements are presented in this paper. The application of these rules to open-chain compounds is also described; their application to cyclic compounds is described in the following papers.

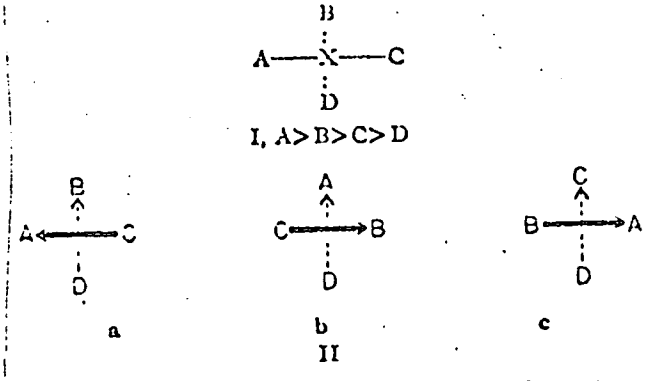

Atomic Asymmetry.—The tetrahedral system, xABCD, can be described as a left-handed screw

pattern of polarizability when it has the absolute configuration shown in the Fischer projection I and when A > B > C > D in polarizability.[10] If our working hypothesis is really useful, then we may expect all asymmetric atoms having configuration I to make rotatory contributions of the same sign[4]; this statement is operationally meaningless, however, until we can develop some standard method for assigning polarizability rank to the substituents A, B, C and D.[11] It is found that an empirical sequence of polarizabilities (Table I) can be established by noting the sign of $[M]_D$ of configurationally related compounds *which can reasonably be expected to show essentially pure atomic asymmetry*[12] (Table II).[13] It is clear from the position of the phenyl group in Table I that priority cannot be assigned on the basis of the polarizability (refraction) of the *entire* substituent.[11] The position of the carbon sequence suggests that priority could be assigned on the basis of the polarizability of attachment atoms[11] (as the carbon atom of a methyl group) provided unsaturation is taken into account.[14] We obtain, thus, the empirical atomic asymmetry rule: *An asymmetric atom in the absolute configuration I is dextrorotatory*[4] *when the polarizabilities of the substituent attachment atoms*[14] *decrease in the order: A > B > C > D.*[15] Under this rule, a formally asymmetric atom carrying two or more alkyl groups will be considered to be, *per se*, optically inactive although it may provide a sterically asymmetric environment conducive to the development of conformational asymmetry (below).

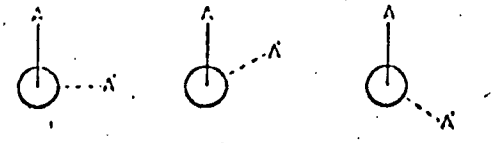

IX

Conformational Asymmetry.—A twisted chain of four atoms, A-C-C-A', displays its asymmetry most clearly when it is viewed along the C-C bond, as in the Newman projections IX; the conformational asymmetry of a complex structure is most conveniently analyzed by systematic inspection of all bonds for units of this nature. It is found empirically that *the conformational units IXb and IXc can be considered to be dextrorotatory*[4,16] *in the absolute configurations shown*[11] *and to make contributions to* $[M]_D$ *which can be expressed mathematically*[17]

$$\Delta[M] = +k \cdot A \cdot A'$$

where A and A' are *functions* of the polarizabilities of the terminal atoms[18] and k a constant which appears to be the same for IXb and IXc.[18] It is of interest that this dextrorotatory conformational unit can be described as a left-handed screw pattern of polarizability[19] (compare the asymmetric atom, above). It is to be expected that the magnitude of the rotatory effect of one of these conformational units would be increased if one (or both) of the terminal bonds were multiple. The basic rule of conformational asymmetry is made operational by the assumption that the rotatory effects of conformational units are additive in full conformations, as Xa ("staggered") and Xb ("eclipsed") which, on this basis, have the rotatory power

$$[M] = +k(A \cdot A' - A \cdot H - A' H + H \cdot H)$$
$$= +k(A - H)(A' - H)$$

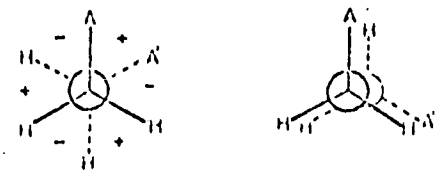

It is found empirically that rotatory powers[4] can be assigned to the full conformations (Xa) (Table I) which, used in conjunction with a simple method of conformational analysis (below), permit predictions of the sign and magnitude of rotation of simple open-chain compounds (this paper). It is shown in part II that these same rotation constants can be used with saturated cyclic compounds *where this method of conformational analysis is not needed.* It will be noted (Table I) that these rotatory values fall into a sequence paralleling the empirical polarizability sequence found for compounds showing pure atomic asymmetry; it has already been pointed out that these values can roughly be calculated from refractions by use of an empirical equation.[15]

The working rules of the simple method of conformational analysis used here are: (1) Only conformations corresponding to energy minima will be prevalent enough to produce appreciable rotatory effects. (2) The five atom conformation XI is "prohibited" when the terminal atoms are *both* larger than hydrogen, the strain here being comparable to that found in a 1,3-diaxially substituted cyclohexane. (3) The conformation XII is "prohibited" when the atoms A, B and C are *all* larger than hydrogen.[20] (4) *In the first approximation*, all allowed conformations are considered equally probable. This rule cannot be justified theoretically but is necessary for a simple analysis of flexible compounds; it may well be that it works because there is some compensation of errors in the method.

In addition to these rules, it is assumed that the rotatory contributions of individual conformations are additive.

XI XII

Tetrahydropyran Derivatives.—The principles which permit the present major simplification and extension of Whiffen's treatment of conformational asymmetry[5] appear to be contradicted at three important points by Whiffen's work. These contradictions can be met only by showing that the present treatment allows a satisfactory calculation of the rotations of the pyranose sugars and their methyl glycosides by use of empirical rotation constants consistent (as some of Whiffen's are not) with the principles used here. It is shown below that these rotations can, indeed, be calculated using *six* such constants (*rounded to the nearest five degrees*); Whiffen used *seven* unrelated and unrounded constants in the same calculations.

One of the present constants [$k_{(C-H)(O-H)} = +50°$] corresponds in form to Whiffen's constant II,[5] for which he gives a value of $+34°$[12]; as shown above and in part I, the present value is suitable for use with acyclic alcohols and is generally

better than Whiffen's value when terpene and steroid alcohols are considered. The second of the present constants [$k(O - H)^2 = +45°$] corresponds in form and magnitude to Whiffen's constant F and is, as Whiffen has shown,[5,11] suitable for calculating the rotations of the cyclitols; as shown above, it forms a consistent series with the values for $k(C - H)(O - H)$ and $k(C - H)^2$ used in part I. This constant will also be used to compute the rotation of asymmetric conformations about bond $C_1 - C_2$, where one of the hydroxy groups is glycosidic. Whiffen has used a constant G (+32°) for this purpose; acceptance of his value would require a repudiation of the central principle that the rotatory power of the asymmetric conformation XXXVIII is independent of the nature of Y.

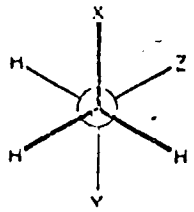

$$[M] = k(X - H)(Z - H)$$

XXXVIII

The tetrahydropyran ring, in contrast to cyclohexane, has an axis of polarizability difference (between O and C_4). If the axial substituents at C_1 and C_5 are different (as in XXXIX), they will form an axis of polarizability difference which will form a screw pattern of polarizability with the ring axis. This pattern, as seen in projection in XLI, has the character of a left-handed screw and should (part I) be dextrorotatory. Since the conformational asymmetry effect of the hydroxy group is $+ - k(O - H)$, we may expect XXXIX to be strongly dextrorotatory; the empirical value used here is +100°, to be compared with Whiffen's value $J = +113°$. An axial hydroxy group at C_2 or C_4 as shown in XL produces the same permolecular pattern XLI, here opposed by the weak net levorotatory conformational effect: $-k(C - O)(O - H) = ca. -5°$. The total rotatory effect of XL is estimated here to be +60°; Whiffen's constant I (+43°) fills the corresponding role in his calculations.[15] An additional constant is required for the hexoses since the hydroxy methyl group is in a sterically asymmetric environment; the two "allowed" conformations of this group as found in D-hexoses are seen in XLII. The empirical value +25° is used here for this system; Whiffen uses a value of +30°. The positive sign of this value is consistent with the smaller size of the ether oxygen as compared to C_4 *and its substituents;* the magnitude of this constant cannot be predicted. A final constant is required for calculations of the rotation of methyl glycosides. This constant reflects the fact that the methoxy group

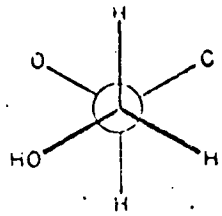

$+k(O - H)^2 = +45°$

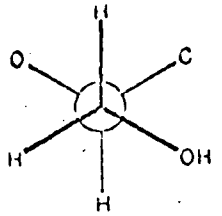

$-k(C - H)(O - H) = -30°$

$+25°$

XLII

Table X

Rotation Constants for Use with Carbohydrates

Notation: Present	Notation: Whiffen[5]	Δ[M]: Whiffen[5]	Δ[M]: Present
$k(O - H)(O - H)$	F	+45°	+45°
	G	+32°	
$k(C - H)(O - H)$	H	+34°	+30°
XXXIX[a]	J	+113°	+100°
XL[a,b]	I	+43°	+60°
XLII		+30°	+25°
XLV[a]		−100°	−105°

[a] These values can be, roughly, calculated by letting the permolecular effect be +65° and by assigning the value: $k(E - H)(C - H) = -30°$, where E represents an unshared pair of electrons on oxygen. On this basis XXXIX becomes: $65 + k(C - E)(O - H) - k(O - H)(C - H) = +107$; XL becomes: $65 - k(C - O)(O - H) = 69$ (using the value $k(O - H)^2 = 45$) and XLV becomes: $-k(C - E)(O - H) = -92°$. [b] The empirical values give better fits and are used in Table XI.

is in a sterically asymmetric environment. In the β-D-hexosides (XLIII), for example, the asymmetric conformation XLV should predominate; this conformation should be levorotatory but its magnitude of rotation cannot be predicted. A value of −105° is used here (Whiffen uses −100°); a value of +105° is, then, required for α-D-hexosides (XLIV).

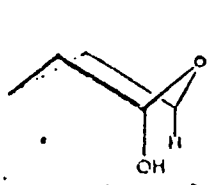

XXXIX, +100°

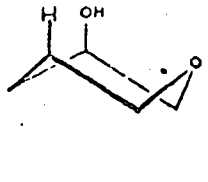

XL, +60°

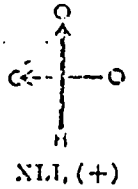

XLI, (+)

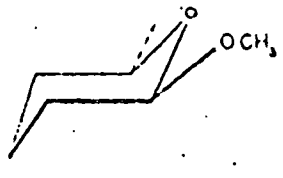

XLIII, β

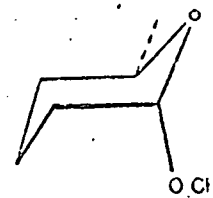

XLIV, α

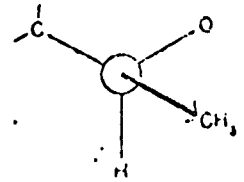

XLV, $-kC(O - H) = -105°$

Example:

Calculated molecular rotation for Methyl α-D-Galactopyranoside in the C1 conformation

	Contribution from bond	Value
C_1-C_2	k (O-H)(O-H)	+45
C_2-C_3	k (O-H)(O-H)	+45
C_3-C_4	k (O-H)(O-H)	+45
C_4-C_5	- k (O-H)(C-H)	-50
C_5-O_r	-	-
O_r-C_1	-	-

Plus

Permolecular effect of axial C(1)-OCH_3(XXXIX) +100

Permolecular effect of axial C(4)-OH (XL) +60

Plus

The empirical value for the hydroxymethyl group for a D sugar = +25

The empirical value to give the methyl α-D-glycoside = +105

∴ Calculated methyl α-D-galactoside value = 375

Observed value $[M]^{Na}$ = 380

3. Lemieux and Martin[12]:

the empirical rules that were first suggested by Whiffen[3] and later elaborated by Brewster[4]. This communication provides further experimental evidence for the utility of such rules. However, to do so, we need to propose new values for the contributions to rotation made by certain asymmetric conformational units found in *saturated* oxygenated compounds wherein neighboring groups are encountered that have staggered arrangements, or at least approximately so. Whiffen proposed it to be "unwise to obtain numerical values from the minimum requisite number of compounds and better to use such values as a guide and adjust them to give the best overall fit with the experimental values." Our basic assumption in developing the numerical values for contributions to rotation by asymmetric conformational units contradicts this proposal. Instead, we believe it more *useful* to

arrive at values by using the rotations of closely related structures, including whenever possible simple model compounds that contain structural units present in the more complex carbohydrate structures. This procedure is considered more useful since it allows predictions of the rotation of more-complex, related structures of fixed conformation. The resultant values are generally in better accord with observation than are those obtained from the more general approaches employed either by Whiffen[3] or by Brewster[4]. Thus, the procedure should be more reliable in attaching significance to differences between calculated and observed rotations. This expectation appears, as will be seen, well justified by the results achieved. Also, Brewster found it necessary to invoke the concept of permolecular dissymmetry in his treatment of the rotations of carbohydrates. We have found, following Whiffen's procedure, that the rotation thus assigned can be attributed to the occurrence of asymmetric conformational units formed by carbon and oxygen atoms in *gauche* relationship, as long as different values are assigned depending on whether the bridging atoms are both carbon (C/C, O/C or O/O) or one is oxygen (C/C_o or O/C_o).

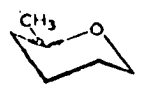

7

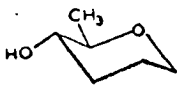

9

Analysis of the asymmetric conformation units present in *R*-2-methyltetrahydropyran in conformation 7 which has the methyl group in equatorial orientation shows that these cancel to zero. Both Whiffen[3] and Brewster[4] have pointed out that in the absence of differences in the contributions to rotation arising from such asymmetric conformational units (pair-wise contributions[5]) only small rotations are to be expected; that is, the presence of the asymmetric carbon in 7 on its own is not expected to render the compound appreciably optically active and, indeed, as seen in Table I the molecular rotation was less than 5° in all the solvents reported. In the case of compound 9, analysis of the asymmetric conformational units present in the chair form indicated shows the following differences: O/C−(O/H+C/H−H/H). The rotation of 9 was found to be +14° in water. As mentioned above, it is *arbitrarily* assumed for the purposes of this presentation that the contributions O/H, C/H, and H/H are negligibly small as compared to the O/C contribution. Since it seems reasonable to expect the term O/H+CH−H/H to be positive, the O/C contribution is estimated to be somewhat lower than the rotation of 9. Therefore, the difference between the rotation of 9 and 7, namely 14−4 = 10°, is considered a better approximate value for the O/C contribution than is the rotation of 9.It is emphasized again that this assumption is made both for reasons of convenience and better overall agreement as are other basically false assumptions implicit to this approach; namely, that the molecules are in perfect chair forms (indeed appreciable contributions to rotation may even arise from neighboring substituents wrongly assumed to be in a perfect antiparallel arrangement), that interactions further extended than for neighboring atoms make no contributions (no permolecular contributions), and that solvent effects are not present. In this light, we assign a contribution to rotation of +10° when in the structures under consideration there exists an oxygen and a carbon in *gauche* relationship and bridged by two carbon atoms and describing a right-handed screw pattern of asymmetry; *i.e.*, as shown in the following asymmetric unit.

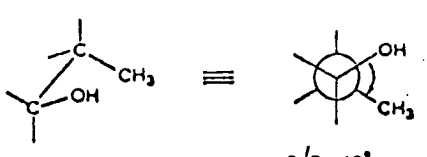

O/C = 10°

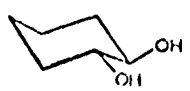

11

D-*threo*-1,2-Cyclohexanediol (11) differs in asymmetric conformational units from cyclohexanol by 2(H/H-O/H)-(O/O-H/H), and this difference is considered to be the origin of the molar rotation (−48°) of the compound. Consideration of the content of Table II shows that the choice of O/O = 45°, as initially proposed by Whiffen[3], provides an excellent basis for estimating the molar rotations of compounds with known conformations wherein these asymmetric conformational units occur.

In his empirical rules to correlate rotation with the structure of methyl glycopyranosides, Brewster[4] assigned a contribution of ± 105° (depending on the configuration) to the conformational unit defined by the acetal linkage as shown in 14. That this carbon–oxygen bridged, asymmetric conformational-unit, which we specify as O/C_o,

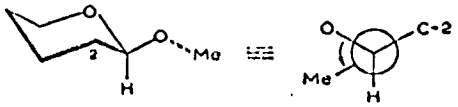

14

should make a strong contribution to rotation is evident from the rotations of the aldopyranoses listed in Table IV having the 1-substituent axial. It is seen that a value of + 115° for the O/C_o unit described by the axial oxygen atom and C-5 provides a good correspondence between predicted and observed rotations. The value of 115° for O/C_o corresponds to the value of 113° assigned by Whiffen[3] to his rotational parameter *J*.

Table VI shows that good agreement is achieved in the calculation of the molar rotations for 1-axial methyl α-D-glycopyranosides if it is assumed that the orientation of the methyl group is entirely that of the enantiomer of 14 (that is, + O/C_o). However, the agreement is not nearly as acceptable for the 1-equatorial methyl glycopyranosides (Table VII), since in all of the examples given the difference between the calculated and found values is negative.

the effect of introducing an hydroxyl group at C-6 of a 6-deoxy-D-hexopyranose structure is to increase the rotation by about 25°

Example:

Calculated Molecular Rotation of Methyl α-D-Galactopyranoside in the C1 Conformation

	Contribution from bond	Value
C_1–C_2	+ O/O − O/C + O/C	+45
C_2–C_3	+ O/O	+45
C_3–C_4	+ O/O − O/C	+35
C_4–C_5	+ O/O − O/C − O/C	+25
C_5–O_r	+ C/C_o	−
O_r–C_1	+ O/C_o − C/C_o	+115

Plus

The empirical value for the hydroxymethyl group of a D sugar = 25

Plus the empirical value to give the methyl α-D glycoside (+ O/C_O) = 115

∴ Calculated methyl α-D-galactoside value = 405

Observed value $[M]^{Na}$ = 380

B. Calculation of the Linkage Rotations

Rees[15]:

We start by asking whether any part of the total optical rotation may be identified as a specific contribution by the linkage stereochemistry. *We recognize the fundamental unsoundness of the van't Hoff superposition principle and Hudson's rules which are derived from it, and the following discussion depends in no way on these ideas.* The true principles to be applied in additive and subtractive treatment of optical rotation contributions within a molecule have been enunciated by Kauzmann.[16] He has pointed out that the quantum theories of optical rotation do *not* suggest that the behaviour is a result of any property of individual groups such as the electronic motions in an asymmetric carbon atom, but is rather a result of the *modification* of such motions by interactions between groups. The optical rotation should not be seen as a sum of contributions from isolated groups but as a sum of interaction effects between groups. The terms to be considered[16] are of the type AB ('pairwise interactions'), ABC ('three-way interactions'), ABCD ('four-way interactions), and so on. The interactions may be through coulombic, dipole, or quadrupole perturbation of electronic transitions, strong dispersion forces, charge-transfer effects, or through covalent bonds.[17] Within this context, we now define the linkage rotation for a given wavelength by equation (1) where $[M_{NR}]$

$$[A] = [M_{NR}] - \{[M_{MeN}] + [M_R]\} \qquad (1)$$

is the molecular rotation for a given disaccharide which contains a nonreducing (N) and a reducing (R) residue, $[M_{MeN}]$ is the molecular rotation of the methyl glycoside of N having the same anomeric configuration as the disaccharide, and $[M_R]$ is the rotation of the reducing sugar. For the present, we assume that mutarotation equilibrium is the same for R and NR, but possible complications will be considered later. In most of the examples to be given in this paper, [A] will actually be calculated by the use of corresponding equations for disaccharide glycosides or other derivatives for which this problem does not arise.

The value for [A] represents the optical rotation due to interactions across the glycosidic linkage, minus any contribution to $[M_{MeN}]$ and $[M_R]$ by interactions of the glycosidic methyl and of the hydrogen lost from R in formal elimination to give NR. The positive terms would include any influence of one residue on the ring conformation of the other, any strong forces of attraction and repulsion which, by perturbing electronic motions, have different effects on the refractive indices to left- and right-handed circularly polarized light, and any interactions through the glycosidic bonding system. To interpret [A], we must make assumptions about which of these effects are likely to be important. From this stage of the argument onwards, therefore, the treatment is justified only to the extent that it works.

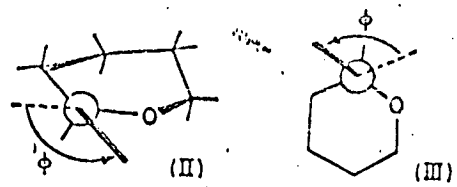

Configurations at C(1), viewed from O(1): β (II) and α (III)

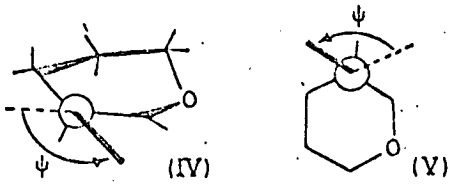

Configurations at non-anomeric carbon atoms, viewed from the oxygen to which it is bonded: equatorial oxygen (IV) and axial (V). C(4) is shown here for illustration but the same considerations apply for C(2) and C(3)

because the sugar residue to be considered at this stage are stable in the Reeves C1 conformation, we shall attempt to account for linkage rotations in terms of interactions between bonded atoms. Since Brewster's methods and parameters work so well for other molecules,[11,13] including carbohydrates,[12] we shall use them here. The notation is also his, except for ϕ and ψ which, for consistency,[4,16] have the positive directions shown (II—V). Each angle is zero when the relevant

C-O and C-H bonds are eclipsed and is denoted $\Delta\phi$ or $\Delta\psi$ to avoid confusion with an earlier [4] convention for the origin. Each chain of four atoms makes a contribution which depends on the dihedral angle, and which is positive when the angle has a right-handed screw sense.[11,15] Taking cellobiose (I) as an example, the interaction C(2)-C(1)-O-C(4′) makes the contribution [14,15] (3) in which the constant (see XLV [12]) is

$$[\Phi_1] = \text{constant} \times \sin\theta \qquad (3)$$

$2/\sqrt{3} \times (105) \approx 120°$ for the wavelength of the sodium D line and θ is the dihedral angle, actually $(2\pi/3 + \Delta\phi)$. Thus we obtain equation (4). In general, the value of

$$[\Phi_1]_D = 120 \sin(2\pi/3 + \Delta\phi) \qquad (4)$$

the constant depends on the nature of the atoms concerned, but a central C-O bond is common to all the interactions we shall need to estimate and, for terminal atoms, the data (see Table 1 [11] and Table 2 [14]) show that oxygen has about the same rotational rank as carbon bonded to a hydroxy-group, while hydrogen atoms can be neglected. The other terms are then as shown in equations (5), (6), and (7) for O(5)-C(1)-O-C(4′), C(1)-O-C(4′)-C(5′), and C(1)-O-C(4′)-C(3′) respectively.

$$[\Phi_2]_D = -120 \sin(2\pi/3 - \Delta\phi) \qquad (5)$$

$$[\Phi_3]_D = -120 \sin(2\pi/3 - \Delta\phi) \qquad (6)$$

$$[\Phi_4]_D = 120 \sin(2\pi/3 + \Delta\phi) \qquad (7)$$

To estimate $[A]_D$, we must also subtract the C_{methyl}-O-C(1)-O(5) and C_{methyl}-O-C(1)-C(2) interactions which were implicit in $[M_{MeN}]$ [see (1)], and for which the combined value is actually [12] $-105°$. For β-linked disaccharides in which the nonreducing residue is D and has the Reeves C1 conformation, therefore we obtain equation (8) which readily simplifies to (9). We prefer

$$[A^{\beta}_{calc}]_D = [\Phi_1]_D + [\Phi_2]_D + [\Phi_3]_D + [\Phi_4]_D + 105 \qquad (8)$$

$$[A^{\beta}_{calc}]_D = 105 - 120(\sin\Delta\phi + \sin\Delta\psi) \qquad (9)$$

to take account of the methyl group in this way rather than in equation (1) because $[A_{obs}]$ is then based only on direct measurements and the theoretical parameters are all contained in $[A_{calc}]$. A different expression (10) must be used for α-linked disaccharides because the correction then [12] has a different sign. The sign of the

$$[A^{\alpha}_{calc}]_D = -105 - 120(\sin\Delta\phi + \sin\Delta\psi) \qquad (10)$$

first term in equations (2) and (3) must be reconsidered [12] if the nonreducing residue has the L configuration or the Reeves 1C conformation.

Example:

Calculation of the Observed and calculated Values of the Linkage Rotation of Methyl β-Cellobioside

Observed Linkage Rotation:

The molecular rotations observed in this study (Chapters 1 and 2) are used to demonstrate the calculation of the observed molecular rotation

	$[M]^{25°C}_{Na}$
Methyl β-cellobioside	-64.6°
Methyl β-D-glucopyranoside	-62.0°

$$[\Lambda_{obs}] = [M_{NR}] - ([M_{MeN}] + [M_R])$$

Both $[M_{MeN}]$ and $[M_R]$ are in this case methyl β-D-glucopyranoside.

$\therefore [\Lambda_{obs}] = -64.6^\circ - (-124.0^\circ)$

$= 59.4^\circ$

Calculated Linkage Rotation:

The values of ϕ and ψ which have been calculated [49] from crystal coordinates [92] would correspond to $\Delta\phi = 42^\circ$, $\Delta\psi = -18^\circ$

$[\Lambda_{calc}] = 105 - 120 (\sin 42^\circ - \sin 18^\circ)$

$= 62^\circ$

This excellent agreement of the observed and calculated linkage rotations strongly suggests that the solution and crystal conformations are similar.

APPENDIX 2

THE VARIATION OF THE COMPENSATED MOLECULAR ROTATION (c.m.r.) OF THE MONOSACCHARIDE METHYL GLYCOSIDES WITH TEMPERATURE, AT λ_{546}

APPENDIX 2

The Variation of the Compensated Molecular Rotation (c.m.r.) with Temperature at λ_{546}

Sample	Solvent	Value of c.m.r. at the temperature indicated (degrees)							
		20	25	30	40	50	60	70	80
Me α-D-glucopyranoside	H_2O	357.7	357.9	358.2	358.7	359.2	359.6	360.1	360.6
	DMSO	351.1	351.1	351.1	351.0	351.0	350.8	350.6	350.3
	Dioxan	358.7	359.8	361.0	362.7	364.3	365.4	365.8	366.0
Me α-D-xylopyranoside	H_2O	292.3	292.5	292.6	293.0	293.3	293.6	294.1	294.4
	DMSO	282.8	282.8	282.8	282.7	282.5	282.0	281.3	280.4
	Dioxan	314.7	314.7	314.6	314.5	314.2	313.9	313.3	312.7
Me α-D-mannopyranoside	H_2O	174.4	174.9	175.5	176.6	177.7	178.8	179.9	181.0
	DMSO	162.9	164.8	166.5	169.9	172.7	175.2	177.5	179.6
	Dioxan	251.6	251.1	250.1	249.0	246.7	243.8	240.2	235.6
Me α-D-galactopyranoside	H_2O	440.7	439.1	437.8	435.6	433.9	432.2	430.7	429.4
	DMSO	396.0	394.8	393.8	391.9	390.1	388.5	387.2	386.0
	Dioxan	357.6	359.3	360.9	364.0	367.0	369.6	371.6	373.1

APPENDIX 2 (Continued)

Sample	Solvent	Value of c.m.r. at the temperature indicated (degrees)							
		20	25	30	40	50	60	70	80
Me β-L-arabinopyranoside	H_2O	455.1	454.3	453.5	452.0	450.4	448.9	447.3	445.8
	DMSO	390.8	389.2	387.8	384.8	381.9	379.2	376.0	374.3
	Dioxan	393.4	393.5	393.6	393.6	393.4	392.5	391.3	390.0
3,6 Anhydro-me-α-D-galacto-	H_2O	163.8	162.8	161.7	159.7	157.7	156.0	154.3	152.7
pyranoside	DMSO	150.9	151.0	151.1	151.3	151.5	151.7	151.9	152.1
	Dioxan	174.0	173.9	173.8	173.6	173.4	173.2	172.9	172.7
Me β-D-glucopyranoside	H_2O	-73.6	-73.2	-72.8	-72.1	-71.4	-70.8	-70.3	-69.9
	DMSO	-76.2	-75.0	-73.7	-71.5	-69.5	-67.8	-66.4	-64.7
	Dioxan	-80.6	-79.6	-78.7	-77.1	-75.9	-75.3	-74.9	-74.7
Me β-D-xylopyranoside	H_2O	-125.6	-125.1	-124.5	-123.6	-122.9	-122.3	-121.9	-121.6
	DMSO	-111.9	-111.5	-111.1	-110.4	-110.0	-109.9	-110.1	-110.5
	Dioxan	-133.2	-133.9	-134.5	-135.8	-137.0	-138.2	-139.5	-140.7

APPENDIX 2 (Continued)

Sample	Solvent	Value of c.m.r. at the temperature indicated (degrees)							
		20	25	30	40	50	60	70	80
Me β-D-galactopyranoside	H_2O	-1.0	-1.6	-2.2	-3.4	-4.5	-5.7	-6.9	-8.1
	DMSO	-27.1	-27.2	-27.2	-27.2	-27.2	-27.2	-27.2	-27.2
	Dioxan	-57.7	-57.1	-56.7	-55.7	-55.0	-54.5	-54.1	-53.9
Styracitol (1,5 anhydro mannitol)	H_2O	-97.5	-97.6	-97.6	-97.7	-97.8	-97.9	-98.0	-98.0
	DMSO	-101.0	-99.9	-98.9	-97.1	-95.5	-94.0	-92.8	-91.7

APPENDIX 3

THE VARIATION OF THE COMPENSATED MOLECULAR AND SPECIFIC ROTATIONS OF THE DISACCHARIDE GLYCOSIDES WITH TEMPERATURE, AT λ_{546}

APPENDIX 3

The Variation of the Compensated Molecular and Specific (in brackets) Rotations with Temperature at λ_{546}

Sample	Solvent	Value of c.m.r. and c.s.r.(in brackets) at the temperature indicated							
		20	25	30	40	50	60	70	80
Methyl β-cellobioside	H_2O	-77.5	-76.7	-75.5	-74.5	-73.2	-72.3	-71.5	-70.8
		(-21.8)	(-21.6)	(-21.3)	(-21.0)	(-20.6)	(-20.3)	(-20.0)	(-19.8)
	DMSO	-82.2	-80.9	-79.4	-76.8	-74.5	-72.5	-70.7	-69.0
		(-23.3)	(-22.8)	(-22.3)	(-21.5)	(-20.9)	(-20.2)	(-19.9)	(-19.5)
Methyl β-maltoside	H_2O	338.5	338.6	338.8	339.1	339.5	339.8	340.3	340.7
Monohydrate		(90.5)	(90.5)	(90.6)	(90.7)	(90.8)	(90.9)	(91.0)	(91.1)
	DMSO	252.4	254.7	257.2	261.5	265.8	269.6	273.2	276.6
		(67.5)	(68.1)	(68.7)	(69.9)	(71.0)	(72.1)	(73.0)	(73.9)
	Dioxan	248.4	252.1	255.7	262.9	269.7	275.8	279.7	284.0
		(66.5)	(67.5)	(68.4)	(70.3)	(72.1)	(73.7)	(75.0)	(75.8)
Methyl α-sophoroside	H_2O	267.4	268.5	267.7	267.9	268.1	268.2	268.3	268.2
		(75.1)	(75.1)	(75.2)	(75.3)	(75.4)	(75.4)	(75.3)	(75.3)
	DMSO	265.5	265.9	266.4	267.2	267.7	267.7	267.3	266.6
		(74.4)	(74.6)	(74.8)	(75.0)	(75.1)	(75.1)	(75.0)	(74.8)

Sample	Solvent	Value of c.m.r. and c.s.r.(in brackets) at the temperature indicated							
		20	25	30	40	50	60	70	80
α,α-Trehalose	H_2O	739.3	739.3	739.2	739.1	739.0	738.9	738.7	738.6
		(215.9)	(215.9)	(215.9)	(215.9)	(215.9)	(215.9)	(215.8)	(215.7)
	DMSO	685.6	686.6	687.5	689.4	690.9	692.1	693.0	693.7
		(200.4)	(199.7)	(200.9)	(201.4)	(201.8)	(202.2)	(202.4)	(202.7)
1,5 Anhydro 4-(O-β-D-glucopyranosyl)-D-sorbitol	H_2O	111.5	111.2	111.0	110.4	109.8	109.0	108.1	107.2
		(34.2)	(34.2)	(34.1)	(33.9)	(33.7)	(33.5)	(33.2)	(32.9)
	DMSO	91.9	91.5	91.1	90.2	89.2	88.0	86.7	85.4
		(28.2)	(28.1)	(28.0)	(27.6)	(27.3)	(26.9)	(26.6)	(26.2)

APPENDIX 4

ALGFIT : COMPUTER PROGRAMME FOR THE DETERMINATION OF ALGINATE BLOCK STRUCTURE

ALGFIT

```
50 PRINT,"YOU DONT SUCCEED"
100 $FILE EDSM,EDSALT,GPH,
110 + SSDJPH,F347PH,AUSTPH,F387PH,CL47PH,CL41PH,CJL44
120 EXTERNAL LEASQ
130 DIMENSION WL(33),Y(66),KALG(33),KBLO(33)
140 DIMENSION MAP(65),F(3),DF(3)
150 REAL MM(33),MG(33),GG(33)
160 COMMON MM,MG,GG,KBLO,KALG,WL,Y,NV
170 1 READ(1) AWL,AMM
180 READ(2) AWL,AMG
190 READ(3) AWL,AGG
200 IF (270.0-AWL) 1,2,2
210 2 N=0.4*(AWL-187.5)+0.5
220 MM(N)=AMM
230 MG(N)=AMG
K40 GG(N)=AGG
250 WL(N)=AWL
260 KBLO(N)=1
270 IF(ENDFILE 1) 1,99
280 99:PRINT,"FILE NUMBER",
281 REWIND 1;REWIND 2 ;REWIND 3
290 INPUT,NFILE
300 3 READ(NFILE) AWL,ALG
310 IF (270.0-AWL) 3,4,4
320 4 N=0.4*(AWL-187.5)+0.5
330 Y(N)=ALG
340 KALG(N)=0
350 IF(ENDFILE NFILE)3,5
360 5 REWIND NFILE
370 PRINT,"ESTIMATED FRACTIONS OF M,ALT + G",
3X0 INPUT,F
390 NV=3
400 PRINT, "ITERATE? TABLE? GRAPH",
410 INPUT, KIT,KTAB,KGR
420 DO 41 I=1,3; 41:DF(I)=0.1
430 ERR=1.0E-9
440 IF(KIT-"YES") 40,98,40
450 98 PRINT,"FORCE FIT TO 1.00",
T60 INPUT,KFF
470 IF(KFF-"YES") 39,97,39 ;97:
480 NV=2
490 39 CALL RESET (NV)
500  CALL SIMPLX(LEASQ,DIFF,NV,F,DF,2000,25,ERR,NITER)
510 IF (KFF-"YES") 95,94,95; 94:F(3)=1.0-F(1)-F(2); 95:
520 PRINTF1,NITER,DIFF,F
530 F1:FORMAT (/I5," ITERATIONS, RESIDUAL SUM OF SQ'S =",F8.4//
540 +   "CALCULATED PROPORTIONS ARE",F6.3," :",F6.3," :",F6.3)
550 40:
560 6 TOT=0.0
570 IF (KTAB-"NO") 114,113,114; 114:
```

ALGFIT CONTINUED

```
580 PRINT,↑↑,"     WAVELENGTH      ALGINATE        FITTED        DIFFERENCE
590 113:
600 DO 22 I=1,33
610 IF (KALG(I)*KBLO(I)) 22,22,10
620 10 YCALC=ABS(F(1))*MM(I)+ABS(F(2))*MG(I)+ABS(F(3))*GG(I)
630 Y(33+I)=YCALC
640 IF (KTAB-"NO") 112,22,112; 112:
650 DIFF=ABS(Y(I)-YCALC)
660 PRINT,WL(I),Y(I),YCALC,DIFF
670 22 CONTINUE
680 IF (KGR-"YES") 99,7,99
690 7 MBL=" "
700 MI="1"
710 IBIG=1
720 ISML=1
730 PRINT,↑↑,"GRAPH",↑
740 DO 101 J=2,66
750 IF(Y(J)-Y(IBIG)) 102
760 IBIG=J; GOTO 101
770 102 IF(Y(ISML)-Y(J)) 101
780 ISML=J
790 101:
800 YBG=AMAX1(Y(IBIG),0.0)
810 YSM=AMIN1(Y(ISML),0.0)
820 YRNGE=YBG-YSM
830 ISTEP=IFIX(YRNGE/6.3)+1
840 B10.0/ISTEP
850 A=B*YBG
860 IBL=A+1.5
870 DO 111 JJ=1,33; J=34-JJ
880 IF(KALG(J)*KBLO(J)) 109,108
890 109:
900 DO 103 I=1,64
910 103 MAP(I)=" "
920 MAP(IBL)="1"
921 OBS=A-B*Y(J)+1.0
922 CAL=A-B*Y(J+33)+1.0
930 NOBS=OBS+0.5
940 NCAL=CAL+0.5
950 IF(ABS(OBS-CAL)-1.0) 105,104,104
960 105 MAP(NOBS)="*"
970 GOTO 106
980 104 MAP(NOBS)="."
990 MAP(NCAL)="+"
1000 106
1010 NPR=MAX0(NOBS,NCAL,IBL)
1020 PRINT 107, WL(J),(MAP(I),I=Q,NPR)
1030 107 FORMAT (F6.1,2X,64A1)
1040 GOTO 111
1050 108 IZ=7+IBL
```

ALGFIT CONTINUED

```
1060 PRINT 110,(MBL,I=1,IZ),MI
1070 110 FORMAT(72A1)
1080 111:
1090 PRINT, '"ONE INCH REPRESENTS",ISTEP,"    CARY INCHES",'
1100 GOTO 99
1110 STOP; END
1120 $USE SIMPLX
1130 SUBROUTINE LEASQ(TOT,F)
1140 COMMON MM,MG,GG,KBLO,KALG,WL,Y,NV
1150 DIMENSION WL(33),Y(66),KALG(33),KBLO(33)
1160 REAL MM(33),MG(33),GG(33),F(3)
1170 IF (NV-2) 6,7,6
1180 7 F(3)=1.0-F(1)-F(2)
1190 6:
1200 II=0
1210 TOT=0.0
1220 DO 1 J=1,33
1230 I=34-J
1240 IF (KALG(I)*KBLO(I)) 1,1,2
1250 2 IF (II) 4,3,4
1260 3 II=1
1270 WF=1.0
1280 GO TO 5
1290 4 WF=1.0/(1.0+5.0*ABS(Y(I)-YOLD))
1300 5 YOLD=Y(I)
1310 YCALC=ABS(F(1))*MM(I)+ABS(F(2))*MG(I)+ABS(F(3))*GG(I)
1320 TOT=TOT+(Y(I)-YCALC)**2*WF
1330 1 CONTINUE
1340 RETURN; END
1350 SUBROUTINE MONITR (IV,PREC,VAL,ARR,LOW,IRTN)
1360 DIMENSION ARR(20,20)
1370 GO TO 15
1380 ENTRY RESET (NNV)
1390 ITIM=0
1400 NV=NNV
1410 RETURN; 15:
1420 IF (ITIM) 10,11,10; 12
1430 IF (NV-2) 1,2,1; 2:ARR(LOW,3)=1.0-ARR(LOW,1)-ARR(LOW,2); 1:
1440 PRINT F1, IV,VAL,ARR(LOW,1),ARR(LOW,2),ARR(LOW,3)
1450 F1:FORMAT ("EVS = ",I5,",  VAL = ",F7.5,10X,
1460 +    "M:A:G = ",3F5.3)
1470 PRINT,"CARRY ON",
1480 INPUT, KCO
1490 IF (KCO-"YES") 3,4,3
1500 3:IRTN=-1
1510 4:RETURN
1520 11:PRINT, "QUIET",; INPUT, KQU
1530 ITIM=-1
1540 10:IF (KQU-"YES") 12,4,12
```